

Molecular and functional characterisation of a new mammalian  
family of proton-coupled amino acid transporters

Martin Foltz

Vollständiger Abdruck der von der Fakultät Wissenschaftszentrum Weihenstephan für Ernährung, Landnutzung und Umwelt der Technischen Universität München zur Erlangung des akademischen Grades eines

Doktors der Naturwissenschaften

genehmigten Dissertation.

Vorsitzender: Univ.-Prof. Dr. rer. nat. Michael Schemann

Prüfer der Dissertation:

1. Univ.-Prof. Dr. rer. nat. Hannelore Daniel
2. Hochschuldozentin Dr. rer. nat. Ellen I. Closs,  
Johannes Gutenberg-Universität Mainz
3. Univ.-Prof. Dr. rer. nat. habil. Siegfried Scherer

**Die Dissertation wurde am 16.09.2004 bei der Technischen Universität München eingereicht und durch die Fakultät für Ernährung, Landnutzung und Umwelt am 15.12.2004 angenommen.**



---

The presented thesis is based on following peer-reviewed original papers and submitted manuscripts

- I Boll M, Foltz M, Rubio-Aliaga I, Kottra G, and Daniel H. Functional characterization of two novel mammalian electrogenic proton dependent amino acid cotransporters. **J. Biol. Chem.**, 277, 22966-22973 (2002)
- II Boll M, Foltz M, Rubio-Aliaga I, and Daniel H. A cluster of proton/amino acid transporter genes in the human and mouse genomes. **Genomics**, 82, 47-56 (2003)
- III Boll M<sup>#</sup>, Foltz M<sup>#</sup>, Anderson CMH, Oechsler C, Kottra G, Thwaites DT, and Daniel H. Substrate recognition by the mammalian proton-dependent amino acid transporter PAT1. **Mol. Membr. Biol.**, 20, 261-269 (2003) <sup>#</sup>authors contributed equally
- IV Rubio-Aliaga I, Boll M, Vogt-Weisenhorn DM, Foltz M, Kottra G, and Daniel H. The proton/amino acid cotransporter PAT2 is expressed in neurons with a different subcellular localization than its paralog PAT1. **J. Biol. Chem.** 279, 2754-2760 (2004)
- V Foltz M, Boll M, Raschka L, Kottra G, and Daniel H. A novel bifunctionality: PAT1 and PAT2 mediate electrogenic proton/amino acid and electroneutral proton/fatty transport. **FASEB J.** 18, 1758-60 (2004)
- VI Foltz M, Dietz V, Boll M, Kottra G, and Daniel H. Kinetics of bidirectional H<sup>+</sup> and substrate transport by the proton-dependent amino acid symporter PAT1. **Biochem. J.** 384, accepted and in press (doi:10.1042/BJ20041519)
- VII Foltz M, Oechsler V, Boll M, Kottra G, and Daniel H. Substrate specificity and transport mode of the proton dependent amino acid transporter mPAT2. **Eur. J. Biochem.** 271, 3340-3347 (2004)
- VIII Anderson CMH, Grenade DS, Boll M, Foltz M, Wake KA, Kennedy DJ, Munck LK, Miyauchi S, Taylor PM, Campbell FC, Munck BG, Daniel H, Ganapathy V, and Thwaites DT. PAT1 (SLC36A1) is a nutrient and drug transporter in human and rat small intestine. **Gastroenterology** 127: 1410-1422 (2004)

## TABLE OF CONTENTS

<b>SUMMARY</b>	1
<b>INTRODUCTION</b>	3
1. Preface	4
2. Brief history of the discovery of amino acid transport processes	5
3. The amino acid/auxin permease family	8
4. Physiological importance of small, neutral amino acids and their derivatives serving as substrates of the PAT-carriers	12
4.1 Glycine	12
4.2 Alanine	12
4.3 Proline	13
4.4 Amino acid derivatives and D-amino acids	13
5. Transport systems for small, neutral amino acids and amino acid derivatives	15
5.1 Glycine transporting systems	15
5.2 Alanine transporting systems	15
5.3 Proline transporting systems	17
5.4 Transport systems for GABA, betaine, taurine and D-amino acids	18
6. System PAT: Mammalian proton-coupled amino acid transport	20
7. Identification and cloning of a mammalian proton/amino acid symporter family	24
<b>AIMS AND ACHIEVEMENTS OF THE THESIS</b>	29
<b>RESULTS AND DISCUSSION</b>	33
1. Revelation of two new mammalian proton/amino acid transporters: General characteristics	35
2. The PATs represent a new mammalian subgroup within the AAAP-family	37
3. Specific functional characteristics of PAT1 and PAT2	40
3.1 Minimal structural requirements of aliphatic amino acid PAT substrates	41
3.2 Driving forces for PAT-mediated transport	43
3.3 Bidirectional transport	44
3.4 Kinetic binding model	44
3.5 Lack of a proton-leak pathway	45

---

4. PAT1 and PAT2 as potential delivery systems for short-chain fatty acids	47
5. <i>Caenorhabditis elegans</i> homologs of the mammalian PAT transporters	50
6. Proposed physiological and pharmacological roles of the PAT transporters	51
7. Potential pathological implications of PAT1 and PAT2	57
8. Future perspectives	59
<b>ZUSAMMENFASSUNG</b>	61
<b>REFERENCES</b>	65
<b>ABBREVIATIONS</b>	75
<b>APPENDIX 1</b>	77
<b>APPENDIX 2</b>	87
<b>APPENDIX 3</b>	99
<b>APPENDIX 4</b>	109
<b>APPENDIX 5</b>	117
<b>APPENDIX 6</b>	139
<b>APPENDIX 7</b>	171
<b>APPENDIX 8</b>	181
<b>ACKNOWLEDGEMENT</b>	195
<b>CURRICULUM VITAE</b>	199
<b>LIST OF SCIENTIFIC PUBLICATIONS</b>	201

*This thesis is dedicated to my parents  
Barbara Foltz  
and Gerhard Foltz  
for their love and their encouragement*

## SUMMARY

Proton-coupled amino acid transport (PAT) systems in the apical membrane of epithelial cells of the small intestine and the renal tubule have been demonstrated by use of the human intestinal cell line Caco-2 and renal brush border membrane vesicles. The present thesis summarises the revelation of the molecular entity of the PAT system and provides deeper insights into this new mammalian family of proton/amino acid cotransporters. The identified family comprises four structural similar murine and human transport proteins (proton/amino acid transporter, PAT1 - 4), all consisting of around 500 amino acid residues with 11 predicted transmembrane spanning domains. Orthologous proteins of this family are found in lower and higher eukaryotes. The murine PATs exhibit a distinct mRNA expression pattern, with PAT1 found *inter alia* in epithelial cells of small intestine and kidney. Moreover, the PAT1 protein is localised in the brush border membrane of murine and human small intestine. After expression in *Xenopus laevis* oocytes PAT1 mediates proton-coupled, electrogenic transport of small and neutral amino acids such as Gly, Ala, and Pro, the corresponding D-isomers and of a variety of amino acid derivatives, e.g. GABA, betaine, and taurine. The apparent affinities for these substrates are in the range of 1 - 10 mM. Beside these physiological substrates PAT1 transports efficiently selected pharmacological compounds. As shown recently, PAT1 resembles in all features the functionally described PAT system in intestinal and renal epithelial cells. The transporter PAT2, expressed in the central nervous system, lung, heart, and brain exhibits similar transport characteristics as PAT1. However, PAT2 is in comparison to PAT1 a high affinity transporter, with 10 to 30-times higher affinities for the identical substrates (app.  $K_m$ -values of 100 - 1000  $\mu$ M) but has in general a narrower substrate spectrum. So far, PAT3 and PAT4 remain orphan transporters with no assigned function. Critical structural elements in aliphatic amino acid substrates of PAT1 and PAT2 were identified *a)* an non-substituted carboxyl-group, *b)* a small size of the amino acid side chain, and *c)* a short spacer distance between the charged amino and carboxyl groups. A free amino group within a substrate is not required. Additionally, short-chain fatty acids were shown to serve as substrates of PAT1 and PAT2. In contrast to amino acids, the short-chain fatty acids are transported in an electroneutral manner. Both transporters seems to bind proton and substrate in an ordered binding mode with the proton binding first. Functional differences in transport characteristics between PAT1 and PAT2 were observed in regard to the proton activation constants, suggesting that PAT2 transports at physiological pH values under proton-saturated conditions, whereas PAT1 can be regulated in transport activity by changes in extracellular pH, i.e. via a cooperation with the  $\text{Na}^+/\text{H}^+$ -exchanger NHE3. This novel family of proton/amino acid symporters takes an exceptional position within mammalian physiology.







# INTRODUCTION

## 1. Preface

From bacteria to humans, amino acids play a fundamental role in a multitude of biological processes such as biosynthesis of proteins, metabolism of hormones and nitrogen, cell growth and cell differentiation as well as neurotransmission. Since the hydrophobic domain of the plasma membrane is not permeable for amino acids, transport of amino acids into and out of cells via specific membrane proteins is essential to life.

At the end of the 1980s Sheikh and co-workers discovered in renal luminal membrane vesicles isolated from pars convoluta of rabbit proximal tubules that an inward directed proton gradient can drive the transport of L-alanine into the vesicles both in the presence and in the absence of sodium ions (Jorgensen KE et al., 1987). This was a novel finding, as the proton gradient serving as a driving force was thought to be restricted to yeast and bacteria, whereas the transmembrane sodium gradient provides mainly the driving force in cells of higher eukaryotes. A proton-driven amino acid transport system was also found to exist in the brush border membrane of the human intestinal cell line Caco-2 (Thwaites DT et al., 1993a). Following investigations into proton-driven amino acid transport processes in the apical membrane of intestinal and renal tubular epithelial cells have demonstrated their existence in different species using classical methods such as flux studies with brush border membrane vesicles (BBMV), cell culture flux studies, *in vitro* perfusion studies or based on intracellular pH measurements. It was convincingly shown that these transporters are secondary active, solely driven by a transmembrane electrochemical proton gradient and confined to small and neutral amino acids such as glycine, alanine and proline and selected amino acid derivatives. The transport system was based on its features designated as **Proton Amino Acid Transport system (system PAT)**. For almost 20 years the underlying protein(s) and gene(s) encoding this transport activity were not known. In 2001 the first two murine cDNAs encoding proton amino acid cotransporters were cloned in our laboratory (Boll M et al., 2002).

This present work has been carried out to characterise the cloned murine transporters as well as the human orthologs on the molecular and functional level. Therefore, molecular biological, electrophysiological and histological methods were used. Specific transport characteristics of the cloned transporters were studied predominantly by using the *X. laevis* oocyte expression system. The putative molecular structures as well as tissue expression patterns and cellular localisation were analysed and, if procurable, potential physiological functions are discussed in the context of PAT-functions and tissue and cellular localisation, respectively.

## 2. Brief history of the discovery of amino acid transport processes

The ability to take up specific substances from the external environment into cells is essential to life. In mammalian species, absorption and reabsorption of nutrients for nutrient homeostasis of the organism takes place in the small intestine and the kidney. At the level of the cell, the plasma membrane segregate intra- and extracellular compartments and cells therefore need the ability for uptake and release of a multitude of compounds. Processes of solute transport into cells and across epithelia have been the subject of intensive research. Initially nutrient transfer from the intestinal lumen into the blood as well as across other epithelia was thought to occur by passive diffusion. However, it is established now that absorption of nutrients is for the most part an active process, involving a variety of specific transport systems that carry sugars, amino acids, peptides, lipids and other substances into the body.

Basic studies of amino acid transport into animal cells go back to the beginning of the twentieth century. In 1913 van Slyke and Meyer were able to show that amino acids can be accumulated against a concentration gradient in specific tissues (van Slyke DD et al., 1913). More detailed descriptions of specific transport processes were provided in the early sixties with the pioneer work in the laboratory of Halvor Christensen (Oxender D et al., 1963). Many following investigations have established that there are more than 20 different transport activities as derived from studies using intact tissues, preparations of cell membranes, like brush border membrane vesicles or proteoliposomes, primary cell cultures and stable cell lines. In this pre-cloning period some seminal concepts regarding amino acid transport were developed. It was shown that amino acids can be taken up against a concentration gradient into epithelial cells by mechanisms using an ion-electrochemical gradient, mainly a  $\text{Na}^+$  gradient, across the apical membrane of the cell (Crane RK, 1965). Additionally, the paradigm has loomed that transport of the different classes of amino acids is mediated by several independent transport systems with broad and overlapping substrate specificities. Transport was shown to be stereoselective, with L-amino acids as preferred substrates. Further characterisation of the underlying mechanisms revealed, that transport can occur besides using the ion gradients in a cotransport mode also in antiport or equilibrative uniport modes (Figure 1). The physiologically identified amino acid transport activities have been subdivided into systems with abbreviations related to their substrate specificity. An immense number of tissues have been investigated for amino acid transport activity. It became evident that some amino acid transport systems are found in almost all tissues, alluding to a housekeeping function, whereas other systems were found to be restricted to specific tissues or cell types, suggesting a specialised function of these transporter systems.

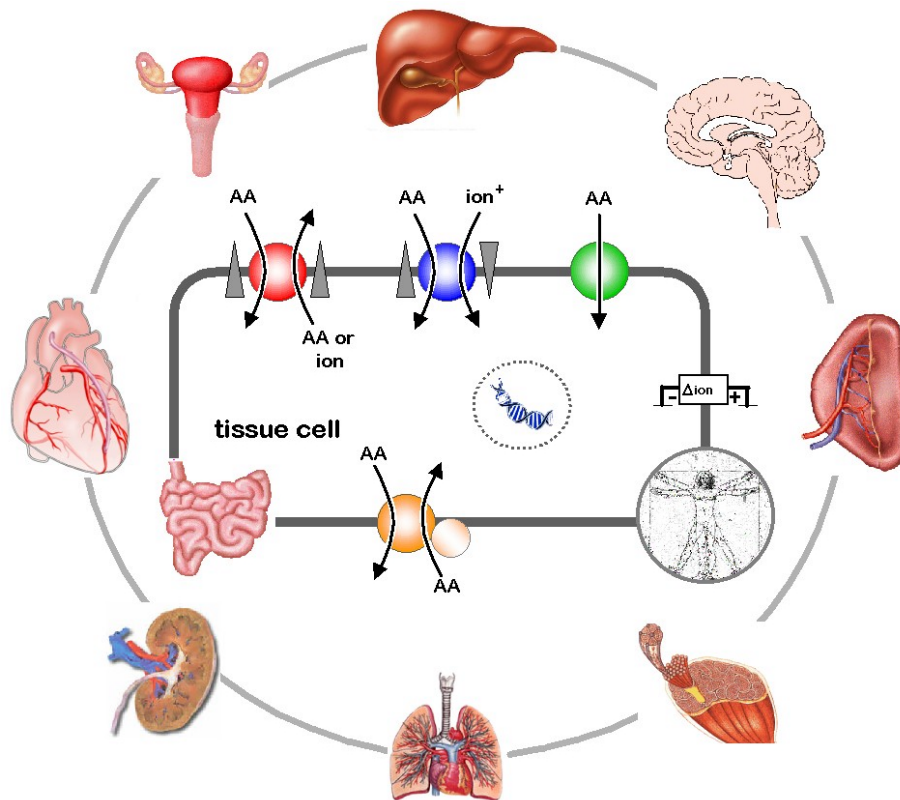


**Figure 1: Utilisation of circulating amino acids in the human organism.** Amino acids (AA) are taken up from the extracellular environment into organs using tissue specific transport systems. Transporters can function either in an antiporter (red), symporter (blue) or equilibrative (green) mode. Efflux of amino acids out of the cell often is mediated by exchangers (orange).

A new era began in 1990 with the identification of the first mammalian amino acid transporter cDNA encoding for a  $\gamma$ -aminobutyric acid (GABA) transporter in human brain (Guastella J et al., 1990), followed by cloning of the first  $\alpha$ -amino acid transport protein, mediating transport of cationic amino acids (Kim JW et al., 1991; Wang H et al., 1991). Subsequently, new molecular biological techniques, oocyte expression systems and homology screening were the starting point for the identification of a wide spectrum of plasma membrane amino acid transporters. Up to now there are more than 30 cDNAs known which encode proteins with different amino acid transport activities. Many of the cloned amino acid transporters exhibit characteristics corresponding to a distinct physiologically identified system. Moreover, the genomic analysis has allowed most mammalian amino acid transporter related gene products to be grouped in 12 solute carrier (SLC) families (Hediger MA, 2004). However, some of the classical transport systems are still missing on the molecular level and, *vice versa*, some cloned transporters could not yet be assigned to a classical transport system. The major amino acid transporting systems of mammalian cells are summarised in Table 1, subdivided into  $\text{Na}^+$ -dependent and  $\text{Na}^+$ -independent pathways for neutral, cationic and anionic amino acids. Representative cDNAs are designated that have been cloned and show the corresponding transport activity to a physiologically identified amino acid transport system, when expressed in a target cell.

classic system	example gene	SLC number designation	superfamily designation	transport type coupling ions	amino acid substrates
<b>sodium dependent systems for neutral amino acids</b>					
A	SNAT1	SLC38A1	ATF	C/ Na <sup>+</sup>	G A S C Q N H M
ASC	ASCT1	SLC1A4	SDS	A/ Na <sup>+</sup>	A S C
B <sup>0</sup>	B <sup>(0)</sup> AT1	SLC6A19	SDS	C/ Na <sup>+</sup>	
BETA	GAT1	SLC6A1	NTS	C/ Na <sup>+</sup> , Cl <sup>-</sup>	GABA
Gly	GlyT2	SLC6A9	NTS	C/ Na <sup>+</sup> , Cl <sup>-</sup>	G
IMINO	---	---	---	C/ Na <sup>+</sup>	P
N	SNAT5	SLC38A5	ATF	C/ Na <sup>+</sup> + E/ H <sup>+</sup>	Q N H S (G A)
PHE	---	---	---	C/ Na <sup>+</sup>	F M
PROT	PROT	SLC6A7	NTS	C/ Na <sup>+</sup> , Cl <sup>-</sup>	P
<b>sodium independent systems for neutral amino acids</b>					
asc	Asc1/4F2hc*	SLC7A10	APC + 4F2hc	preferentially E	G A S C T
PAT	PAT1	SLC36A1	APC	C/ H <sup>+</sup>	G A P GABA
L	LAT1/4F2hc*	SLC7A5	APC + 4F2hc	E	H M L I V F Y W Q
T	TAT1	SLC16A1	Monocarboxylate	F	W, Y, F
<b>sodium dependent systems for anionic amino acids</b>					
X <sup>C</sup>	xCT/4F2hc*	SLC7A11	APC + 4F2hc	E	cystine
<b>sodium independent systems for anionic amino acids</b>					
X <sup>AG</sup>	EAAT1	SLC1A3	SDS	C/ Na <sup>+</sup> , H <sup>+</sup> , K <sup>+</sup>	E D
<b>sodium dependent systems for cationic amino acids</b>					
B <sup>0,+</sup>	ATB(0,+)	SLC6A14	NTS	C/ Na <sup>+</sup> , Cl <sup>-</sup>	K R A S C T N Q H
<b>sodium independent systems for cationic amino acids</b>					
b <sup>0+</sup>	b(0,+)/AT/rBAT	SLC7A9	APC + rBAT	E	K R A S C T N Q H
y <sup>+</sup>	Cat-1	SLC7A1	APC	E (F)	R K H
y <sup>+</sup> L	y+LAT1/4F2hc*	SLC7A7	APC + 4F2hc	E	K R Q H M L

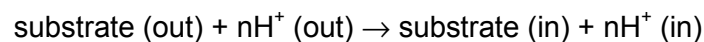
**Table 1: Mammalian amino acid transporters, designations, mechanisms and substrate specificities.** Genes coding for a definite transport activity are shown. Systems are classified in the solute carrier (SLC) series ([www.bioparadigms.org/slc/menu.asp](http://www.bioparadigms.org/slc/menu.asp)) according to the HUGO Nomenclature Committee database ([www.gene.ucl.ac.uk/hugo](http://www.gene.ucl.ac.uk/hugo)). Additionally, according to protein sequence homology they are designated to five superfamilies: Amino acid-polyamine-choline transporter family (APC), sodium dicarboxylate symporter superfamily (SDS), neurotransmitter superfamily (NTS), amino acid transporter superfamily 1 (ATF1), amino acid transporters within the major facilitator superfamily (MFS). Transporter type: cotransporter (C), facilitated transporter (F), exchanger (E), antiporter (A). \*Heterodimeric transporter, for transport activity association with the glycoprotein rBAT or 4F2hc is essential. Amino acid transporters have been extensively reviewed, information presented in the table was mainly taken from Hyde et al. (2003), and was completed referring to the literature by Malandro and Kilberg (1996), Palacin et al. (1998), Wipf et al. (2000), and Saier (2000).



Individual members of the AAAP family are exclusively found in eukaryotes, 15 AAAP paralogous are found in *Saccharomyces cerevisiae*, more than 40 in *Arabidopsis thaliana*, 11 in *Caenorabditis elegans* and annotation of the public human genome database reveals currently 15 AAAP members in *Homo sapiens*. In contrast, AAAP members can not be found in any bacterial genome (<http://66.93.129.133/transporter/wb/index2.html>).

The AAAP members exhibit minimal sequence conservation ( $\leq 25\%$  sequence identity) within the family in spite of the fact that all of its members are derived from eukaryotes. The proteins differ in length between 400 and 710 amino acid residues, but most of them consist of 400 to 500 residues. Nevertheless, AAAP members feature beside functional similarities also structural similarities and secondary structure models have been shown to possess conserved regions. All AAAP proteins exhibit very similar hydropathy profiles leading to proposed membrane topology models with 11, sometimes 10, putative transmembrane  $\alpha$ -helical domains (TMD) (Young GB et al., 1999; Saier MHJ, 2000). One homologue, NAT2/AAP1 of *Arabidopsis thaliana* was proofed to possess 11 TMDs (Chang HC et al., 1997).

Cloned AAAP transporters from *Arabidopsis thaliana*, when expressed in yeast or oocytes, were found to operate as sodium-independent, proton-coupled symporters for a wide spectrum of amino acids (Fischer WN et al., 2002). The generalised transport reaction catalysed by non-mammalian proteins of the AAAP family can be described as follows:



Mammalian organisms also express transport proteins belonging to the AAAP family. However, the mammalian members do not display this strict proton symport coupling. Most animal transporters usually couple amino acid uptake to a  $\text{Na}^+$  gradient, but the mammalian AAAP members show at least a  $\text{H}^+$  sensitivity,  $\text{H}^+$  exchange activity or even a  $\text{H}^+$  cotransport mode. The mammalian AAAP proteins exhibit weak but significant similarities to the plant and lower eukaryotic AAAP transporters. By means of their protein sequence data they are clustered into three subgroups, the VGAT (vesicular GABA transporter) transporter category (also known as VIAAT = vesicular inhibitory amino acid transporter, SLC32A1), transporters belonging to the system A and N category and the LYAAT (lysosomal amino acid transporter) group (Sagne C et al., 2001), the latter has been renamed to PAT group (Boll M et al., 2004).

The first identified mammalian member of the AAAP family was the VGAT/VIAAT transporter (SLC32A1). This protein is responsible for packaging of the inhibitory neurotransmitters GABA and glycine into neuronal synaptic vesicles (McIntire SL et al., 1997). The driving force for this transport is the proton gradient between the intravesicular space and the cytoplasm.

The proton gradient is generated by a vesicular  $H^+$  ATPase which leads to an intravesicular acidification (Sagne C et al., 1997). VGAT/VIAAT functions in an antiport mode, allowing the accumulation of GABA and glycine by utilisation of the outwardly directed proton gradient. (McIntire SL et al., 1997). Figure 3 describes schematically the function of VGAT/VIAAT. The VGAT branch comprises a single member with mammalian paralogues found in human, rat and mouse (Gasnier B, 2004).

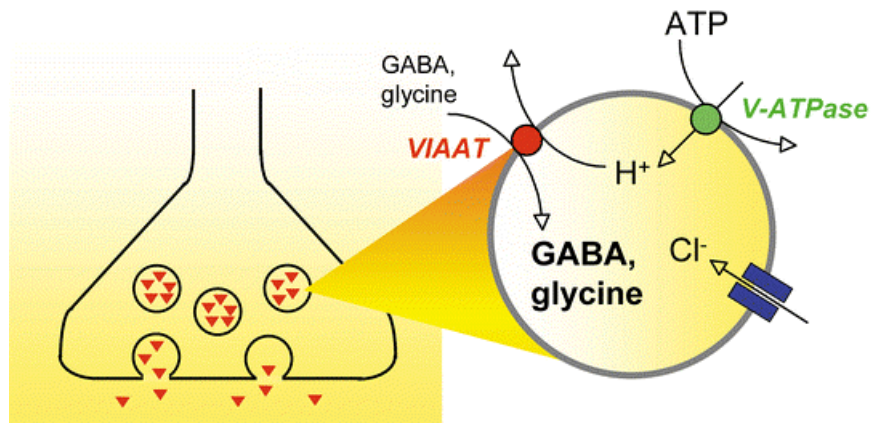


**Figure 3: Schematic diagram of function of VGAT/VIAAT in the loading of inhibitory amino acids into synaptic vesicle.** (taken from Gasnier 2004, Pflügers Archiv) Secretory vesicles are charged positively and acidified by an electrogenic  $H^+$  ATPase and by a chloride channel which provides an electrical shunt for efficient proton pumping. VGAT/VIAAT exchanges vesicular protons for cytosolic GABA or glycine, thus allowing their secretion from nerve terminals

The second mammalian AAAP subfamily is composed of the amino acid transporters belonging to the system A and system N transporter class (SLC38 transporter family, particulars in Introduction, Section 5.2). Although the system N and system A transporters share high protein sequence similarities, they exhibit differences in terms of their substrate specificity and functional properties (Mackenzie B et al., 2004). Transporters of the system A subtype are expressed ubiquitously, mediate uptake of small, aliphatic amino acids with alanine as a favored substrate and are considered to be the major provider of these amino acids in most cell types. System A carriers act as rheogenic  $Na^+$ /substrate symporters. They possess a proton sensing site, sensitive to low pH, resulting in a decline of transport activity (Mackenzie B et al., 2004). In contrast, system N transporters couple the  $Na^+$ /amino acid symport to the exchange of one proton, this would predict an electroneutral transport mode. In fact the transport is electrogenic, but this is due to an uncoupled ion conductance observed after expression in *Xenopus laevis* oocytes (Chaudhry FA et al., 2001). They exhibit a more restricted substrate profile than system A transporters, with glutamine as a preferred substrate. System N transporters mediate glutamine flux from astrocytes to neurons in the central nervous system, where glutamine serves as precursor of the excitatory neurotransmitter glutamate (Mackenzie B et al., 2004).

The third mammalian AAAP subfamily has recently been identified with the cloning of the first mammalian amino transporter which acts, like the non-mammalian AAAP members, in a proton/substrate symport mode. This transporter was cloned *in silico* by data base search for mammalian homologs of the VGAT/VIAAT transporter (Sagne C et al., 2001). After transfection in COS-7 cells (fibroblast-like cells growing as monolayers), this transporter mediated uptake of small and neutral amino acids such as alanine and proline as well as the neurotransmitter GABA. Uptake rates were sodium-independent but increased by lowering extracellular pH, suggesting a proton/amino acid symport mode. Immunohistochemical studies with a specific antibody and colocalisation with marker-protein antibodies revealed that this transporter is expressed in glutamatergic and GABAergic neurons. The authors were able to show that this protein is mainly found in these neurons in the lysosomal membrane and therefore this transporter was named **LYsosomal Amino Acid Transporter-1** (LYAAT-1). The proposed transport mechanism of rLYAAT-1 is outlined in Figure 4.

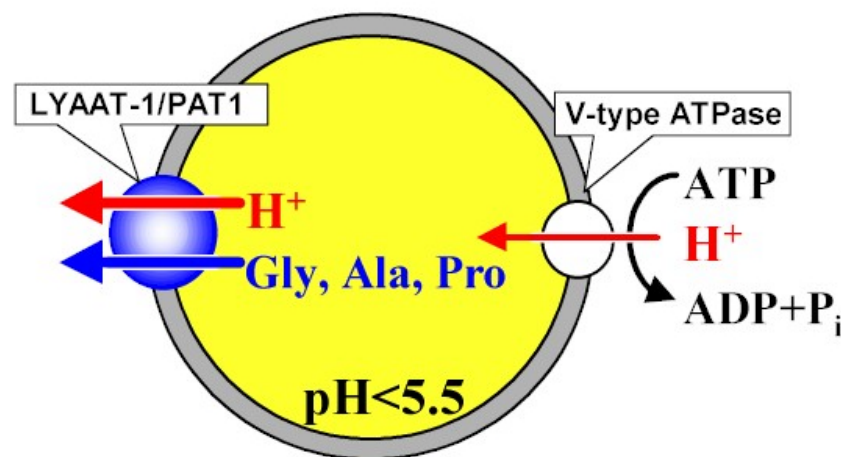


**Figure 4: Schematic diagram of the role of LYAAT-1 in efflux of amino acids from lysosomes.** (Boll et al. 2004, Pflügers Archiv) The lysosomal amino acid transporter-1 (LYAAT1) transporter functions in brain neurons as an export system of small amino acids from lysosomes.

With experimental work summarised here it was demonstrated that the cloned transporter PAT1 from mouse small intestine represents the murine orthologue of the rat LYAAT-1 transporter and that the other identified PAT transporters (PAT2 - 4) build together with the rLYAAT1 transporter the third mammalian subbranch of the AAAP-family.

#### **4. Physiological importance of small, neutral amino acids and their derivatives serving as substrates of the PAT-carriers**

Prokaryotes and eukaryotes require a set of 20 proteinogenic amino acids for synthesis of small peptides and large proteins that may consist of more than 1000 amino acid residues. Next to the utilisation for protein biosynthesis various proteinogenic amino acids and certainly a variety of non-proteinogenic amino acid derivatives possess specified functions in various biological processes. In this section a brief overview is provided on the role of individual amino acids and amino acid derivatives identified as PAT substrates.

##### **4.1 Glycine**

Glycine, a non-essential amino acid, is one of the most interesting amino acids. It plays a role in protein primary structure as it serves as a flexible link in proteins by its small size and allows the formation of  $\alpha$ -helices and  $\beta$ -turns. In addition to its role in peptide and protein structure, glycine serves as an extracellular signalling molecule, as a modifier of molecular activity via conjugation or by glycine-extensions of hormone precursors, and as an osmoprotectant. Best examined is its role as an inhibitory neurotransmitter, however, glycine is also involved in the excitatory neurotransmission (Lopez-Corcuera B et al., 2001; Legendre P, 2001). Glycine-mediated inhibitory neurotransmission is essential in reflex reactions, in the locomotor behaviour and in transmission of sensory signals. Glycine plays also an inhibitory or modulatory role in nerve fibres of the spinal cord and brain stem as well as in several other areas of the central nervous system (Lopez-Corcuera B et al., 2001; Legendre P, 2001). The inhibitory effects of glycine are mediated via ligand-gated chloride channel receptors (heteromeric or homomeric GlyR receptors), whereas the excitatory effects are mediated via binding at glutamate receptors of the excitatory NMDA (N-methyl-D-aspartate) subtype. Activation of the NMDA glutamate receptor requires beside binding of glutamate also glycine binding (Legendre P, 2001; Klein RC et al., 2001; Breitingner HG et al., 2002). Recently a novel NMDA subtype of the glutamate receptor was demonstrated to be solely activated by glycine (Chatterton JE et al., 2002). In addition, glycine is involved in the biosynthesis of creatine, porphyrin and purine. Glycine is conjugated with bile acids and used in liver, beside other substrates, for conjugation with xenobiotics and biliary elimination (Wheeler MD et al., 1999). Glycine is also a component of the antioxidant peptide glutathione.

##### **4.2 Alanine**

Alanine is an amino acid which links glucose, tricarboxylic acid cycle and amino acid metabolism via its reaction with  $\alpha$ -ketoglutarate to form pyruvate and glutamate, a process catalysed by the alanine aminotransferase. In the glucose-alanine-cycle alanine acts as the

primary glucogenic amino acid. At lower blood glucose levels alanine is released from peripheral tissues, basically from muscle cells, and is extracted by the liver and used in gluconeogenesis. Subsequently, *de novo* synthesised glucose is released from the liver into the blood and serves as energy substrate in peripheral tissues (Felig P, 1973; Palmer TN et al., 1985). In addition, alanine seems to play a role as a metabolic fuel in GABAergic neurons. Here, alanine supplies an amino group for the conversion of  $\alpha$ -ketoglutarate from the tricarboxylic acid cycle to glutamate which is utilised for GABA synthesis. The carbon skeleton of alanine (pyruvate) is converted to acetyl CoA which is metabolised in the tricarboxylic acid cycle (Schousboe A et al., 2003).

#### 4.3 Proline

Proline is formally not an amino acid, but an imino acid. It is an important building block in proteins but no additional particular physiological function has been described. Proline is a major amino acid in collagen proteins. It is hydroxylated in the protein complex and lacks a hydrogen on the  $\alpha$ -amino group, so it cannot donate a hydrogen bond to stabilise an  $\alpha$ -helix or a  $\beta$ -sheet leading to a kink in the peptide chain. Therefore, proline is responsible for the spacial constitution of the collagen fibres. Proline is often found at the end of  $\alpha$ -helices or in turns or loops. Unlike other amino acids which exist almost exclusively in the trans-form in polypeptides, proline exists also in the cis-configuration in peptides. The cis and trans forms are nearly isoenergetic. The cis/trans isomerisation can play an important role in the folding of proteins and turns proline containing peptide bonds into structures with a degree of high resistance to almost all mammalian proteolytic enzymes (Vanhoof G et al., 1995).

Since glycine, alanine and proline are found in plasma at much lower levels than inside mammalian cells (Divino-Filho JC et al., 1997), active transport systems in the cells, able to transport the amino acids against a concentration gradient into the cell, are required.

#### 4.4 Amino acid derivatives and D-amino acids

GABA is the most important inhibitory neurotransmitter in the central nervous system. GABA is converted from glutamate by the action of glutamate decarboxylase. Like glycine, the GABAergic effects are mediated via ligand-gated chloride channel receptors (GABA<sub>A</sub> receptors) or via G protein-coupled receptors (GABA<sub>B</sub> receptors) (Wong CG et al., 2003). GABA mediates the majority of inhibitory signals in the brain, and perturbations in GABAergic inhibition can result in seizures. This seems to be the case in epilepsy and a targeting of GABAergic neurotransmission is used in therapy. However, psychiatric diseases such as schizophrenia and spasticity have also been related to disorders of GABAergic function in the brain (Wong CG et al., 2003). Beside its function in the central nervous system, GABA also was shown to function as a neurotransmitter in pancreas and in the gastrointestinal tract (Nichols K et al., 1995; Sha L et al., 2001).

Betaine and taurine are besides myo-inositol and sorbitol the key organic osmolytes for cell volume regulation. In muscle cells they are found in high intracellular concentrations (Lang F et al., 1998). For maintaining cell volume, betaine and taurine are either transported into the shrunken cells or are rapidly released during cell swelling. Efflux of betaine and taurine is acutely regulated by a specific channel protein, permeable for organic osmolytes (Lang F et al., 1998). Betaine was also proposed to serve as an important methylating agent when normal methylating pathways are impaired, e.g. by ethanol consumption or certain drugs. It has been shown that betaine is able to remethylate homocysteine and remove S-adenosylhomocysteine, and for that overcomes the harmful effects of ethanol consumption on methionine metabolism. It may therefore be effective in correcting methylation defects and in treating liver diseases. Betaine may also have therapeutic applications under conditions of impaired folate, vitamin B12 or methionine metabolism (Barak AJ et al., 2003).

Taurine is mainly used in the liver for the formation of hydrophilic conjugates in the phase 2 reaction of biotransformation of apolar, lipophilic and consequently poorly excretable compounds, e.g. bile acids and xenobiotics.

D-amino acids have so far not been considered to be important in human physiology. New findings however suggest that at least D-serine may play a role in human brain. A mammalian enzyme, designated as serine racemase, converting L-serine into D-serine has been cloned from mammalian glia cells (Wolosker H et al., 1999). D-serine is found in the mammalian forebrain, striatum and cortex. Levels of D-serine in these regions of the mammalian brain are approximately one third of those of the L-isomer. (Hashimoto A et al., 1993; Schell MJ et al., 1995; Hashimoto A et al., 1995). Up to now a specific receptor for D-serine have not been found, but in fact D-serine was shown to be a selective and potent agonist at the glycine binding site of the NMDA receptor. D-serine seems to be a normal stimulus for the glycine site of this receptor with a potency in activation similar to glycine (Kemp JA et al., 1993).

## 5. Transport-systems for small, neutral amino acids and amino acid derivatives

A multitude of different transport systems for small, aliphatic amino acids and amino acid derivatives have been described and distinguished from each other based on their substrate specificity. In the last ten years many of them have been cloned and characterised on the molecular level. The most important systems transporting with a specificity for small and neutral amino acids and their derivatives are introduced here briefly with respect to molecular architecture and functional features.

### 5.1 Glycine transporting systems

Early investigations identified two glycine transporters in rat brain synaptosomal vesicles which were strictly dependent on  $\text{Na}^+$  and  $\text{Cl}^-$  and that differed in their sensitivity to sarcosine (N-methyl-glycine) and in kinetic properties (Mayor FJ et al., 1981). These observations were confirmed by the cloning of two  $\text{Na}^+$ - and  $\text{Cl}^-$ -dependent glycine transporters from rat brain, designated as GlyT1 (SLC6A9) and GlyT2 (SLC6A5) (Guastella J et al., 1992). GlyT1 and GlyT2 are predominantly expressed in glycinergic neurons of the mammalian brain and spinal cord, and are responsible for re-uptake of glycine from the synaptic cleft (Lopez-Corcuera B et al., 2001; Legendre P, 2001). These transporters exhibit a narrow substrate specificity, transporting only glycine and its derivatives (Lopez-Corcuera B et al., 2001). It was shown that the human GlyT1 transcript is alternatively spliced. Three N-terminal exons and two C-terminal exons exist, which can be combined in multiple ways. Predominantly found are the isoforms GlyT1a-f (Guastella J et al., 1992; Smith KE et al., 1992a; Kim KM et al., 1994; Hanley JG et al., 2000). GlyT1a is the only isoform which is functionally expressed in extraneuronal tissues, with a restricted localisation to the basolateral side of human enterocytes (Christie GR et al., 2001). Due to the limited expression of the GlyT transporters, it can be assumed that these proteins are not responsible for the intestinal absorption and renal reabsorption of glycine or the interorgan flux of glycine between different tissues.

However, different studies suggested that beyond the nervous system specific transporters for glycine, both  $\text{Na}^+$ -dependent,  $\text{Na}^+$ - and  $\text{Cl}^-$ -dependent as well as  $\text{H}^+$ -dependent, may exist in the plasma membrane of various cell types (Rajendran VM et al., 1987). In addition, glycine was shown to be transported as well by transporters of the system A family, although their preferred substrate is alanine.

### 5.2 Alanine transporting systems

Plasma membrane transport of alanine is mediated by various transport proteins. Exchange between tissues is mainly mediated by the system A transporters SNAT1, SNAT2 and SNAT4 (revised nomenclature, **s**odium-coupled **n**eutral **a**mino acid **t**ransporter, see Mackenzie B and Erickson JD, 2004) and by the system ASC transporters. Additionally,

system L and system y<sup>+</sup>L are participating in alanine homeostasis (Palacin M et al., 1998). Moreover, the system B<sup>0</sup> appears to be involved in the absorption of alanine in the small intestine (Kekuda R et al., 1996; Kekuda R et al., 1997).

The transporters of the SNAT family, system ASC and L transporters are present in almost all cell types (Palacin M et al., 1998). SNATs couple amino acid transport to the Na<sup>+</sup> electrochemical potential gradient with a 1:1 flux coupling stoichiometry. They are sensitive to low pH, highest transport activities are observed at a slightly basic pH. Alanine transport by SNATs was shown to be inhibited by the amino acid derivative 2-methylaminoisobutyric acid (MeAIB) which was regarded as routing substrate for these transporters (Reimer RJ et al., 2000). However, the selectivity for MeAIB is often not “clear cut” different from that for alanine and MeAIB is as well accepted by other transporters as well (such as the PAT1 transporter) (Mackenzie B et al., 2003). SNAT2 (previously referred to as ATA2, SA1 and SAT2) was found in almost all tissues examined by northern blot analysis (Hatanaka T et al., 2000). SNAT2 prefers alanine, serine, cysteine, glutamine, asparagine and also proline as substrates, with apparent affinities in the range of 0.25 mM to 1 mM (Hatanaka T et al., 2000). SNAT1 is predominantly expressed in brain, but significant expression is also observed in the retina, placenta and heart, whereas SNAT4 is mainly found in the liver (Hatanaka T et al., 2001). SNAT transport activity is highly regulated in many cell types. This includes an up-regulation during cell-cycle progression and cell growth in many cells and tissues as well as hormonal control by insulin, glucagon, catecholamines, glucocorticoids, various growth factors and mitogens by quite different signalling pathways (McGivan JD et al., 1994).

The system ASC transporters ASCT1 (SLC1A4, also known as SATT) and ASCT2 (SLC1A5, also known as AAAT or hATB0) were first cloned from human brain and mouse testis (Shafqat S et al., 1993; Arriza JL et al., 1993; Utsunomiya-Tate N et al., 1996) and are expressed in a wide variety of tissues. They transport alanine and additionally serine, threonine and cysteine in a sodium-dependent manner. Transport is insensitive to pH and occurs only in exchange with intracellular amino acids associated with movement of one or two sodium ions in both directions in an electroneutral manner (Zerangue N et al., 1996). Under some circumstances binding and transport of substrate induces inward currents, but this is due to a substrate-gated anion conductance and not by the cotransport of ions (Broer A et al., 2000). ASCT1 possibly works in part as a concentrative transporter for alanine as shown in ASCT1 expressing *Xenopus* oocytes (Pinilla J et al., 2001). In the presence of sodium an accumulation of alanine in the oocyte is observed which is sodium-dependent but not coupled to the sodium gradient. Since the authors did not measure the efflux of preloaded alanine from the oocyte and it is well known that *Xenopus laevis* oocytes have a high intracellular amino acid pool (Taylor PM et al., 1996) the data do not allow to distinguish

whether accumulation of alanine occurs in a concentrative manner or by exchange, even though the kinetic data argue for an active transport. The ASCT2 transporter (also known as ATB<sup>0</sup>) has a broader substrate specificity and is thought to be responsible for the bulk of intestinal absorption and renal reabsorption of zwitterionic amino acids (Palacin M et al., 1998). Here it needs to be mentioned that in addition to amino acid transporters, the di- and tripeptide transporters PEPT1 and PEPT2 are also involved in the homeostasis of amino acid nitrogen in the organism. Whether amino acid or peptide transporters are the major player in supplying the body with amino acid nitrogen is currently not known, but it is believed that the peptide transporters are more important (Leibach FH et al., 1996).

The widely expressed heterodimeric system L transporters LAT1, LAT2, y<sup>+</sup>LAT2 and y<sup>+</sup>LAT1 (SLC7A5 - 8) mediate the efflux of alanine from the cell in a sodium-independent manner. They are composed of a catalytic subunit (the light chain) associated via a disulphide bridge with the glycoprotein 4F2hc (the heavy chain). These proteins are obligatory exchangers, they mediate uptake of large branched and aromatic amino acids coupled to the efflux of another amino acid with a 1:1 stoichiometry. Alanine serves as an exchange substrate for these transporters and the function of these transporters is coupled to the existence of transport proteins providing high intracellular concentrations of the exchange substrates, like alanine. In contrast, amino acids with small, non-branched side chains are poor substrates for the system L transporters for uptake into cells. The LAT transporters are mainly expressed at the basolateral side of cells and therefore appear to be involved in transepithelial transport of alanine (Verrey F, 2003).

### 5.3 Proline transporting systems

Transporters mediating specifically transmembrane flux of proline are hitherto not identified at their molecular level with the exception of a brain-specific transporter. Proline is transported to a minor degree by amino acid transport systems for neutral amino acids, such as the system A transporter SNAT2 (Takanaga H et al., 2002) and the system ASC transporters (Barker GA et al., 1999; Pinilla-Tenas J et al., 2003; Yamamoto T et al., 2003). On the other hand, in brain an exclusive proline transport system (system PROT) has been described on functional and molecular level. PROT was first cloned by RT-PCR from rat brain (Fremeau RTJ et al., 1992) and subsequently from human brain (Shafqat S et al., 1995). PROT is exclusively found in brain and here mainly in glutamatergic terminals in the hippocampus, cortex and other forebrain regions (Velaz-Faircloth M et al., 1995; Crump FT et al., 1999; Renick SE et al., 1999). It was shown that the bulk of PROT colocalises with intracellular synaptic vesicles (Renick SE et al., 1999). This transporter binds proline with high-affinity ( $K_m = 10 \mu\text{M}$ ) and transports in a sodium- and chloride-dependent manner (Fremeau RTJ et al., 1992). It is proposed that PROT plays a role in regulating excitatory

synaptic transmission, given that proline enhances glutamatergic signalling in hippocampus (Shafqat S et al., 1995).

On the functional level a proline transport system was identified in epithelial cells of small intestine and kidney of different mammalian species and has been defined as a sodium-dependent transporter of both, aliphatic and cyclic imino acids and for that was designated as system IMINO (Davies S et al., 1987). Beside L- proline substrates of these transport system are hydroxyproline, N-methylated glycines and MeAIB (methyl-amino-isobutyric acid) (Wright EM et al., 1984; Stevens BR et al., 1985; Vilella S et al., 1989; Munck LK et al., 1992). Until now, the IMINO system could not identified on the molecular or genetic level, respectively.

#### **5.4 Transport systems for GABA, betaine, taurine and D-amino acids**

Specialised  $\beta$ - and  $\gamma$ -amino acid transporting systems are responsible for influx and efflux of the amino acid derivatives GABA, betaine and taurine. Molecular cloning studies have revealed the existence of three high-affinity subtypes of GABA transporters (GATs) in the rat and human brain: GAT1 (SLC6A1), GAT2 (SLC6A13), and GAT3 (SLC6A11) (Guastella J et al., 1990; Borden LA et al., 1992). GAT1 and GAT3 are exclusively expressed in the central nervous system, whereas GAT2 is also present in peripheral tissues, mainly in liver and kidney (Lopez-Corcuera B et al., 1992; Liu M et al., 1999). In brain, the GATs are expressed in neurons as well as in glia cells and are responsible for the re-uptake of GABA from the synaptic cleft. The GATs are operating in a sodium- and chloride-dependent manner (Chen NH et al., 2004). Alongside the GATs, GABA is also transported by BGT-1 (Betaine/GABA Transporter 1, SLC6A12) in addition to betaine. BGT-1 is predominantly expressed in brain and kidney. This protein seems to be involved in cell volume regulation (Bitoun M et al., 2000). Similarly, a high affinity taurine transporter TAUT (SLC6A6) was cloned from rat brain and subsequently from human placenta. The protein is found in brain, retina, liver and kidney (Smith KE et al., 1992b; Ramamoorthy S et al., 1994). Expression of TAUT was shown to be induced by hypertonicity and by high levels of taurine, suggesting a role of the transporter in regulation of osmotic balance (Takeuchi K et al., 2000; Cammarata PR et al., 2002).

To date, all the identified and cloned amino acid transporters are highly stereoselective systems, accepting, if at all, D-amino acids only with poor affinity and low transport rates. The sole exception is the Asc-1 protein (SLC7A10) cloned from human brain (Nakauchi J et al., 2000). This transporter can bind D-serine with high affinity ( $K_m = 30 \mu\text{M}$ ) and might transport physiologically D-serine in brain in a sodium-independent manner, typical for the system ASC (Nakauchi J et al., 2000).

Despite the fact that a huge number of amino acid transporter cDNAs has been identified and subsequently characterised, some transporters are still missing on the molecular level.

Although their transport characteristics are well described on functional levels for intestinal and renal transport of betaine and taurine in different cell systems, this(these) transporter(s) has (have) not been cloned yet. Moreover, there is strong evidence for a transport system existing in the apical membrane of enterocytes and renal epithelial cells that couples transport of small amino acids and their derivatives to proton movement instead of sodium cotransport. This transport activity was named system PAT (Thwaites DT et al., 1995b). In the following sections the system PAT is described in detail.

## 6. System PAT: Mammalian Proton-coupled Amino Acid Transport

In prokaryotes proton coupled transport systems for various nutrients are well described and have been characterised in detail. Phenomenological similar systems were not anticipated to exist in eukaryotes or even mammals. However, the ability of a proton electrochemical gradient to energise the net uptake of solutes for example across the brush border membrane of mammalian epithelial cells was shown first for the di- and tripeptide transporters PEPT1 and PEPT2. In 1983 Ganapathy and Leibach demonstrated that transport of the dipeptide glycyl-proline across the brush border membrane of small intestinal cells is stimulated by an cell-inward directed proton gradient (Ganapathy V et al., 1983). This pH dependency was also shown for the renal peptide transporters (Ganapathy V et al., 1982a and b; Ganapathy V et al., 1983). Flux coupling experiments revealed later that the peptide transporters indeed act as substrate/proton symporters and independent from sodium or chloride gradients (Kottra G et al., 2002). Beside the PEPTs, only the sugar transporter SGLT1 (sodium/glucose transporter 1) was shown to act in a proton symport mode under sodium-free conditions. Although, naturally driven by a sodium gradient, sodium can be replaced by protons in SGLT1 resulting in transport rates of about 30% of the Na<sup>+</sup>/glucose rates (Wright EM et al., 1994). The identification of other solute transporters linked to a proton rather than to a sodium-electrochemical gradient has received little attention.

Particularly the studies by Thwaites et al. (Thwaites DT et al., 1993a; Thwaites DT et al., 1993b; Thwaites DT et al., 1994; Thwaites DT et al., 1995a; Thwaites DT et al., 1995b; Thwaites DT et al., 1995c; Thwaites DT et al., 1999a; Thwaites DT et al., 1999b; Thwaites DT et al., 2000) and of the laboratory around Sheikh (Roigaard-Petersen H et al., 1984; Roigaard-Petersen H et al., 1987; Jorgensen KE et al., 1987; Jessen H et al., 1988a; Jessen H et al., 1988b; Roigaard-Petersen H et al., 1988; Roigaard-Petersen H et al., 1989; Jessen H et al., 1989; Roigaard-Petersen H et al., 1990; Jessen H et al., 1991a; Jessen H et al., 1991b; Jessen H et al., 1991c; Jessen H et al., 1992) provided evidence for the existence of a proton-driven amino acid transporter PAT in the apical membrane of mammalian intestinal and renal epithelial cells. This functional studies were carried out mainly in the human cancer cell line Caco-2, which exhibits after differentiation typical characteristics of enterocytes. BBMVs prepared from renal and intestinal epithelial cells were also employed.

Jorgensen and Sheikh were the first to demonstrate that transport of L-alanine into vesicles from kidney whole cortex is mediated by both Na<sup>+</sup>-dependent and Na<sup>+</sup>-independent but electrogenic, processes, indicating the presence of an active, Na<sup>+</sup>-independent transporter in these vesicles (Jorgensen KE et al., 1987). By preparing BBMVs either from *pars convoluta* or *pars recta* it became clear that the Na<sup>+</sup>-unspecific transport system for L-alanine was

exclusively localised to the *pars convoluta*. A closer examination of the mechanism of transport of L-alanine in vesicles from *pars convoluta* revealed that an  $H^+$  gradient ( $pH_{out} > pH_{in}$ ) could drive the transport of L-alanine into the vesicles in the absence of sodium (Jorgensen KE et al., 1987). Using Caco-2 cells, L-proline was shown to be transported under  $Na^+$ -free conditions in a pH dependent manner across intact intestinal cell monolayers. That proline transport was associated with transport of  $H^+$  across the apical membrane was revealed by a simultaneously decline of intracellular pH, measured with the pH-sensitive fluorescent dye BCECF (2',7'-bis(2-carboxyethyl)-5(6)-carboxyfluorescein). Moreover, the authors were also able to demonstrate that the pH-dependent L-proline transport is electrogenic by measuring short circuit currents (Thwaites DT et al., 1993b). Further studies proved that the driving force for this transport in human intestinal and rabbit renal cells is a cell inwardly directed pH gradient and that amino acid influx is coupled to an intracellular acidification. The proton gradient is generated in the intestine and renal epithelial cells by the activity of the  $Na^+/H^+$  exchanger 3 (NHE3), which in turn is coupled to the  $Na^+$  gradient generated by a  $Na^+/K^+$  ATPase (Figure 5).

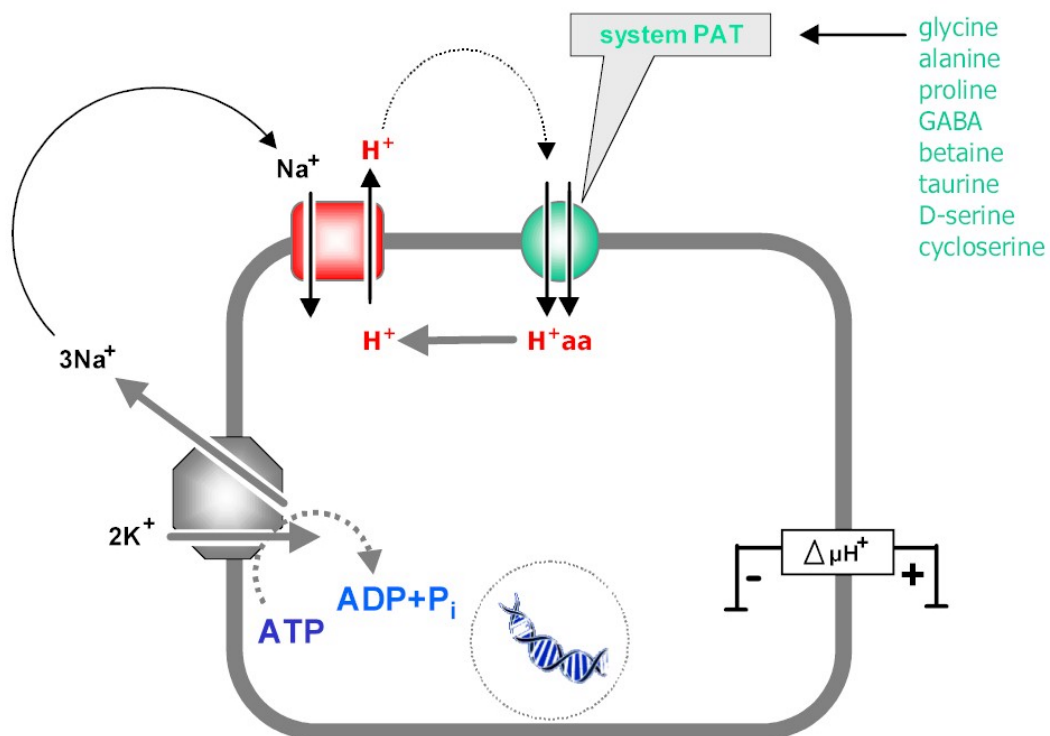


**Figure 5: Proposed transport mode of the PAT activity found in the apical membrane of small intestinal and renal epithelial cells.**

The system PAT was found to transport only the small and neutral amino acids glycine, alanine, proline and to some extent serine (Roigaard-Petersen H et al., 1987; Jorgensen KE et al., 1987; Jessen H et al., 1988b; Roigaard-Petersen H et al., 1988; Kapoor M et al., 1988a; Kapoor M et al., 1988b; Roigaard-Petersen H et al., 1990; Nicklin PL et al., 1992; Thwaites DT et al., 1993b; Thwaites DT et al., 1994; Thwaites DT et al., 1995bb; Jessen H et al., 1996; Thwaites DT et al., 1999).

Although system PAT appeared to be very restrictive regarding the amino acid side chain, it was also shown that derivatives of these small and neutral amino acids were accepted as substrates as well. In intestinal as well as renal epithelial cells from human, rabbit and rat it was demonstrated that in addition to glycine, alanine and proline also hydroxyproline,  $\beta$ -alanine, sarcosine, betaine, taurine, MeAIB and GABA were taken up into cells in a symport mode with protons (Jessen H et al., 1988a; Roigaard-Petersen H et al., 1989; Jessen H et al., 1989; Ranaldi G et al., 1994; Thwaites DT et al., 1995b; Thwaites DT et al., 1995c; Thwaites DT et al., 1999). Selected D-amino acids such as D-alanine, D-proline, D-cycloserine were shown to interact with the substrate binding site of this transport system by competitive inhibition (Jessen H et al., 1988a; Roigaard-Petersen H et al., 1989; Ranaldi G et al., 1994; Thwaites DT et al., 1995b; Thwaites DT et al., 1995c). Another characteristic of the system PAT is that both glycine and the imino acids proline and hydroxyproline are transported by the same carrier (Roigaard-Petersen H et al., 1984; Thwaites DT et al., 1995b). The affinities of these amino acids and derivatives to system PAT in Caco-2 cells are similar to the affinities described in renal brush border membrane vesicles and are in the range of 2 - 10 mM (Tab. 2).

substrate	in vitro $K_m$ values (mM)	
	Caco-2	renal BBMV
glycine	5.3 $\pm$ 0.4	3.9
L-alanine	5.7 $\pm$ 0.7	4.4
L-proline	9.2 $\pm$ 0.9	4.5
L-serine	+	3.7
GABA	1.95 $\pm$ 0.78	not tested
$\beta$ -alanine	8.1 $\pm$ 1.1	4.0
hydroxy-L-proline	+	7.0
taurine	+	2.9
D-alanine	+	7.9 $\pm$ 0.4
D-proline	+	3.9
hydroxy-D-proline	not tested	9.7
D-cycloserine	15.8 $\pm$ 2.0	not tested

**Table 2: Apparent affinities of system PAT substrates.**  $K_m$  values are taken from the literature on  $\text{Na}^+$ -independent, proton-driven transport activity, as found in the apical membranes of Caco-2 cells and in renal brush border membrane vesicles (BBMV) from pars convoluta. +, no  $K_m$  values were determined but compounds showed first order inhibition kinetics for uptake of a PAT substrate.

In spite of the strong evidence for a mammalian amino acid transport system that acts like the prokaryotic and lower eukaryotic solute transporters as a proton/substrate symporter in epithelial cells of the small intestine and kidney and being different from the other  $\text{Na}^+$ -

coupled solute transporters, the existence of a PAT protein was mistrusted by many scientists. The doubts were supported by the fact that a cDNA coding for a protein that exhibits PAT-like activity could not be identified for long time.

In 2001 Sagne C et al. described the cloning of the first mammalian amino acid transport protein acting as a proton/amino acid symporter. They cloned the transporter from rat brain and detected the protein in neuronal lysosomes by immunohistochemical studies. It was therefore designated as rat lysosomal amino acid transporter-1 (rLYAAT-1). After transfection of COS-7 cells with rLYAAT-1 cDNA, the cells displayed an elevated uptake of proline, alanine and GABA. Inhibition studies with GABA as a tracer revealed that out of the 20 proteinogenic amino acids only glycine, proline and alanine were able to inhibit uptake of GABA. Transport rates of GABA increased with decreasing extracellular pH and were independent of sodium. The affinity of GABA for transport by rLYAAT-1 was determined with around 0.5 mM. The authors found the LYAAT-1 mRNA in most of the tissues examined, inter alia in brain, lung, kidney and liver. Expression of rLYAAT-1 in small intestine was not investigated (Sagne C et al., 2001). The authors hypothesised that rLYAAT-1 could be responsible for the export of amino acids derived from protein breakdown in lysosomes by using the proton gradient between lysosome and cytoplasm (higher lysosomal and lower cytoplasmic proton concentrations). However, it was not analysed whether rLYAAT-1 is expressed always and exclusively in the lysosomal membrane or whether this is dependent on the tissue where the protein is expressed. Moreover, only basic functional data of rLYAAT-1 expressed in COS-7 cells were obtained and a link to the transporters of the PAT system was not made.

Almost simultaneously we identified and cloned the murine orthologue of rLYAAT-1, which was designated as PAT1. Identification of PAT1 and the other members of the PAT-family is described in the following section.

## 7. Identification and cloning of a mammalian proton/amino acid symporter family

During the last years several eukaryotic genomes were completely sequenced and genome sequence data of man and mouse as well as of several other eukaryotes are available online in different databases. Therefore, so far unknown genes can be identified *in silico*, which represents the cloning of a functional cDNA starting from homology-based sequence-information of genes with known functions. Before cloning of the PAT proteins all functionally described AAAP transporters were scanned for homologous regions using the blastp method. The observation was made that all AAAP members exhibit a common signature within their protein sequence. Furthermore, hydrophobicity plots of functional AAAP members were very similar and predicted that the transporters are also very similar regarding their secondary structure. Most of the functional members analysed were from yeast and plants. They all were shown to transport amino acids and derivatives, mostly by utilising a transmembrane pH gradient. It therefore was suggested that a common motif in the AAAP-gene-family may provide a tool for identification of the not yet identified mammalian proton-dependent amino acid transporters of the PAT system as described in the apical membrane of small intestinal and renal epithelial cells.

As a first step in identifying PAT-relevant sequences out of a whole genome, different sequence databases were searched for sequence intercepts with a common AAAP signature. As search template the protein sequence YKL146w from *Saccharomyces cerevisiae* was used (Boll M. et al., 2002). This sequence is related to the neuronal vesicular GABA-glycine transporter VGAT/VIAAT, the first mammalian AAAP-member that has been cloned. Following databases were mainly used: the murine and human Expressed Sequence Tag (EST) databases, the human genome sequence, and additionally the murine Shotgun-genome sequence database.

In the murine EST database a sequence was found, possessing the AAAP signature. To this sequence, denoted with the accession number AW048509, was no function assigned at that time. The potential complete cDNA was constructed by assembling the corresponding overlapping EST sequences. Subsequently this sequence was used for searching of additional members of this AAAP subfamily in the murine and human genomes. In both, the human as well as in the murine genome four genes from each species were identified. None of the genes was known at this time. Moreover, bioinformatic analysis of the human genome project did not predict the respecting parts of the genome as coding regions. The individual steps of obtaining the complete murine cDNAs of the designated PAT1 - 4 transporters are described here in brief.

In case of the murine PAT2, an EST clone (IMAGp998B154710Q2, RZPD) was identified, containing the complete open reading frame. For identification and assembling of PAT1,

PAT3 and PAT4 from mouse, different strategies were used. At first, using the PAT2 sequence as a template, mammalian EST databases were searched in an attempt to assemble the sequences. Additionally, the human genome and the murine shotgun-genome sequence were analysed for the corresponding transporter genes. When the complete open reading frame (ORF) could not be constructed, putative exons were determined with genescan-programs. The complete 5'-ends of cDNAs were verified and identified by the 5'RACE technique (RACE: rapid amplification of cDNA ends) and the derived cDNA sequences were checked for in vivo expression in murine tissues using RT-PCR.

After assembling of the complete cDNA sequences of the murine PAT1, PAT3 and PAT4, gene-specific primers flanking the ORF were used for RT-PCR to gain functional cDNA clones. PCR-products were cloned into a modified pCRII-vector (Invitrogen). The pCRII vector contained a 700 bp fragment of the rabbit PEPT2 3'-end inclusive poly(A)-tail for stabilising the synthesised cRNA.

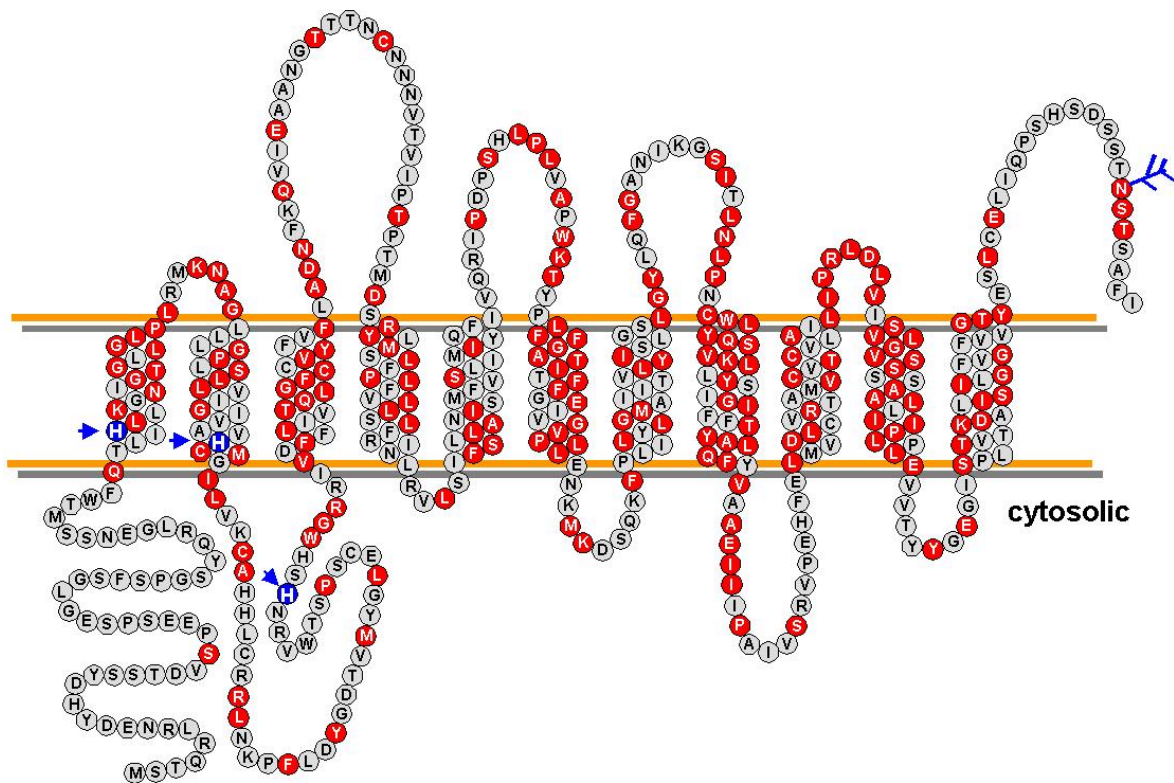


**Figure 6: Proposed membrane topology model of the murine PAT1 transporter.** Amino acids are represented by circles, with the amino acid residue in the one-letter code. Putative transmembrane domains are shown schematically. Red circles (with white letters) represent identical residues in the PAT1 to PAT4 proteins. The conserved putative N-glycosylation site is marked as a branch. The three conserved histidine residues are marked by blue circles and arrows.

The murine sequences have all been verified on cDNA levels and the human sequences were derived from genomic and EST sequences. Hydropathy analysis, using the Kyte and Doolittle algorithm, revealed topology models with 11 TMDs for the human as well as murine PAT1 and PAT2 proteins, as shown for the murine PAT1 model in Figure 6.

Whether the PAT3 and PAT4 proteins exhibit 10 or 11 TMDs is not clear due to lower hydrophobicity values in the region corresponding to TMD 8 in PAT1 and PAT2 (Boll M et al., 2003). Figure 7 shows the sequence alignment of the identified human and murine PAT transporters.

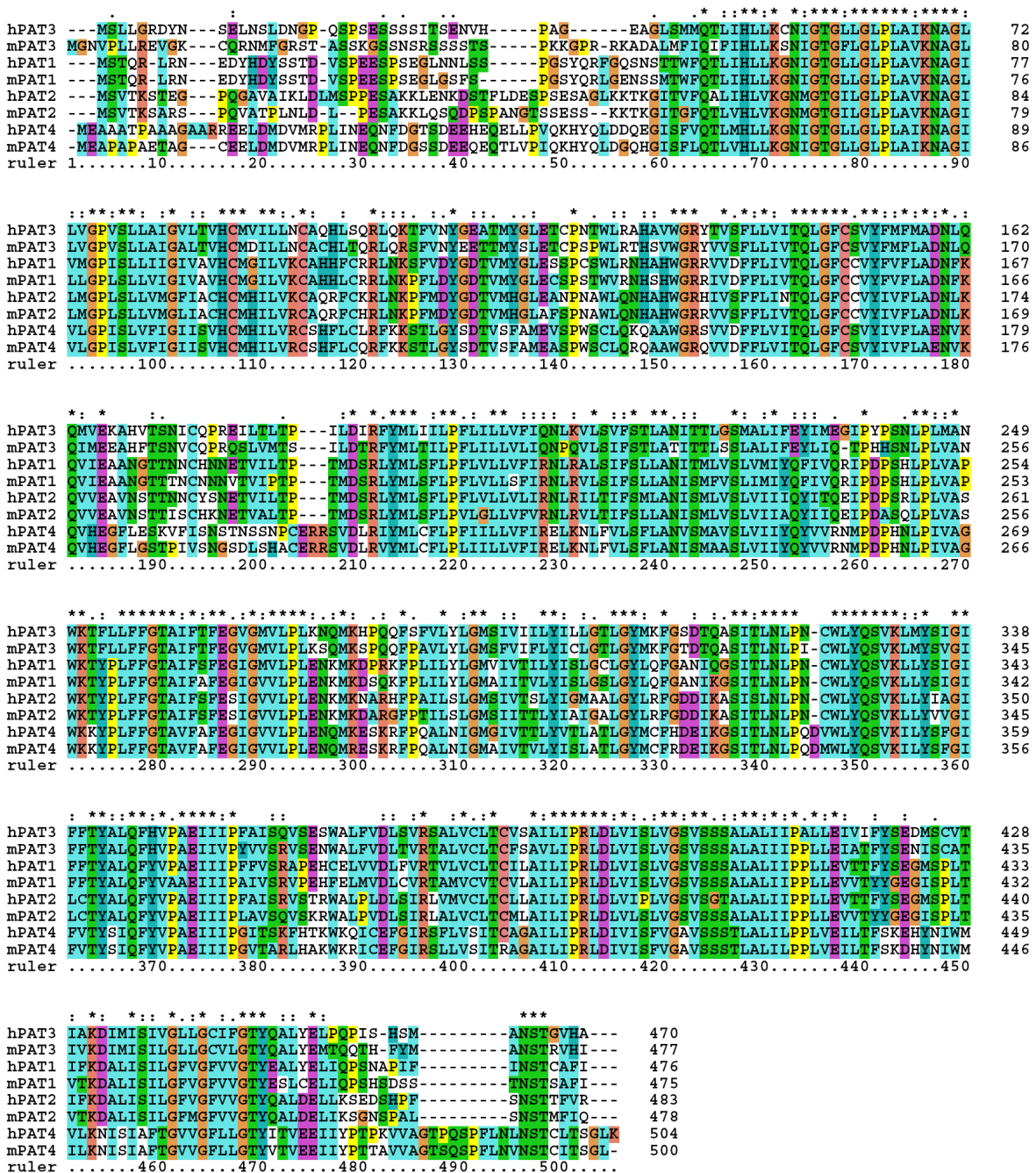


**Figure 7: Multiple sequence alignment of the human and mouse PAT proteins.** The alignment was performed with the ClustalX 1.8 program. Single, fully conserved residue (\*), “strong” groups, fully conserved (:), and “weak” groups, fully conserved (.) are indicated. Amino acids are merged to groups due to their properties (acidic, basic, charged), indicated by different colours. Protein weight matrix according to the Gonnet series (Gonnet Pam250), strong and weak groups are defined as strong score >0.5 and weak score =<0.5, respectively. Gap opening, 10; Gap extension 0.2

The PAT proteins comprise 470 to 483 amino acids. The human and murine PAT proteins are closely related to each other, they show high sequence similarity to each other with 91% (PAT1), 89% (PAT2), 83% (PAT3) and 87% (PAT4) over the entire protein sequence. PAT1 and PAT2 are the most closely related paralogous with an overall similarity of 80%. Within the entire PAT family, a similarity in protein sequence of at least 47% was observed, indicating a high degree of conservation between the proteins. Conserved residues are distributed over the entire protein sequences, with the exception of the 40 to 50 amino-acid-long N-terminal stretch. In the PAT proteins, the N-terminus is predicted to be located in the cytosol, whereas the C-terminus may face the extracellular side. The most closely related mammalian protein is the LYAAT-1 transporter from rat.

Tissue specific expression of the PAT transporters at the mRNA level were determined by northern blot analysis with PAT-specific cDNA probes (Figure 8). The expression pattern of the murine PAT transporters is very heterogeneous. The PAT1 transcript (5.0 kb) was found to be expressed in almost all tissues with high intensity in small intestine, kidney, brain and colon. Strong expression of the PAT2-mRNA (2.5 kb) was detected in lung and heart, weaker signals were also found in kidney, muscle, testes and spleen. PAT3-mRNA (1.9 kb) expression was restricted to small intestine, colon and testes whereas the PAT4-mRNA (5.7 kb) was found in all tissues examined except small intestine. The strong expression of PAT1-mRNA in small intestine and kidney made this potential amino acid transporter to be a good candidate protein for the functionally described PAT-system.

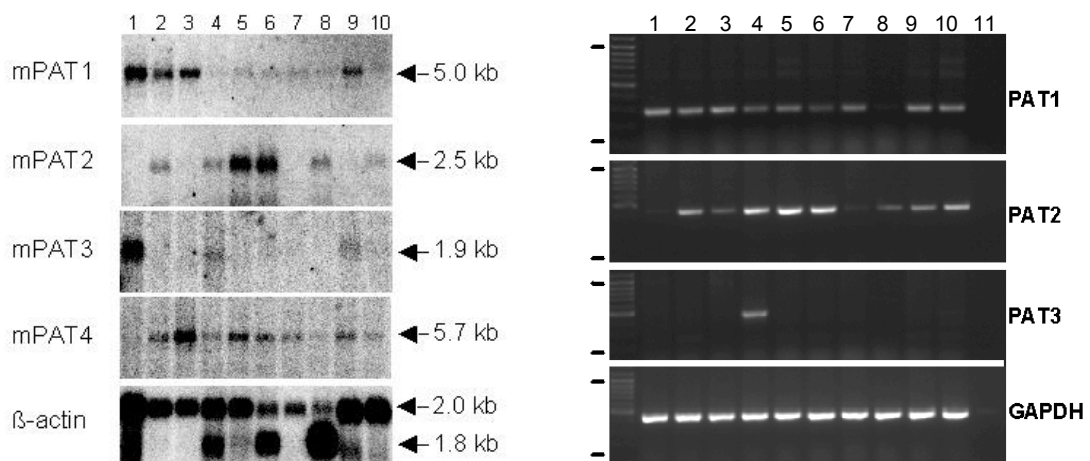


**Figure 8: Tissue distribution of the murine PAT1, PAT2, PAT3 and PAT4 mRNA.** (A) Northern blot was performed with murine Poly(A)-RNA isolated from different tissues using mouse PAT subtype-specific cDNA probes. As a control for the RNA integrity, the blot was also probed for  $\beta$ -actin. (B) 5 $\mu$ g total RNA of the indicated mouse tissue was reverse transcribed with oligo(dT) primers. In the PCR, cDNA specific primers were used to detect the subtype mRNAs. As a control for the RNA integrity, the glyceraldehyde-3-phosphate dehydrogenase (GAPDH) PCR product was amplified. Black lines on the left side indicate the 1000 and 100 bp DNA ladder fragments. 1 small intestine; 2 kidney; 3 brain; 4 testis; 5 lung; 6 heart; 7 liver; 8 muscle; 9 colon; 10 spleen; 11 control.



## **AIMS AND ACHIEVEMENTS OF THE THESIS**



## AIMS AND ACHIEVEMENTS OF THE THESIS

The existence of a proton-dependent transport system for small, neutral amino acids and selected derivatives in the brush border membrane of small intestinal and renal epithelial cells was well documented in various studies without knowing the responsible genes and proteins. By functional studies it was convincingly shown that glycine, alanine, proline and inter alia the neurotransmitter GABA are taken up into epithelial cells, energised by a proton-driven mechanism. In our laboratory four novel mammalian genes were identified, possibly encoding these proton-driven amino acid transport proteins.

The main intention of the present Ph.D. project was to assess whether the cloned transporters PAT1 - 4 from mouse and man indeed mediate amino acid uptake after heterologous expression. It could be demonstrated that mouse and human PAT1 and PAT2 proteins are proton-driven transporters for small and neutral amino acids and selected derivatives. PAT1 represents in comparison to PAT2 a low affinity, high capacity system and is postulated to be the molecular entity of the described system PAT in renal and intestinal epithelial cells. So far, PAT3 and PAT4 remain orphan transporters as no function could be assigned to these proteins. Several approaches were used to characterise PAT1 and PAT2 in more detail. After expression of the transporters in *Xenopus laevis* oocytes the functional characteristics of the transporters were specified with electrophysiological, tracer-flux studies and intracellular pH measurements to elucidate substrate selectivity and specificity. Ion, pH as well as membrane potential dependencies were determined; minimal structural requirements for substrate recognition and transport were characterised and the transport mode was investigated. Moreover, short-chain fatty acids were identified as a new class of substrates for the PAT1 and PAT2 transporters.

To gain insights into potential physiological functions of the PAT1 and PAT2 transporters, cellular and subcellular localisation of the transporters in selected tissues and cell lines were determined with immunohistochemical and immunofluorescence approaches using PAT1- and PAT2-specific antibodies. Furthermore, fusion proteins of the PAT2 transporter with GFP enabled a localisation of the transporter in the plasma membrane, at least in part, in HeLa cells and in the neuronal cell lines GT1 and N2A.

Based on amino acid sequence, orthologous proteins in *C. elegans* and *D. melanogaster* were identified and their phylogenetic relationship was determined. Two closely related proteins of PAT1 from *C. elegans* were cloned, but after expression in *X. laevis* oocytes no transport activity could be detected.



## **RESULTS AND DISCUSSION**



## 1. Revelation of two new mammalian proton/amino acid transporters: General characteristics

The PAT system was previously shown to exist in the apical membrane of small intestinal and renal epithelial cells (Roigaard-Petersen H et al., 1990; Thwaites DT et al., 1995b). At the beginning of the project underlying this thesis the molecular identity of the underlying gene and protein was not known. By homology screening, with the yeast sequence AVT3 (Vacuolar Amino Acid Transporter 3) (Rusnak R et al., 2001) as a template two closely related murine transporter proteins, designated as mPAT1 and mPAT2, were identified in mammalian EST databases. To determine whether these transporters indeed function as rheogenic amino acid transporters, the transporters were expressed in *X. laevis* oocytes and the two electrode voltage clamp technique (TEVC) as well as flux studies were applied to characterise their transport function [Appendix 1].

Both murine PAT transporters displayed very similar functional properties when expressed in *X. laevis* oocytes. Both transporters mediate uptake only of the small and neutral amino acids glycine, alanine, and proline. Transport is electrogenic and was shown to be enhanced by hyperpolarising membrane potentials. Interestingly, in contrast to many other mammalian solute transporters murine PAT1 and PAT2 activity does not depend on the presence of  $\text{Na}^+$ ,  $\text{Cl}^-$ , or  $\text{K}^+$  but is strongly dependent on the extracellular  $\text{H}^+$  concentration. A decrease in extracellular pH leads to a significant increase of transport activity of both, PAT1 and PAT2 [Appendix 1, Fig. 3]. A strongly decreased uptake of proline into HeLa cells overexpressing PAT1 in presence of the protonophore nigericin, which dissipates the chemical proton gradient ( $\Delta\text{pH}$ ) across the plasma membrane without affecting the electrical gradient, confirmed our finding that  $\Delta\text{pH}$  is the major driving force for PAT1 (Wreden CC et al., 2003).

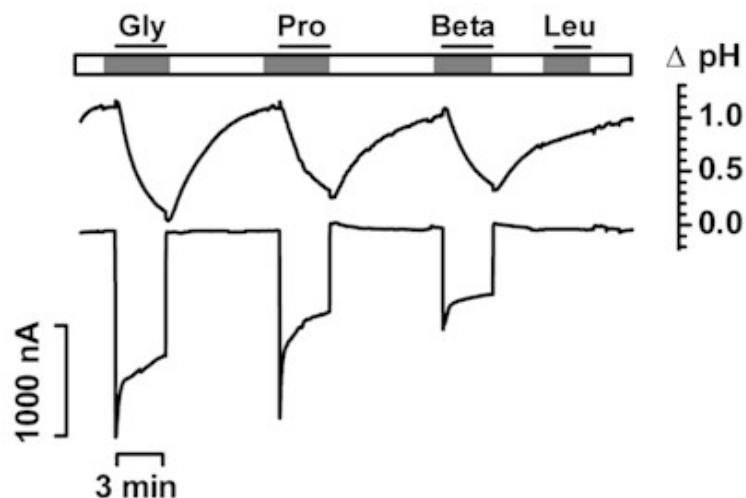


**Figure 9: Amino acid induced intracellular pH changes in mPAT1 expressing *X. laevis* oocytes:** Oocytes were clamped to a membrane potential of  $-60$  mV and pH changes were recorded with a hydrogen-ion selective microelectrode (upper trace) simultaneously with the changes in holding currents (lower trace). White boxes indicate perfusion with  $\text{Na}^+$  containing buffer at pH 7.4, grey boxes indicate perfusion of  $\text{Na}^+$  containing buffer at pH 6.5. Presence of amino acids at concentrations of 20 mM each is indicated by black lines.

That protons are directly transported by the PAT proteins across the plasma membrane was demonstrated by substrate-induced intracellular acidification as measured with hydrogen-selective microelectrodes (Figure 9). Net charge movement across the membrane results almost exclusively from proton influx, since the amino acids are almost exclusively zwitterionic in the pH range studied. Charge to flux coupling experiments revealed that movement of one amino acid across the membrane is coupled to the movement of one proton. This was shown for the murine PAT1 as well as the PAT2 protein [Appendix 1, Fig. 4]. This stoichiometry seems to be conserved in the PAT family as the rat orthologue PAT1/LYAAT-1 has also been shown to couple current stoichiometrically to transport with a rate of 1:1 (Wreden CC et al., 2003).

Regarding amino acid substrates, both transporters display a quite narrow substrate specificity. As substrates are accepted amino acids with a small and apolar side chain, like glycine, alanine, and proline, whereas the hydroxy-group containing L-serine is only poorly transported. Although PAT1 and PAT2 seem to be very restrictive regarding substrate recognition for binding and transport, it was shown that they do accept also the D-isomers of alanine, proline, and serine as well as small  $\beta$ -amino acids,  $\gamma$ -amino acids, and N-substituted amino acids [Appendix 1, 2, 6 and 7]. It was shown that  $\beta$ -alanine, GABA, and betaine are good substrates for PAT1, but poor substrates for PAT2. In general, the PAT2 protein exhibits higher affinities to L-amino acid substrates than the paralog PAT1. The transport characteristics of the PAT1 protein regarding substrate specificity, affinity, and enantioselectivity and transport mode turned out to be very similar to the transport system in the apical membrane of the human intestinal cell line Caco-2 described by Thwaites et al. (Thwaites DT et al., 1993b; Thwaites DT et al., 1994; Thwaites DT et al., 2000). The facts that PAT1 was cloned by RT-PCR from murine small intestinal RNA and that it is strongly expressed in the small intestine, also supported the assumption that PAT1 represents the molecular identity of the proton-dependent amino acid transport activity described in Caco-2 cells [Appendix 1, Table 1]. This hypothesis was confirmed later by the cloning of human PAT1 from Caco-2 cells and by the identification of the PAT1 protein in the apical membrane of enterocytes (Chen Z et al., 2003a).

In conclusion, with the PAT1 and the PAT2 proteins two transporters of a new mammalian family of amino acid transporters were identified. This was also the first description of mammalian amino acid transporters acting as proton-coupled cotransporters. Although the cellular and subcellular localisation is not yet finally determined, these transporters may act as plasma membrane carriers for small neutral amino acids and their derivatives in several tissues and cell types.

## 2. The PATs represent a new mammalian subgroup within the AAAP-family

During the ongoing cloning work in our laboratory the cloning of a lysosomal amino acid transporter from *Rattus norvegicus*, named rLYAAT-1 was published (Sagne C et al., 2001). At this time, LYAAT-1 was the only functionally known and characterised mammalian homologue of the murine PAT1 and PAT2 transporters. LYAAT-1 represents the rat orthologue of the murine PAT1 protein. More members of the PAT/LYAAT family have meanwhile been identified at the molecular level. The rat orthologue (rPAT2) of the murine PAT2 was cloned from a lung cDNA library and was functionally characterised after expression in *X. laevis* oocytes (Chen Z et al., 2003b). Additionally, rPAT2 was also isolated from sciatic nerve and was found to be a “protein rich in transmembrane domains” and therefore was designated as tramdorin-1 (transmembrane domain rich protein). The function of tramdorin-1 was not analysed (Bermingham JRJ et al., 2002), but the sequence shows 99% identity to rPAT2. Differences are most likely due to polymorphisms or sequencing errors and therefore these two proteins are identical. Moreover, we were able to clone the human PAT1 transporter from Caco-2 cells and homology screening of a human testis cDNA library enabled us to clone hPAT2. Additionally, basic functional features of the human transporters PAT1 and PAT2 were determined [Appendix 2, Fig. 7]. Human PAT1 was also cloned and characterised by Chen Z et al. in 2003. The newly identified family of mammalian proton-coupled amino acid transporters include two orphan members found in the human, mouse, and rat genome, designated as PAT3 and PAT4 [Appendix 2, Fig. 4] (Chen Z et al., 2003a; Boll M et al., 2004).

Functionally, all transporters of the PAT family characterised so far represent mammalian proton/amino acid symporters. They have been shown, except the orphan members PAT3 and PAT4, to mediate uptake of glycine, alanine, and proline after expression in a heterologous cell system. Transport activity is independent of Na<sup>+</sup> and Cl<sup>-</sup>, but strongly dependent on pH and leads to a pronounced intracellular acidification, indicating a proton/amino acid symport mode [Appendix 1 and 2] (Sagne C et al., 2001; Chen Z et al., 2003a; Chen Z et al., 2003b). The proteins all consist of about 500 amino acids and are predicted to possess 11 transmembrane domains [Appendix 2, Fig. 1 and 2] (Chen Z et al., 2003a; Wreden CC et al., 2003). The PAT proteins show high sequence similarity to each other, including the orphan members PAT3 and PAT4. On protein level an identity of at least 48% within the PAT family is found. Table 3 summarises the features of cloned and characterised members of the mammalian PAT family of proton/amino acid symporters with respect to their main substrates, tissue distribution, and chromosomal localisation.

Protein name	Human gene name	Alias	amino acid substrate	transport type/ coupling ions	Tissue distribution (mRNA level)	human gene locus	species counterparts cloned
PAT1	SLC36A1	LYAAT-1	G, A, P, GABA, D-Pro, D-Ala, MeAIB	C/H <sup>+</sup>	brain (neurons), small intestine, colon, kidney, lung, liver, spleen	5q33.1	mouse, rat
PAT2	SLC36A2	Tramdorin1	G, A, P	C/H <sup>+</sup>	lung, heart, kidney	5q33.1	mouse, rat
PAT3	SLC36A3	-	-	orphan	testes	5q33.1	mouse
PAT4	SLC36A4	LYAAT2	-	orphan	brain, lung, heart, colon	11q14.3	mouse

**Table 3: The mammalian proton coupled amino acid transporter family SLC36.** Adapted from Boll et al. (2004)

The PAT transporters are belonging to the eukaryotic AAAP transporter family (Young GB et al., 1999). Phylogenetic analysis revealed that the PAT/LYAAT proteins form a third subgroup within the mammalian AAAP family, in addition to the VGAT/VIAAT and the system A/N transporter branches (Figure 10). A comparison of the amino acid sequences of PAT1 and PAT2 with proteins of the two other mammalian AAAP subgroups revealed that the identified PATs are only distantly related to these branches. They exhibit 36% or 33% similarity and 19% or 17% identity with the VGAT/VIAAT and the system A/N transporters, respectively. Nevertheless, all related mammalian AAAP proteins show amino acid transport activity combined with a proton sensitivity.

By database search for PAT homologous proteins several yet “hypothetical” proteins from *D. melanogaster* and *C. elegans* were found with significant sequence similarity to the human and mouse PAT proteins. So far only for the *unc-47* gene, the *C. elegans* orthologue of VGAT, a physiological function has been assigned (McIntire SL et al., 1997). In *C. elegans* 6 proteins and in *D. melanogaster* 8 proteins were identified as potential PAT-like proteins at a threshold level of at least 45% similarity (Figure 10). PAT-like genes were also found in the plant *A. thaliana* as well as in the malaria mosquito *Anopheles gambiae*. A survey of the human and mouse genome sequences revealed no additional PAT like proteins. In the *C. elegans* and *D. melanogaster* genomes only one VGAT-like protein but no clearly defined system A/N protein was found. The large number of PAT-like proteins as found in *D. melanogaster* and *C. elegans* as compared to the 4 PAT proteins found in mammals and the low number of Na<sup>+</sup>-driven transporters in *C. elegans* and *D. melanogaster* suggests that these organisms are evolutionary still closer to the prokaryotes and simple eukaryotes. Although not yet well defined, the more prominent numbers of Na<sup>+</sup>-dependent transporters in higher eukaryotes appears to have co-evolved with the appearance of Na<sup>+</sup>/K<sup>+</sup> ATPase. The proton-driven systems as found in mammals may in turn be coined the “archaic nutrient transporters”.

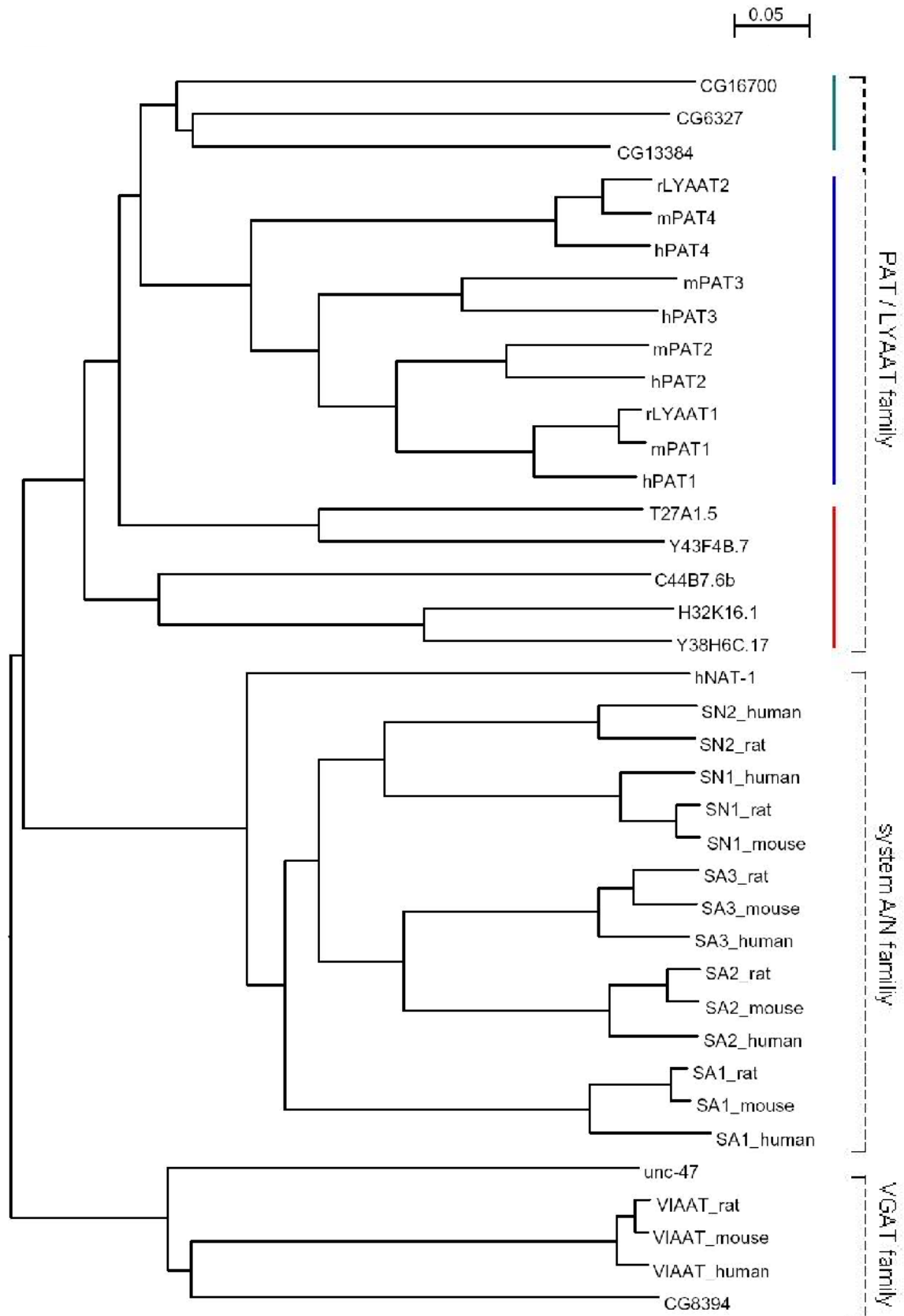


**Figure 10: Dendrogram of AAAP members from invertebrates and mammals.** Clustering of the AAAP superfamily in the three mammalian subfamilies is demonstrated. The closely related PAT-like proteins out of *D. melanogaster*, (green) and *C. elegans* (red) to mammalian PATs (blue) are shown. The Dendrogram was constructed by the neighbour joining method using the ClustalX 1.8 program. The scale bar indicates the distance between the proteins (0.05 = 1 exchange per 20 amino acid residues).

### 3. Specific functional characteristics of PAT1 and PAT2

As mentioned before the general transport characteristics of proton/substrate cotransport appears to be conserved throughout the mammalian PAT family. The orthologous proteins in mouse, rat, and human seem to have similar, if not even identical functional characteristics, such as identical substrate specificity, similar affinities, and inhibition constants (Figure 11) (Sagne C et al., 2001; Chen Z et al., 2003a; Chen Z et al., 2003b; Wreden CC et al., 2003).

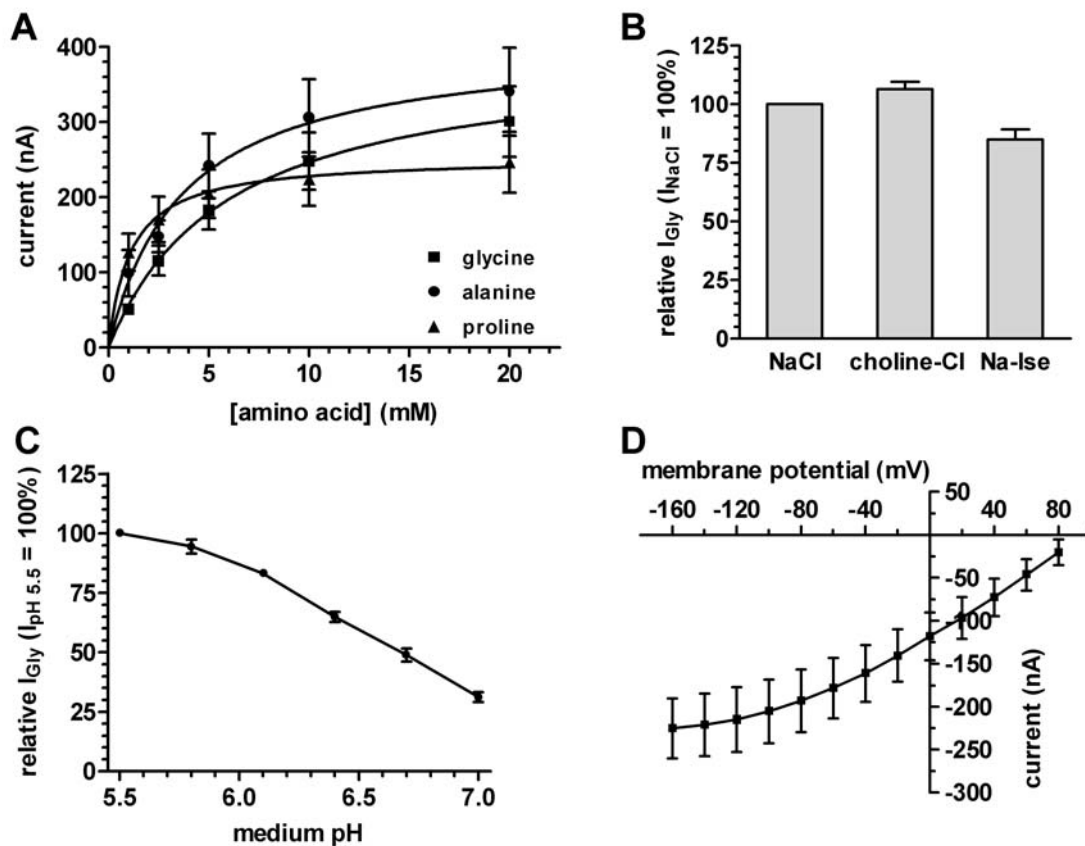


**Figure 11: Functional characteristics of the human PAT1 transporter:** Experiments were performed with hPAT1 expressing oocytes under TEVC conditions. Results are shown as the mean  $\pm$  SEM of at least 8 different oocytes of different batches. (A) Substrate-dependent transport kinetics induced by perfusion of glycine (filled square), alanine (rhombus) and proline (open triangle). (B) Effect of equimolar replacement of 100 mM NaCl by choline-Cl or Na<sup>+</sup>-isethionate on glycine evoked currents. (C) Proton-dependent inward currents under  $V_{max}$  conditions (50 mM glycine). (D) Membrane potential dependency of glycine-induced inward currents.

Despite the fact that both, PAT1 and PAT2, display an overall similar substrate specificity, the PAT isoforms 1 and 2 possess distinct differences in transport function.

PAT1 is in comparison to PAT2 a low affinity transport system. The apparent  $K_m$  values for its substrates are in the millimolar range (2 - 15 mM). In contrast, the apparent affinities of PAT2 substrates are in the micromolar range (100 - 1000  $\mu$ M), and around 10 to 30-times higher than the corresponding affinity for PAT1 under identical conditions (see Table 4 on page 39). The observed apparent affinities are in conformity with the results obtained in other expression systems (Sagne C et al., 2001; Chen Z et al., 2003a; Wreden CC et al., 2003).

### 3.1 Minimal structural requirements of aliphatic amino acid PAT substrates

By testing a large set of aliphatic amino acids and structurally related compounds the structural requirements underlying the substrate specificity of PAT1 [Appendix 3] and PAT2 [Appendix 7] were defined.

This series of experiments revealed that PAT1 exhibits a broader substrate specificity than originally expected, including the osmolytes sarcosine and betaine, the D-amino acids D-serine, and D-alanine as substrates (Table 4) [Appendix 3, Fig. 3]. The critical structural elements for PAT1 substrates are *a*) an unsubstituted negatively charged carboxyl-group, *b*) a small size of the amino acid side chain (maximal 2 CH<sub>2</sub>-units), and *c*) a short spacer distance between the charged amino and carboxyl groups (maximal 3 CH<sub>2</sub>-unit). On the other hand, a free amino group within the PAT1 substrate is not essential and the carboxyl group is exchangeable by a sulfonic acid group, as in taurine or by a sulfinic acid group, as in hypotaurine (Figure 12).

Similar criteria apply also for the substrate recognition pattern of PAT2, when high affinity ( $K_m = 0.1 - 1$  mM) and low affinity substrates ( $K_m = 5 - 15$  mM) are considered [Appendix 7, Table 1]. The differences to PAT1 are *a*) the maximal spacer distance between amino and carboxyl group in a PAT2 substrates should consist of maximal 2 CH<sub>2</sub>-units, as GABA is not accepted as substrate, and *b*) a more sensitive interaction between the amino group of the substrate and the respective binding pocket of PAT2, as betaine seems not to be recognised by PAT2, whereas it represents a good substrate of PAT1 [Appendix 7, Fig. 1].

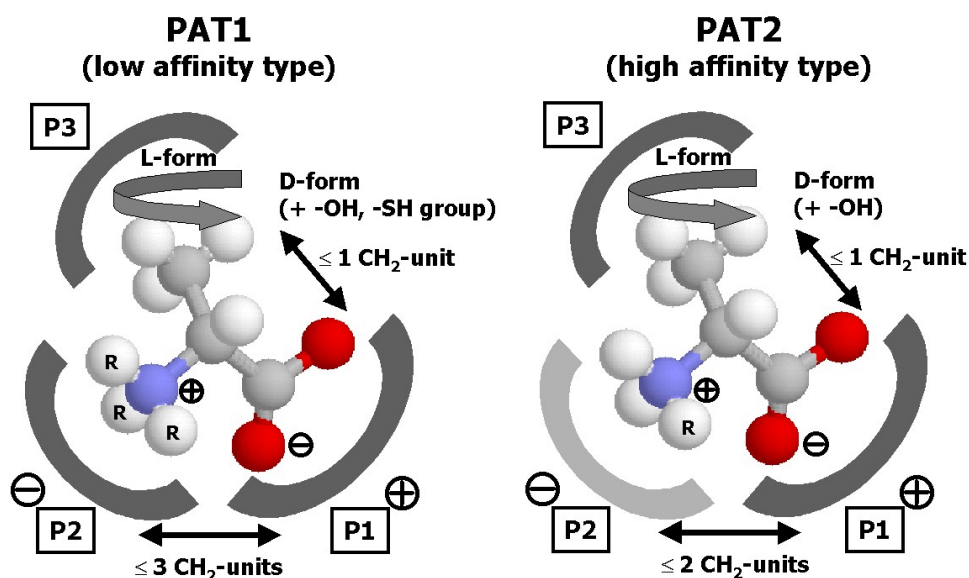


**Figure 12: Proposed model of the substrate binding site of the transporters PAT1 and PAT2.** The substrate binding is shown here schematically for the model substrate L-alanine. The binding site of both transporters is proposed to possess three binding pockets. P1 for the binding of the negatively charged carboxyl group, P2 for the positively charged amino group and P3 for the interaction with the side chain of the amino acid substrate. The P2 binding site in PAT1 accepts a up to triple-methylated amino group (indicated by R), whereas for high affinity binding in PAT2 the amino acid should carry only an one-methylated group. In the D-configuration of amino acid substrates the P3 binding pocket accepts additionally side chains containing hydroxyl groups (PAT1 and PAT2) and thiol groups (only PAT1). The maximal distance between the amino and the carboxy terminus of amino acid substrates consists in PAT1 of 3 CH<sub>2</sub>-units and in PAT2 of 2 CH<sub>2</sub>-units.

However, when based only on the high affinity substrates, PAT2 is more strict in substrate recognition and transport. Figure 12 shows that PAT2 recognises only  $\alpha$ -amino acids (with the exception of D-Pro) and tolerates only one substitution at the amino group of the substrate, as in sarcosine and proline (which possesses due to its ring structure an imino group). Interestingly, beside L-Pro also D-Pro and OH-Pro are recognised as high affinity substrates by PAT2. This is noteworthy, since D-Pro is the only D-amino acid, and OH-Pro is the only polar amino acid, which is accepted by PAT2. An explanation might be that the ring structure of proline, which changes the orientation of the amino acid within the substrate binding site, avoids a negative interference between a polar group in the side chain with the binding site. Whether additional proline derivatives are also accepted by PAT2, as shown recently for PAT1 (Metzner L et al., 2004), is presently not known.

substrate	apparent $K_m$ -value (mM)				
	mPAT1	hPAT1	mPAT2	Caco-2	renal BBMV
glycine	7.0 ± 0.7	6.8 ± 0.2	0.59 ± 0.04	5.3 <sup>&amp;</sup>	3.9
L-alanine	7.5 ± 0.6	3.1 ± 0.5	0.26 ± 0.05	5.7 <sup>&amp;</sup>	4.4
D-alanine	6.3 ± 0.7	2.9 ± 0.9 <sup>#</sup>	6.5 ± 1.1	+ <sup>&amp;</sup>	7.9
L-proline	2.8 ± 0.1	0.9 ± 0.2	0.12 ± 0.02	9.2 <sup>&amp;</sup>	4.5
D-proline	2.6 ± 0.3	2.5 ± 0.3 <sup>#</sup>	0.29 ± 0.03		3.9
L-serine	68.8 ± 5.2	29.1 ± 7.8 <sup>#</sup>	42.6 ± 3.9	+ <sup>&amp;</sup>	
D-serine	15.6 ± 1.4	3.8 ± 0.4 <sup>#</sup>	14.7 ± 0.4	+ <sup>&amp;</sup>	
D-cysteine	33.2 ± 1.2	3.5 ± 0.5 <sup>#</sup>	no substrate		
$\beta$ -alanine	5.2 ± 0.2		14.8 ± 1.5	8.1 <sup>&amp;</sup>	4.0
GABA	3.1 ± 0.2	2.1 ± 0.2 <sup>#</sup>	30.9 ± 0.1	1.95 <sup>&amp;</sup>	
5-APA	38 ± 1		no substrate		
sarcosine	3.2 ± 0.3		0.20 ± 0.01	+ <sup>&amp;</sup>	
N,N-dimethyl-glycine	8.5 ± 0.5		+		
betaine	5.4 ± 0.3		> 25 mM	+ <sup>&amp;</sup>	
taurine	8.3 ± 0.6	+	no substrate	+ <sup>&amp;</sup>	2.9
hypotaurine	+				
L- $\alpha$ -ABA	48 ± 8		20 ± 1.5		
DL- $\beta$ -aminobutyric acid	4.1 ± 0.6		nd	+ <sup>&amp;</sup>	
hydroxy-L-Pro	10.7 ± 0.9	4.6 ± 0.8 <sup>#</sup>	0.70 ± 0.04	+ <sup>&amp;</sup>	7
L-pipecolic acid	21.3 ± 1.9				
D-pipecolic acid	5.7 ± 0.3				
Nipecotic acid	3.1 ± 0.3		no substrate	+ <sup>&amp;</sup>	
Isonipecotic acid	2.0 ± 0.1		no substrate	+ <sup>&amp;</sup>	
L-cycloserine	9.9 ± 1.6		+		
D-cycloserine	5.4 ± 0.6		+	15.8 <sup>&amp;</sup>	
MeAIB	8.2 ± 0.5	1.5 ± 0.2 <sup>#</sup>	+	6.2 <sup>&amp;</sup>	

**Table 4: Apparent affinities of various compounds for interaction with the murine transporters PAT1 and PAT2.** Concentration-dependent substrate evoked currents were determined in *X. laevis* oocytes expressing the respective transporter. After Eadie-Hofstee-transformation, the  $K_m$  values were calculated by linear regression analysis. Data represent the mean ± SEM of  $n \geq 6$  oocytes of at least two different batches. (#)  $K_i$ -values taken from Chen Z et al., 2003a; (&) taken from Thwaites et al., 1993-2000; (+) compound is transported but kinetic is lacking.

The transport properties of the cyclic amino acid derivatives fit into the proposed binding pocket model for PAT1 and PAT2 (Figure 12), with the addition that a longer side chain is accepted (maximally 4 CH<sub>2</sub>-units) based on the ring structure. Nipecotic and isonipecotic acid are good substrates for PAT1 but are not transported by PAT2, due to the side chain restriction (nipecotic acid) and backbone length exclusion (isonipecotic acid).

### 3.2 Driving forces for PAT-mediated transport

Despite the fact that both transporters are electrogenic proton symporters, PAT1 is much more affected in transport activity by lowering extracellular pH than PAT2. For example, decreasing extracellular pH from 7.5 to 5.5 leads to a more than 6-fold increase in transport activity of PAT1, whereas PAT2 activity is stimulated less than 2-fold. Additionally, PAT1 was shown to possess an even higher sensitivity towards changes in membrane potential, e.g. hyperpolarisation leads to a much stronger increase in PAT1 transport activity, than that of PAT2 [Appendix 1, Fig. 2]. Studies in HeLa cells overexpressing PAT1, and by using the ionophore nigericin confirmed that the proton gradient across the membrane is a driving force for transport (Wreden C.C. et al. 2003). These effects are mirrored in the dependency of K<sub>m</sub> values on extracellular pH. It was demonstrated that the apparent substrate affinities of PAT1 and PAT2 strongly increase by lowering the extracellular pH, with more pronounced effects in case of PAT1 [Appendix 6, Fig. 2 and Appendix 7, Fig. 3].

As expected (on the basis of the different pH dependencies), PAT1 and PAT2 differ remarkable in their affinities for the cotransported proton. PAT1 exhibits an apparent H<sup>+</sup> binding affinity of about 100 nM [Appendix 6, Fig. 1], corresponding to an pH value of 7.0, which is 200-fold lower than the proton affinity reported for the PAT2 of 0.5 nM, corresponding to a pH value of 9.3 [Appendix 7, Fig. 5]. This suggests that the PAT1 operates with high transport rates at more acidic conditions typically present on cell membranes where the PAT1 activity is likely to be operational, as in the small intestine (pH 6.1 - pH 6.8) (McEwan GT et al., 1988; Daniel H et al., 1989) and neuronal lysosomes (≤ pH 5.5) (Golabek AA et al., 2000). Whereas PAT1 in the lysosomal membrane seems to operate close to its maximal capacity, in the brush border membrane of the small intestine PAT1 activity can be altered by the activity of the Na<sup>+</sup>/H<sup>+</sup> exchanger NHE3 [Appendix 8].

Such a cooperation has been reported already for the proton-coupled peptide transporter PEPT1 (Thwaites DT et al., 2002), and additionally, an activation of PAT1 activity by NHE3 has been shown in the Caco2 cell system (Thwaites DT et al., 1999). In contrast, PAT2 reaches its half maximal transport activity at a pH of 9.3, and thus operates under proton saturation even at blood pH.

### 3.3 Bidirectional transport

PAT1- as well as PAT2-mediated transport was shown to be bidirectional. Both carriers are able to transport in both directions (inward or outward) with the direction of transport determined by the sum of the individual driving forces, the electrical, chemical, and substrate gradients. PAT1 and PAT2 mediated transport in the outward direction is also concentration-dependent and exhibits a dependence on membrane potential. This was shown by using the giant patch clamp technique (GPC) [Appendix 4, Fig.6 and Appendix 6, Fig. 8]. The PAT1 substrate specificity is symmetric in the inward and outward transport direction, as the affinity pattern from the cytosolic side is almost identical to that from the external surface (i.e. substrates with high affinities at the external surface exhibits also relative high affinities at the cytosolic binding site). However, the overall substrate affinities are asymmetric with generally around 7-fold lower affinities in the inward facing state [Appendix 6, Fig. 8]. For example, glycine exhibits for the outward facing PAT1 protein an apparent affinity of  $7.0 \pm 0.7$  mM, whereas from the cytosolic side the  $K_m$  value is  $37 \pm 8$  mM. This suggests major conformational differences of the substrate binding pocket in its inside- and outside-facing states.

The efflux mode of PAT1 and PAT2 might also be of physiological importance, since the outward transport was shown to occur even at negative potentials, which resembles physiological conditions [Appendix 6, Fig. 6]. PAT1 expressing oocytes showed, after injection of radiolabelled L-proline, efflux of this amino acid in the absence of an outwardly directed pH gradient. This efflux mode was strongly stimulated by the addition of extracellular amino acid substrates with half maximal transactivation constants of about 1 mM. Whereas the major physiological function of PAT1 is a net accumulative transport in the normal cellular setting, especially in membranes possessing a pH gradient, under certain conditions PAT1 may even serve as an electrogenic proton/amino acid efflux transporter. This would be of interest in cell types with high intracellular concentrations of Gly, Ala, and Pro and a negligible pH gradient across the membrane, e.g. in muscle cells.

### 3.4 Kinetic binding model

Detailed kinetic analyses of PAT1 currents induced by the reference substrate glycine under various conditions provided a basis for a six state ordered binding model for PAT1 (Figure 13) [Appendix 6, Fig. 3]. This binding model exhibits a mirror symmetry, i.e. has the same chronology for binding from outside and inside, in which the preferred route is for  $H^+$  to bind first (step 1). The  $H^+$  binding induces a conformational change of the transporter, that permits the amino acid to bind (step 2). The fully loaded  $H^+$ /amino acid cotransport complex then undergoes an additional conformational change and delivers simultaneously the  $H^+$  and amino acid binding site to the cytoplasmic surface of the membrane (step 3), where the

ligands are released into the cell interior (step 4 and 5). The final step in the transport cycle is the return of the binding sites to the external face of the membrane (step 6).

Although such a detailed analysis was not performed for the high affinity type transporter PAT2, it was observed that the affinity of protons for PAT2 is not significantly affected by the amino acid substrate, whereas the affinity of substrates is significantly dependent on the extracellular proton concentration [Appendix 7, Fig. 4]. This suggest also a distinct binding mode analogous to that in PAT1.

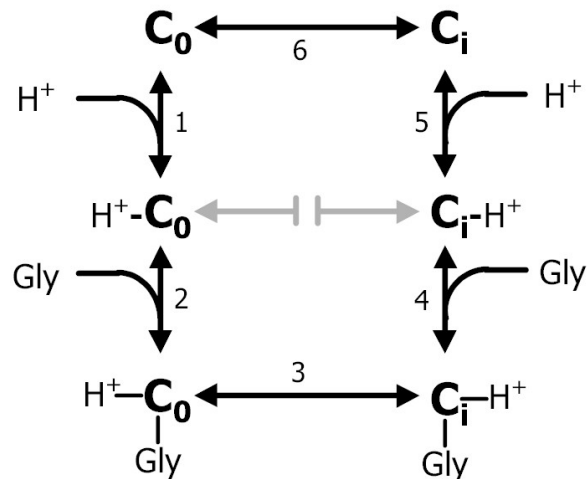


**Figure 13: Six-state ordered binding model for the proton/amino acid transporter PAT1.** States  $C_0$  and  $C_i$  face the external and internal membrane surfaces, respectively. In the absence of substrates the transporter exists in 2 stages ( $C_0$  and  $C_i$ ). At the external surface one  $H^+$  binds to the transporter to form the complex  $C_0-H^+$  (step 1). After binding of glycine (step 2) the fully loaded transporter undergoes a conformational change (step 3), to face the internal membrane surface, and releases its substrates (step 4 and 5). A  $H^+$  “leak” pathway (directly conformational change from stage  $C_0-H^+$  to  $C_i-H^+$ ) was not detectable.

### 3.5 Lack of a proton-leak pathway

The question was addressed whether both transporters might exhibit an intrinsic proton leak by a translocation of the transporter not loaded with a substrate. No evidence for an uncoupled  $H^+$  flux was found for PAT1 and PAT2. It was demonstrated that pH jumps using perfusion solutions with varying pH levels resulted only in a minimal shift in reversal potential, not significantly different from that observed in water-injected control oocytes [Appendix 6, Fig. 4 and Appendix 7, Fig. 5]. Moreover, PAT1 oocytes also showed no alterations in  $pH_{in}$  by applying acidic perfusion solutions in the absence of substrates [Appendix 6, Fig. 4].

That the affinity of the proton to PAT1 and PAT2 is much more dependent on the membrane potential than the affinities of the amino acid substrates may be explained by their different charge. Furthermore, the effect that the binding of protons depends strongly on voltage might be due to an “ion-well” effect, assuming that the proton by entering the binding site of the external faced transporter has to cross a part of the transmembrane voltage (Jauch P et al., 1986).

Beside the strong potential dependence of proton affinity, the maximum currents for proton-driven transport were only very moderately voltage-dependent in case of PAT1. This

suggests that membrane voltage has only a little effect on the reorientation of the empty transporter from the internal to the external surface of the membrane, although this conformational change is usually the rate-limiting transport step (Jauch P et al., 1986).

Both transporters share general features, such as the voltage dependence of affinities, the ordered binding mechanism with the ion binding first, and the “ion-well” effect, with the proton-coupled peptide transporter PEPT1 but also with the sodium-coupled transporter SGLT1 and the system A transporter SA2 (Mackenzie B et al., 1996; Loo DD et al., 1998; Chaudhry FA et al., 2002), the latter belonging to the same superfamily as PAT1.

#### 4. PAT1 and PAT2 as potential delivery system for short-chain fatty acids

It was established that a free amino group in a substrate is not essential for substrate recognition by the PAT transporters. Therefore it was hypothesised that the transporters may also be able to recognise and transport the corresponding physiologically important short-chain fatty acids (SCFA) acetate, propionate and butyrate. This was tested by a combination of electrophysiological analysis with uptake and inhibition experiments, and intracellular pH measurements. It was demonstrated that SCFAs are indeed substrates of PAT1 and PAT2, which are transported in contrast to the amino acid substrates in an electroneutral manner. If this is of physiological relevance has to be shown.

With glycine and proline as substrates it was demonstrated that acetate, butyrate and propionate are competing substrates for uptake by PAT1 and PAT2 [Appendix 5, Fig. 2]. In contrast, lactate and pyruvate did not interfere with the substrate binding site of the PAT carriers showing that only unsubstituted monocarboxylic acids are recognised. This is in accordance with previous observations that amino acids with polar side chains are only poorly recognised by PAT1 [Appendix 1 and 2] (Chen Z et al., 2003a). Using radiolabelled acetate and propionate it was furthermore shown that expression of PAT1 and PAT2 in oocytes increased SCFA uptake and that this influx is inhibited by amino acids [Appendix 5, Fig. 3]. However, electrophysiology failed to demonstrate any associated transport currents when SCFAs were applied but recordings of the intracellular pH established that SCFA uptake is associated with proton influx under voltage clamp conditions. This strongly suggests that SCFA influx occurs by proton symport most likely by transport of the SCFA anion with a proton in a 1:1 flux coupling stoichiometry (Figure 14) as shown previously also for proline [Appendix 1, Fig. 4].

The initial rates of intracellular acidification induced by the different SCFAs were dependent on the PAT expression level. Higher expression of PAT1 (measured as the integrated glycine-induced current) led to a faster initial acidification, whereas in control oocytes acidification was unaffected. Initial rates of intracellular acidification by PAT1 caused by either butyrate or glycine uptake were similar whereas in case of propionate, acidification was 2-fold higher than with glycine. Similarly, acetate induced also 2-fold higher acidification rates than glycine. This suggests that the maximal transport rates of PAT1 for propionate and acetate uptake are higher than those for glycine. That PAT1 possesses different maximal transport rates for its substrates was shown also for glycine and betaine which have almost the same apparent substrate affinity, but betaine induces only 60% of the maximal currents of glycine.

Acetate, propionate and butyrate displayed concentration-dependent inhibition of amino acid influx. The apparent  $K_i$  values (5.6 - 12.0 mM) for PAT1 are in the same range as the apparent  $K_m$  (1 - 15 mM) found for the amino acid substrates. In comparison, PAT2 displays

affinities in the range of 100 - 700  $\mu\text{M}$  for Gly, Ala, Pro, but displays much lower affinities for butyrate (7.6 mM). This confirms the observation that PAT2 is more restrictive with regard to the structural requirements in substrates for high affinity recognition than PAT1.

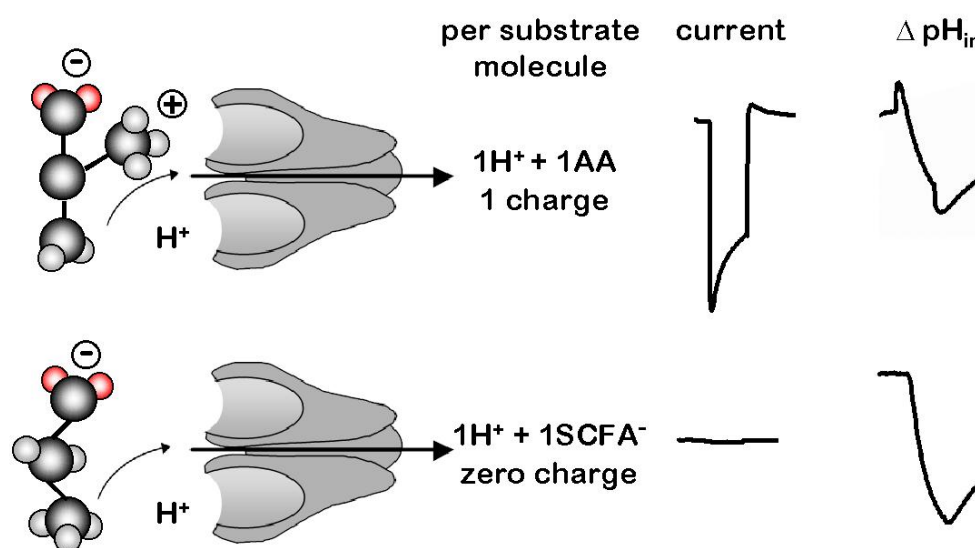


**Figure 14: A scheme for the transport of neutral amino acids and anionic monocarboxylic acids by PAT1 and PAT2.** The substrate binding pockets of the PAT transporters can accommodate neutral amino acids as well as the analogous negatively charged SCFAs. Amino acid substrates induce inward currents in PAT expressing oocytes and lead to a strong intracellular acidification. Transport of the negatively charged SCFA substrate results in an electroneutral transport mode by simultaneously acidification inside the cell.

PAT1 and PAT2 are two of the few known transporters for which transport of short-chain fatty acids has been described on the molecular level. Up to date, only two additional transporter proteins that mediate uptake of SCFAs have been characterised at the molecular level, the **monocarboxylate transporter** MCT1 (SLC16A1) and the **sodium-coupled monocarboxylate transporter** SMCT (SLC5A8).

MCT1 was shown to catalyse the proton-coupled transport of monocarboxylates such as lactate, pyruvate and ketone bodies (Halestrap AP et al., 1999; Halestrap AP et al., 2004). In addition, MCT1 also recognises acetate, propionate and butyrate as substrates, as shown after expression of MCT1 in *Xenopus laevis* oocytes and after transfection into MDA-MB231 cells (Broer S et al., 1998; Tamai I et al., 1999). MCT1 is expressed in almost all tissues, inter alia in caecum, colon and in kidney cortex (Halestrap AP et al., 1999; Halestrap AP et al., 2004). However, it is still under discussion whether MCT1 localises to the apical or basolateral surface in this epithelial tissues (Garcia CK et al., 1995; Lambert DW et al., 2002).

SMCT mediates  $\text{Na}^+$ -coupled SCFA transport after expression in *X. laevis* oocytes (Miyachi S et al., 2004). This transporter is abundantly expressed in the colon and was cloned from a human intestinal RNA-pool. The substrate specificity of SMCT is similar to that of MCT1, given that lactate, pyruvate, and the SCFAs acetate, butyrate, and propionate have been

shown to be transported by SMCT. However, this transporter exhibits no sequence similarity to MCT1 (Miyachi S et al., 2004) and localisation of the SMCT1 protein has not been determined yet (Miyachi S et al., 2004).

Transmembrane transport of SCFAs is assumed to occur by *a*) non-ionic diffusion, *b*) SCFA/anion-exchange and *c*) SCFA/proton symport mechanisms. The quantitative contribution and importance of each process to the overall SCFA uptake is discussed controversially. Permeation of a non-dissociated SCFA occurs rapidly by its neutral character followed by a fast intracellular dissociation (Ruppin H et al., 1980; Charney AN et al., 1998). Hereby, the driving force is the transmembrane concentration gradient of the protonated SCFA and the transmembrane pH gradient. In particular in colonic tissues, various studies have assessed the transport mode for SCFAs (that are produced in huge quantities by bacterial fermentation) and it is believed that SCFA transport here occurs via a bicarbonate/SCFA exchange mechanism (Mascolo N et al., 1991; Reynolds DA et al., 1993; von Engelhardt W et al., 1994; Ritzhaupt A et al., 1998; Tyagi S et al., 2002). Besides anion exchange processes, also a proton/SCFA symport mechanism was proposed. Studies in the intestinal epithelial cell line Caco-2 (Stein J et al., 2000) and in isolated epithelial cells from rabbit proximal colon (DeSoignie R et al., 1994) provided evidence for such a proton/SCFA cotransport system.

In summary, it is demonstrated that the mammalian PAT proteins 1 and 2 are novel bifunctional proton-coupled symporters that operate in an electrogenic mode with amino acid substrates such as glycine, alanine, proline or GABA or in an electroneutral mode when the substrates lack an amino group. The demonstration of PAT-mediated proton/SCFA symport suggests a new function of these transporters in mammalian physiology.

## 5. *Caenorhabditis elegans* homologues of the mammalian PAT transporters

Homology searching of the *Caenorhabditis elegans* genome sequence revealed the presence of 6 genes encoding close homologues to the mammalian PAT family, each having at least 48% similarity with the PAT1 transporter. A dendrogram constructed from the predicted protein sequences is shown in Figure 15A. Two of the six *C. elegans* homologues (T27A1.5 and Y43F4B.7) are more closely related to the mammalian transporters than to the other predicted *C. elegans* amino acid transporters. However, all six *C. elegans* homologues possess a highly conserved region which is also found in the mammalian PAT proteins (Figure 15B), and the closest relationship to mammalian proteins is found for the mammalian PAT proteins. The high homology of T27A1.5 and Y43F4B.7 with the mammalian PATs suggests that (at least) these two genes possibly encode for *C. elegans* proton/amino acid transporters.

Using total RNA from mixed stage *C. elegans* and specific primers for the 6 different *C. elegans* PAT-like genes, the full length cDNAs of T27A1.5, Y43F4B.7, and F59B2.2 were amplified. The cDNAs were sequenced and were identical to the *C. elegans* data base entries. After cloning of the DNA products into a cRNA expression vector (pCRII, Invitrogen) the cRNA was synthesised. However, injection of the respective cRNA into *Xenopus laevis* oocytes resulted neither in electrogenic transport of any given amino acid nor in an enhanced uptake of one of the mammalian PAT amino acid substrates (Gly, Ala, and Pro). Whether this is due to a lack of expression of the respective transport protein abundantly enough or improper targeting of the expressed protein to the oocyte membrane is not known.

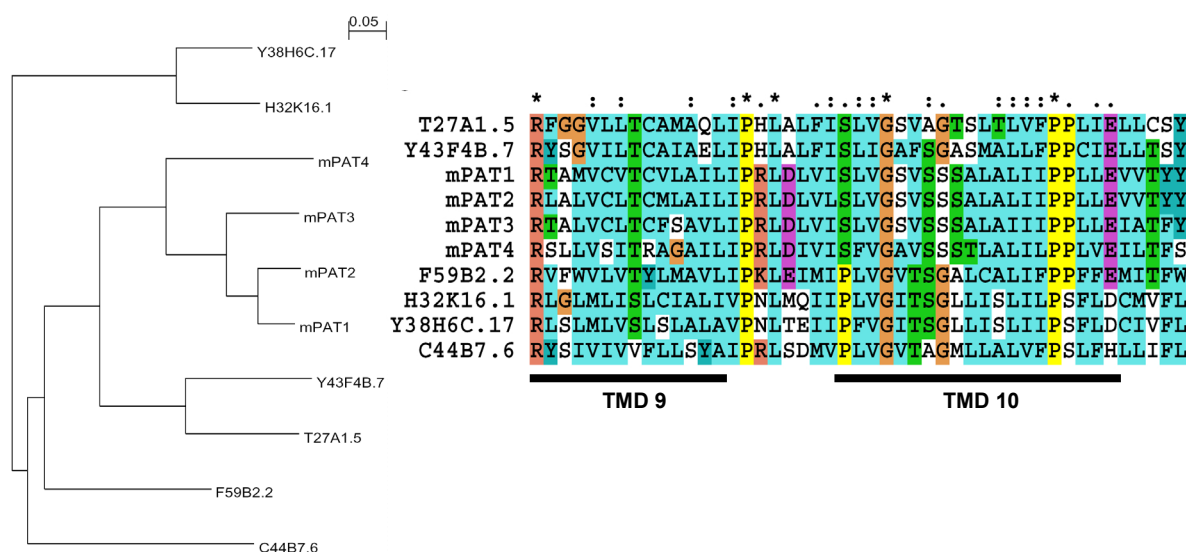


**Figure 15: Six *C. elegans* genes are closely related to the mammalian PAT family.**

**A:** Dendrogram of mammalian PAT proteins and *C. elegans* homologues. The dendrogram was prepared by amino acid sequence alignment and neighbour joining method using the ClustalX 1.8 program. **B:** Multiple sequence alignment of a highly conserved region in the PAT proteins. Using the Block Maker program (Henikoff S et al., 1995) 5 highly conserved regions were identified, the highest conserved region is shown. Single, fully conserved residue (\*), "strong" groups, fully conserved (:), and "weak" groups, fully conserved (.) are indicated.

## 6. Proposed physiological and pharmacological roles of the PAT transporters

Almost 20 years ago it was reported that selected amino acids in mammals may be absorbed in a proton-dependent manner (Jorgensen KE et al., 1987), and several functional studies have been conducted to characterise this process. The cloning of the corresponding gene and the identification of a new family of proton/amino acid transporters in mammals substantially advances our knowledge of these transporters in respect to kinetics, specificity, ion coupling and tissue distribution. However, data on endogenous functional expression of the PAT proteins are very limited and defined physiological roles of the PAT transporters can not be predicted.

Prime substrates for the PAT carriers are the amino acids glycine, L-alanine and L-proline. These compounds have been shown to be transported by the cloned transporters after heterologous expression in different cell systems [Appendix 1] (Chen Z et al., 2003a, b; Sagne C et al., 2001; Wreden CC et al., 2003).

Expression of the PAT1 protein in the apical membrane of Caco-2 cells was demonstrated by Chen Z. et al. (2003a) and that PAT1 is in fact expressed in the luminal membrane of mouse small intestine is demonstrated in Fig. 16.

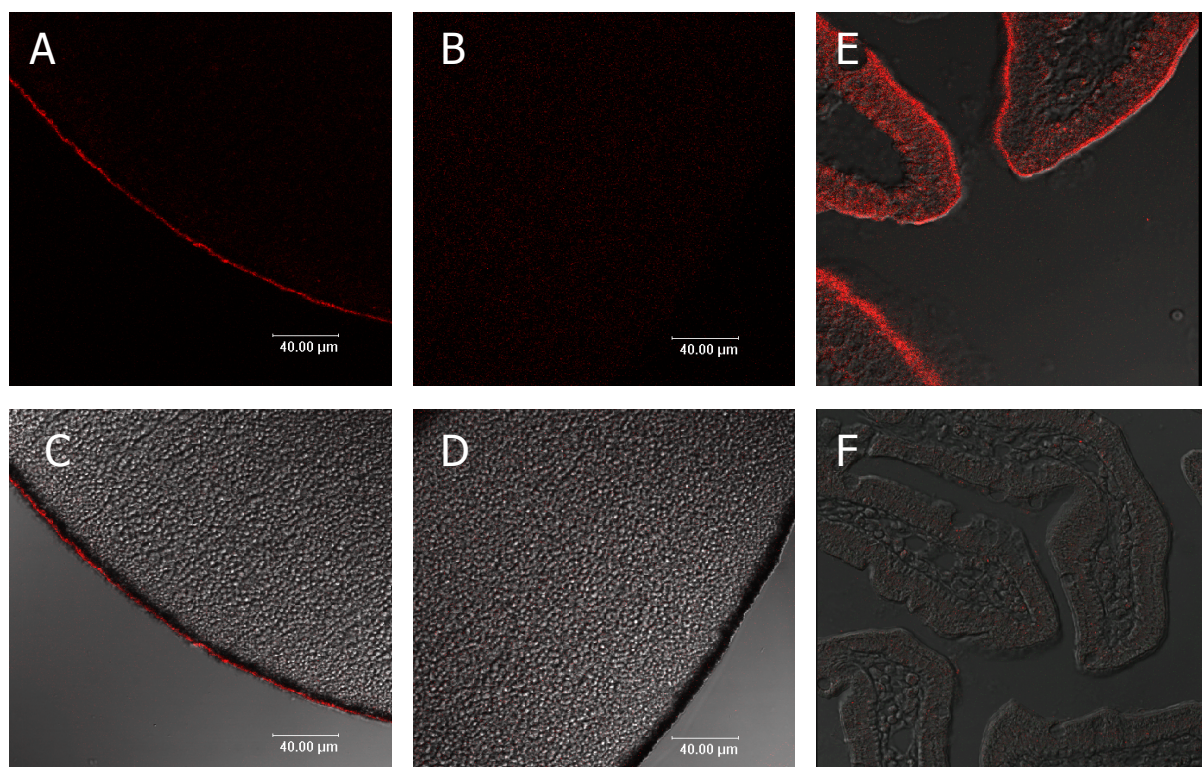


**Figure 16: Immunofluorescence detection of PAT1 in murine small intestine and PAT1 expressing *X. laevis* oocytes.** A-D, for determination of PAT1 antibody specificity immunofluorescence studies were performed using 8 μm cross sections of *X. laevis* oocytes injected with mPAT1 cRNA (A) or *X. laevis* oocytes injected with water (B) and incubated with anti-PAT1 antibody. C, and D are phase contrast micrographs of the A, and B, respectively. Immunofluorescent detection of mPAT1 in mouse small intestine was performed using either the anti-PAT1 antibody alone (E) or following pre-incubation of the antibody with antigenic peptide (F). The antibody was raised against rat PAT1 specific residue 16 amino acids long at the intracellular N-terminus of PAT1. These residues are fully conserved between mouse and rat. (The antibody was kindly provided by Bruno Giros, Paris).

Very recently it has been demonstrated in the Thwaites laboratory that the PAT1 protein is localised in the brush border membrane also in the human intestine [Appendix 8, Fig. 4]. PAT1 as a low-affinity, high capacity transporter most likely plays an important role in both nutrient and drug absorption from the intestinal lumen into enterocytes.

During protein digestion the intestinal lumen contains a huge spectrum of proteolytic degradation products, including small peptides and free amino acids. These products have to enter the enterocytes via specific transport proteins. PAT1 transports Gly, Ala and Pro with high transport rates, but also  $\beta$ -amino acids ( $\beta$ -Ala), N-methylated amino acids (e.g. betaine) and sulphur-containing derivatives (taurine, high abundant in meat, fish) are accepted as substrates. Therefore, PAT1 is so far the only protein entity identified in the mammalian small intestine transporting this combination of substrates. The system A transporter SNAT2 (SLC38A2), also expressed in the small intestine, mediates uptake of Gly, Ala, Pro, but it excludes the other substrates mentioned (Mackenzie B et al., 2004). Different transport proteins for the osmolytes betaine and taurine are known. However, the betaine and GABA transporter BGT-1 (SLC6A12) is generally localised in the basolateral membrane for example in renal epithelial cells and shows strong expression in brain (Chen NH et al., 2004). The transporter TAUT (SLC6A6) which transports taurine with high affinity is also expressed mainly in kidney and brain, but is not found in the small intestine (Chen NH et al., 2004). Taken this into consideration it seems reasonable, to postulate that PAT1 is the transporter responsible for the absorption of the osmolytes betaine and taurine within mammalian intestine.

Only two amino acid transport systems within the mammalian small intestine have been described functionally to transport the imino acid proline. The rat "imino acid carrier" and the IMINO system detected in rabbit jejunal brush border membrane vesicles. The substrate selectivity of the partially  $\text{Na}^+$ -dependent rat "imino acid carrier" is very similar to that of PAT1, as glycine, proline, sarcosine, methyl-aminoisobutyric acid, GABA, and  $\beta$ -alanine are accepted as substrates (Newey H et al., 1964; Daniels VG et al., 1969; De la NJ et al., 1971). Additionally, PAT1 function has been demonstrated to be partial  $\text{Na}^+$ -dependent, due to a functional cooperation with the  $\text{Na}^+/\text{H}^+$  exchanger NHE3 [Appendix 8, Fig. 1-3]. In contrast, the rabbit IMINO acid carrier excludes a variety of PAT1 substrates, inter alia glycine, GABA, taurine, and  $\beta$ -alanine and is strictly dependent on sodium (Wright EM et al., 1984; Stevens BR et al., 1987; Munck LK et al., 1992). Therefore, PAT1 appears to represent the human and mouse homologue of the "imino acid carrier" described in rat, whereas the IMINO acid carrier is clearly a different entity [Appendix 8, Fig. 5].

By using a different driving force (the pH gradient) as most of the other amino acid cotransporters (mainly using the  $\text{Na}^+$  gradient) PAT1 provides an additional route in overall amino acid absorption. The existence of PAT1-mediated transport of MeAIB in a mammalian

tissue has been demonstrated for the first time only very recently using intact rat small intestinal tissue preparations [*Appendix 8, Fig. 6*].

Other proton-dependent transporters involved in intestinal amino acid absorption are peptide transporters. The high capacity di- and tripeptide transporter PEPT1, which is strongly expressed in the apical membrane of the small intestine, is additionally responsible for efficient uptake of amino acid nitrogen by transporting peptide-bound amino acids (Daniel H, 2004). The importance of this system in overall amino acid absorption is demonstrated by the fact, that patients with genetic defects in intestinal transport proteins transporting essential amino acids do not develop a deficiency when the essential amino acid is supplied in peptide-bound form as shown for lysine in cystinuria patients (Hellier MD et al., 1971; de Sanctis L et al., 2001).

PAT1 also seems to provide a route for oral absorption of therapeutic compounds. So far, PAT1 is the only intestinal transporter that has been shown to transport the orally administered compounds D-serine and D-cycloserine, and betaine (Table 4). D-serine and D-cycloserine are used in the treatment of affective disorders as schizophrenia, ataxia and post traumatic stress disorder, whereas betaine is used in the treatment of homocystinuria (Smolin LA et al., 1981; Heresco-Levy U et al., 2002; Evins AE et al., 2002; Ogawa M et al., 2003). Additionally, we demonstrated convincingly that the antiepileptic drug vigabatrin is a good PAT1 substrate. Vigabatrin displays high affinity to human as well as murine PAT1 (unpublished observation). Also a couple of other GABA analogues and derivatives, which are used to treat affective disorders, have been shown to be transported efficiently via PAT1 [*Appendix 8, Fig. 5*]. Moreover, in a very recent study, transport of various pharmacologically active proline- and GABA-derivatives was investigated using the classical Caco-2 model (Metzner L et al., 2004). The oral availability of all these compounds is quite high and PAT1 in the small intestine is the best candidate to be responsible for the efficient uptake of these compounds.

The expression of PAT1 in the colon in combination with its ability to transport short-chain fatty acids and D-amino acids suggests an additional physiological role. In the colon huge quantities of SCFAs emerge from bacterial fermentation of non-digestible carbohydrates. Concentrations of SCFAs between 70 mM and 120 mM have been reported and also significant quantities of D-amino acids, especially D-serine and D-alanine are produced by the colonic microflora (Bergman EN, 1990). It seems plausible to postulate that these fermentation products are absorbed in the colon, at least in part, via PAT1. SCFAs are important in maintaining the mucosal barrier in the colon, they are regarded as a major energy source and have been shown to act in a beneficial, protective manner against colon cancer. Portal blood of different species has concentrations of SCFAs in the range from 0.4 mM to 5.3 mM (Pomare EW et al., 1985; Bergman EN, 1990) and SCFAs delivered to the

circulation serve as metabolic fuel of the liver and other peripheral tissues (Remesy C et al., 1980; Bergman EN, 1990). D-serine, absorbed by PAT1 in the colon, may exert an influence on glutamatergic neurotransmission in the brain by binding to the D-serine sensitive glycine binding site of the NMDA receptor. D-Serine is present in the systemic circulation and has access to the central nervous system, given that the heterodimeric amino acid transporter LAT1, which has also the ability to transport D-serine, is expressed at the blood brain barrier (Boado RJ et al., 1999). PAT1 is also strongly expressed in choroid plexus, but is not found in the cerebral blood brain barrier (Agulhon C et al., 2003). Furthermore, NMDA-receptors have been found to be functionally expressed in several non-neuronal tissues such as pancreas, skin, fat and bone (Skerry TM et al., 2001).

With regard to NMDA receptors, a potential physiological role of PAT2 has also to be addressed. Immunohistochemical and functional studies indicated that PAT2 in mouse brain is expressed in neurons which are positive for the NMDA subtype glutamate receptor subunit NR1 [*Appendix 4, Fig. 3*]. Within these neurons PAT2 localises mainly to the endoplasmatic reticulum and recycling endosomes, and only a small amount of PAT2 is targeted to the plasma membrane. Functional characterisation revealed that PAT2-type transport is bidirectional, most likely not affected by pH alterations and translocates glycine with a considerably low affinity (in comparison to other neuronal glycine transport systems), which is able to bind at the NMDA glutamate receptor subunit NR1. Therefore, by regulating extracellular glycine levels it is possible that PAT2 modulates the activity of the NMDA glutamate receptor. A similar mechanism has been proposed for the glycine transporter GlyT1 in nerve terminals (Lopez-Corcuera B et al., 2001). However, it needs to be mentioned that a colocalisation between PAT2 and the NMDA glutamate receptor could not be shown within the synapse. Based on mRNA level, PAT2 is expressed in a variety of tissues [*Appendix 2, Fig. 6*], inter alia bone and fat tissue (Bermingham JRJ et al., 2004), but the cell types that express PAT2 outside the CNS have not been determined. Expression of NMDA glutamate receptors has been found in bone as well as in adipocytes and it seems to be that glutamate/glycine signalling is important for metabolism in these tissues (Skerry TM et al., 2001) and functions similarly to their neuronal counterparts (Gu Y et al., 2002).

Beside PAT2 also the PAT1 protein is expressed in the central nervous system (Sagne C et al., 2001; Boll M et al., 2002; Wreden CC et al., 2003; Agulhon C et al., 2003). PAT1 has been cloned from rat brain as a transporter mainly localised in the lysosomal membrane (Sagne C et al., 2001), but localisation in synaptic vesicles and plasma membranes has been demonstrated at least in neuronal cell cultures (Wreden CC et al., 2003). In the central nervous system amino acids play roles as neurotransmitters, synaptic modulators and precursors of neurotransmitters. Degradation of membrane proteins after endocytosis (for termination of signalling by receptor internalisation, elimination of misfolded proteins) within

lysosomes and subsequent release of the endproducts from lysosomes, maintain protein turnover. Therefore, PAT1 driven by the acidic intralysosomal pH may serve to maintain low concentrations of glycine, alanine and proline within the lumen of the lysosomes and thereby save neuronal metabolic energy by providing these amino acids for protein biosynthesis or for neurotransmitter storage and release. Defects in lysosomal release mechanisms have been described to result in affected disorders, like cystinosis, which results from mutations in a lysosomal cystine efflux transporter (Kalatzis V et al., 2001).

Another physiological important annotation is the distinct subcellular localisation of the PAT1 protein in different tissues/cell types. PAT1 is expressed in the brush border membrane of human [Appendix 8, Fig. 4] and mouse (Fig. 16) small intestine and is exclusively expressed in the apical membrane in Caco-2 cells (Chen Z. et al 2003a), whereas in the rat cortex and hippocampus PAT1 is mainly detected in the membrane of lysosomes (Sagne C. et al. 2001). Simultaneously expression of PAT1 in both compartments, plasma membrane as well as lysosomal membrane, has been shown *in vitro* in cultures of hippocampal neurons (Wreden CC et al. 2003). The latter investigators found that endogenous PAT1 is functionally expressed at the cell surface of hippocampal neurons and also localises to intracellular compartments, like lysosomes and synaptic vesicles as shown with the colocalisation markers LAMP1 (lysosomal membrane glycoprotein 1) and synaptophysin (Wreden CC et al., 2003). Additional data on endogenous expression and subcellular localisation of the PAT1 protein in other tissues than brain and small intestine are not yet available. Whether the PAT1 protein is targeted to the apical membrane of epithelial cells or to intracellular lysosomal membranes or to both compartments is obviously dependent on the tissue and/or cell type where the protein is expressed. Splice variants leading to different protein localisations in distinct cellular regions have been reported for many proteins. For example, the DMT1+IRE (divalent metal transporter 1, iron responsive element) but not its isoform DMT1-IRE (lacking the iron response element), is localised in the apical membrane of enterocytes mediating the uptake of Fe<sup>2+</sup> and other divalent cations (Garrick MD et al., 2003). On the other hand DMT1-IRE is expressed in macrophages and sertoli cells in intracellular membranes of phagosomes as well as of lysosomes, indicating an IRE-mediated targeting mechanism in certain cell types. (Tabuchi M et al., 2002). In addition, differentially spliced PAT1 transcripts resulting in proteins with distinct truncated C-termini have been described recently (Bermingham JRJ et al., 2004). The functions of the truncated PAT1 proteins have not been characterised. They may be non-functional proteins or may inhibit the function of normal PAT1 by interaction with intracellular proteins required for targeting of PAT1 into a specific compartment (Bermingham JRJ et al., 2004).

Whether the truncated PAT proteins are functionally expressed in extraintestinal and extraneuronal tissues, must be determined by combined immunohistochemical studies and transport measurements with e.g. membrane preparations of the selected tissues.

PAT1 and PAT2 have been shown to be expressed in a variety of tissues on mRNA level, but the physiological function of both transporters in these tissues is also not known. However, both nutritional and pharmacological relevant roles of PAT1 can be anticipated in renal tissues by its potential involvement in the reabsorption of amino acids and derivatives from the primary filtrate. Proton-dependent amino acid transport activity has been shown in the proximal tubule of rabbit kidney (Jessen H et al., 1988b). The characteristics of this transport system is, based on substrate affinity and specificity very similar to the PAT1 system in small intestinal cells, but hitherto the PAT1 protein has not been localised in cells of the renal tubular system. The proton/peptide transporters PEPT1 as well as PEPT2 are also functionally expressed in the apical membrane of renal tubular cells, suggesting that proton-dependent transport processes play an important role in kidney.

In analogy to the high affinity type peptide transporter PEPT2 a physiological function of the PAT2 transporter may be postulated for lung tissues. The PEPT2 protein has been demonstrated to be localised in the human lung, more precisely in the alveolar type II pneumocytes. PEPT2 is functional in these cells, as revealed by uptake studies with PEPT2 specific substrates (Groneberg DA et al., 2001; Groneberg DA et al., 2002; Groneberg DA et al., 2004) Type II pneumocytes are responsible for the secretion of surfactant proteins, which serve to regulate alveolar surface tension. The surfactants are essential for lung function, but an excess of these proteins would lead to obstruction of the airway epithelia. Therefore, enzymes for surfactant degradation and uptake mechanisms for the degradation products contribute to a normal lung function (Mager S et al., 2003). In the alveolar lumen high concentrations of free amino acids have been reported and several transporters have been identified in the luminal membrane of alveolar epithelial cells, which might be involved in removing of protein degradation products (Mager S et al., 2003). PAT2 is expressed at high levels in the murine lung and also the mRNA of the orphan transporter PAT4 is abundantly found here (Introduction, figure 8) [*Appendix 2, Fig. 6*]. However, given that the cell types that express PAT2 and/or PAT4 have not been determined and functional evidence for a proton-activated transport system for small and neutral amino acids in alveolar epithelia is missing, it is too early to propose a physiological role of PAT2 in airway epithelia.

Further immunolocalisation studies in combination with functional studies in specific cell lines and/or membrane preparations of different tissues will eventually define the physiological roles of the PATs. Similarly, animal models with a targeted inactivation of the genes encoding the PAT proteins should reveal the physiological functions of the carriers in metabolism.

## 7. Potential pathological implications of PAT1 and PAT2

The observed substrate specificity of PAT1 and PAT2 as well as their chromosomal localisation makes these transporters candidate genes for inherited diseases and the cause of specific aminoacidurias.

PAT1 and/or PAT2 could play a role in the autosomal recessive disease iminoglycinuria (OMIM 242600). This disorder is characterised by a selective urinary loss of the imino acids proline and hydroxyproline as well as of glycine due to a defect in renal tubular reabsorption (Rosenberg LE et al., 1968). However, iminoglycinuria features a genetic heterogeneity with some patients showing only a hyperglycinuria after glycine loading (Scriver CR, 1989). Similar transport defects in the intestinal absorption of these amino acids are also reported (Scriver CR, 1989). Proline, hydroxyproline and glycine are high affinity substrates of the PAT transporters and PAT1 and PAT2 have been shown to be strongly expressed in kidney [Appendix 1, Fig. 6 and Appendix 2, Fig. 6]. Moreover, PAT1 has been shown to be functionally expressed in the small intestine (also PAT2 is abundant in the small intestine but with very low expression levels). This suggests that this protein is involved in iminoglycinuria. However, alanine which is a high affinity PAT1 and PAT2 substrate is not elevated in the urine of iminoglycinuric patients (Scriver CR, 1989). Admittedly, for alanine a variety of renal amino acid transport systems (e.g. system b<sup>0+</sup>) are known to be involved in its tubular reabsorption (Palacin M et al., 1998), which may compensate a defect in another specific transport system. So far, no other transport system is known (at its functional as well as molecular level) which substrates specificity fits better within the pattern of urinary amino acid loss of iminoglycinuria, neither the Na<sup>+</sup>-dependent glycine transporters (GLYT1 and GLYT2, which do not recognise proline as substrate) nor the Na<sup>+</sup>-dependent IMINO system (which does not accept glycine as a substrate) (Ganapathy V et al., 1983; Guastella J et al., 1992; Liu QR et al., 1992). Further studies by means of PAT1 and PAT2 immunolocalisation in the mammalian kidney and the genetic mapping are needed to investigate the role of both PAT transporters in iminoglycinuria.

The localisation of the human PAT1 - 3 transporters on chromosome 5 within in the region q31-q33 makes them candidates to be involved in the development of the symptoms observed in the so called 5q-Syndrome. This myelodysplastic haematological disorder has been mapped to the same region and is characterised by the loss of a part of chromosome 5, with a minimum region containing 34 genes including the PAT1 - 3 genes. A consequence of this deletion is a refractory macrocytic anaemia and the formation of megakaryocytes within the bone marrow (Van den Berghe H et al., 1997). That the mRNA of PAT2 is expressed in myelin protein zero positive (P0+) bone marrow cells has been shown by Bermingham JR et al. (2004). The authors assume, based on the knowledge that maturation of megakaryocytes requires NMDA glutamate receptor signalling, that a loss of PAT2 could lead to an altered

glutamnergic signalling (due to the loss of transport of the NMDA glutamate receptor ligands glycine) and thereby contribute to the aetiology of this myelodysplastic disease. However, the 5q-Syndrome does not represent a single-gene disorder, it is rather a contiguous gene syndrome resulting from defects in several genes. Of key importance in the development of the 5q-Syndrome is most likely the involvement of Interleukin-5 gene (an eosinophil differentiation factor), and the neighbouring genes as CDC25C (a mitosis inducer), Interleukin-3 (a haematopoietic colony-stimulating factor), and CSF2 (necessary for the survival, proliferation, and differentiation of haematopoietic progenitor cells) (Van den Berghe H et al., 1997).

Malfunctions of the PAT1 system is clearly not the cause for the autosomal recessive Hartnup disorder (OMIM 234500) in which transport of neutral amino acids is impaired. The severe symptoms in Hartnup disease are mostly caused by the lack of intestinal uptake and renal reabsorption of tryptophan (which is not a PAT1 substrate) (Levy HS, 1995). Beside tryptophan also glutamine, valine, phenylalanine, leucine, asparagine, isoleucine, threonine, histidine, serine and the PAT1 substrate alanine show reduced intestinal absorption and are found in high concentrations in urine (Levy HS, 1995). However, also a partial contribution of PAT1 can be excluded, as urine levels of proline, hydroxyproline, (in addition to methionine and arginine) are unchanged in the Hartnup disorder (Levy HS, 1995). Only very recently it has been demonstrated that Hartnup disease is caused by mutations in the gene of the neutral amino acid transporter B(0)AT1 (SLC6A19) which is expressed in renal proximal tubules and small intestinal epithelia (Seow HF et al., 2004; Kleta R et al., 2004).

It is also important to mention that PAT1 function may be affected in certain disease states. This could be due to an altered function of the sodium/proton exchanger NHE3, which is responsible for maintaining a constant intracellular pH and generates the pH gradient and thereby perpetuates the driving force of PAT1. That proton-driven solute transport is impaired by inhibition of NHE3, via a downregulation by protein kinase A following an increase of cAMP levels, has been demonstrated for the peptide transporter PEPT1 in Caco-2 cells (Thwaites DT et al., 2002). An inhibition of NHE3 is also induced by the enteric neuropeptide VIP (vasoactive intestinal peptide) and inhibition of PEPT1 transport by VIP has also been demonstrated (Anderson CM et al., 2003). Several pathophysiological conditions are known which increase plasma VIP levels, e.g. enterotoxin-induced diarrhoea and VIP-producing tumours. Additionally, the cholera enterotoxin can directly increase intracellular cAMP levels (Field M, 2003). Under these conditions PAT1 function may be indirectly impaired and result in a decreased absorption nutrients and orally administered drugs transported by PAT1.

## 8. Future perspectives

Identification of the PAT genes enabled us and others to predict preliminary the structure of the proteins and to describe in detail the functional characteristics of the mammalian PAT transporters. Future studies have to address the protein structure, targeting, regulation and further physiological function of PAT1 and PAT2. Furthermore, the functions of the orphan members PAT3 and PAT4 are still unknown.

In this thesis the minimal molecular requirements in PAT substrates are presented and functional groups in substrates that may interact with residues in the transporter protein have been defined. However, nothing is known about the protein structure and which amino acid residues in the transporter are important for substrate and proton binding. Within the PAT family two conserved histidyl-residues have been identified and predicted to reside in trans-membrane segments. Do they contribute to proton binding? What determines the difference in affinity and specificity between PAT1 and PAT2, although both transporters share such a high similarity in protein sequence? Construction of several chimeric proteins consisting of either PAT1 and PAT2 regions and generation of deletion mutants would be very helpful to answer these questions. The predicted topology models have to be experimentally verified and it has to be clarified whether the PATs are functionally inserted in the plasma membrane as homo-monomeric or homo-oligomeric proteins.

For a better understanding of the physiological role of the transporters, it is important to know in which organs the PAT proteins are functionally expressed and in which subcellular compartment they are localised. Another interesting question is, which molecular determinants lead to the divergent targeting of the PAT1 protein to the lysosomal membrane and/or to the plasma membrane. There may be not yet identified regulatory subunits present which control and direct the transporter to the distinct compartment.

It has been shown for several plasma membrane amino acid transporters that they are regulated via several proteinkinases. PAT1 as well as PAT2 possess recognition sites for proteinkinase C and A. The proteinkinase C recognition site is fully conserved in PAT1, as this motif is found in the human, rat, and mouse sequence. Therefore, PAT1 might be regulated in transport activity by hormones or metabolic changes via PKC signalling pathway. For PAT2 it has been shown that the protein is localised in part in recycling endosomes in neuronal cells, indicating that this transporter may undergo a recycling by retrieval and fusion of plasma membrane vesicles containing the transporter.

The observation that the PATs are expressed in extra-epithelial tissues is of particular interest and leads to the question of what physiological role the PAT1 and PAT2 proteins are

playing in these organs. Are they implicated in the intracellular distribution of amino acids and/or do they play a role in the intercellular and interorgan flux of amino acids?

Understanding the molecular functions of this interesting transporter family, which is widespread in nature and is found in humans but also in plants, yeast and lower eukaryotes and that mediates transmembrane transport of amino acids and amino acid derivatives could provide new insights into the physiology of life.

## ZUSAMMENFASSUNG



## ZUSAMMENFASSUNG

Die Epithelzellen von Dünndarm und Niere besitzen die Fähigkeit, aus dem Lumen kleine, neutrale Aminosäuren und deren Derivate in einem protonengekoppelten Transportschritt aufzunehmen (System PAT). In dieser Arbeit wird die molekulare Grundlage für diese Transportaktivität erstmals beschrieben und eine neu identifizierte Familie von Protonen-Aminosäure-Transportern (PAT) in Säugetieren charakterisiert. Die PAT-Familie umfasst vier Mitglieder (PAT1 - 4), die eine sehr hohe Ähnlichkeit hinsichtlich ihrer Aminosäuresequenz und putativen Membrantopologie aufweisen (11 Transmembrandomänen). Orthologe Proteine dieser Familie wurden in *Drosophila melanogaster* und *Caenorhabditis elegans* identifiziert. Die murinen Transporter zeigen auf mRNA-Ebene ein heterogenes Expressionsmuster. PAT1 wird unter anderem sehr stark in der Niere und im Dünndarm exprimiert. Das PAT1-Protein konnte mittels eines spezifischen Antikörpers in der Bürstensaummembran des Dünndarmes der Maus nachgewiesen werden. Auf funktioneller Ebene entsprechen die Transportcharakteristika des heterolog exprimierten PAT1 dem aus transportphysiologischen und biochemischen Studien bekannten System PAT. Die durch PAT1 vermittelte Aufnahme von Gly, Ala, Pro, deren D-Isomere und einer Vielzahl von Aminosäurederivaten, wie Betain, GABA und Taurin ist elektrogen und protonengekoppelt. Neben diesen physiologischen Substraten konnten ebenso pharmakologisch und therapeutisch relevante Verbindungen als Substrate von PAT1 identifiziert werden. Die Affinitäten der PAT1-Substrate liegen im Bereich von 1 - 10 mM. PAT2 ist stark im zentralen Nervensystem, der Lunge und dem Herzen exprimiert. PAT2 besitzt ähnliche Transporteigenschaften wie PAT1, weist aber 10 - 30mal höhere Affinitäten (100 - 1000  $\mu$ M) zu den identischen Substraten auf als PAT1 und hat ein engeres Substratspektrum. Den Transportern PAT3 und PAT4 konnte bisher noch keine Funktion zugeordnet werden. Folgende strukturelle Eigenschaften von aliphatischen Aminosäuren konnten als essentielle Parameter für den Transport von PAT1 und PAT2 determiniert werden: a) eine nicht-substituierte Carboxylgruppe, b) eine kurze Seitenkette der Aminosäure und c) eine maximale Distanz von 3 bzw. 2  $\text{CH}_2$ -Gruppen zwischen Amino- und Carboxylgruppe. Eine freie Aminogruppe ist nicht essentiell für den PAT1 und PAT2 vermittelten Transport. Dies erklärt auch, dass kurzkettige Fettsäuren als Substrate fungieren, die im Gegensatz zu den Aminosäuren elektroneutral transportiert werden. Beide Transporter binden ein Proton und ein Substrat in einem geordneten Mechanismus, bei dem zuerst das Proton an den Transporter bindet. PAT1 und PAT2 weisen unterschiedliche Protonenaktivierungskonstanten auf. PAT2 transportiert bei physiologischem pH unter  $\text{H}^+$ -Sättigung, PAT1 scheint dagegen durch eine funktionelle Kooperation mit dem  $\text{Na}^+/\text{H}^+$ -Austauscher NHE3 in seiner Aktivität regulierbar. Diese neue Protonen-Aminosäure-Transporter-Familie nimmt eine Ausnahmestellung in der Säugetierphysiologie ein.



## REFERENCES

## REFERENCES

- [1] Agulhon, C; Rostaing, P; Ravassard, P; Sagne, C; Triller, A; Giros, B (2003) Lysosomal amino acid transporter LYAAT-1 in the rat central nervous system: an in situ hybridization and immunohistochemical study. *J Comp Neurol* **462**: 71-89.
- [2] Anderson, CM; Mendoza, ME; Kennedy, DJ; Raldua, D; Thwaites, DT (2003) Inhibition of intestinal dipeptide transport by the neuropeptide VIP is an anti-absorptive effect via the VPAC1 receptor in a human enterocyte-like cell line (Caco-2). *Br J Pharmacol* **138**: 564-573.
- [3] Arriza, JL; Kavanaugh, MP; Fairman, WA; Wu, YN ; Murdoch, GH; North, RA; Amara, SG (1993) Cloning and expression of a human neutral amino acid transporter with structural similarity to the glutamate transporter gene family. *J Biol Chem* **268**: 15329-15332.
- [4] Barak, AJ; Beckenhauer, HC; Mailliard, ME; Kharbanda, KK; Tuma, DJ (2003) Betaine lowers elevated s-adenosylhomocysteine levels in hepatocytes from ethanol-fed rats. *J Nutr* **133**: 2845-2848.
- [5] Barker, GA; Wilkins, RJ; Golding, S; Ellory, JC (1999) Neutral amino acid transport in bovine articular chondrocytes. *J Physiol* **514**: 795-808.
- [6] Bergman, EN (1990) Energy contributions of volatile fatty acids from the gastrointestinal tract in various species. *Physiol Rev* **70**: 567-590.
- [7] Bermingham, JRJ and Pennington, J (2004) Organization and expression of the SLC36 cluster of amino acid transporter genes. *Mamm Genome* **15**: 114-125.
- [8] Bermingham, JRJ; Shumas, S; Whisenhunt, T; Sirkowski, EE; O'Connell, S; Scherer, SS; Rosenfeld, MG (2002) Identification of genes that are downregulated in the absence of the POU domain transcription factor pou3f1 (Oct-6, Tst-1, SCIP) in sciatic nerve. *J Neurosci* **22**: 10217-10231.
- [9] Bitoun, M and Tappaz, M (2000) Gene expression of the transporters and biosynthetic enzymes of the osmolytes in astrocyte primary cultures exposed to hyperosmotic conditions. *Glia* **32**: 165-176.
- [10] Boado, RJ; Li, JY; Nagaya, M; Zhang, C; Pardridge, WM (1999) Selective expression of the large neutral amino acid transporter at the blood-brain barrier. *Proc Natl Acad Sci U S A* **96**: 12079-12084.
- [11] Boll, M; Daniel, H; Gasnier, B (2004) The SLC36 family: proton-coupled transporters for the absorption of selected amino acids from extracellular and intracellular proteolysis. *Pflugers Arch* **447**: 776-779.
- [12] Boll, M; Foltz, M; Rubio-Aliaga, I; Daniel, H (2003) A cluster of proton/amino acid transporter genes in the human and mouse genomes. *Genomics* **82**: 47-56.
- [13] Boll, M; Foltz, M; Rubio-Aliaga, I; Kottra, G; Daniel, H (2002) Functional characterization of two novel mammalian electrogenic proton-dependent amino acid cotransporters. *J Biol Chem* **277**: 22966-22973.
- [14] Borden, LA; Smith, KE; Hartig, PR; Branchek, TA; Weinshank, RL (1992) Molecular heterogeneity of the gamma-aminobutyric acid (GABA) transport system. Cloning of two novel high affinity GABA transporters from rat brain. *J Biol Chem* **267**: 21098-21104.
- [15] Breiting, HG and Becker, CM (2002) The inhibitory glycine receptor-simple views of a complicated channel. *Chembiochem*. **3**: 1042-1052.
- [16] Broer, A; Wagner, C; Lang, F; Broer, S (2000) Neutral amino acid transporter ASCT2 displays substrate-induced Na<sup>+</sup> exchange and a substrate-gated anion conductance. *Biochem J* **346**: 705-710.
- [17] Broer, S; Schneider, HP; Broer, A; Rahman, B; Hamprecht, B; Deitmer, JW (1998) Characterization of the monocarboxylate transporter 1 expressed in *Xenopus laevis* oocytes by changes in cytosolic pH. *Biochem J* **333**: 167-174.
- [18] Cammarata, PR; Schafer, G; Chen, SW; Guo, Z; Reeves, RE (2002) Osmoregulatory alterations in taurine uptake by cultured human and bovine lens epithelial cells. *Invest Ophthalmol Vis Sci* **43**: 425-433.
- [19] Chang, HC and Bush, DR (1997) Topology of NAT2, a prototypical example of a new family of amino acid transporters. *J Biol Chem* **272**: 30552-30557.
- [20] Charney, AN; Micic, L; Egnor, RW (1998) Nonionic diffusion of short-chain fatty acids across rat colon. *Am J Physiol* **274**: 518-524.
- [21] Chatterton, JE; Awobuluyi, M; Premkumar, LS; Takahashi, H; Talantova, M; Shin, Y; Cui, J; Tu, S; Sevarino, KA; Nakanishi, N; Tong, G; Lipton, SA; Zhang, D (2002) Excitatory glycine receptors containing the NR3 family of NMDA receptor subunits. *Nature* **415**: 793-798.

- [22] Chaudhry, FA; Krizaj, D; Larsson, P; Reimer, RJ; Wreden, C; Storm-Mathisen, J; Copenhagen, D; Kavanaugh, M; Edwards, RH (2001) Coupled and uncoupled proton movement by amino acid transport system N. *EMBO* **20**: 7041-7051.
- [23] Chaudhry, FA; Schmitz, D; Reimer, RJ; Larsson, P; Gray, AT; Nicoll, R; Kavanaugh, M; Edwards, RH (2002) Glutamine uptake by neurons: interaction of protons with system a transporters. *J Neurosci* **22**: 62-72.
- [24] Chen, NH; Reith, ME; Quick, MW (2004) Synaptic uptake and beyond: the sodium- and chloride-dependent neurotransmitter transporter family SLC6. *Pflugers Arch* **447**: 519-531.
- [25] Chen, Z; Fei, YJ; Anderson, CM; Wake, KA; Miyauchi, S; Huang, W; Thwaites, DT; Ganapathy, V (2003a) Structure, function and immunolocalization of a proton-coupled amino acid transporter (hPAT1) in the human intestinal cell line Caco-2. *J Physiol* **546**: 349-361.
- [26] Chen, Z; Kennedy, DJ; Wake, KA; Zhuang, L; Ganapathy, V; Thwaites, DT (2003b) Structure, tissue expression pattern, and function of the amino acid transporter rat PAT2. *Biochem Biophys Res Commun* **304**: 747-754.
- [27] Christie, GR; Ford, D; Howard, A; Clark, MA; Hirst, BH (2001) Glycine supply to human enterocytes mediated by high-affinity basolateral GLYT1. *Gastroenterology* **120**: 439-448.
- [28] Crane, RK (1965) Na<sup>+</sup>-dependent transport in the intestine and other animal tissues. *Fed Proc* **24**: 1000-1006.
- [29] Crump, FT; Fremeau, RT; Craig, AM (1999) Localization of the brain-specific high-affinity l-proline transporter in cultured hippocampal neurons: molecular heterogeneity of synaptic terminals. *Mol Cell Neurosci* **13**: 25-39.
- [30] Daniel, H (2004) Molecular and integrative physiology of intestinal Peptide transport. *Annu Rev Physiol* **66**: 361-384.
- [31] Daniel, H; Fett, C; Kratz, A (1989) Demonstration and modification of intervillous pH profiles in rat small intestine in vitro. *Am J Physiol* **257**: G489-G495
- [32] Daniels, VG; Newey, H; Smyth, DH (1969) Stereochemical specificity of neutral amino acid transfer systems in rat small intestine. *Biochim Biophys Acta* **183**: 637-639.
- [33] Davies, S; Maenz, DD; Cheeseman, CI (1987) A novel imino-acid carrier in the enterocyte basolateral membrane. *Biochim Biophys Acta* **896**: 247-255.
- [34] De la, NJ; Newey, H; Smyth, DH (1971) Transfer of alanine isomers by rat small intestine. *J Physiol* **214**: 105-114.
- [35] de Sanctis, L; Bonetti, G; Bruno, M; De Luca, F; Bisceglia, L; Palacin, M; Dianzani, I; Ponzzone, A (2001) Cystinuria phenotyping by oral lysine and arginine loading. *Clin Nephrol* **56**: 467-474.
- [36] DeSoignie, R and Sellin, JH (1994) Propionate-initiated changes in intracellular pH in rabbit colonocytes. *Gastroenterology* **107**: 347-356.
- [37] Divino-Filho, JC; Barany, P; Stehle, P; Furst, P; Bergstrom, J (1997) Free amino-acid levels simultaneously collected in plasma, muscle, and erythrocytes of uraemic patients. *Nephrol Dial Transplant* **12**: 2339-2348.
- [38] Evins, AE; Amico, E; Posever, TA; Toker, R ; Goff, DC (2002) D-Cycloserine added to risperidone in patients with primary negative symptoms of schizophrenia. *Schizophr Res* **56**: 19-23.
- [39] Felig, P (1973) The glucose-alanine cycle. *Metabolism* **22**: 179-207.
- [40] Field, M (2003) Intestinal ion transport and the pathophysiology of diarrhea. *J Clin Invest* **111**: 931-943.
- [41] Fischer, WN; Loo, DD; Koch, W; Ludewig, U; Boorer, KJ; Tegeder, M; Rentsch, D; Wright, EM; Frommer, WB (2002) Low and high affinity amino acid H<sup>+</sup>-cotransporters for cellular import of neutral and charged amino acids. *Plant J* **29**: 717-731.
- [42] Fremeau, RTJ; Caron, MG; Blakely, RD (1992) Molecular cloning and expression of a high affinity L-proline transporter expressed in putative glutamatergic pathways of rat brain. *Neuron* **8**: 915-926.
- [43] Ganapathy, V and Leibach, FH (1982a) Peptide transport in intestinal and renal brush border membrane vesicles. *Life Sci* **30**: 2137-2146.
- [44] Ganapathy, V and Leibach, FH (1982b) Peptide transport in rabbit kidney. Studies with L-carnosine. *Biochim Biophys Acta* **691**: 362-366.
- [45] Ganapathy, V and Leibach, FH (1983a) Role of pH gradient and membrane potential in dipeptide transport in intestinal and renal brush-border membrane vesicles from the rabbit. Studies with L-carnosine and glycyl-L-proline. *J Biol Chem* **258**: 14189-14192.

- [46] Ganapathy, V; Roesel, RA; Howard, JC; Leibach, FH (1983b) Interaction of proline, 5-oxoproline, and pipercolic acid for renal transport in the rabbit. *J Biol Chem* **258**: 2266-2272.
- [47] Garcia, CK; Brown, MS; Pathak, RK; Goldstein, JL (1995) cDNA cloning of MCT2, a second monocarboxylate transporter expressed in different cells than MCT1. *J Biol Chem* **270**: 1843-1849.
- [48] Garrick, MD; Dolan, KG; Horbinski, C; Ghio, AJ; Higgins, D; Porubcin, M; Moore, EG; Hainsworth, LN; Umbreit, JN; Conrad, ME; Feng, L; Lis, A; Roth, JA; Singleton, S; Garrick, LM (2003) DMT1: a mammalian transporter for multiple metals. *Biometals* **16**: 41-54.
- [49] Golabek, AA; Kida, E; Walus, M; Kaczmarski, W; Michalewski, M; Wisniewski, KE (2000) CLN3 protein regulates lysosomal pH and alters intracellular processing of Alzheimer's amyloid-beta protein precursor and cathepsin D in human cells. *Mol Genet Metab* **70**: 203-213.
- [50] Groneberg, DA; Eynott, PR; Doring, F; Thai, DQ; Oates, T; Barnes, PJ; Chung, KF; Daniel, H; Fischer, A (2002) Distribution and function of the peptide transporter PEPT2 in normal and cystic fibrosis human lung. *Thorax* **57**: 55-60.
- [51] Groneberg, DA; Fischer, A; Chung, KF; Daniel, H (2004) Molecular mechanisms of pulmonary peptidomimetic drug and peptide transport. *Am J Respir Cell Mol Biol* **30**: 251-260.
- [52] Groneberg, DA; Nickolaus, M; Springer, J; Doring, F; Daniel, H; Fischer, A (2001) Localization of the Peptide Transporter PEPT2 in the Lung : Implications for Pulmonary Oligopeptide Uptake. *Am J Pathol* **158**: 707-714.
- [53] Gu, Y; Genever, PG; Skerry, TM; Publicover, SJ (2002) The NMDA type glutamate receptors expressed by primary rat osteoblasts have the same electrophysiological characteristics as neuronal receptors. *Calcif Tissue Int* **70**: 194-203.
- [54] Guastella, J; Brecha, N; Weigmann, C; Lester, HA; Davidson, N (1992) Cloning, expression, and localization of a rat brain high-affinity glycine transporter. *Proc Natl Acad Sci U S A* **89**: 7189-7193.
- [55] Guastella, J; Nelson, N; Nelson, H; Czyzyk, L ; Keynan, S; Miedel, MC; Davidson, N; Lester, HA; Kanner, BI (1990) Cloning and expression of a rat brain GABA transporter. *Science* **249**: 1303-1306.
- [56] Halestrap, AP and Meredith, D (2004) The SLC16 gene family-from monocarboxylate transporters (MCTs) to aromatic amino acid transporters and beyond. *Pflugers Arch* **447**: 619-628.
- [57] Halestrap, AP and Price, NT (1999) The proton-linked monocarboxylate transporter (MCT) family: structure, function and regulation. *Biochem J* **343**: 281-299.
- [58] Hanley, JG; Jones, EM; Moss, SJ (2000) GABA receptor rho1 subunit interacts with a novel splice variant of the glycine transporter, GLYT-1. *J Biol Chem* **275**: 840-846.
- [59] Hashimoto, A; Nishikawa, T; Oka, T; Takahashi, K (1993) Endogenous D-serine in rat brain: N-methyl-D-aspartate receptor-related distribution and aging. *J Neurochem* **60**: 783-786.
- [60] Hashimoto, A; Oka, T; Nishikawa, T (1995) Extracellular concentration of endogenous free D-serine in the rat brain as revealed by in vivo microdialysis. *Neuroscience* **66**: 635-643.
- [61] Hatanaka, T; Huang, W; Ling, R; Prasad, PD; Sugawara, M; Leibach, FH; Ganapathy, V (2001) Evidence for the transport of neutral as well as cationic amino acids by ATA3, a novel and liver-specific subtype of amino acid transport system A. *Biochim Biophys Acta* **1510**: 10-17.
- [62] Hatanaka, T; Huang, W; Wang, H; Sugawara, M; Prasad, PD; Leibach, FH; Ganapathy, V (2000) Primary structure, functional characteristics and tissue expression pattern of human ATA2, a subtype of amino acid transport system A. *Biochim Biophys Acta* **1467**: 1-6.
- [63] Hediger, MA (2004) The ABCs of solute carriers: physiological, pathological and therapeutic implications of human membrane transport proteins. *Pflugers Arch* **447**: 465-817.
- [64] Hellier, MD; Perrett, D; Holdsworth, CD; Thirumalai, C (1971) Absorption of dipeptides in normal and cystinuric subjects. *Gut* **12**: 496-497.
- [65] Henikoff, S; Henikoff, JG; Alford, WJ; Pietrokovski, S (1995) Automated construction and graphical presentation of protein blocks from unaligned sequences. *Gene* **163**: GC17-GC26
- [66] Heresco-Levy, U; Kremer, I; Javitt, DC; Goichman, R; Reshef, A; Blanaru, M ; Cohen, T (2002) Pilot-controlled trial of D-cycloserine for the treatment of post-traumatic stress disorder. *Int J Neuropsychopharmacol* **5** : 301-307.
- [67] Hyde, R; Taylor, PM; Hundal, HS (2003) Amino acid transporters: roles in amino acid sensing and signalling in animal cells. *Biochem J* **373**: 1-18.
- [68] Jauch, P and Lauger, P (1986) Electrogenic properties of the sodium-alanine cotransporter in pancreatic acinar cells: II. Comparison with transport models. *J Membr Biol* **94**: 117-127.

- [69] Jessen, H; Jorgensen, KE; Roigaard-Petersen, H; Sheikh, MI (1989) Demonstration of H<sup>+</sup>- and Na<sup>+</sup>-coupled co-transport of beta-alanine by luminal membrane vesicles of rabbit proximal tubule. *J Physiol* **411**: 517-528.
- [70] Jessen, H; Roigaard, H; Jacobsen, C (1996) Uptake of neutral alpha- and beta-amino acids by human proximal tubular cells. *Biochim Biophys Acta* **1282**: 225-232.
- [71] Jessen, H and Sheikh, MI (1991a) Renal transport of taurine in luminal membrane vesicles from rabbit proximal tubule. *Biochim Biophys Acta* **1064**: 189-198.
- [72] Jessen, H and Sheikh, MI (1991c) Stoichiometric studies of beta-alanine transporters in rabbit proximal tubule. *Biochem J* **277**: 891-894.
- [73] Jessen, H and Sheikh, MI (1992) L-tryptophan uptake by segment-specific membrane vesicles from the proximal tubule of rabbit kidney. *Biochem J* **286**: 103-110.
- [74] Jessen, H; Vorum, H; Jorgensen, KE; Sheikh, MI (1988a) Characteristics of D-alanine transport by luminal membrane vesicles from pars convoluta and pars recta of rabbit proximal tubule. *Biochim Biophys Acta* **942**: 262-270.
- [75] Jessen, H; Vorum, H; Jorgensen, KE; Sheikh, MI (1988b) Energetics of renal Na<sup>+</sup> and H<sup>+</sup>/L-alanine co-transport systems. *Biochem J* **256**: 299-302.
- [76] Jessen, H; Vorum, H; Jorgensen, KE; Sheikh, MI (1991b) Na<sup>(+)</sup>- and H<sup>(+)</sup>-gradient-dependent transport of alpha-aminoisobutyrate by luminal membrane vesicles from rabbit proximal tubule. *J Physiol* **436**: 149-167.
- [77] Jorgensen, KE and Sheikh, MI (1987) Renal transport of neutral amino acids. Cation-dependent uptake of L-alanine by luminal-membrane vesicles. *Biochem J* **248**: 533-538.
- [78] Kalatzis, V; Cherqui, S; Antignac, C; Gasnier, B (2001) Cystinosin, the protein defective in cystinosis, is a H<sup>(+)</sup>-driven lysosomal cystine transporter. *EMBO J* **20**: 5940-5949.
- [79] Kapoor, M; Babbar, HS; Jaswal, VM; Mahmood, A (1988a) Effect of pH on sodium dependent and independent glycine uptake in rat small intestine. *Indian J Biochem Biophys* **25**: 276-278.
- [80] Kapoor, M; Babbar, HS; Jaswal, VM; Mahmood, A (1988b) pH-dependent glycine uptake in the presence and absence of sodium ions from rat small intestine. *Biochem Med. Metab Biol* **40**: 118-122.
- [81] Kekuda, R; Prasad, PD; Fei, YJ; Torres-Zamorano, V; Sinha, S; Yang-Feng, TL; Leibach, FH; Ganapathy, V (1996) Cloning of the sodium-dependent, broad-scope, neutral amino acid transporter Bo from a human placental choriocarcinoma cell line. *J Biol Chem* **271**: 18657-18661.
- [82] Kekuda, R; Torres-Zamorano, V; Fei, YJ; Prasad, PD; Li, HW; Mader, LD; Leibach, FH; Ganapathy, V (1997) Molecular and functional characterization of intestinal Na<sup>(+)</sup>-dependent neutral amino acid transporter B0. *Am J Physiol* **272**: G1463-G1472
- [83] Kemp, JA and Leeson, PD (1993) The glycine site of the NMDA receptor--five years on. *Trends Pharmacol Sci* **14**: 20-25.
- [84] Kim, JW; Closs, EI; Albritton, LM; Cunningham, JM (1991) Transport of cationic amino acids by the mouse ecotropic retrovirus receptor. *Nature* **352**: 725-728.
- [85] Kim, KM; Kingsmore, SF; Han, H; T.L.; Godinot, N; Seldin, MF; Caron, MG; Giros, B (1994) Cloning of the human glycine transporter type 1: molecular and pharmacological characterization of novel isoform variants and chromosomal localization of the gene in the human and mouse genomes. *Mol Pharmacol* **45**: 608-617.
- [86] Klein, RC and Castellino, FJ (2001) Activators and inhibitors of the ion channel of the NMDA receptor. *Curr Drug Targets* **2**: 323-329.
- [87] Kleta, R; Romeo, E; Ristic, Z; Ohura, T; Stuart, C; Arcos-Burgos, M; Dave, MH; Wagner, CA; Camargo, SR; Inoue, S; Matsuura, N; Helip-Wooley, A; Bockenbauer, D; Warth, R; Bernardini, I; Visser, G; Eggermann, T; Lee, P; Chairoungdua, A; Jutabha, P; Babu, E; Nilwarangkoon, S; Anzai, N; Kanai, Y; Verrey, F; Gahl, WA; Koizumi, A (2004) Mutations in SLC6A19, encoding B(0)AT1, cause Hartnup disorder. *Nat Genet* [doi:10.1038/ng1405]
- [88] Kottra, G; Stamford, A; Daniel, H (2002) PEPT1 as a paradigm for membrane carriers that mediate electrogenic bidirectional transport of anionic, cationic, and neutral substrates. *J Biol Chem* **277**: 32683-32691.
- [89] Lambert, DW; Wood, IS; Ellis, A; S.P. (2002) Molecular changes in the expression of human colonic nutrient transporters during the transition from normality to malignancy. *Br J Cancer* **86**: 1262-1269.
- [90] Lang, F; Busch, GL; Volkl, H (1998) The diversity of volume regulatory mechanisms. *Cell Physiol Biochem* **8**: 1-45.
- [91] Legendre, P (2001) The glycinergic inhibitory synapse. *Cell Mol Life Sci* **58**: 760-793.

- [92] Leibach, FH and Ganapathy, V (1996) Peptide transporters in the intestine and the kidney. *Annu Rev Nutr* **16**: 99-119.
- [93] Levy, H.S. (1995) Hartnup Disorder. In: *The Metabolic Basis of Inherited Disease* (Scriver, C.R., Beaudet, A.L., Sly, W.S. & Valle, D. eds.), pp. 3629-3642. McGraw-Hill, New York, NY.
- [94] Liu, M; Russell, RL; Beigelman, L; Handschumacher, RE; Pizzorno, G (1999) beta-alanine and alpha-fluoro-beta-alanine concentrative transport in rat hepatocytes is mediated by GABA transporter GAT-2. *Am J Physiol* **276**: G206-G210
- [95] Liu, QR; Nelson, H; Mandiyan, S; Lopez-Corcuera, B; Nelson, N (1992) Cloning and expression of a glycine transporter from mouse brain. *FEBS Lett* **305**: 110-114.
- [96] Loo, DD; Hirayama, BA; Gallardo, EM; Lam, JT ; Turk, E; Wright, EM (1998) Conformational changes couple Na<sup>+</sup> and glucose transport. *Proc Natl Acad Sci U S A* **95**: 7789-7794.
- [97] Lopez-Corcuera, B; Geerlings, A; Aragon, C (2001) Glycine neurotransmitter transporters: an update. *Mol Membr Biol* **18**: 13-20.
- [98] Lopez-Corcuera, B; Liu, QR; Mandiyan, S; Nelson, H; Nelson, N (1992) Expression of a mouse brain cDNA encoding novel gamma-aminobutyric acid transporter. *J Biol Chem*. **267**: 17491-17493.
- [99] Mackenzie, B and Erickson, JD (2004) Sodium-coupled neutral amino acid (System N/A) transporters of the SLC38 gene family. *Pflugers Arch* **447**: 784-795.
- [100] Mackenzie, B; Loo, DD; Fei, Y; Liu, WJ; Ganapathy, V; Leibach, FH; Wright, EM (1996) Mechanisms of the human intestinal H<sup>+</sup>-coupled oligopeptide transporter hPEPT1. *J Biol Chem* **271**: 5430-5437.
- [101] Mackenzie, B; Schafer, MK; Erickson, JD; Hediger, MA; Weihe, E; Varoqui, H (2003) Functional properties and cellular distribution of the system A glutamine transporter SNAT1 support specialized roles in central neurons. *J Biol Chem* **278**: 23720-23730.
- [102] Mager, S and Sloan, J (2003) Possible role of amino acids, peptides, and sugar transporter in protein removal and innate lung defense. *Eur J Pharmacol* **479**: 263-267.
- [103] Malandro, MS and Kilberg, MS (1996) Molecular biology of mammalian amino acid transporters. *Annu Rev Biochem* **65**: 305-336.
- [104] Mascolo, N; Rajendran, VM; Binder, HJ (1991) Mechanism of short-chain fatty acid uptake by apical membrane vesicles of rat distal colon. *Gastroenterology* **101**: 331-338.
- [105] Mayor, FJ; Marvizon, JG; Aragon, MC; Gimenez, C; Valdivieso, F (1981) Glycine transport into plasma-membrane vesicles derived from rat brain synaptosomes. *Biochem J* **198**: 535-541.
- [106] McEwan, GT; Daniel, H; Fett, C; Burgess, MN; Lucas, ML (1988) The effect of Escherichia coli STa enterotoxin and other secretagogues on mucosal surface pH of rat small intestine in vivo. *Proc R.Soc.Lond.B.Biol Sci* **234**: 219-237.
- [107] McGivan, JD and Pastor-Anglada, M (1994) Regulatory and molecular aspects of mammalian amino acid transport. *Biochem J* **299**: 321-334.
- [108] McIntire, SL; Reimer, RJ; Schuske, K; Edwards, RH; Jorgensen, EM (1997) Identification and characterization of the vesicular GABA transporter. *Nature* **389**: 870-876.
- [109] Metzner, L; Kalbitz, J; Brandsch, M (2004) Transport of Pharmacologically Active Proline Derivatives by the Human Proton-Coupled Amino Acid Transporter hPAT1. *J Pharmacol Exp Ther* **309**: 28-35.
- [110] Miyauchi, S; Gopal, E; Fei, YJ; Ganapathy, V (2004) Functional Identification of SLC5A8, a Tumor Suppressor Down-regulated in Colon Cancer, as a Na<sup>+</sup>-coupled Transporter for Short-chain Fatty Acids. *J Biol Chem* **279**: 13293-13296.
- [111] Munck, LK and Munck, BG (1992) The rabbit jejunal 'imino carrier' and the ileal 'imino acid carrier' describe the same epithelial function. *Biochim Biophys Acta* **1116**: 91-96.
- [112] Nakauchi, J; Matsuo, H; Kim, DK; Goto, A; Chairoungdua, A; Cha, SH; Inatomi, J; Shiokawa, Y; Yamaguchi, K; Saito, I; Endou, H; Kanai, Y (2000) Cloning and characterization of a human brain Na<sup>(+)</sup>-independent transporter for small neutral amino acids that transports D-serine with high affinity. *Neurosci Lett* **287**: 231-235.
- [113] Newey, H and Smyth, DH (1964) The transfer system for neutral amino acids in the rat small intestine. *J Physiol* **170**: 328-343.
- [114] Nichols, K; Staines, W; Wu, JY; Krantis, A (1995) Immunopositive GABAergic neural sites display nitric oxide synthase-related NADPH diaphorase activity in the human colon. *J Auton Nerv Syst* **50**: 253-262.
- [115] Nicklin, PL; Irwin, WJ; Hassan, IF; Mackay, M (1992) Proline uptake by monolayers of human intestinal absorptive (Caco-2) cells in vitro. *Biochim Biophys Acta* **1104**: 283-292.

- [116] Ogawa, M; Shigeto, H; Yamamoto, T; Oya, Y; Wada, K; Nishikawa, T; Kawai, M (2003) D-cycloserine for the treatment of ataxia in spinocerebellar degeneration. *J Neurol Sci* **210**: 53-56.
- [117] Oxender, D and Christensen, HN (1963) Distinct mediating systems for the transport of neutral amino acids by the Ehrlich cell. *J Biol Chem* **238**: 3686-3699.
- [118] Palacin, M; Estevez, R; Bertran, J; Zorzano, A (1998) Molecular biology of mammalian plasma membrane amino acid transporters. *Physiol Rev* **78**: 969-1054.
- [119] Palmer, TN; Caldecourt, MA; Snell, K; Sugden, MC (1985) Alanine and inter-organ relationships in branched-chain amino and 2-oxo acid metabolism. *Biosci Rep* **5**: 1015-1033.
- [120] Pinilla-Tenas, J; Barber, A; Lostao, MP (2003) Transport of proline and hydroxyproline by the neutral amino-acid exchanger ASCT1. *J Membr Biol* **195**: 27-32.
- [121] Pinilla, J; Barber, A; Lostao, MP (2001) Active transport of alanine by the neutral amino-acid exchanger ASCT1. *Can J Physiol Pharmacol* **79**: 1023-1029.
- [122] Pomare, EW; Branch, WJ; Cummings, JH (1985) Carbohydrate fermentation in the human colon and its relation to acetate concentrations in venous blood. *J Clin Invest* **75**: 1448-1454.
- [123] Rajendran, VM; Barry, JA; Kleinman, JG; Ramaswamy, K (1987) Proton gradient-dependent transport of glycine in rabbit renal brush-border membrane vesicles. *J Biol Chem* **262**: 14974-14977.
- [124] Ramamoorthy, S; Leibach, FH; Mahesh, VB; Han, H; Yang-Feng, T; Blakely, RD ; Ganapathy, V (1994) Functional characterization and chromosomal localization of a cloned taurine transporter from human placenta. *Biochem J* **300**: 893-900.
- [125] Ranaldi, G; Islam, K; Sambuy, Y (1994) D-cycloserine uses an active transport mechanism in the human intestinal cell line Caco 2. *Antimicrob Agents Chemother* **38**: 1239-1245.
- [126] Reimer, RJ; Chaudhry, FA; Gray, AT; Edwards, RH (2000) Amino acid transport system A resembles system N in sequence but differs in mechanism. *Proc Natl Acad Sci U S A* **97**: 7715-7720.
- [127] Remesy, C; Demigne, C; Chartier, F (1980) Origin and utilization of volatile fatty acids in the rat. *Reprod Nutr Dev* **20**: 1339-1349.
- [128] Renick, SE; Kleven, DT; Chan, J; Stenius, K; Milner, TA; Pickel, VM; Fremeau, RTJ (1999) The mammalian brain high-affinity L-proline transporter is enriched preferentially in synaptic vesicles in a subpopulation of excitatory nerve terminals in rat forebrain. *J Neurosci* **19**: 21-33.
- [129] Reynolds, DA; Rajendran, VM; Binder, HJ (1993) Bicarbonate-stimulated [<sup>14</sup>C]butyrate uptake in basolateral membrane vesicles of rat distal colon. *Gastroenterology* **105**: 725-732.
- [130] Ritzhaupt, A; Ellis, A; Hosie, KB; S.P. (1998) The characterization of butyrate transport across pig and human colonic luminal membrane. *J Physiol* **507**: 819-830.
- [131] Roigaard-Petersen, H; Jacobsen, C; Iqbal, SM (1987) H<sup>+</sup>-L-proline cotransport by vesicles from pars convoluta of rabbit proximal tubule. *Am J Physiol* **253** : 15-20.
- [132] Roigaard-Petersen, H; Jacobsen, C; Jessen, H; Mollerup, S; Sheikh, MI (1989) Electrogenic uptake of D-imino acids by luminal membrane vesicles from rabbit kidney proximal tubule. *Biochim Biophys Acta* **984**: 231-237.
- [133] Roigaard-Petersen, H; Jacobsen, C; Sheikh, MI (1988) Transport of L-proline by luminal membrane vesicles from pars recta of rabbit proximal tubule. *Am J Physiol* **254**: F628-F633
- [134] Roigaard-Petersen, H; Jessen, H; Mollerup, S; Jorgensen, KE; Jacobsen, C; Sheikh, MI (1990) Proton gradient-dependent renal transport of glycine: evidence for vesicle studies. *Am J Physiol.* **258**: F388-F396
- [135] Roigaard-Petersen, H and Sheikh, MI (1984) Renal transport of neutral amino acids. Demonstration of Na<sup>+</sup>-independent and Na<sup>+</sup>-dependent electrogenic uptake of L-proline, hydroxy-L-proline and 5-oxo-L-proline by luminal-membrane vesicles. *Biochem J* **220**: 25-33.
- [136] Rosenberg, LE; Durant, JL; Elsas, LJ (1968) Familial iminoglycinuria. An inborn error of renal tubular transport. *N Engl J Med* **278**: 1407-1413.
- [137] Ruppin, H; Bar-Meir, S; Soergel, KH; Wood, CM; Schmitt, MGJ (1980) Absorption of short-chain fatty acids by the colon. *Gastroenterology* **78**: 1500-1507.
- [138] Russnak, R; Konczal, D; McIntire, SL (2001) A family of yeast proteins mediating bidirectional vacuolar amino acid transport. *J Biol Chem* **276**: 23849-23857.
- [139] Sagne, C; Agulhon, C; Ravassard, P; Darmon, M; Hamon, M; El Mestikawy, S ; Gasnier, B; Giros, B (2001) Identification and characterization of a lysosomal transporter for small neutral amino acids. *Proc Natl Acad Sci U S A* **98**: 7206-7211.

- [140] Sagne, C; El Mestikawy, S; Isambert, MF; Hamon, M; Henry, JP; Giros, B; Gasnier, B (1997) Cloning of a functional vesicular GABA and glycine transporter by screening of genome databases. *FEBS Lett* **417**: 177-183.
- [141] Saier, MHJ (2000) Families of transmembrane transporters selective for amino acids and their derivatives. *Microbiology*. **146**: 1775-1795.
- [142] Schell, MJ; Molliver, ME; Snyder, SH (1995) D-serine, an endogenous synaptic modulator: localization to astrocytes and glutamate-stimulated release. *Proc Natl Acad Sci U S A* **92**: 3948-3952.
- [143] Schousboe, A; Sonnewald, U; Waagepetersen, HS (2003) Differential roles of alanine in GABAergic and glutamatergic neurons. *Neurochem Int* **43**: 311-315.
- [144] Scriver, C.R. (1989) Familial renal iminoglycinuria. In: *The Metabolic Basis of Inherited Disease* (Scriver, C.R., Beaudet, A.L., Sly, W.S. & Valle, D., eds.), pp. 2529-2538. McGraw-Hill, New York, NY.
- [145] Seow, HF; Broer, S; Broer, A; Bailey, CG; Potter, SJ; Cavanaugh, JA; Rasko, JE (2004) Hartnup disorder is caused by mutations in the gene encoding the neutral amino acid transporter SLC6A19. *Nat Genet* [doi:10.1038/ng1406]
- [146] Sha, L; Miller, SM; Szurszewski, JH (2001) Electrophysiological effects of GABA on cat pancreatic neurons. *Am J Physiol Gastrointest Liver Physiol* **280**: G324-G331
- [147] Shafiqat, S; Tamarappoo, BK; Kilberg, MS; Puranam, RS; McNamara, JO; Guadano-Ferraz, A; Freneau, RTJ (1993) Cloning and expression of a novel Na(+)-dependent neutral amino acid transporter structurally related to mammalian Na+/glutamate cotransporters. *J Biol Chem* **268**: 15351-15355.
- [148] Shafiqat, S; Velaz-Faircloth, M; Henzi, VA; Whitney, KD; T.L.; Seldin, MF; Freneau, RTJ (1995) Human brain-specific L-proline transporter: molecular cloning, functional expression, and chromosomal localization of the gene in human and mouse genomes. *Mol Pharmacol* **48**: 219-229.
- [149] Skerry, TM and Genever, PG (2001) Glutamate signalling in non-neuronal tissues. *Trends Pharmacol Sci* **22**: 174-181.
- [150] Smith, KE; Borden, LA; Hartig, PR; Branchek, T; Weinshank, RL (1992a) Cloning and expression of a glycine transporter reveal colocalization with NMDA receptors. *Neuron* **8**: 927-935.
- [151] Smith, KE; Borden, LA; Wang, CH; Hartig, PR; Branchek, TA; Weinshank, RL (1992b) Cloning and expression of a high affinity taurine transporter from rat brain. *Mol Pharmacol* **42**: 563-569.
- [152] Smolin, LA; Benevenga, NJ; Berlow, S (1981) The use of betaine for the treatment of homocystinuria. *J Pediatr* **99**: 467-472.
- [153] Stein, J; Zores, M; Schroder, O (2000) Short-chain fatty acid (SCFA) uptake into Caco-2 cells by a pH-dependent and carrier mediated transport mechanism. *Eur J Nutr* **39**: 121-125.
- [154] Stevens, BR and Wright, EM (1985) Substrate specificity of the intestinal brush-border proline/sodium (IMINO) transporter. *J Membr Biol* **87**: 27-34.
- [155] Stevens, BR and Wright, EM (1987) Kinetics of the intestinal brush border proline (Imino) carrier. *J Biol Chem* **262**: 6546-6551.
- [156] Tabuchi, M; Tanaka, N; Nishida-Kitayama, J; Ohno, H; Kishi, F (2002) Alternative splicing regulates the subcellular localization of divalent metal transporter 1 isoforms. *Mol Biol Cell* **13**: 4371-4387.
- [157] Takanaga, H; Tokuda, N; Ohtsuki, S; Hosoya, K; Terasaki, T (2002) ATA2 is predominantly expressed as system A at the blood-brain barrier and acts as brain-to-blood efflux transport for L-proline. *Mol Pharmacol* **61**: 1289-1296.
- [158] Takeuchi, K; Toyohara, H; Sakaguchi, M (2000) A hyperosmotic stress-induced mRNA of carp cell encodes Na(+)- and Cl(-)-dependent high affinity taurine transporter. *Biochim Biophys Acta* **1464**: 219-230.
- [159] Tamai, I; Sai, Y; Ono, A; Kido, Y; Yabuuchi, H; Takanaga, H; Satoh, E; Ogihara, T; Amano, O; Izeki, S; Tsuji, A (1999) Immunohistochemical and functional characterization of pH-dependent intestinal absorption of weak organic acids by the monocarboxylic acid transporter MCT1. *J Pharm Pharmacol* **51**: 1113-1121.
- [160] Taylor, PM; Kaur, S; Mackenzie, B; Peter, GJ (1996) Amino-acid-dependent modulation of amino acid transport in *Xenopus laevis* oocytes. *J Exp Biol* **199**: 923-931.
- [161] Thwaites, DT; Armstrong, G; Hirst, BH; Simmons, NL (1995c) D-cycloserine transport in human intestinal epithelial (Caco-2) cells: mediation by a H(+)-coupled amino acid transporter. *Br J Pharmacol*. **115**: 761-766.
- [162] Thwaites, DT; Basterfield, L; McCleave, PM; Carter, SM; Simmons, NL (2000) Gamma-Aminobutyric acid (GABA) transport across human intestinal epithelial (Caco-2) cell monolayers. *Br J Pharmacol*. **129**: 457-464.

- [163] Thwaites, DT; Ford, D; Glanville, M; Simmons, NL (1999a) H(+)/solute-induced intracellular acidification leads to selective activation of apical Na(+)/H(+) exchange in human intestinal epithelial cells. *J Clin Invest*. **104**: 629-635.
- [164] Thwaites, DT; Kennedy, DJ; Raldua, D; Anderson, CM; Mendoza, ME; Bladen, CL; Simmons, NL (2002) H/dipeptide absorption across the human intestinal epithelium is controlled indirectly via a functional Na/H exchanger. *Gastroenterology* **122**: 1322-1333.
- [165] Thwaites, DT; McEwan, GT; Brown, CD; Hirst, BH; Simmons, NL (1993a) Na(+)-independent, H(+)-coupled transepithelial beta-alanine absorption by human intestinal Caco-2 cell monolayers. *J Biol Chem* **268**: 18438-18441.
- [166] Thwaites, DT; McEwan, GT; Brown, CD; Hirst, BH; Simmons, NL (1994) L-alanine absorption in human intestinal Caco-2 cells driven by the proton electrochemical gradient. *J Membr Biol* **140**: 143-151.
- [167] Thwaites, DT; McEwan, GT; Cook, MJ; Hirst, BH; Simmons, NL (1993b) H(+)-coupled (Na(+)-independent) proline transport in human intestinal (Caco-2) epithelial cell monolayers. *FEBS Lett* **333**: 78-82.
- [168] Thwaites, DT; McEwan, GT; Hirst, BH; Simmons, NL (1995a) H(+)-coupled alpha-methylaminoisobutyric acid transport in human intestinal Caco-2 cells. *Biochim Biophys Acta* **1234**: 111-118.
- [169] Thwaites, DT; McEwan, GT; Simmons, NL (1995bb) The role of the proton electrochemical gradient in the transepithelial absorption of amino acids by human intestinal Caco-2 cell monolayers. *J Membr Biol* **145**: 245-256.
- [170] Thwaites, DT and Stevens, BC (1999b) H+-zwitterionic amino acid symport at the brush-border membrane of human intestinal epithelial (CACO-2) cells. *Exp Physiol* **84**: 275-284.
- [171] Tyagi, S; Venugopalakrishnan, J; Ramaswamy, K; Dudeja, PK (2002) Mechanism of n-butyrate uptake in the human proximal colonic basolateral membranes. *Am J Physiol Gastrointest Liver Physiol* **282**: G676-G682
- [172] Utsunomiya-Tate, N; Endou, H; Kanai, Y (1996) Cloning and functional characterization of a system ASC-like Na+-dependent neutral amino acid transporter. *J Biol Chem* **271**: 14883-14890.
- [173] Van den Berghe, H and Michaux, L (1997) 5q-, twenty-five years later: a synopsis. *Cancer Genet Cytogenet* **94**: 1-7
- [174] Van Slyke, DD and Meyer, GM (1913) The fate of protein digestion products in the body III: The absorption of amino-acids from the blood by the tissues. *J Biol Chem*. **16**: 197-212.
- [175] Vanhoof, G; Goossens, F; De, M, I; Hendriks, D; Scharpe, S (1995) Proline motifs in peptides and their biological processing. *FASEB J* **9**: 736-744.
- [176] Velaz-Faircloth, M; Guadano-Ferraz, A; Henzi, VA; Fremeau, RTJ (1995) Mammalian brain-specific L-proline transporter. Neuronal localization of mRNA and enrichment of transporter protein in synaptic plasma membranes. *J Biol Chem* **270**: 15755-15761.
- [177] Verrey, F (2003) System L: heteromeric exchangers of large, neutral amino acids involved in directional transport. *Pflugers Arch* **445**: 529-533.
- [178] Vilella, S; Cassano, G; Storelli, C (1989) How many Na+-dependent carriers for L-alanine and L-proline in the eel intestine? Studies with brush-border membrane vesicles. *Biochim Biophys Acta* **984**: 188-192.
- [179] von Engelhardt, W; Gros, G; Burmester, M; Hansen, K; Becker, G; Rechkemmer, G (1994) Functional role of bicarbonate transport across guinea-pig isolated caecum and proximal colon. *J Physiol* **477**: 365-371.
- [180] Wang, H; Kavanaugh, MP; North, RA; Kabat, D (1991) Cell-surface receptor for ecotropic murine retroviruses is a basic amino-acid transporter. *Nature* **352**: 729-731.
- [181] Wheeler, MD; Ikejima, K; Enomoto, N; Stacklewitz, RF; Seabra, V; Zhong, Z; Yin, M; Schemmer, P; Rose, ML; Rusyn, I; Bradford, B; Thurman, RG (1999) Glycine: a new anti-inflammatory immunonutrient. *Cell Mol Life Sci* **56**: 843-856.
- [182] Wipf, D; Ludewig, U; Tegeder, M; Rentsch, D; Koch, W; Frommer, WB (2002) Conservation of amino acid transporters in fungi, plants and animals. *Trends Biochem Sci* **27**: 139-147.
- [183] Wolosker, H; Blackshaw, S; Snyder, SH (1999) Serine racemase: a glial enzyme synthesizing D-serine to regulate glutamate-N-methyl-D-aspartate neurotransmission. *Proc Natl Acad Sci U S A* **96**: 13409-13414.
- [184] Wong, CG; Bottiglieri, T; Snead, OC3 (2003) GABA, gamma-hydroxybutyric acid, and neurological disease. *Ann.Neurol*. **54**: S3-S12
- [185] Wreden, CC; Johnson, J; Tran, C; Seal, RP; Copenhagen, DR; Reimer, RJ; Edwards, RH (2003) The H+-coupled electrogenic lysosomal amino acid transporter LYAAT1 localizes to the axon and plasma membrane of hippocampal neurons. *J Neurosci* **23**: 1265-1275.

- 
- [186] Wright, EM; Loo, DD; Panayotova-Heiermann, M; Lostao, MP; Hirayama, BH; Mackenzie, B; Boorer, K; Zampighi, G (1994) 'Active' sugar transport in eukaryotes. *J Exp Biol* **196**: 197-212.
- [187] Wright, EM and Pearce, BE (1984) Identification and conformational changes of the intestinal proline carrier. *J Biol Chem* **259**: 14993-14996.
- [188] Yamamoto, T; Nishizaki, I; Furuya, S; Hirabayashi, Y; Takahashi, K; Okuyama, S; Yamamoto, H (2003) Characterization of rapid and high-affinity uptake of L-serine in neurons and astrocytes in primary culture. *FEBS Lett* **548**: 69-73.
- [189] Young, GB; Jack, DL; Smith, DW; Saier, MHJ (1999) The amino acid/auxin:proton symport permease family. *Biochim.Biophys.Acta* **1415**: 306-322.
- [190] Zerangue, N and Kavanaugh, MP (1996) ASCT-1 is a neutral amino acid exchanger with chloride channel activity. *J Biol Chem* **271**: 27991-27994.

## ABBREVIATIONS

AAAP	amino acid/auxin permease family	RNA	ribonucleic acid
APC	amine-polyamine-choline transporter superfamily	RT-PCR	reverse transcription polymerase chain reaction
ASC	neutral amino acid transporter family	RZPD	Deutsches Ressourcenzentrum fuer Genomforschung GmbH
ATF1	amino acid transporter superfamily 1	SCFA	short-chain fatty acid
AVT-3	amino acid vacuolar transporter 3	SDS	sodium dicarboxylate symporter superfamily
BBMV	brush border membrane vesicle	SGLT1	sodium/glucose transporter 1
BCECF	2,7-bis-(carboxyethyl)-5-(and-6)-carboxyfluorescein	SLC	solute carrier
BGT-1	Betaine/GABA Transporter 1	SMCT	sodium monocarboxylate cotransporter
cAMP	cyclo adenosine monophosphate	SNAT	sodium-coupled neutral amino acid transporter (formerly system N/A transporter)
cDNA	copy-deoxyribonucleic acid	TAUT	taurine transporter
DMT	divalent metal ion transporter	TEVC	two electrode voltage clamp
DNA	deoxyribonucleic acid	TMD	transmembrane domain
EST	expressed sequence tag	VGAT/VIAAT	vesicular GABA transporter / vesicular inhibitory amino acid transporter
GABA	$\gamma$ -amino butyric acid	VIP	vasoactive intestinal peptide
GAT	GABA transporter,		
GlyT	high affinity type glycine transporter		
GPC	giant patch clamp		
HUGO	human genome project		
IRE	iron responsive element		
LAMP1	lysosomal membrane glycoprotein 1		
LAT	heterodimeric amino acid transporter light chain		
LYAAT	lysosomal amino acid transporter		
MCT1	monocarboxylate transporter 1		
MeAIB	methyl-amino-isobutyric acid		
MFS	amino acid transporters within the major facilitator superfamily		
mRNA	messenger ribonucleic acid		
NAT2/AAP	<i>A. thaliana</i> neutral amino acid transporter/amino acid permease		
NHE3	sodium/proton exchanger 3		
NMDA	N-methyl-D-aspartate		
NTS	neurotransmitter superfamily		
ORF	open reading frame		
PAT	proton/amino acid transporter		
PCR	polymerase chain reaction		
PEPT	peptide transporter		
PROT	brain-specific high affinity type proline transporter		
RACE	rapid amplification of cDNA ends		



## APPENDIX 1

published in *Journal of Biological Chemistry*

## Functional Characterization of Two Novel Mammalian Electrogenic Proton-dependent Amino Acid Cotransporters\*

Received for publication, January 14, 2002, and in revised form, April 5, 2002  
Published, JBC Papers in Press, April 16, 2002, DOI 10.1074/jbc.M200374200

Michael Boll, Martin Foltz, Isabel Rubio-Aliaga, Gabor Kottra, and Hannelore Daniel‡

From the Molecular Nutrition Unit, Institute of Nutritional Sciences, Technical University of Munich, D-85350 Freising-Weihenstephan, Germany

We cloned two cDNAs encoding proton/amino acid cotransporters, designated as mPAT1 and mPAT2, from murine tissues. They were identified by sequence similarity to the amino acid/auxin permease family member of lower eukaryotes. We functionally characterized both transporters by flux studies and electrophysiology after expression in *Xenopus laevis* oocytes. Both mPAT1 and mPAT2 induced a pH-dependent electrogenic transport activity for small amino acids (glycine, alanine, and proline) that is altered by membrane potential. Direct evidence for amino acid/H<sup>+</sup>-symport was shown by intracellular acidification, and a flux coupling stoichiometry for proline/H<sup>+</sup>-symport of 1:1 was determined for both transporters. Besides small apolar L-amino acids, the transporters also recognize their D-enantiomers and selected amino acid derivatives such as  $\gamma$ -aminobutyric acid. The mPAT1 transporter, the murine orthologue of the recently cloned rat LYAAT-1 transporter, can be considered as a low affinity system when compared with mPAT2. The mRNA of mPAT1 is highly expressed in small intestine, colon, kidney, and brain; the mPAT2-mRNA is mainly found in heart and lung. Phenotypically, the PAT1 transporter possesses the same functional characteristics as the previously described proton-dependent amino acid transport process in apical membranes of intestinal and renal epithelial cells.

One of the largest families of amino acid transporters identified so far is the amino acid/auxin permease (AAAP)<sup>1</sup> family (1, 2). This protein family is widespread in nature, with members found in yeast, plants, invertebrates, and mammals. Although their amino acid sequences appear very divergent, a common signature has been identified, and secondary structure predictions show conserved similarities (2). Accordingly, most members of the AAAP family possess 11 membrane-spanning domains with very similar hydrophathy profiles. Functionally characterized members as AAP1 and AVT1 found in *Saccharomyces cerevisiae* and *Arabidopsis thaliana* operate as

proton symporters for amino acids and selected derivatives such as auxins (2–4). Three subfamilies within the AAAP family that show low although significant similarities (20–30%) have been identified so far in mammalian organisms. They are represented by the VGAT transporter group, the system A/N transporter group, and the LYAAT branch (5).

The vesicular  $\gamma$ -aminobutyric acid (GABA) transporter VGAT was the first identified mammalian member of the AAAP family with an assigned function (6). It mediates the uptake of the inhibitory neurotransmitters GABA and glycine into synaptic vesicles (6, 7). The driving force of VGAT is the electrochemical proton gradient generated by the vesicular H<sup>+</sup>-ATPase (8). Cytoplasmic GABA and glycine can therefore be accumulated within the vesicles via a proton antiport mechanism (6). The system A/N transporter group also belong to the AAAP family. System N plays an important role especially in the homeostasis of glutamine in brain, where it serves as a delivery system for the precursor of the excitatory amino acid glutamate (9). The system N-mediated glutamine influx is coupled to the cotransport of one Na<sup>+</sup> ion in antiport with one H<sup>+</sup> ion (9). Although system A transporters are highly homologous to system N, they show a very different substrate specificity as well as a different ion-substrate flux coupling ratio (10). System A transporters prefer alanine and most of the other neutral amino acids and are considered to provide bulk quantities of these amino acids in most cell types. System A carriers act as Na<sup>+</sup>/amino acid symporters. Although transport by system A is sensitive to low pH, no proton exchanger activity has been shown in contrast to system N (11).

Recently, Sagne *et al.* (5) report the cloning of the first mammalian proton/amino acid symporter from rat brain, which is also a member of the AAAP family (5). This lysosomal amino acid transporter, designated as LYAAT-1, when transfected in CV-1 cells mediated the uptake of small amino acids such as alanine and proline and the neurotransmitter GABA. The observation of an enhanced transport activity by low extracellular pH suggested a proton-symport mechanism for amino acid influx. The LYAAT-1 transcripts were identified in glutamatergic and GABAergic neurons in rat brain. The LYAAT-1 protein was localized in the lysosomal membrane in these neurons, although when expressed heterologously, it mediated plasma membrane amino acid uptake (5).

The first members of the system A/N subfamily, the SN1 protein, and LYAAT-1 have been identified by data base search for mammalian homologues of the VGAT transporter (5, 6, 9). We searched for mammalian AAAP family members based on the *S. cerevisiae* protein sequence YKL146wp, which had been identified by genome-scanning analysis as a putative amino acid transport protein. Recently it was shown that YKL146wp indeed codes for a protein that represents a vesicular amino acid transporter, designated as AVT3 (4). Here we report the identification and characterization of two new members, the

\* The costs of publication of this article were defrayed in part by the payment of page charges. This article must therefore be hereby marked "advertisement" in accordance with 18 U.S.C. Section 1734 solely to indicate this fact.

The nucleotide sequence(s) reported in this paper has been submitted to the GenBank™/EBI Data Bank with accession number(s) AF453743 (mPAT1) and AF453744 (mPAT2).

‡ To whom correspondence should be addressed. Tel.: 49-8161-71-3400; Fax: 49-8161-71-3999; E-mail: daniel@wzw.tum.de.

<sup>1</sup> The abbreviations used are: AAAP, amino acid/auxin permease; PAT, proton/amino acid transporter; GABA,  $\gamma$ -aminobutyric acid; VGAT, vesicular GABA transporter; LYAAT-1, lysosomal amino acid transporter 1; EST, expressed sequence tag; ORF, open reading frame; MES, 4-morpholineethanesulfonic acid; contig, group of overlapping clones; EGFP, enhanced green fluorescent protein.

## Mammalian Proton/Amino Acid Cotransporters

22967

murine orthologue of rLYAAT-1, designated as mPAT1, and an additional member of this subfamily, designated as mPAT2. Both transporters, when expressed in *Xenopus laevis* oocytes, show the functional characteristics of electrogenic H<sup>+</sup>/amino acid symporters. The mPAT2 transporter displays the characteristics of a high affinity system with a more restricted substrate specificity than mPAT1.

## EXPERIMENTAL PROCEDURES

**cDNA Cloning**—The yeast protein sequence YKL146wp belonging to the AAAP family was blasted (tblastn method) against murine and human EST sequences. Two closely related cDNA sequences were identified that were so far not linked to any functionally known cDNA. The EST clone 1920302 (designated as mPAT2) from a murine 14 days-post-coital embryonic cDNA library was purchased from the Resource Center/Primary Data base of the German Human Genome Project (IMAGp998B154710Q2, RZPD, Berlin, Germany). The original cDNA in the pME18S-FL3 vector was cut with *XhoI* and *EcoRI* and ligated in pCRII (BD Pharmingen) to allow cRNA transcription using the T7 polymerase promoter. The major part of the open reading frame (ORF) of the mPAT1-cDNA was available by the assembly of EST sequences. The 5'-untranslated cDNA end including the start codon was identified using the 5'-rapid amplification of cDNA ends system (BD Pharmingen). The complete ORF of mPAT1 was amplified with a high fidelity *Taq* polymerase (Elongase, Invitrogen) using the primers mPAT1-F-140 (GTCAGACTCACTCCATAGTAC) and mPAT1-B1571 (AGACACACAGGGTGAGGCTG) with small intestinal RNA (5  $\mu$ g). The numbering of the primers is according to their position in relation to the first base of the start codon. Two independently amplified PCR products were cloned in the pCRII vector, and both strands were sequenced using the Thermo Sequenase Cy5 dye terminator kit with an automated DNA sequencer (ALF Express, AP Biotech). The PCR products were subcloned directionally in the pCRII vector in which an ~700-bp 3' end fragment of the rabbit PEPT2 (GenBank™ accession number U32507), including the poly(A) tail, was introduced. This usually stabilizes the synthesized cRNA for efficient expression in *X. laevis* oocytes. The expression of mPAT1-cRNA with the additional 3' end was more than 50-fold higher than that of the mPAT1-cRNA without the additional 3' end (data not shown).

**Sequence Analysis**—For homology searches on DNA and protein levels, the BLAST programs were used (www.ncbi.nlm.nih.gov/blast). Transmembrane regions of PAT proteins were predicted with DNASIS (Hitachi) using the Kyte and Doolittle algorithm with a window size of 18 amino acids. Multiple sequence alignments (neighbor joining method) were performed with the CLUSTALW program (www.ebi.ac.uk/clustalw/).

***X. laevis* Oocytes Handling and cRNA Injection**—Oocytes were treated with collagenase A (Roche Diagnostics) for 1.5–2 h at room temperature in Ca<sup>2+</sup>-free ORII solution (82.5 mM NaCl, 2 mM KCl, 1 mM MgCl<sub>2</sub> and 10 mM HEPES (pH 7.5) to remove follicular cells. After sorting, healthy oocytes of stage V and VI were kept at 18 °C in modified Barth solution containing 88 mM NaCl, 1 mM KCl, 0.8 mM MgSO<sub>4</sub>, 0.4 mM CaCl<sub>2</sub>, 0.3 mM Ca(NO<sub>3</sub>)<sub>2</sub>, 2.4 mM NaHCO<sub>3</sub>, and 10 mM HEPES (pH 7.5). The next day oocytes were injected with 27 nl of sterile water (control) or 27 nl of mPAT1- or mPAT2-cRNA solution at concentrations between 0.2 and 1.5  $\mu$ g/ $\mu$ l for initial functional tests. For detailed functional characterization 10 ng of mPAT1 or 25 ng of mPAT2-cRNA were injected into oocytes. The oocytes were kept in modified Barth solution at 18 °C until further use (3–5 days after injection).

**Amino Acid Uptake**—10 oocytes (water or cRNA injected) per uptake experiment were preincubated at room temperature for 2 min in Na<sup>+</sup>-free standard uptake buffer (100 mM choline chloride, 2 mM KCl, 1 mM MgCl<sub>2</sub>, 1 mM CaCl<sub>2</sub>, 10 mM MES (pH 6.5)). The buffer was then replaced by the respective uptake buffer supplemented with 100  $\mu$ M amino acid and the corresponding <sup>3</sup>H-labeled L-amino acid as a tracer (5  $\mu$ Ci/ml). Uptake experiments were performed for 10 min because pilot experiments showed linearity in amino acid uptake during this time period (data not shown). The oocytes were washed 3 times with 3 ml of ice-cold wash buffer (uptake buffer containing 20 mM glycine) and distributed to individual vials. After oocyte lysis in 10% SDS, radioactivity was counted by liquid scintillation. Uptake solutions for the determination of pH-dependent uptake of L-proline were buffered with 10 mM MES/KOH (pH 5.5–6.5), HEPES/KOH (pH 7.0–8.0), or TRIS/HCl (pH 8.5).

**Two-electrode Voltage Clamp**—Two-electrode voltage clamp experiments were performed as described previously (12). Briefly, the oocyte was placed in an open chamber and continuously superfused with incubation buffer (100 mM choline chloride, 2 mM KCl, 1 mM MgCl<sub>2</sub>, 1 mM CaCl<sub>2</sub>, 10 mM MES, or HEPES at pH 5.5–8.5) in the absence or

presence of amino acids. Oocytes were voltage-clamped at –60 mV, and current-voltage (I-V) relations were measured using short (100 ms) pulses separated by 200-ms pauses in the potential range –160 to +80 mV. I-V measurements were made immediately before and 20–30 s after substrate application when current flow reached steady state. The current evoked by mPAT1 or mPAT2 at a given membrane potential was calculated as the difference between the currents measured in the presence and the absence of substrate. In studies investigating the cation or anion dependence of mPAT transport activity, 100 mM NaCl was equimolar replaced by either choline chloride, sodium isethionate, or potassium chloride.

H<sup>+</sup>/L-proline coupling stoichiometry was determined by direct comparison of net inward charge with [<sup>3</sup>H]proline accumulation in individual oocytes under voltage clamp as described (11). Oocytes were clamped at V<sub>m</sub> = –60 mV and superfused with standard Na<sup>+</sup>-free medium (pH 6.5) plus 500  $\mu$ M L-[<sup>3</sup>H]proline (ICN, 10  $\mu$ Ci/ml) for 5 min before washing out with Na<sup>+</sup>-free medium. Oocytes were solubilized, and the <sup>3</sup>H content was measured by liquid scintillation counting. The proline-evoked current was integrated with time to obtain the proline-dependent charge (Q<sup>Pro</sup>) and converted to a molar equivalent using the Faraday conversion.

Michaelis-Menten kinetics were constructed from experiments employing 5 different amino acid concentrations in Na<sup>+</sup>-free buffer at pH 6.5 with 6 individual mPAT1- or mPAT2-expressing oocytes from at least two different oocyte batches for each substrate. Substrate-evoked currents were transformed according to Eadie-Hofstee, and after linear regression, the substrate concentrations that cause half-maximal transport activity (apparent K<sub>m</sub>) were derived.

**Intracellular pH Recordings**—Intracellular pH of oocytes injected with mPAT1 or mPAT2-cRNA was measured using ion-selective microelectrodes filled with the proton ionophore I mixture B (Fluka). The electrodes were calibrated using solutions with different pH values, and only electrodes with a slope of >55 mV/pH unit and stable calibration were used. On basis of the calibration curves for the pH-sensitive electrode, the chemical potential for H<sup>+</sup> of oocytes was calculated as the difference between the membrane potential, measured simultaneously with a 3 M KCl microelectrode, and the electrochemical potential of the pH-sensitive electrode.

**RNA Isolation and Northern Blot Analyses**—Total RNA from different murine tissues were isolated with RNawiz (Ambion) following the supplier's protocol. Poly(A)<sup>+</sup> RNA samples were purified with Dynabeads (DynaL Biotech). 2  $\mu$ g of poly(A)<sup>+</sup> RNA and RNA standard (Promega) were separated by electrophoresis on a 1% agarose gel under denaturing conditions and subsequently transferred to a positively charged membrane (Hybond N, AP Biotech). The blot was hybridized with subtype-specific mPAT-cDNA, [ $\alpha$ -<sup>32</sup>P]dATP (ICN)-radiolabeled by random priming (AP Biotech), for 1 h in Express Hyb solution (BD Pharmingen CLONTECH) at 68 °C after high stringency washing. For detection of bound radioactivity, the blot was exposed on a PhosphorScreen and detected with Cyclone phosphorimaging (Packard BioScience). For a demonstration of RNA loading, the blot was hybridized with a  $\beta$ -actin cDNA probe.

**Transient Transfection of the mPAT2-EGFP-cDNA Construct in HeLa Cells**—The ORF of mPAT2 was amplified with the ELongase *Taq* polymerase (Invitrogen) and the mPAT2-cDNA as template using the primers mPAT2-F-*EcoRI* (TGAATTCATGTCTGTGACCAAGAGTGC) and mPAT2-B-*EcoRI* (AGAATTCCTGAATAAACATGGTGGAGTTGG). In both primer sequences an *EcoRI* restriction site was introduced to allow the ligation of the PCR product into the *EcoRI* site of the pEGFP-N2 vector (Invitrogen), which had the mPAT2 and the EGFP-coding region in the same frame. Insertion of the mPAT2 ORF in the right direction was checked by PCR. The mPAT2 cDNA insert was sequenced on both strands. For transfection, HeLa cells were grown on six-well plates to a confluency of about 70%. 2  $\mu$ g of the mPAT2-pEGFP construct was transfected using the SuperFect transfection reagent following the instructions of the manufacturer (Qiagen). Two days after transfection the cells were examined with a confocal laser-scanning microscope (Leica TCS) for the appearance of green fluorescence. Staining of acidic organelles with LysoTrackerRed was performed according to the supplier's protocol (Molecular Probes). The functionality of the mPAT2-EGFP fusion protein was tested after injection of its cRNA into *X. laevis* oocytes. Therefore, the mPAT2-EGFP-cDNA insert was cut with *XhoI* and *MunI* and subcloned into the pCRII vector including the rabbit PEPT2 3' end, as also used for enhanced expression of mPAT1. Uptake of radiolabeled glycine, alanine, and proline (100  $\mu$ M) into oocytes expressing mPAT2-EGFP was significantly increased ( $p < 0.01$ , Student's paired *t* test) when compared with the uptake in water-injected control oocytes. Similar to wild type mPAT2, proline uptake in



## Mammalian Proton/Amino Acid Cotransporters

22969

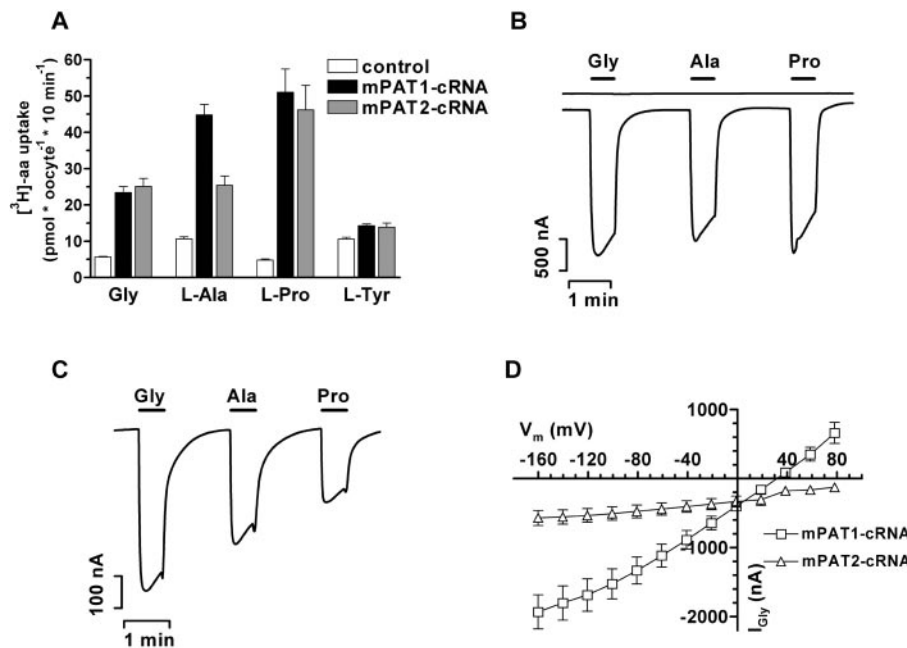


**FIG. 2. Basic functional characteristics of the mPAT1 and mPAT2 transporters expressed in *X. laevis* oocytes.** *A*, oocytes ( $n = 10$ ) were incubated in  $\text{Na}^+$ -free uptake buffer at pH 6.5 for 10 min with  $100 \mu\text{M}$   $^3\text{H}$ -labeled amino acids as indicated. The uptake rates of Gly, Ala, and Pro were elevated in mPAT1 (black bars)- and mPAT2 (gray bars)-expressing oocytes, whereas tyrosine uptake was not significantly different when compared with uptake in control oocytes (white bars). Applications of Gly, Ala, and Pro (20 mM) induced positive inward currents in mPAT1 (*B*)- and mPAT2 (*C*)-expressing oocytes at a holding potential of  $-60$  mV under  $\text{Na}^+$ -free conditions at a pH of 6.5. The upper trace in *B* represents the current recordings in water-injected control oocytes. *D*, the glycine-evoked currents in mPAT1- and mPAT2-cRNA-injected oocytes are dependent on the membrane potential. Hyperpolarization of the membrane increased glycine-evoked currents more potently in mPAT1 than in mPAT2 expressing oocytes ( $n = 3$ ).

the transport currents of mPAT1 and mPAT2, we first studied the effect of different cations and anions on the glycine-evoked currents. Replacement of  $\text{Na}^+$  by choline or  $\text{K}^+$  and  $\text{Cl}^-$  by isethionate had no significant effect on normalized mPAT1 and mPAT2 transport activity (Fig. 3A). On the other hand, lowering the extracellular pH led to a pronounced increase in mPAT1 and mPAT2 mediated L-proline influx (Fig. 3B). The mPAT1 transport activity was much more strongly influenced by changes of the extracellular pH than that of mPAT2. The uptake rate of  $100 \mu\text{M}$  L-Pro at pH 5.5 was 6-fold higher than that at pH 7.5 in mPAT1-expressing oocytes, whereas its stimulation in mPAT2-expressing oocytes was only increased by 45%. Direct evidence for a proton/amino acid symport mechanism was obtained by measuring intracellular pH changes by a hydrogen ion-selective electrode simultaneously with changes in membrane potential when perfusing oocytes in the absence or presence of 20 mM glycine or proline. As shown in Fig. 3C, the addition of glycine and proline to the perfusate led to an intracellular acidification as well as to a depolarization of oocytes expressing mPAT1. These effects were completely reversed by washing out the amino acids. The same effect was observed for glycine in mPAT2-expressing oocytes, whereas leucine, which is no substrate of the transporters, failed to induce an acidification and membrane depolarization. Water-injected control oocytes did not respond to the addition of any applied amino acid (data not shown).

The  $\text{H}^+/\text{L}$ -proline-coupling stoichiometry was directly determined by comparing the L-proline-dependent charge ( $Q^{\text{Pro}}$ ) with the concomitant accumulation rate of L- $^3\text{H}$ proline in individual oocytes voltage-clamped at  $-60$  mV (Fig. 4A).  $Q^{\text{Pro}}$  correlated with the  $^3\text{H}$  accumulation in a linear fashion with a slope of 0.97 (mPAT1) and 1.28 (mPAT2). The  $\text{H}^+/\text{L}$ -proline-coupling coefficients ( $n$ ) were  $1.22 \pm 0.04$  (mPAT1) and  $1.28 \pm 0.08$ , and the mean  $Q^{\text{Pro}}$  values were not significantly different from the  $^3\text{H}$  accumulation rates in a paired *t* test (Fig. 4B). This convincingly shows that the  $\text{H}^+$ -coupled L-proline transport via

mPAT1 and mPAT2 occurs with 1:1 stoichiometry.

Both transporters are very restrictive regarding substrate recognition. We tested all 20 proteinogenic L-amino acids for their ability to induce positive inward currents in mPAT1- and mPAT2-expressing oocytes at concentrations of 20 mM. Only amino acids with short side chains such as glycine, alanine, proline, and to a much smaller extent serine were able to interact with the transporters substrate binding sites (Fig. 5, A and B). No other proteinogenic amino acid was able to induce inward current significantly above background oocyte activity. On the other hand, the transporters are not very enantioselective, as shown by the inward currents induced by D-alanine, D-proline, and D-serine in Fig. 5, C and D. In oocytes expressing mPAT1 D-alanine- and D-proline-evoked currents were almost as high as those of glycine, whereas in the case of mPAT2, all D-enantiomers induced less than 30% of the glycine currents. In addition,  $\beta$ -alanine and the neurotransmitter GABA induced positive inward currents more potently in mPAT1- than in mPAT2-expressing oocytes (Fig. 5, C and D).

Dose-response experiments for currents in voltage-clamped oocytes injected with mPAT1- or mPAT2-cRNA were performed for selected amino acids and derivatives. Net substrate-evoked currents at five different concentrations were calculated, and after Eadie-Hofstee transformation and linear regression analysis, the apparent affinities ( $K_m$  values) were determined. Table I summarizes the obtained apparent  $K_m$  values. The proteinogenic amino acid with the highest affinity was L-Pro, with apparent  $K_m$  values of 2.8 mM (mPAT1) and 0.12 mM (mPAT2). In general, mPAT2 was found to have a more than 10-fold higher affinity for all three L- $\alpha$ -amino acids when compared with the affinities of mPAT1. The very low affinity of L-serine of  $>40$  mM for both transporters shows the very strict specificity, as the introduction of the polar hydroxy group almost abolishes affinity. D-Alanine has almost the same affinity for both transporters ( $K_m$  values of 6.3 and 6.5 mM for mPAT1 and mPAT2, respectively), again demonstrating that mPAT2 is more enan-

22970

## Mammalian Proton/Amino Acid Cotransporters

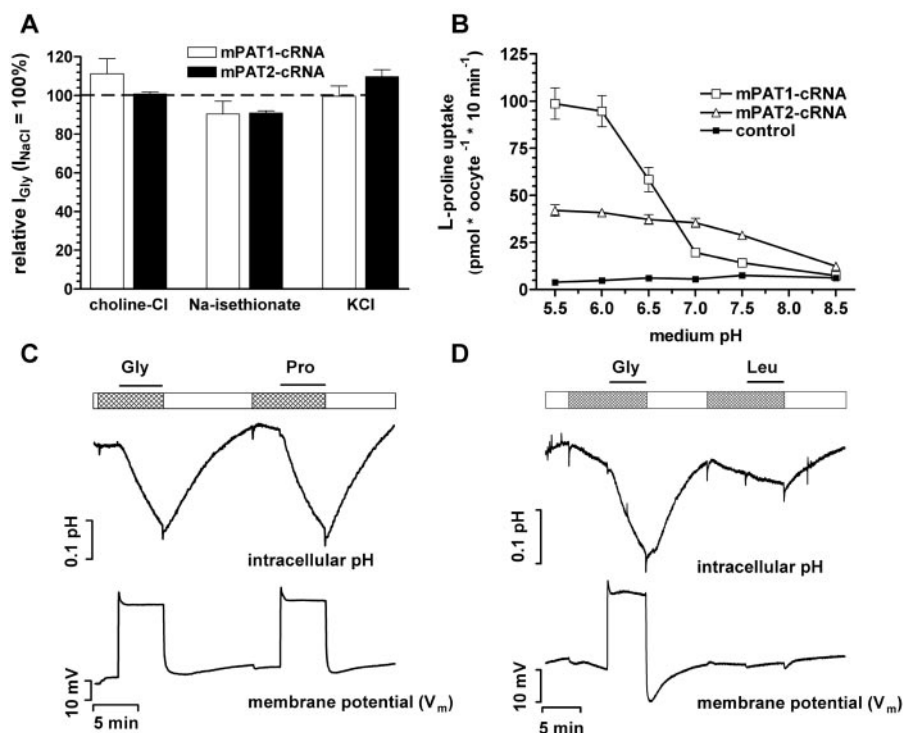


**FIG. 3. Ion dependence of mPAT1- and mPAT2-mediated transport activity.** *A*, the equimolar replacement of 100 mM NaCl by choline chloride, Na<sup>+</sup> isethionate, or KCl had no significant effect on glycine-evoked currents under voltage clamp conditions (−60 mV, 20 mM Gly, pH 6.5, *n* = 6 oocytes). Currents are normalized to the glycine-evoked currents in NaCl-containing medium. *B*, oocytes (*n* = 10) were incubated in Na<sup>+</sup>-free uptake buffer for 10 min with 100 μM L-[<sup>3</sup>H]proline at different medium pH values (pH 5.5–8.5). At pH 8.5 there was hardly any stimulation of proline uptake in cRNA-injected oocytes, whereas the uptake at pH 5.5 was stimulated 26-fold (mPAT1) and 11-fold (mPAT2) when compared with the uptake of water-injected oocytes. Intracellular pH changes in mPAT1 (*C*)- and mPAT2 (*D*)-expressing oocytes were recorded with a hydrogen ion-selective electrode (upper traces) simultaneously with the changes in membrane potential (lower traces). The time periods when oocytes were perfused with Na<sup>+</sup>-containing buffer at pH 7.4 (white boxes) and pH 6.5 (checkered boxes) and when 20 mM of the amino acid was present (black lines) are indicated. In mPAT1-expressing oocytes, the addition of 20 mM Gly and L-Pro led to a membrane depolarization and a concomitant intracellular acidification. The same effect of Gly but not of L-Leu was observed in mPAT2-expressing oocytes.

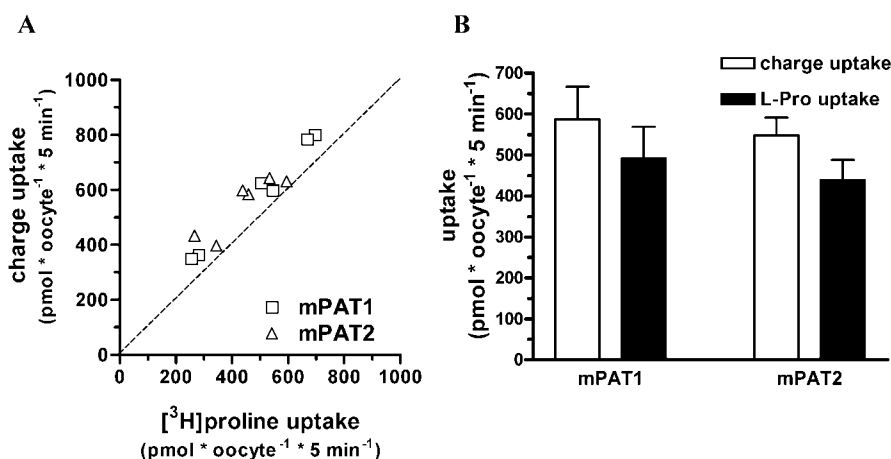


**FIG. 4. H<sup>+</sup> L-proline-coupling coefficient determined by L-[<sup>3</sup>H]proline uptake under voltage clamp conditions.** Oocytes were clamped at −60 mV, and 500 μM L-[<sup>3</sup>H]proline was applied for 5 min at a medium pH of 6.5. *A*, the proline-dependent charge ( $Q^{Pro}$ ) was compared with the concomitant tracer accumulation rate in the same oocytes expressing mPAT1 (squares) or mPAT2 (triangles). Tracer uptake in control oocytes ( $42.2 \pm 3.8$  pmol·5 min<sup>−1</sup>, *n* = 5 oocytes) was first subtracted. The ratio of  $Q^{Pro}:^3H$  was  $1.22 \pm 0.04$  for mPAT1 and  $1.28 \pm 0.08$  for mPAT2 (mean ± S.E., *n* = 6 oocytes), and there was no significant difference between  $Q^{Pro}$  (open bars) and <sup>3</sup>H (filled bars) accumulation (*B*) according to Student's paired *t* test.

tioselective than mPAT1. In addition, GABA is a very good substrate of mPAT1 ( $K_m = 3.1$  mM) but a poor substrate of mPAT2 ( $K_m = 30.9$  mM). In summary, mPAT2 therefore represents a high affinity-type PAT transporter and is more restrictive in substrate recognition when compared with the low affinity type mPAT1.

**Tissue Distribution of the mPAT Subtypes**—Northern blot analyses revealed that the mPAT mRNAs are differentially

expressed in murine tissues (Fig. 6A). The 5.0-kb mPAT1 transcript could be detected at higher levels in small intestine, kidney, brain, and colon. After longer exposure times, faint bands were also visible in all other tissues tested, excluding testis (data not shown). The mPAT2 mRNA (2.5 kb) was most abundantly expressed in lung and heart. Weaker signals could also be detected in kidney, testis, muscle, and spleen.

**Subcellular Localization of an mPAT2-EGFP Fusion Protein**

## Mammalian Proton/Amino Acid Cotransporters

22971

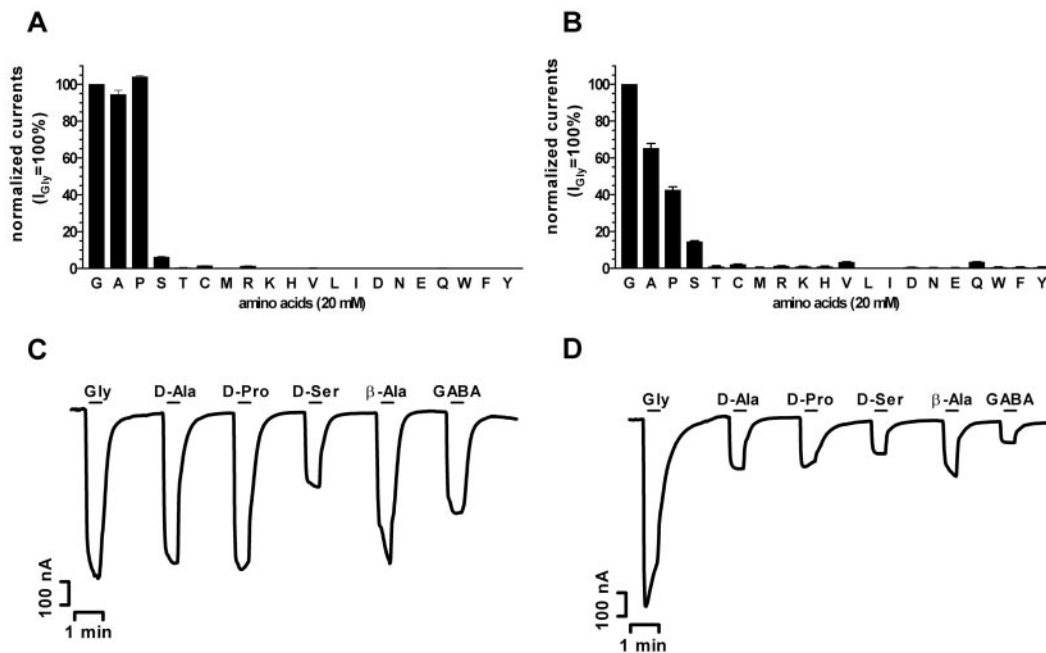


FIG. 5. **Substrate specificity of the mPAT1 and the mPAT2 transporter.** Oocytes expressing mPAT1 (A) or mPAT2 (B) were held at a membrane potential of  $-60$  mV and perfused with Na<sup>+</sup>-free buffer at pH 6.5 in the absence or presence of 20 mM indicated amino acid (one-letter code). The amino acid-evoked currents are displayed relative to glycine-induced currents ( $I_{Gly} = 1856 \pm 171$  and  $623 \pm 40$  nA for mPAT1 and mPAT2, respectively) as the mean  $\pm$  S.E. ( $n = 6$  oocytes). Amino acid-evoked currents in water-injected oocytes were, when detectable, subtracted. The lower panel shows representative current traces obtained in oocytes expressing mPAT1 (C) and mPAT2 (D) when perfused with selected D-amino acids,  $\beta$ -alanine, and GABA at concentrations of 20 mM in Na<sup>+</sup>-free buffer at pH 6.5. The time period when the compound was present in the perfusate is marked by the black lines.

TABLE I  
Apparent affinities of selected amino acids and derivatives of proton/amino acid cotransporters

Substrate-dependent transport kinetics of mPAT1 and mPAT2 were determined by two-electrode voltage clamp for the substrates indicated (5 concentrations) in Na<sup>+</sup>-free uptake solution (pH 6.5). Substrate-evoked currents were transformed according to Eadie-Hofstee, and  $K_m$  values were calculated by linear regression analysis. Data represent the mean  $\pm$  S.E. of six oocytes. For comparison,  $K_m$  values taken from the literature (in parentheses) on PAT-like transport activity, as found in the apical membranes of Caco-2 cells and in renal brush border membrane vesicles (BBMV) from pars convoluta, are shown. ND, not determined.

Substrate	$K_m$ value		<i>In vitro</i> $K_m$ value	
	mPAT1	mPAT2	Caco-2	Renal BBMV
		<i>mM</i>		<i>mM</i>
Glycine	$7.0 \pm 0.7$	$0.59 \pm 0.04$	$5.3 \pm 0.4$ (13)	$3.9$ (17)
L-Alanine	$7.5 \pm 0.6$	$0.26 \pm 0.05$	$5.7 \pm 0.7$ (14)	$4.4$ (18)
L-Proline	$2.8 \pm 0.1$	$0.12 \pm 0.02$	$9.2 \pm 0.9$ (15)	$4.5$ (19)
L-Serine	$69 \pm 5$	$43 \pm 4$	ND	ND
D-Alanine	$6.3 \pm 0.7$	$6.5 \pm 1.1$	ND	$7.86 \pm 0.38$ (20)
GABA	$3.1 \pm 0.2$	$30.9 \pm 0.1$	$1.95 \pm 0.78$ (16)	ND

*in Transfected HeLa Cells*—Although functional expression in oocytes suggested the transporters to be integral plasma membrane proteins, we used the EGFP-tagging approach to study the cellular localization of mPAT2. The mPAT2 protein, when tagged C-terminally with the EGFP protein was obviously translocated to the plasma membrane of HeLa cells (Fig. 6B). Substantial fluorescence was also found in the perinuclear compartment, most likely represented by the endoplasmic reticulum and the Golgi apparatus. However, currently we do not have any direct experimental evidence for this assumption. Because the rat orthologue of mPAT1, the rLYAAT-1 protein, has been colocalized in rat brain to lysosomes in neurons (5), we performed costaining experiments of the mPAT2-EGFP fusion protein in transfected HeLa cells with the LysoTrackerRed dye, which accumulates in acidic compartments, mainly lysosomes. When fluorescence of both dyes was merged, no significant colocalization was observed, suggesting that mPAT2 is not an integral protein of lysosomal membranes, at least not when overexpressed in HeLa cells (Fig. 6B).

## DISCUSSION

We identified by homology screening in expressed sequence tag databases two closely related murine transporter proteins, designated as mPAT1 and mPAT2, which belong to the eukaryotic AAAP family (2). The two deduced proteins could be functionally characterized as rheogenic proton/amino acid symporters with a specificity for amino acids with small side chains. Together with the rat LYAAT-1 transporter (the orthologue of PAT1), the mPAT proteins build a new subfamily next to the VGAT and system A/N transporter subfamilies within the phylogenetic tree of the AAAP family. Similar to mPAT1/rLYAAT-1 (5), a human orthologue of mPAT2 can be identified in the first version of the human genome. That the PAT2 gene is indeed expressed in human tissues *in vivo* is demonstrated by the presence of cDNA sequence fragments in the public EST data base (e.g. GenBank<sup>TM</sup> accession numbers BE501426 and BF511146).

Both mPAT transporters display similar functional properties when expressed in *X. laevis* oocytes. We show that the PAT

22972

## Mammalian Proton/Amino Acid Cotransporters

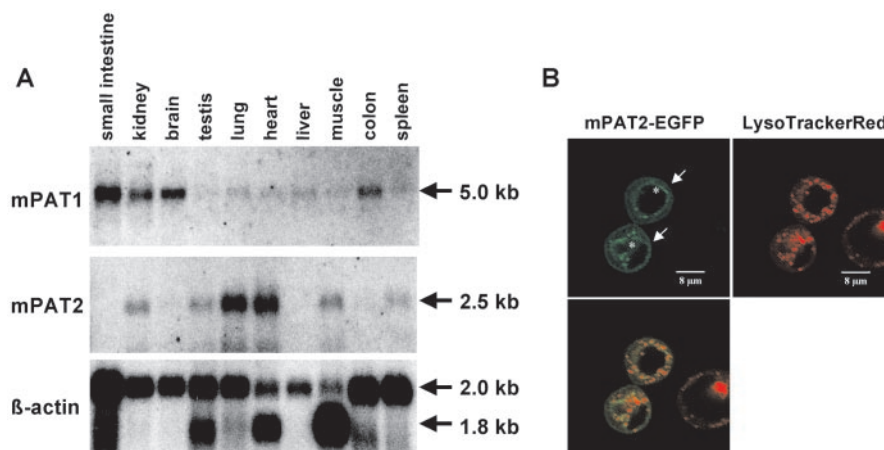


FIG. 6. Tissue distribution of the mPAT mRNA subtypes and subcellular localization of the mPAT2-EGFP fusion protein. *A*, the Northern blot was performed on murine Poly(A)<sup>+</sup> RNA isolated from different tissues using mPAT subtype-specific cDNA probes. As a control for the RNA integrity, the blot was also probed for  $\beta$ -actin. *B*, after transfection of a mPAT2-EGFP construct in HeLa cells, most of the green fluorescence appeared in the perinuclear region (asterisks) but also partly in the plasma membrane (arrows, upper left). Cells were stained with the LysoTrackerRed dye, which accumulates in acidic organelles, mainly lysosomes (upper right). In the superimposed image hardly any colocalization is observed (lower image). Scale bars are shown in the upper images.

carriers increase specifically the influx of small amino acids and demonstrate for the first time the electrogenic nature of the transport mechanism. Because all substrate amino acids are zwitterionic in the pH range studied, net charge movement across the plasma membrane is due to  $H^+$  influx stoichiometrically coupled to amino acid import. This was directly proven by a substrate-specific intracellular acidification induced by mPAT transport activity. No evidence was found for interactions of other tested cations or anion ( $Na^+$ ,  $K^+$ ,  $Cl^-$ ), suggesting that protons are the only ionic species cotransported with amino acids by mPAT1 and mPAT2. Transport activity of mPAT1 was highly dependent on membrane voltage and on extracellular pH in contrast to mPAT2, found to be only slightly influenced by both factors. This suggests that activity of mPAT1, but less so mPAT2, could be regulated by changes in membrane potential and pH within the physiological range. Whether these factors influence only the transport velocity or also substrate or  $H^+$  affinities has to be determined.

Both transporters display a narrow substrate specificity, preferentially accepting amino acids with small apolar side chains, such as glycine, alanine, and proline, whereas L-Ser is only poorly recognized. The mPAT2 protein has much higher affinities to the amino acids than mPAT1, with affinities 12–29-fold higher for Gly, L-Ala, and L-Pro under the same experimental conditions. The introduction of a hydroxy group (L-Ser) in the side chain dramatically diminishes the substrate affinity for both transporters (10- and >70-fold) in comparison to the  $K_m$  observed for L-Ala. Moreover, the introduction of a sulfhydryl group as in L-Cys abolishes substrate binding completely. The mPAT2 transporter shows a more restrictive substrate recognition pattern and a more pronounced enantioselectivity with only small neutral L- $\alpha$ -amino acids serving as high affinity substrates, whereas GABA and  $\beta$ -alanine are only poorly transported. Besides these functional differences, the mRNA transcripts of the transporters also show differential expression patterns in murine tissues. The mPAT1 mRNA has been detected in most of the examined tissues, with abundant expression in small intestine, colon, kidney, and brain, whereas highest signal levels of the mPAT2 mRNA were obtained in heart and lung. The physiological significance of the differential distribution of proton-dependent small amino acid transporters with different functional properties in the organism has to be investigated.

The only functionally known and characterized mammalian

homologue of the new murine PAT transporters is the lysosomal amino acid transporter (rLYAAT-1) from *Rattus norvegicus*. It most likely represents the first lysosomal proton/amino acid symporter found in mammals (5). rLYAAT-1, which has been functionally characterized after transient transfection in the fibroblast cell line CV-1, displays a very similar substrate specificity and shows similar kinetics as mPAT1, which represents the murine orthologue. Only two minor differences were obtained regarding functional properties. First, L-serine did not inhibit GABA uptake into rLYAAT-1-transfected CV-1 cells at a concentration of 0.5 mM (5), whereas in our experiments 20 mM L-serine induced significant inward currents in mPAT1-expressing oocytes. The most simple explanation might be the very low affinity of this amino acid to mPAT1, with an apparent  $K_m$  value of 69 mM, which may prevent inhibition. Second, the GABA affinity for rLYAAT-1 has been determined with a  $K_m$  value of 0.5 mM (5), whereas GABA displayed a  $K_m$  of 3.1 mM in the case of mPAT1. This difference, however, may be explained by the different experimental conditions such as pH (5.5 versus 6.5) and membrane potential (open circuit versus voltage-clamped) or species differences (rat versus mouse).

Regarding the physiological importance of the PAT carriers in mammals, it may be considered that the two proteins described here are as well lysosomal transporters responsible for the export of small amino acids from the lysosomal lumen into the cytoplasm. However, as already stated by Sagne *et al.* (5), no direct functional evidence for such systems has been found in lysosomal preparations. Moreover, the functionally characterized lysosomal small amino acid transport systems f and p have significantly different substrate specificities and affinities and appear not to act as proton symporters (21). On the other hand, in comparing our functional data with amino acid influx studies in cell lines and membrane vesicle preparations, we found a striking similarity between mPAT1 and the proton-dependent amino acid transport systems previously identified in the apical membrane of the intestinal Caco-2 cells (13–16) and renal brush border membrane vesicle preparations (17–20). These transport systems in apical membranes of intestinal and renal tubular epithelial cells have been well characterized, and it was convincingly shown that they are secondary active systems for the same small amino acids (Gly, Ala, Pro) and selected derivatives. The substrate specificity and kinetics of mPAT1 is identical to the transport system described in Caco-2 cells, which preferentially transports small apolar amino acids,

## Mammalian Proton/Amino Acid Cotransporters

22973

selected D-amino acids (e.g. D-Ala and D-Ser), the  $\beta$ -amino acid  $\beta$ -alanine, and the neurotransmitter GABA (13). Moreover, the stoichiometry of the transport system was proposed to be 1:1 (14), as found for mPAT1. The substrate affinities, as available from the literature, are in the same range as determined for mPAT1 (see Table I for  $K_m$  values; Refs. 13–21). Minor differences in affinities may again be due to different experimental conditions such as medium pH or membrane potential. The mPAT1 transcript is in addition abundantly expressed in the small intestine and kidney, giving further evidence for its potential role as a transport system in the apical membrane of enterocytes and kidney tubular cells. In addition, when performing reverse transcriptase-PCR with Caco-2 cell RNA and human PAT1-specific primers, we amplified a PCR product with the predicted size (data not shown).

Expression of mPAT1 and mPAT2 in oocytes and of rLYAAT in CV-1 cells clearly demonstrated that the proteins serve as plasma membrane carriers; however, this could be an artifact of overexpression. Nevertheless, our transfection experiments with the mPAT2-EGFP fusion protein did not reveal evidence for a lysosomal localization of this protein in HeLa cells. Based on this circumstantial evidence we have chosen the more general designation PAT for the two new proton amino acid cotransporters to indicate that they are not *a priori* lysosomal carriers, although the rLYAAT-1 protein was exclusively expressed *in vivo* in neuronal lysosomes of the rat brain (5). Immunohistochemical studies in other tissues than brain have so far not been performed. Consequently, nothing is known currently about the subcellular localization of the mPAT1/LYAAT-1 proteins in tissues such as small intestine and kidney. Nevertheless it might be that the mPAT1/LYAAT-1 protein is targeted in a cell-specific manner to reach either the plasma membrane or the lysosomes. Such cell type-specific targeting has already been shown for other membrane proteins including the epithelial peptide transporter PEPT1, which is mainly found in the apical plasma membrane of intestinal and renal epithelial cells (22, 23), but it is also found in lysosomes of pancreatic acinar cells (24). Therefore, it could be that the PAT proteins serve as both proton-dependent plasma membrane import transporters and lysosomal exporters for small amino acids.

In conclusion, we have identified, cloned, and functionally characterized two mammalian electrogenic H<sup>+</sup>/amino acid symporters with a high selectivity for amino acids with apolar

and small side chains as well as related compounds. Although their cellular localization has not yet been finally determined, they may serve as plasma membrane and/or lysosomal carriers. The characteristics, in particular of mPAT1, resemble in view of the mode of operation, substrate specificity, substrate affinity, and enantioselectivity the functions of apical membrane carriers identified in intestine and kidney for which the protein entities had not been identified until now.

## REFERENCES

- Saier, M. H., Jr. (2000) *Microbiology* **146**, 1775–1795
- Young, G. B., Jack, D. L., Smith, D. W., and Saier, M. H., Jr. (1999) *Biochim. Biophys. Acta* **1415**, 306–322
- Boorer, K. J., Frommer, W. B., Bush, D. R., Kreman, M., Loo, D. D., and Wright, E. M. (1996) *J. Biol. Chem.* **271**, 2213–2220
- Russnak, R., Konczal, D., and McIntire, S. L. (2001) *J. Biol. Chem.* **276**, 23849–23857
- Sagne, C., Agulhon, C., Ravassard, P., Darmon, M., Hamon, M., El Mestikawy, S., Gasnier, B., and Giros, B. (2001) *Proc. Natl. Acad. Sci. U. S. A.* **98**, 7206–7211
- McIntire, S. L., Reimer, R. J., Schuske, K., Edwards, R. H., and Jorgensen, E. M. (1997) *Nature* **389**, 870–876
- Sagne, C., El Mestikawy, S., Isambert, M. F., Hamon, M., Henry, J. P., Giros, B., and Gasnier, B. (1997) *FEBS Lett.* **417**, 177–183
- Forgac, M. (1999) *J. Biol. Chem.* **274**, 12951–12954
- Chaudhry, F. A., Reimer, R. J., Krizaj, D., Barber, D., Storm-Mathisen, J., Copenhagen, D. R., and Edwards, R. H. (1999) *Cell* **99**, 769–780
- Reimer, R. J., Chaudhry, F. A., Gray, A. T., and Edwards, R. H. (2000) *Proc. Natl. Acad. Sci. U. S. A.* **97**, 7715–7720
- Yao, D., Mackenzie, B., Ming, H., Varoqui, H., Zhu, H., Hediger, M. A., and Erickson, J. D. (2000) *J. Biol. Chem.* **275**, 22790–22797
- Kottra, G., and Daniel, H. (2001) *J. Physiol.* **536**, 495–503
- Thwaites, D. T., McEwan, G. T., and Simmons, N. L. (1995) *J. Membr. Biol.* **145**, 245–256
- Thwaites, D. T., McEwan, G. T., Brown, C. D., Hirst, B. H., and Simmons, N. L. (1994) *J. Membr. Biol.* **140**, 143–151
- Thwaites, D. T., McEwan, G. T., Cook, M. J., Hirst, B. H., and Simmons, N. L. (1993) *FEBS Lett.* **333**, 78–82
- Thwaites, D. T., Basterfield, L., McCleave, P. M., Carter, S. M., and Simmons, N. L. (2000) *Br. J. Pharmacol.* **129**, 457–464
- Roigaard-Petersen, H., Jessen, H., Mollerup, S., Jorgensen, K. E., Jacobsen, C., and Sheikh, M. I. (1990) *Am. J. Physiol.* **258**, F388–F396
- Jorgensen, K. E., and Sheikh, M. I. (1987) *Biochem. J.* **248**, 533–538
- Roigaard-Petersen, H., Jacobsen, C., Jessen, H., Mollerup, S., and Sheikh, M. I. (1989) *Biochim. Biophys. Acta* **984**, 231–237
- Jessen, H., Vorum, H., Jorgensen, K. E., and Sheikh, M. I. (1988) *Biochim. Biophys. Acta* **942**, 262–270
- Pisoni, R. L., Flickinger, K. S., Thoene, J. G., and Christensen, H. N. (1987) *J. Biol. Chem.* **262**, 6010–6017
- Bockman, D. E., Ganapathy, V., Oblak, T. G., and Leibach, F. H. (1997) *Int. J. Pancreatol.* **22**, 221–225
- Ogihara, H., Saito, H., Shin, B. C., Terado, T., Takenoshita, S., Nagamachi, Y., Inui, K., and Takata, K. (1996) *Biochem. Biophys. Res. Commun.* **220**, 848–852
- Shen, H., Smith, D. E., Yang, T., Huang, Y. G., Schnermann, J. B., and Brosius, F. C., III (1999) *Am. J. Physiol.* **276**, F658–F665



## APPENDIX 2

published in *Genomics*

ACADEMIC  
PRESSAvailable online at [www.sciencedirect.com](http://www.sciencedirect.com)

SCIENCE @ DIRECT®

Genomics 82 (2003) 47–56

GENOMICS

[www.elsevier.com/locate/ygeno](http://www.elsevier.com/locate/ygeno)

## A cluster of proton/amino acid transporter genes in the human and mouse genomes<sup>☆</sup>

Michael Boll,\* Martin Foltz, Isabel Rubio-Aliaga, and Hannelore Daniel

*Molecular Nutrition Unit, Institute of Nutritional Sciences, Technical University of Munich, Hochfeldweg 2, D-85350 Freising-Weihenstephan, Germany*

Received 14 November 2002; accepted 27 March 2003

### Abstract

We recently cloned and functionally characterized two novel proton/amino acid transporters (PAT1 and PAT2) from mouse. Here we report the isolation of the corresponding cDNAs of the human orthologues and one additional mouse and human PAT-like transporter cDNA, designated PAT3. The PAT proteins comprise 470 to 483 amino acids. The mouse PAT3 mRNA is expressed in testis of adult mice. In the human and mouse genomes the genes of the PAT transporters (designated *SLC36A1–3* and *Slc36a1–3*, respectively) are clustered on human chromosome 5q33.1 and in the syntenic region of mouse chromosome 11B1.3. PAT-like transporter genes are present as well in the genomes of other eukaryotic organisms such as *Drosophila melanogaster* and *Caenorhabditis elegans*. For the PAT3 subtype transporter, we could not yet identify its function. The human PAT1 and PAT2 transporters when functionally expressed in *Xenopus laevis* oocytes show characteristics similar to those of their mouse counterparts.

© 2003 Elsevier Science (USA). All rights reserved.

Members of the eukaryote-specific amino acid/auxin permease (AAAP)<sup>1</sup> transporter family are found in virtually all eukaryotic organisms, like yeasts, plants, invertebrates, and vertebrates [1,2]. In mammals three different subfamilies of the AAAP transporter class have been so far identified, including the vesicular GABA transporter (VGAT) [3], the various system A/N transporters [4–7], and the LYAAT/PAT subfamily [8,9]. Although the amino acid sequences between the subgroups are quite divergent, a common signature within the protein sequences is found [1]. Moreover the proposed membrane topology, so far exclusively based on hydropathy analysis [3,4,8], is very similar and suggests that most of the mammalian AAAP family members com-

prise 11 putative transmembrane domains. All mammalian AAAP transporters that have been functionally characterized possess two common features. First, they all recognize amino acids or closely related compounds as substrates [3,5,9] and second, the transporters' function is altered by changes in the intra- or extracellular proton concentration, with protons serving either as cotransported ions (PAT transporters) [8,9] or antiport ions (VGAT and system N transporters) [3,4] or as negative regulators of activity (system A transporters) [5].

The first mammalian AAAP transporter, the vesicular GABA transporter (VGAT, VIAAT), was identified by two independent studies [3,10] based on the previous characterization of the *Caenorhabditis elegans* mutant *unc-47*. The *unc-47* phenotype is caused by the selective impairment of GABAergic neurotransmission, and the *unc-47* gene was identified by positional cloning. By sequence homology screening, the mammalian orthologous cDNAs were cloned, and their overexpression in neuronal cells identified a GABA/H<sup>+</sup> antiport mechanism [3,10]. The VGAT protein has been localized to synaptic vesicles of selected neurons in various regions of the brain that are known to play a role in GABAergic and/or glycinergic neurotransmission [3].

<sup>☆</sup> Sequence data from this article have been deposited with the GenBank Data Libraries under Accession No. AY162213 (human PAT1), AY162214 (human PAT2), AY162215 (human PAT3), and AF453745 (mouse PAT3).

\* Corresponding author. Fax: +49-8161-71-3999.

E-mail address: [boll@wzw.tum.de](mailto:boll@wzw.tum.de) (M. Boll).

<sup>1</sup> Abbreviations used: PAT, proton/amino acid transporter; SLC, solute carrier; AAAP, amino acid/auxin permease; VGAT, vesicular GABA transporter; VIAAT, vesicular inhibitory amino acid transporter; LYAAT, lysosomal amino acid transporter; TMD, transmembrane domain; EST, expressed sequence tag; RACE, rapid amplification of cDNA ends.

Therefore, VGAT is responsible for the uptake and storage of GABA and glycine in synaptic vesicles [11].

The second AAAP subfamily contains the amino acid transport systems A and N. Both transporter types play important roles in the homeostasis of various neutral amino acids. So far three different subtypes of system A (SAT1–3/ATA1–3) and two subtypes of system N (SN1 and SN2) have been cloned from different mammalian species [4–7]. The system A and N proteins show a high similarity of >60% to one another [5]. Both transporter subtypes are localized in the plasma membrane. In brain, system SN1 is localized exclusively in astrocytic cells, whereas system A shows neuronal expression [4,12]. Both carriers seem to play a central role in the intercellular transport of glutamine between astrocytes and neurons in its delivery as a precursor for glutamate [13]. In addition to their function in neurotransmission, system A and N transporters are key players in the interorgan fluxes of neutral amino acid, especially of alanine and glutamine [5,14].

The third mammalian subgroup of AAAP transporters is at present represented by the rat LYAAT1 and the mouse PAT1 and PAT2 transporters. LYAAT1 and PAT1 are orthologues, identified independently by Sagne et al. [8] and our lab [9] by homology-based cloning. Very recently, Chen et al. [15] reported the cloning of a human PAT1 cDNA from a human Caco-2 cDNA library. PAT1 and PAT2 are proton-dependent transporters for small amino acids, such as glycine, alanine, and proline. Uptake of these amino acids by the mouse PAT1 and PAT2 transporters is electrogenic and leads to an intracellular acidification suggesting a proton/amino acid symport mechanism [9]. In addition to L- $\alpha$ -amino acids,  $\beta$ -alanine and GABA have been shown to interact with the transporters' binding site. Whereas the  $K_m$  values for substrates of PAT1 range from 2.5 to 15 mM, PAT2 represents the high-affinity subtype with  $K_m$  values for the same substrates that are generally less than 0.6 mM. The transporters' mRNAs are differentially expressed in mouse tissues as determined by Northern blot analysis. The PAT1 mRNA has been detected in virtually all tissues examined, with high expression levels in brain, small intestine, colon, and kidney. Moreover, the PAT1/LYAAT1 protein has been detected in lysosomes of neurons in rat brain [8]. In contrast to PAT1/LYAAT1, we could not detect the PAT2 transporter in lysosomes when using an EGFP-fusion protein, but showed its presence in the plasma membrane when overexpressed in HeLa cells [9]. We therefore propose that the PAT2 transporter plays a role in the influx of small amino acids into selected cells. It seems like these two transporters play a dual role in the mammalian organism, mediating the efflux of small amino acids from lysosomes into the cytosol and in epithelial cells with an apical localization mediating the uptake of small amino acids into the cell [8,9]. The expression pattern of the PAT2 mRNA seems more restricted and particularly high expression levels were observed in lung and heart but lower levels are also found in kidney, testis, muscle, and spleen [9].

Here we present the cloning of the human PAT1 and PAT2 cDNAs, as well as the identification of a new PAT member, designated PAT3, from mouse and human. Interestingly, all three genes encoding the PAT transporters are located in the human as well as in the mouse genome in a chromosomal region spanning less than 250 kb. The human genes, designated *SLC36A1–3*, are located on chromosome 5q33.1 and the mouse genes *Slc36a1–3* on chromosome 11B1.3. To assess whether the human transporters have functions similar to those of their murine counterparts, we determined their transport characteristics after heterologous expression.

## Results and discussion

### *Identification of the mouse PAT3 and the human PAT1-3 transporter cDNAs*

We previously identified two cDNAs (PAT1 and PAT2) from mouse [9], encoding proton/amino acid symport activity as shown by tracer flux studies and electrophysiological analysis after expression in *Xenopus laevis* oocytes. Here, we report the cloning of the human PAT1 transporter cDNA by a reverse transcriptase PCR approach, using Caco-2 cell RNA as a template, and the cloning of the human PAT2 cDNA from a human adult testis cDNA library by homology screening. In addition, we were able to identify a third PAT cDNA, designated PAT3, in the human and mouse genome. The complete open reading frame (ORF) of the mouse PAT3 transporter was amplified by RT-PCR, whereas the human PAT3 ORF sequence was obtained by assembling RT-PCR product sequences from different cDNA regions, and the 5' end sequence was obtained by 5'RACE. The cloning of a human PAT1 cDNA from a Caco-2 cell cDNA library was very recently reported [15] but its sequence is not yet publicly available and therefore no comparison at the nucleotide sequence level was possible.

An alignment of the human and mouse PAT proteins is shown in Fig. 1. The PAT proteins comprise 470 to 483 amino acids. The human and mouse orthologous proteins share a high similarity to each other with 91 (PAT1), 89 (PAT2), and 83% (PAT3) over the entire protein sequence. The mouse and human PAT1 and PAT2 proteins are the most closely related paralogs, with an overall similarity of ~80%. Conserved residues are distributed over the entire protein sequences, with the exception of the ~40- to 50-amino-acid-long N-terminal stretch. Using the Kyte and Doolittle algorithm for hydropathy analysis, an 11-transmembrane-domain (TMD) topology is predicted for the PAT1 and PAT2 proteins, as shown for the mouse PAT1 model in Fig. 2. In the human and mouse PAT3 sequences, the region that corresponds to TMD 8 in PAT1 and PAT2 does not reveal a clear-cut hydrophobicity profile so that either 10 or 11 TMDs are predicted for this transporter



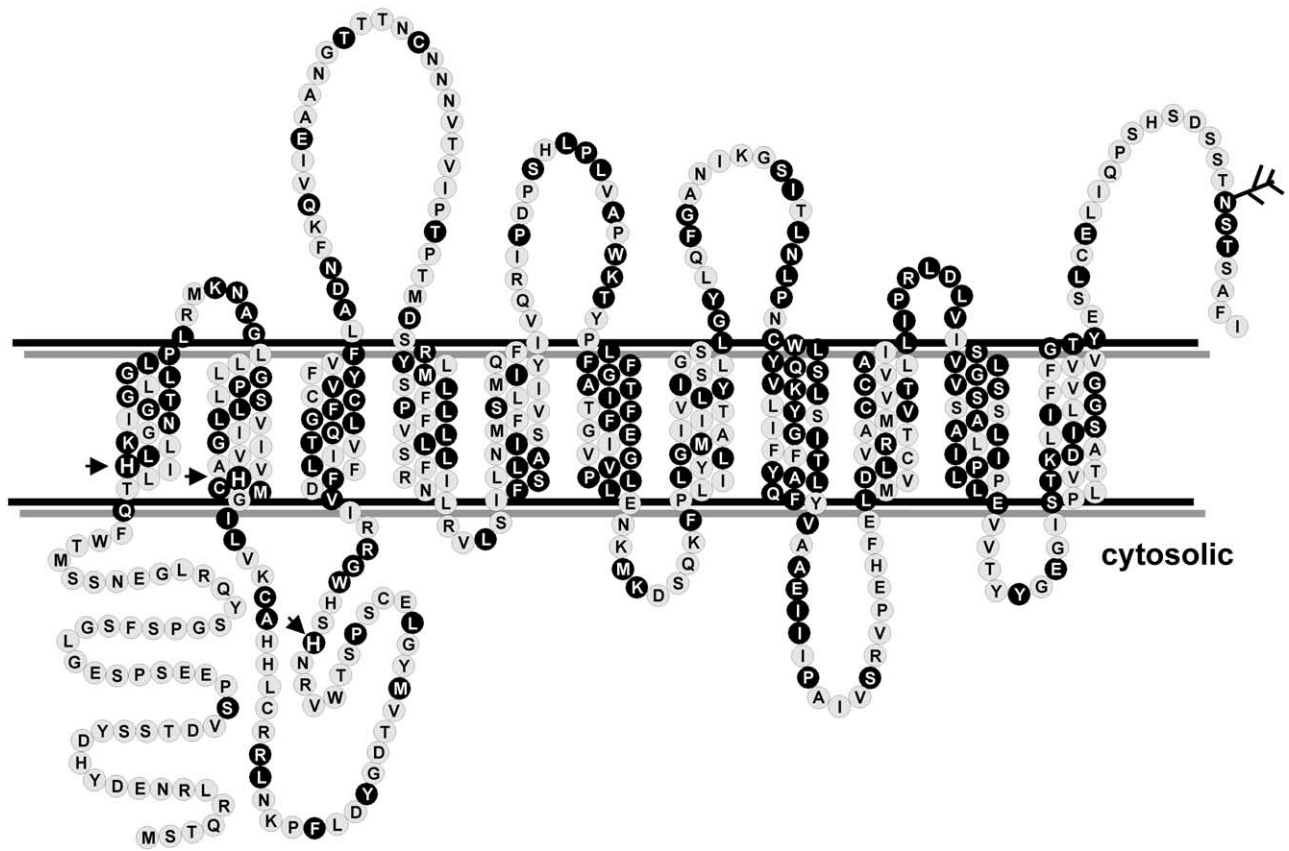


Fig. 2. Topology model of the mouse PAT1 protein. Amino acids are represented by circles, with the amino acid residue in the one-letter code. Putative transmembrane domains are shown schematically. Black circles (with white letters) represent identical residues in the PAT proteins, shown in Fig. 1. The conserved putative N-glycosylation site is marked as a branch. The three conserved histidine residues are marked by arrows.

respectively. Conserved amino acid residues are essentially spread over the entire protein sequences with the exception of the predicted cytosolic N-terminal stretch. Although the transporter proteins of the different subfamilies are distantly related on the molecular level, they all share the two functional features of high proton selectivity and sensitivity and amino acid transport specificity.

Sagne et al. reported that LYAAT1 homologues are found in other organisms, like in *Drosophila melanogaster* and *C. elegans* [8]. We extended this analysis and searched databases for the other AAAP members in these two model organisms. In *D. melanogaster* there are most likely 24 and in *C. elegans* 14 members of the AAAP family found in the available genome databases, of which only unc-47 (the *C.*

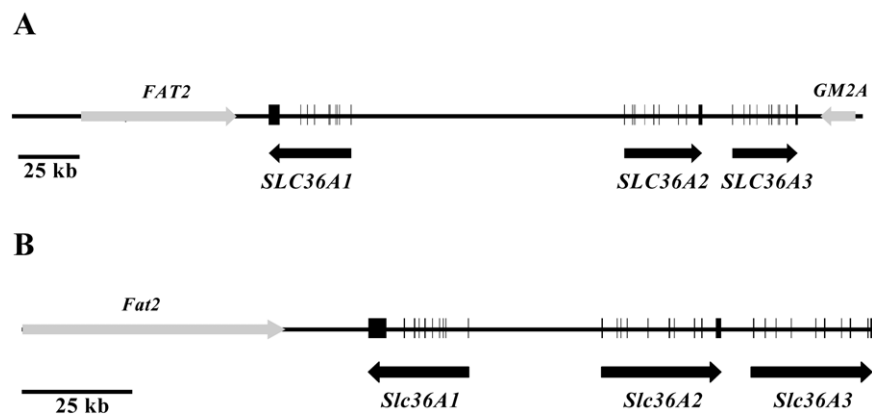


Fig. 3. Genomic organization of the human and mouse *SLC36/Slc36* genes. (A) The exon/intron organization of the *SLC36A1–3* genes on human chromosome 5q33.1 and (B) their orthologous genes *Slc36a1–3* on mouse chromosome 11B1.3 are shown. The flanking human genes *FAT2* and *GM2A*, as well as the mouse *Fat2* gene, are shown for orientation.

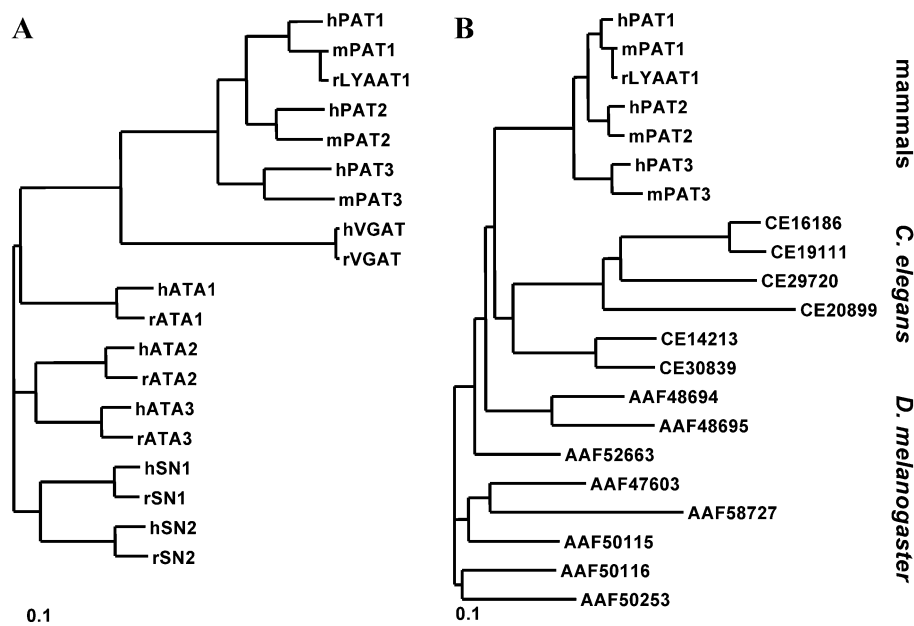


Fig. 4. Dendrograms of the mammalian AAAP and the eukaryotic PAT-like family members. Dendrograms were constructed by the neighbor-joining algorithm using the ClustalW program. (A) Dendrogram of the mammalian members of the AAAP family, demonstrating a classification of the proteins into three different subfamilies. (B) Dendrogram of the PAT and PAT-like proteins in mammals, *D. melanogaster*, and *C. elegans*. The scale bars indicate the distances between the proteins.

*elegans* VGAT ortholog) has yet been assigned a physiological function [3,10]. All other AAAP proteins are deduced only by genome scan analysis and homology search. Comparing those AAAP-like transporter proteins with human and mouse protein sequences, 8 deduced proteins of *D. melanogaster* and 6 proteins of *C. elegans* show highest similarity to the mammalian PAT transporters. Fig. 4B shows a dendrogram of the PAT-like proteins of various mammals as well as *D. melanogaster* and *C. elegans*. The PAT-like proteins in *D. melanogaster* have a similarity of 42–53% with the mammalian PAT proteins, nearly in same range as the *C. elegans* PAT-like proteins, with a similarity range of 43–51%. Therefore, the PAT transporters display a fairly high degree of evolutionary conservation, which predicts also in the invertebrates a distinct physiological role in amino acid transport.

It needs to be emphasized that all lower eukaryotes and prokaryotes use predominantly a transmembrane electrochemical proton gradient as the driving force for nutrient uptake, including the uptake of amino acids. It is believed that during evolution in higher eukaryotes the transmembrane  $\text{Na}^+$  gradient generated by  $\text{Na}^+/\text{K}^+$  ATPase and  $\text{Na}^+/\text{H}^+$  exchangers has taken over the role of plasma membrane electrochemical proton gradients in providing the driving force for the majority of electrogenic transport systems. The high number of PAT-like proteins in *D. melanogaster* and *C. elegans* compared to the low number identified in mammals may reflect the substitution of PAT-like proteins with those that utilize  $\text{Na}^+$  gradients and that belong to other protein families. As already stated, we could identify only one additional PAT-like gene in mammals,

including *Homo sapiens*, with a location on human chromosome 11q21, and there is also no evidence from the mammalian EST sequence databases for more than a total of four PAT transporter cDNAs. For the VGAT transporter, one ortholog in *C. elegans* (*unc-47*), as well as one in *D. melanogaster* (AAF58280, deduced protein), was found. None of the systems A and N transporter-like genes/proteins could be detected in the genome/protein sequence database of either organism (data not shown), suggesting that the systems A and N transporters may represent the evolutionarily more recent family branch of genes in the transition from proton-gradient-driven to sodium-gradient-driven electrogenic membrane transporters.

Comparing the amino acid sequences of all identified PAT-like proteins, several highly conserved regions can be identified. The multiple sequence alignment in Fig. 5 represents one of the most highly conserved regions within the PAT proteins. The consensus sequence derived from the alignment is [FLVI]-R-x(3)-[VLM]-x(6)-[AS]-x(2)-[IVL]-P-x-[LI]-x(3)-[ILMVT]-[SPGE]-[LF]-[VIFE]-G-[ASIV]-[FVTL]-[CSA]-[GSLF]-x(2)-[LICM]-[AGNST]-[LMFI]-[IVLA]-x-P-[PASV]-[LFVIC]-[LIF]. This region comprises a part of TMD 9, the fifth luminal loop, and TMD 10, according to the topology model shown in Fig. 2. This consensus sequence of the PAT proteins is not completely represented in the other AAAP-like transporter proteins [1].

#### *Tissue-specific expression of the PAT3 mRNA in mice*

The mRNAs of the PAT1 and PAT2 subtypes display different expression patterns in mouse tissues. Whereas

52

*M. Boll et al. / Genomics 82 (2003) 47–56*

		TMD 9	TMD 10	
hPAT1	378	VRTVLVCLTCILAILIPRLDLVISLVGSVSSSALALIIPPLL	420	
hPAT2	385	IRLVMVCLTCLLAILIPRLDLVISLVGSVSGTALALIIPPLL	427	
hPAT3	368	VRSALVCLTCVSAILIPRLDLVISLVGSVSSSALALIIPALL	410	
mPAT1	377	VRTAMVCVTCVLAILIPRLDLVISLVGSVSSSALALIIPPLL	419	
mPAT2	380	IRLALVCLTCMLAILIPRLDLVLSLVGSVSSSALALIIPPLL	422	
mPAT3	380	VRTALVCLTCFSAVLIIPRLDLVISLVGSVSSSALALIIPPLL	422	
AAF47603	363	FRAIVLLTFGCAVAIPDLSVFLSLVGSFCLSILGLIFPVLL	405	
AAF48694	375	FRTFMVLVTLAIAEMVPALGLFISLIGALCSTALALVFPPVI	417	
AAF48695	371	LRFFMVMMTFGVALVVPKLNLFISLIGALCSTCLAFVIVLI	413	
AAF50115	372	VRTGLVLTFFLLAVAI PNLELFISLFGALCLSALGLAFPALI	414	
AAF50116	410	LRVFLVLLCGGIAVALPNLGPFIISLIGAVCLSTLGMIVPATI	452	
AAF50253	405	LRTVLVTAAVVLAVAVPTIGPFMGLIGAFCSILGLIFPVVI	447	
AAF52663	397	LRVVLVTFLLATCI PNLSIIISLVGAVSSSALALIAPPPII	439	
AAF58727	366	VRLFLFLTGAVAIGVFNLAALTELEGAFSLSNLLNLLCPALI	408	
CE14213	358	IRFGGVLTCAMAQLIPHLALFISLVGSVAGTSLTLVFPPLI	400	
CE16186	388	LRLGLMLISLCIALIVPNMQIIPVGIITSGLLISLILPSFL	430	
CE19111	373	LRLSMLVSLSLALAVPNLTEIIPFVGITSGLLISLIIPPSFL	415	
CE20899	363	FRVFWLVVTYLMAVLI PKLEIMIPLVGVTSALCALIFPPFF	405	
CE29720	347	FRYSIVLVFLLSYAIPRLSDMPLVGVGTAGMLLALVFPSLF	389	
CE30839	368	ARYSGVILTCAIAELIPHLALFISLIGAFSGASMALLFPPCI	410	
		* : : * : . : * . : * :		

Fig. 5. Multiple alignment of a highly conserved region in the PAT proteins. Using the Block Maker program, highly conserved regions in the PAT proteins were identified. The consensus sequence derived from the multiple alignment is noted in the text.

the PAT1 mRNA is highly expressed in small intestine, colon, kidney, and brain, the mouse PAT2 mRNA is abundantly detected in lung and heart [9]. In contrast, the PAT3 mRNA has a very restricted expression pattern. By using reverse transcription PCR, a specific band could be detected only in testis of adult mice (Fig. 6), whereas specific PCR products could be amplified for PAT1 and PAT2 in all tissues tested, with variable signal intensities. PAT1 mRNA was hardly detectable in skeletal muscle and PAT2 mRNA in small intestine and liver. Based on Northern blot analysis, the PAT2 mRNA was not detectable in small intestine, brain, liver, or colon [9], but by employing RT-PCR we were able to amplify the PAT2 mRNA in virtually all tissues examined, which was also the case for the PAT1 mRNA. Therefore, the expression patterns of PAT1 and PAT2 mRNA do not differ very much, but as shown previously, the absolute expression levels in the various tissues are strikingly different [9]. On the other hand, the apparent exclusive expression of PAT3 mRNA in the testis in adult male mice addresses the question of its physiological role in this organ. What has not been shown yet is whether PAT3 expression is sex-specific or whether PAT3 mRNA can also be found in the female reproductive tissues. Furthermore, the cell specificity of its expression and the subcellular localization of PAT3 have to be determined before its physiological role can be predicted or proven. The mRNA expression of the various human orthologous PAT transporters is evident, as for all three subtypes various sequence fragments are present in the EST sequence database (data not shown).

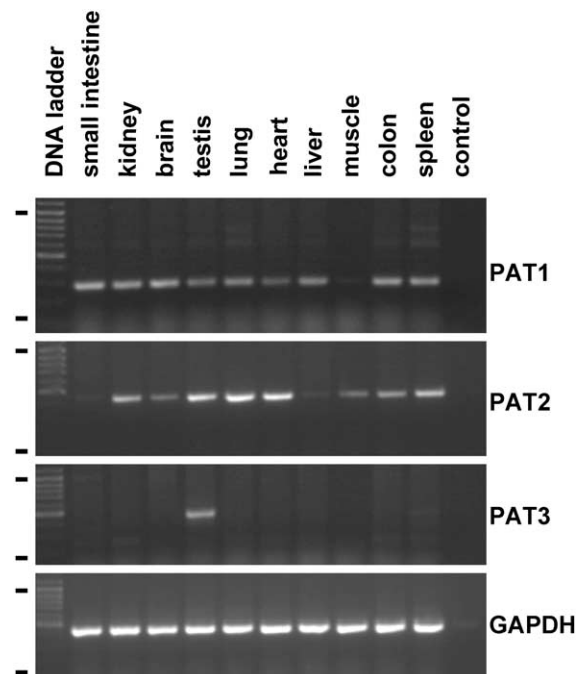


Fig. 6. Tissue distribution of the PAT1, PAT2, and PAT3 mRNA in mouse. 5  $\mu$ g of total RNA of the indicated mouse tissues was reverse transcribed with oligo(dT) primers. In the PCR, cDNA-specific primer pairs were used to detect the subtype mRNAs. The expected sizes of the PCR products were 289 (PAT1), 460 (PAT2), and 454 bp (PAT3). As a control for the RNA integrity, the glyceraldehyde-3-phosphate dehydrogenase (GAPDH) PCR product was amplified (expected size 453 bp). On the left side, black lines indicate the 100 and the 1000 bp DNA ladder fragments.

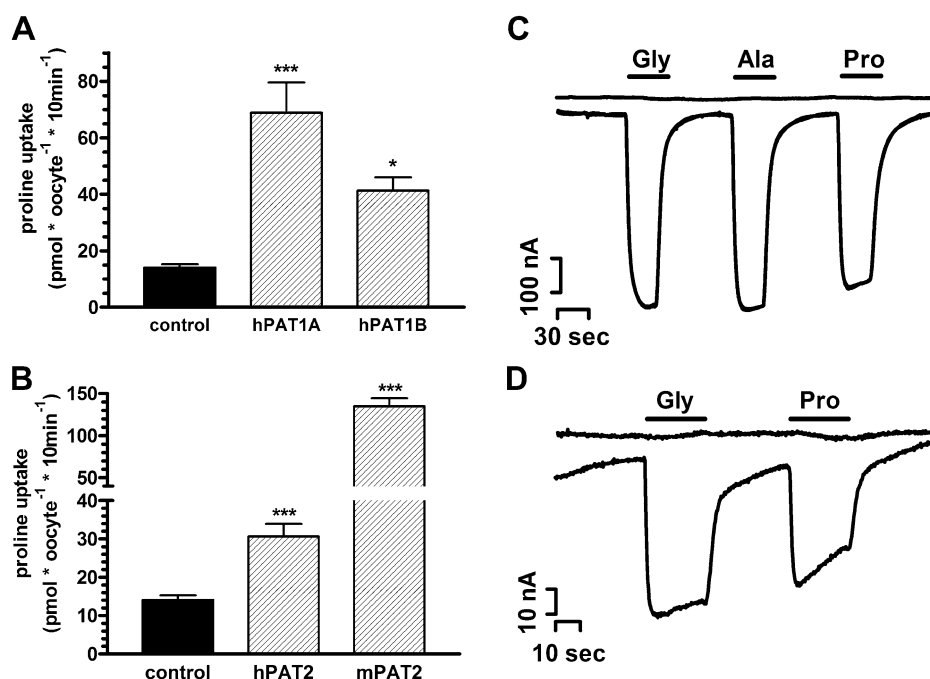


Fig. 7. Functional expression of the human PAT1 and PAT2 transporters in *X. laevis* oocytes. (A and B) Oocytes ( $n = 10$ ) were incubated in  $\text{Na}^+$ -free uptake buffer at pH 6.5 for 10 min with  $100 \mu\text{M}$   $^3\text{H}$ -labeled L-proline. The mean uptake rates ( $\pm\text{SEM}$ ) of L-proline in water-injected oocytes (black bars) and in PAT1- (A) and PAT2- (B) expressing oocytes (hatched bars) are shown. Significant differences between uptake rates are marked (\*\* $p < 0.001$ , \* $p < 0.05$ ). (C and D) Oocytes expressing human PAT1 (C) or human PAT2 (D) were held at a membrane potential of  $-40 \text{ mV}$  and perfused with  $\text{Na}^+$ -free buffer at pH 6.5 in the absence or presence of the indicated amino acids at 20 mM. Water-injected oocytes (control, upper trace) did not respond in holding currents to the addition of the amino acids.

#### Functional expression of the PAT transporters in *X. laevis* oocytes

Based on the well-characterized function of the murine PAT1 and PAT2 proteins [9] all three independently cloned mouse PAT3 cDNAs were also tested for amino acid transport function after expression of the cRNA in *X. laevis* oocytes. None of the 20 proteinogenic amino acids, provided in concentrations of 10 mM, was able to induce any inward currents in voltage-clamped oocytes injected with the PAT3 cRNA (data not shown). Uptake of radiolabeled glycine, alanine, and proline (each  $100 \mu\text{M}$ ) was also not enhanced in PAT3 cRNA-injected oocytes compared to water-injected control oocytes (data not shown). So, currently we cannot assign a transport function for the PAT3 protein, which may depend on (a) a very low functional expression level in oocytes or (b) a lack of translocation of the mature protein to the plasma membrane or (c) a quite different substrate specificity (accepting none of the proteinogenic amino acids as substrate) or (d) a completely different transport mode. Further investigations are needed to elucidate the function of the PAT3 protein.

In contrast to mouse PAT3, transport function of the human PAT1 and PAT2 transporters could be determined and characterized when their cRNAs were injected into *X. laevis* oocytes. Both flux studies using radiolabeled amino acids and the two-electrode voltage-clamp technique allowed electrogenic  $\text{H}^+$ /amino acid symport to be demon-

strated. With radiolabeled proline ( $100 \mu\text{M}$ ) we obtained increased proline influx in human PAT1- as well as in human PAT2-expressing oocytes compared with the uptake in water-injected control oocytes (Figs. 7A and 7B). From the three different PCR products obtained for PAT1, two of the injected human PAT1 cRNAs were able to enhance proline accumulation in oocytes by  $\sim 4.8$ - (clone A) and  $\sim 2.8$ -fold (clone B) over control values (Fig. 7A). The difference in expression level between the two clones, which are identical in the open reading frames, is most likely due to the varying 5' and/or 3' ends and those are longer in the PAT1 clone B. The third clone was not sequenced, because of its lack of functional expression in *X. laevis* oocytes (data not shown). The human PAT2 cRNA caused increased proline uptake by  $\sim 2.1$ -fold over controls. However, the functional expression level was generally much lower than that of the mouse PAT2 protein (Fig. 7B).

Electrogenicity of transport function in human PAT1- and PAT2-expressing oocytes could be shown for a variety of amino acids. The addition of 20 mM glycine to the perfusate induced positive inward currents of around 620 nA at an extracellular pH of 6.5 and a membrane potential clamped at  $-40 \text{ mV}$  (Fig. 7C). The currents induced by alanine and proline were in a range similar to that of those induced by glycine in human PAT1-expressing oocytes. Under the same experimental conditions glycine and proline induced inward currents of  $\sim 60$  and  $\sim 50$  nA in the case of human PAT2, confirming the low functional expression

levels achieved (Fig. 7D). Based on this comparative analysis of functions, the human orthologues appear to have functional characteristics similar if not identical to those of the mouse PAT1 and PAT2 proteins and are electrogenic proton/amino acid symporters with a high selectivity for amino acids with small side chains. This was also recently confirmed for human PAT1 cloned from a Caco-2 cell cDNA library by Chen et al. [15].

In summary, we have identified the human orthologous proteins of the mammalian PAT class of novel proton-dependent amino acid transporters and have added a new mammalian member designated PAT3 with a yet unassigned function. The genes of the three PAT transporters are clustered in the human as well as the mouse genome. The PAT proteins belong to a larger group of amino acid transporters with relatives showing different cellular and subcellular localizations that have in common the specificity to transport selected amino acids and a distinct role of protons in the transport mode. The PAT proteins identified in mammals may resemble the “archaic section” of lower eukaryotic amino acid transporters utilizing a proton motive force that is still present in the mammalian organisms.

## Materials and methods

### Animals

Female *X. laevis* were purchased from Nasco (Fort Atkinson, USA), and adult male mice (C57BL/6) were purchased from Charles River (Sulzfeld, Germany).

### Materials

The 5' RACE system and the high-fidelity *Taq* polymerase ELONGase were purchased from Invitrogen (Groningen, Netherlands), the Retroscript kit from Ambion (Huntingdon, UK), and the oligonucleotide <sup>32</sup>P labeling kit from AP Biotech (Freiburg, Germany). All chemicals including amino acids used were of p.a. quality and purchased from Sigma-Aldrich/Fluka (Deisenhofen, Germany) or Merck (Darmstadt, Germany).

### Cloning of the human PAT1 cDNA

Five micrograms of RNA, isolated from Caco-2 cells (provided by D.T. Thwaites, University of Newcastle upon Tyne, UK), was reverse transcribed with the Retroscript system (Ambion) with oligo(dT) primers. The PCR was performed with 5 µl reverse-transcribed RNA using the ELONGase enzyme mix (Invitrogen) containing proofreading polymerase and the following pairs of human PAT1-specific primers: (a) PAT1-F-14 (ATGCTCCAGCTGCCATGTCCA) and PAT1-B1546 (CTGCAGAGACGAACCCAGATC), (b) PAT1-F-128 (CA GAACCCGAGCAGTGAGTTC) and PAT1-B1546, and

(c) PAT1-F-128 and PAT1-B1532 (ATGAAGGCACAGGTGGAATTG). Primer sequences (numbered according to their relative position to the start codon) were derived from the deduced human *SLC36A1* exons and all PCR products comprise the complete human PAT1 ORF. The obtained PCR products with the expected size were cloned into the pCRII vector (Invitrogen). Several clones were picked and the cDNA inserts were analyzed for their right direction, having the 5' end directed to the T7 promoter of the vector. The cDNA inserts of the three human PAT1 clones (PAT1A–C) were subcloned with *EcoRI* into the pCRII vector, containing ~700 bp of the 3' end of the rabbit PEPT2 cDNA (including the poly(A) tail) at the SP6 site of the MCS to enhance functional expression in *X. laevis* oocytes, as previously reported [9]. After the functional expression of the different human PAT1 clones was tested in *X. laevis* oocytes, the cDNA inserts of both functional PAT1 cDNA clones (clones A and B) were sequenced on both strands. The sequences of both cDNAs were identical within the open reading frame and the sequence has been deposited with GenBank (Accession No. AY162213).

### Cloning of the human PAT2 cDNA

In the first round, GeneFinder cDNA pools from the resource center of the German human genome project (RZPD, Berlin, Germany) containing plasmid DNA of various human cDNA libraries were screened using the PCR method on 96-well microtiter plates. The following primer pairs were used: (a) PAT2-F679 (AACATCAGCATGCTGGTCAGC) and PAT2-B1480 (TGCTGGTAGGCAAGGAGCAG) and (b) PAT2-F184 (CACCTGGTGAAAGGCAACATG) and PAT2-B585 (CAGATCACCGTCTCATTGGA). Primer sequences were derived from the human PAT2 gene sequences, which had been in part obtained by homology search using the mouse PAT2 cDNA sequence as template. We obtained a PCR product with the predicted size in two cDNA pools, containing plasmid DNAs from a human adult testis cDNA library (Library No. 565; RZPD). A high-density colony filter of the cDNA library was ordered and screened with a [<sup>32</sup>P]dATP-labeled PAT2-specific cDNA probe. Two clones were identified and ordered with the RZPD clone IDs DKFZp565L1565Q6 and DKFZp565M0451Q6. Both strands of the cDNA insert of the positive clone DKFZp565M0451Q6 were sequenced (GenBank Accession No. AY162214). The PAT2 cDNA insert, originally in the pAMP1 vector, was subcloned with *EcoRI* into the pCRII vector for cRNA synthesis using the T7 RNA polymerase.

### Identification of the mouse and human PAT3 cDNA

The exons of the *Slc36a3* gene in mouse were partly identified by a homology search in the draft sequences of the mouse genome and the EST sequence database using the

mouse PAT2 sequence as template. Thereby, most of the cDNA sequence could be identified, including the complete untranslated 3' end (e.g., the EST sequences AV284440, BB016045, and BB405219). All mouse PAT3-like EST sequences were derived from cDNA clones from testis-specific cDNA libraries. The missing 5' end of the mouse PAT3 cDNA was obtained by 5'RACE (5'RACE System; Invitrogen). The first-strand cDNA was synthesized from 5  $\mu$ g total testis RNA from mouse with the Superscript RT according to the manufacturer's protocol using the mouse PAT3-specific primer PAT3-B665 (AGGCTGCTCAGG-GTGGTGATG). The PCRs were performed with 5  $\mu$ l RT reaction, SigmaRed Taq (Sigma), the antisense primer PAT3-B595 (ACCAGCAGGATGAGGAAGGGC), and the abridged anchor primer, included in the 5'RACE System. One microliter of the first PCR was subjected to a second round of amplification using the antisense primer PAT3-B411 (CAGCAGGAAGCTCACAACGTAC) and the abridged anchor primer. The obtained PCR product was cloned into the pCRII vector and sequenced. The primer pair PAT3-F-20 (ACCTCTGCTGCCTGTCCATCA) and PAT3-B1488 (GCAAATCCAACAGAGGGTGGA) was used to amplify PCR products comprising the complete mouse PAT3 ORF. Three independently amplified PCR products with the expected size were cloned into the pCRII vector and then subcloned into pCRII including the rabbit PEPT2 3' end. The cDNA inserts of two mouse PAT3 clones were sequenced on both strands (GenBank Accession No. AF453745). The human PAT3 cDNA sequence was partly predicted by sequence homology of the mouse PAT3 cDNA to the human genome sequence (sequence contig NT\_006859.10) and EST sequences (sequence ID AI208756 and AA922218). The 5' end of the cDNA was identified by using the 5'RACE method. The first-strand cDNA was synthesized from 5  $\mu$ g human testis RNA (Ambion) with Superscript RT using the human PAT3-specific primer PAT3-B607 (ACAGGATCAGGAAGGGCAGGA). The PCR was performed with 5  $\mu$ l RT reaction, SigmaRed Taq (Sigma), the antisense primer PAT3-B445 (AGC-CCAGCTGGGTGATGACTA), and the abridged anchor primer. The approximately 700-bp-long PCR product obtained was cloned into the pCRII vector and sequenced. The assembled PAT3 cDNA sequence has been submitted to GenBank (Accession No. AY162215).

#### RNA isolation and RT-PCR

Total RNA from different mouse tissues was isolated with RNAwiz (Ambion) following the supplier's protocol. Four microliters of first-strand cDNA—prepared from 5  $\mu$ g total RNA using oligo(dT) primers and the Retroscript system (Ambion)—was subjected to PCR. PCR amplification was performed for 30 cycles with 94°C denaturation for 30 s, 57°C annealing for 30 s, and 72°C extension for 30 s with the RedTaq polymerase (Sigma). The following gene-specific primer pairs were used for amplification: (i) PAT1-

F88 (GCTACCATGTCCACACAGAGG) and PAT1-B376 (TGCAGTGCACGGCCACGATAC), (ii) PAT2-F679 (AACATCAGCATGCTGGTCAGC) and PAT2-B1138 (TAGACAGGTCCACGGCAGTG), (iii) PAT3-F212 (CT-GTCAGCCTCTTGGCCATCG) and PAT3-B665 (AG-GCTGCTCAGGGTGGTGATG), and (iv) GAPDH-F519 (GACCACAGTCCATGACATCACT) and GAPDH-B971 (TCCACCACCTGTTGCTGTAG). Ten microliters of each PCR was separated by agarose gel electrophoresis and visualized with ethidium bromide.

#### Expression studies in *X. laevis* oocytes

The handling of *X. laevis* oocytes, the in vitro synthesis of cRNA, and the injection of cRNA into oocytes have been described previously [9]. Twenty-five nanograms of human PAT1, 50 ng of human PAT2, and up to 50 ng of mouse PAT3 cRNA were injected into oocytes. Three to five days after injection function was tested by employing flux studies with radiolabeled amino acids or electrophysiological recordings with the two-electrode voltage clamp. In flux studies, 10 oocytes per condition were preincubated at room temperature for 2 min in Na<sup>+</sup>-free standard uptake buffer (100 mM choline chloride, 2 mM KCl, 1 mM MgCl<sub>2</sub>, 1 mM CaCl<sub>2</sub>, 10 mM Mes, pH 6.5). The buffer was then replaced by the respective uptake buffer supplemented with 100  $\mu$ M proline (2  $\mu$ Ci/ml L-[<sup>3</sup>H]proline; ICN). After 10 min incubation, the oocytes were washed three times with 3 ml of ice-cold uptake buffer and distributed to individual vials. After oocyte lysis, radioactivity was counted by liquid scintillation. The two-electrode voltage clamp experiments were performed as described previously [9]. Briefly, oocytes were placed in an open chamber and continuously superfused at a clamped membrane potential of -40 mV with incubation buffer (100 mM choline chloride, 2 mM KCl, 1 mM MgCl<sub>2</sub>, 1 mM CaCl<sub>2</sub>, 10 mM Mes, pH 6.5) in the absence or presence of various amino acids (20 mM).

#### Sequence analyses

Homology searches with nucleotide and protein sequences were performed with various BLAST methods (<http://www.ncbi.nlm.nih.gov/BLAST>) [17]. The multiple alignment of protein sequences and the phylogenetic analyses were performed using the ClustalW 1.7 program package from the European Bioinformatics Institute (<http://www.ebi.ac.uk>) [18]. Searches for consensus patterns within the PAT-like proteins were performed with the Block Maker program (<http://blocks.fhcr.org/>) from the Fred Hutchinson Cancer Research Center (Seattle, WA, USA) [19].

## Acknowledgments

The authors thank Daniela Kolmeder for perfect technical assistance. The work has been funded by the Deutsche Forschungsgemeinschaft to M.B. (Grant BO 1857/1). We thank David T. Thwaites (University of Newcastle, UK) for providing us with Caco-2 RNA.

## References

- [1] G.B. Young, D.L. Jack, D.W. Smith, M.H. Saier Jr., The amino acid/auxin: proton symport permease family, *Biochim. Biophys. Acta* 1415 (1999) 306–322.
- [2] D. Wipf, et al., Conservation of amino acid transporters in fungi, plants and animals, *Trends Biochem. Sci.* 27 (2002) 139–147.
- [3] S.L. McIntire, R.J. Reimer, K. Schuske, R.H. Edwards, E.M. Jorgensen, Identification and characterization of the vesicular GABA transporter, *Nature* 389 (1997) 870–876.
- [4] F.A. Chaudhry, et al., Molecular analysis of system N suggests novel physiological roles in nitrogen metabolism and synaptic transmission, *Cell* 99 (1999) 769–780.
- [5] R.J. Reimer, F.A. Chaudhry, A.T. Gray, R.H. Edwards, Amino acid transport system A resembles system N in sequence but differs in mechanism, *Proc. Natl. Acad. Sci. USA* 97 (2000) 7715–7720.
- [6] M. Sugawara, et al., Cloning of an amino acid transporter with functional characteristics and tissue expression pattern identical to that of system A, *J. Biol. Chem.* 275 (2000) 16473–16477.
- [7] T. Nakanishi, et al., Cloning and functional characterization of a new subtype of the amino acid transport system N, *Am. J. Physiol. Cell Physiol.* 281 (2001) C1757–C1768.
- [8] C. Sagne, et al., Identification and characterization of a lysosomal transporter for small neutral amino acids, *Proc. Natl. Acad. Sci. USA* 98 (2001) 7206–7211.
- [9] M. Boll, M. Foltz, I. Rubio-Aliaga, G. Kottra, H. Daniel, Functional characterization of two novel mammalian electrogenic proton dependent amino acid cotransporters, *J. Biol. Chem.* 277 (2002) 22966–22973.
- [10] C. Sagne, et al., Cloning of a functional vesicular GABA and glycine transporter by screening of genome databases, *FEBS Lett.* 417 (1997) 177–183.
- [11] B. Gasnier, The loading of neurotransmitters into synaptic vesicles, *Biochimie* 82 (2000) 327–337.
- [12] H. Varoqui, H. Zhu, D. Yao, H. Ming, J. D. Erickson, Cloning and functional identification of a neuronal glutamine transporter, *J. Biol. Chem.* 275 (2000) 4049–4054.
- [13] S. Bröer, N. Brookes, Transfer of glutamine between astrocytes and neurons, *J. Neurochem.* 77 (2001) 705–719.
- [14] B.P. Bode, Recent molecular advances in mammalian glutamine transport, *J. Nutr.* 131 (2001) 2475S–2485S.
- [15] Z. Chen, et al., Structure, function and immunolocalization of a proton-coupled amino acid transporter (hPAT1) in the human intestinal cell line Caco-2, *J. Physiol.* 546 (2003) 349–361.
- [16] M. Brandsch, et al., Influence of proton and essential histidyl residues on the transport kinetics of the H<sup>+</sup>/peptide cotransport systems in intestine (PEPT 1) and kidney (PEPT 2), *Biochim. Biophys. Acta* 1324 (2001) 251–262.
- [17] S.F. Altschul, T.L. Madden, A.A. Schäffer, J. Zhang, Z. Zhang, W. Miller, D.J. Lipman, Gapped BLAST and PSI-BLAST: a new generation of protein database search programs, *Nucleic Acids Res.* 25 (1997) 3389–3402.
- [18] V. Lombard, E.B. Camon, H.E. Parkinson, P. Hingamp, G. Stoesser, N. Redaschi, EMBL-Align: a new public nucleotide and amino acid multiple sequence alignment database, *Bioinformatics* 18 (2002) 763–764.
- [19] J.G. Henikoff, S. Henikoff, Blocks database and its applications, *Methods Enzymol.* 266 (1996) 88–105.



## APPENDIX 3

published in *Molecular Membrane Biology*

## Substrate recognition by the mammalian proton-dependent amino acid transporter PAT1

Michael Boll<sup>†#</sup>, Martin Foltz<sup>†#</sup>,  
Catriona M. H. Anderson<sup>‡</sup>, Carmen Oechsler<sup>†</sup>,  
Gabor Kottra<sup>†</sup>, David T. Thwaites<sup>‡</sup> and  
Hannelore Daniel<sup>†\*</sup>

<sup>†</sup> Molecular Nutrition Unit, Technical University of Munich, Hochfeldweg 2, D-85350 Freising-Weihenstephan, Germany

<sup>‡</sup> School of Cell and Molecular Biosciences, Medical School, University of Newcastle upon Tyne, Newcastle upon Tyne NE2 4HH, UK

# These authors contributed equally to this work.

### Summary

The PAT family of proton-dependent amino acid transporters has recently been identified at the molecular level. This paper describes the structural requirements in substrates for their interaction with the cloned murine intestinal proton/amino acid cotransporter (PAT1). By using *Xenopus laevis* oocytes as an expression system and by combining the two-electrode voltage clamp technique with radiotracer flux studies, it was demonstrated that the aliphatic side chain of L- $\alpha$ -amino acids substrates can consist maximally of only one CH<sub>2</sub>-unit for high affinity interaction with PAT1. With respect to the maximal separation between the amino and carboxyl groups, only two CH<sub>2</sub>-units, as in  $\gamma$ -aminobutyric acid (GABA), are tolerated. PAT1 displays no or even a reversed stereoselectivity, tolerating serine and cysteine only in the form of the D-enantiomers. A methyl-substitution of the carboxyl group (e.g. O-methyl-glycine) markedly diminishes substrate affinity and transport rates, whereas methyl-substitutions at the amino group (e.g. sarcosine or betaine) have only minor effects on substrate interaction with the transporter binding site. Furthermore, it has been shown (by kinetic analysis of radiolabelled betaine influx and inhibition studies) that the endogenous PAT system of human Caco-2 cells has very similar transport characteristics to mouse PAT1. In summary, one has defined the structural requirements and limitations that determine the substrate specificity of PAT1. A critical recognition criterion of PAT1 is the backbone charge separation distance and side chain size, whereas substitutions on the amino group are well tolerated.

**Keywords:** Rheogenic, osmolytes, D-amino acids, absorption, proton symporter.

**Abbreviations:** AAAP, amino acid/auxin permease, VGAT, vesicular GABA transporter, PAT, proton/amino acid transporter, GABA,  $\gamma$ -aminobutyric acid, LYAAT, lysosomal amino acid transporter, MES, 4-morpholineethanesulphonic acid, HEPES, 4-(2-hydroxyethyl)-1-piperazineethanesulphonic acid, TRIS, 2-amino-2-(hydroxymethyl)-1,3-propanediol.

\*To whom correspondence should be addressed.  
e-mail: daniel@wzw.tum.de

### Introduction

Members of the eukaryotic amino acid/auxin permease (AAAP) family are found in yeast, plants, invertebrates and mammals (Young *et al.* 1999). In mammals, three different subfamilies of the AAAP transporter class have been identified presently, represented by (i) the vesicular  $\gamma$ -aminobutyric acid (GABA) transporter VGAT (McIntire *et al.* 1997); (ii) a subfamily consisting of various transporters with system A and N activity (Chaudhry *et al.* 1999, Reimer *et al.* 2000, Sugawara *et al.* 2000, Nakanishi *et al.* 2001); and (iii) the lysosomal amino acid and proton/amino acid cotransporters LYAAT/PAT (Sagne *et al.* 2001, Boll *et al.* 2002). Although the amino acid sequences between the subgroups are quite divergent, a common signature motif within the protein sequences is found (Young *et al.* 1999). Moreover, the membrane topologies of the transporters, based on hydropathy analysis, are very similar and suggest that most of the mammalian AAAP family members possess 9–11 transmembrane domains (Chang and Bush 1997).

One of the important common functional features of the transporters within the different subfamilies is that they all show the involvement of a specific proton binding site. VGAT serves as an H<sup>+</sup>/amino acid antiporter (McIntire *et al.* 1997) and system N mediates H<sup>+</sup> efflux during Na<sup>+</sup>/amino acid influx (Chaudhry *et al.* 1999, 2001). System A seems not to translocate H<sup>+</sup>, but its transport activity is strongly inhibited by high external proton concentrations (Reimer *et al.* 2000, Chaudhry *et al.* 2002). Finally, the LYAAT/PAT transporter clones are the first rheogenic H<sup>+</sup>/amino acid cotransporters identified in mammals (Sagne *et al.* 2001, Boll *et al.* 2002). As yet, little functional characterization of the VGAT transporter has been possible due to its exclusive localization in synaptic vesicles. VGAT, when overexpressed in PC12 cells, mediates the uptake of GABA into synaptic vesicles, and this process can partly be blocked by an excess of glycine (McIntire *et al.* 1997, Sagne *et al.* 1997). Whether the VGAT transporter also accepts other amino acids than these two inhibitory neurotransmitters is unknown. The system N transporters SN1 and SN2 prefer mainly glutamine, asparagine and histidine as substrates (Chaudhry *et al.* 1999, Nakanishi *et al.* 2001). System A transporters have a broader substrate specificity, accepting a variety of zwitterionic amino acids, e.g. glutamine, alanine, serine, cysteine and methionine (Reimer *et al.* 2000, Sugawara *et al.* 2000). In addition, the system A transporter subtype ATA3 mediates the uptake of cationic amino acids (Hatanaka *et al.* 2001). The rat LYAAT1, when overexpressed in CV-1 cells, mediates the uptake of small amino acids such as alanine and proline and the neurotransmitter GABA. Immunohistochemistry revealed that the LYAAT1 protein is localized in the lysosomal compartment of glutamatergic and GABAergic neurons in rat brain, where it seems to be responsible for the

efflux of small amino acids from lysosomes (Sagne *et al.* 2001).

One has recently cloned the PAT1 transporter cDNA from mouse intestine (Boll *et al.* 2002), which is the mouse orthologue of rat LYAAT1. When expressed in *Xenopus laevis* oocytes, PAT1 induced a pH-dependent electrogenic transport activity for the proteinogenic amino acids glycine, alanine and proline, the neurotransmitter GABA and the D-amino acid D-alanine. The apparent  $K_m$  values of these amino acids are in the range of 2.8–7.5 mM. Phenotypically, the PAT1 transporter possessed functional characteristics of a proton-coupled amino acid transporter (system PAT) identified in apical membranes of intestinal (Thwaites *et al.* 1993a,b, 1994, 1995a,b,c, 2000, Thwaites and Stevens 1999) and renal (Rajendran *et al.* 1987, Roigaard-Petersen *et al.* 1987, Jessen *et al.* 1988, 1989, 1991, Wunz and Wright 1993) epithelia. The hypothesis, that PAT1 may represent the molecular entity of this intestinal and renal epithelial transport system, was supported by the fact that the PAT1 mRNA was detectable in small intestinal as well as renal tissues (Boll *et al.* 2002). The proton-dependent transport system, as characterized in the human intestinal epithelial (Caco-2) cell monolayers (Thwaites *et al.* 1993a,b, 1994, 1995a,b,c, 2000, Thwaites and Stevens 1999) and renal brush border vesicles (Rajendran *et al.* 1987, Roigaard-Petersen *et al.* 1987, Jessen *et al.* 1988, 1989, 1991, Wunz and Wright 1993), displayed a distinct substrate specificity accepting almost exclusively small apolar amino acids, such as glycine, alanine and proline (Rajendran *et al.* 1987, Roigaard-Petersen *et al.* 1987, Thwaites *et al.* 1993b, 1994, 1995a). In addition, derivatives of small amino acids are also recognized by this transport pathway, examples include the neurotransmitter GABA (Thwaites *et al.* 2000), amino-isobutyric acid (AIB) (Jessen *et al.* 1991, Thwaites *et al.* 1995c),  $\alpha$ -N-methyl-amino-isobutyric acid (MeAIB, regarded as the classical system A substrate) (Thwaites *et al.* 1995b), the osmolytes sarcosine and betaine (Wunz and Wright 1993, Thwaites *et al.* 1995c), small D-amino acids (Jessen *et al.* 1988, Thwaites *et al.* 1995c) and the partial antagonist at the glycine binding site of the NMDA receptor D-cycloserine (Thwaites *et al.* 1995a). That the system described in Caco-2 cells indeed represents the PAT1 protein was most recently shown by Chen *et al.* (2003) with the cloning of the human PAT1 cDNA from the Caco-2 intestinal epithelial cell line and by immunolocalization of the PAT1 protein in the apical membrane of the cells. Although the substrate specificity of the PAT system in the intestine has been carefully characterized, no detailed analysis of the substrate recognition pattern or on transport and affinity of corresponding amino acid derivatives has been performed. Such an analysis has also pharmacological implications, as the PAT-transporters carry the inhibitory neurotransmitters glycine and GABA and structurally-related compounds which may act as agonists or antagonists of the receptors and reuptake pathways including D-serine, D-cycloserine and a range of GABA analogues (Thwaites *et al.* 1995a,c, 2000).

Here, one describes for the first time the analysis of structural features in substrates for their interaction with the PAT1-transporter binding site by determination of the transport rate and the affinity of a large set of test compounds.

The ability of the PAT1-protein to tolerate substrates of variable side chain and backbone length was explored and the role of the terminal head groups was determined. The findings provide insights into the minimal structural requirements for substrate binding to PAT1.

## Results

### *The length of the amino acid side chains and of the backbone determine substrate interaction with the PAT1-binding site*

The substrate selectivity of the murine proton/amino acid symporter PAT1 following expression in *Xenopus laevis* oocytes was determined by using the two electrode voltage clamp technique and competition assays in tracer flux studies. Glycine and L-alanine evoked pronounced positive inward currents in PAT1 expressing oocytes. The introduction of just one additional  $\text{CH}_2$ -unit into the side chain of L-alanine leading to L- $\alpha$ -aminobutyric acid reduced the substrate evoked currents to only  $5.9 \pm 0.3\%$  of those of glycine at a concentration of 20 mM (pH 6.5) (Table 1). The apparent affinity of L- $\alpha$ -aminobutyric acid for PAT1 dropped to  $\sim 48$  mM. A further side chain extension, as in L-norvaline and L-norleucine, abolished any substrate interaction with the transporter (Table 1). These findings were mirrored by the data obtained in tracer flux studies in which uptake of

Table 1. Apparent affinities and PAT1-mediated currents of various compounds tested in this study. Concentration-dependent substrate evoked currents were determined and, after Eadie-Hofstee-transformation, the apparent  $K_m$  has been calculated by linear regression analysis. Values represent the mean  $\pm$  SEM of  $n = 5-7$  oocytes. In the third row, data represent the normalized currents (mean  $\pm$  SEM,  $n = 5-7$ ) of the selected compounds (20 mM) relative to the glycine (20 mM) evoked currents at pH 6.5 at a membrane potential of  $-60$  mV.  $I_{20 \text{ mM}}$  values of compounds not significantly higher than background values in water-injected oocytes ( $p > 0.05$ , students paired  $t$ -test) are given as 0.  $K_m$  and  $\%I_{20 \text{ mM}}$  values taken from previous studies (Boll *et al.* 2002) are marked with asterisks (\*).

Substrate	Apparent $K_m$ value (mM)	$\%I_{20 \text{ mM}}$ ( $I_{\text{Gly}} = 100\%$ )
Elongation of the side chain		
glycine	$7.0 \pm 0.7^*$	100
L-alanine	$7.5 \pm 0.6^*$	$88.5 \pm 2.8^*$
L- $\alpha$ -aminobutyric acid	$48 \pm 8$	$5.9 \pm 0.3$
L-norvaline	nd	0
L-norleucine	nd	0
Elongation of the backbone		
$\beta$ -alanine	$5.2 \pm 0.2$	$103 \pm 0.8$
$\gamma$ -aminobutyric acid	$3.1 \pm 0.2^*$	$51 \pm 0.6$
$\delta$ -aminopentanoic acid	$38 \pm 1$	$16 \pm 1.2$
$\epsilon$ -aminohexanoic acid	nd	0
D-enantiomers		
D-alanine	$6.3 \pm 0.7^*$	$98.2 \pm 1.7$
D-serine	$15.6 \pm 1.4$	$50.9 \pm 1.1$
D-cysteine	$24.0 \pm 0.9$	$69.5 \pm 1.6$
D- $\alpha$ -aminobutyric acid	$36 \pm 2$	$26.5 \pm 0.7$
O-methyl substitution		
O-methyl-glycine	nd	$13.3 \pm 2.4$
O-methyl-alanine	nd	$21.5 \pm 1.9$
N-methylated glycines		
sarcosine	$3.2 \pm 0.3$	$110 \pm 3.7$
N,N-dimethylglycine	$7.8 \pm 0.6$	$74.8 \pm 2.2$
betaine	$5.4 \pm 0.3$	$66.8 \pm 2.3$

## Substrate recognition by PAT1

263

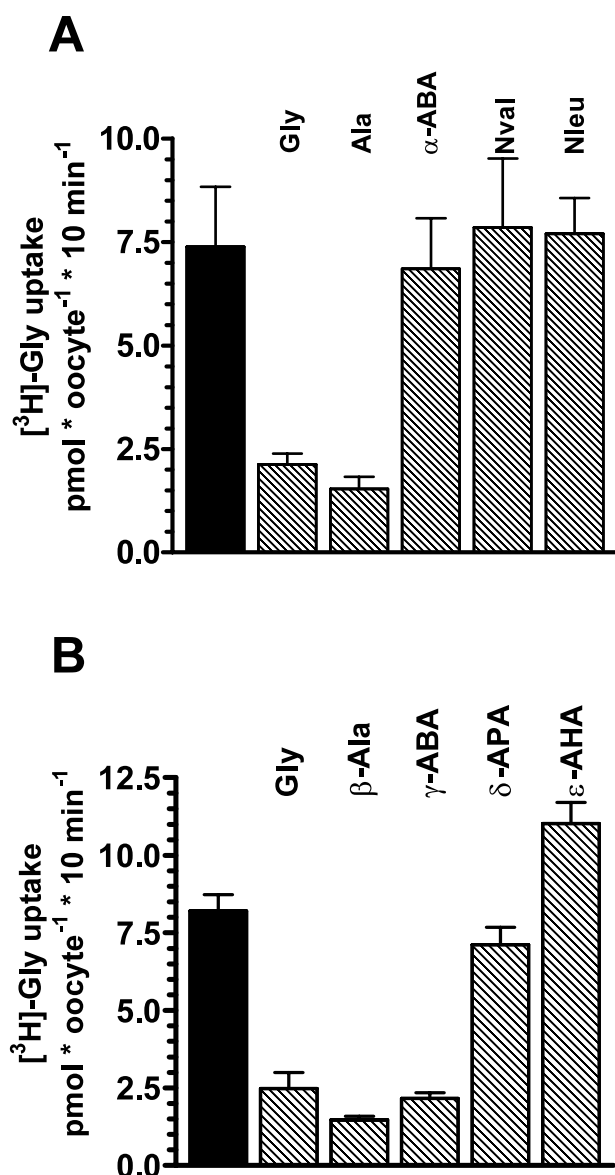


Figure 1. The elongation of the side chain and the backbone of L-amino acids reduces the ability for the interaction with the PAT1 transporter. (a) Inhibition of [<sup>3</sup>H]glycine uptake by L- $\alpha$ -amino acids in PAT1 expressing oocytes. Data represent the PAT1 mediated glycine uptake in the absence (filled bar) or presence (hatched bars) of 10 mM L- $\alpha$ -amino acids in Na<sup>+</sup>-free buffer at pH 6.5 (mean  $\pm$  SEM,  $n = 6-8$ ). (b) Inhibition of glycine uptake by  $\omega$ -amino acids in PAT1 expressing oocytes. The mean  $\pm$  SEM ( $n = 6-8$ ) of PAT1 mediated glycine uptake in the absence (filled bar) or presence (hatched bars) of 10 mM  $\omega$ -amino acids in Na<sup>+</sup>-free buffer at pH 6.5.

radiolabelled glycine (100  $\mu$ M) was reduced by the addition of a 100-fold excess of either glycine or alanine to 28.7  $\pm$  3.6% and 20.8  $\pm$  4.0% of control glycine uptake. Neither 10 mM L- $\alpha$ -aminobutyric acid, nor L-norvaline or L-norleucine reduced glycine transport (Figure 1(a)). Since the resting membrane potential is not controlled in the tracer flux studies, it has been determined based on the inward currents to which extent the apparent substrate affinity is dependent on the membrane voltage. In the range of the natural resting potential of oocytes ( $-20$  to  $-60$  mV), there was no

significant effect on the apparent affinity for example of Gly with a  $K_m$  of 7.3  $\pm$  0.3 at  $-20$  mV and 7.0  $\pm$  0.7 mM at  $-60$  mV. This suggests that the data from tracer flux studies and current measurements performed at  $-60$  mV can be compared, as affinities are not markedly altered by membrane voltage.

As previously shown, LYAAT1/PAT1 proteins transport not only  $\alpha$ -amino acids (Sagne *et al.* 2001, Boll *et al.* 2002). Here, it is determined how an elongation of the backbone in  $\omega$ -amino acids affects substrate interaction with the transporter. Inhibition studies revealed that 10 mM  $\beta$ -alanine and GABA were able to decrease uptake of radiolabelled glycine to 18.0  $\pm$  1.3% and 26.4  $\pm$  2.3%, respectively, whereas 10 mM  $\delta$ -APA or  $\epsilon$ -AHA showed no inhibition (Figure 1(b)). In voltage clamped oocytes expressing mPAT1 20 mM of  $\beta$ -Ala or GABA produced inward currents of 103.0  $\pm$  0.8% and 51.0  $\pm$  0.6%, whereas  $\delta$ -amino pentanoic acid ( $\delta$ -APA) evoked only 16.0  $\pm$  1.2% of the glycine currents and no current response was obtained by 20 mM  $\epsilon$ -aminohexanoic acid ( $\epsilon$ -AHA) at a pH of 6.5 (Table 1).

Michaelis-Menten kinetics for Gly,  $\beta$ -Ala and GABA induced transport currents at a membrane voltage of  $-60$  mV revealed  $K_m$  values of 7.0  $\pm$  0.7, 5.2  $\pm$  0.2 and 3.1  $\pm$  0.2 mM, respectively (Table 1). In contrast, the apparent  $K_m$  of  $\delta$ -APA was  $\sim 38$  mM, demonstrating that the extension of the backbone in  $\omega$ -amino acids by up to 2 CH<sub>2</sub>-units is accepted, but then affinity declines dramatically.

The position of the amino group within the amino acid has a major impact on the ability of substrates to interact with the PAT1-binding site. Figure 2(a) shows in direct comparison based on current-voltage relationships that aminobutyric acid with the amino group in  $\alpha$ -position induces considerably less current than  $\beta$ - and  $\gamma$ -aminobutyric acid and, accordingly, only  $\beta$ - and  $\gamma$ -aminobutyric acid (10 mM) were able to inhibit glycine uptake significantly in PAT1-expressing oocytes (Figure 2(b)).

## PAT1 displays a 'reversed' stereoselectivity

One has demonstrated previously that D-amino acids with small side chains are transported by PAT1 in an electrogenic manner and that the apparent affinities of the L- and D-enantiomer of alanine are not significantly different from each other ( $K_m = 7.5 \pm 0.6$  and 6.3  $\pm$  0.7 mM, respectively) (Boll *et al.* 2002). Here, it is shown that all tested D-amino acids produce higher inward currents than the corresponding L-enantiomers at a concentration of 20 mM (Figure 3(a) and Table 1). These differences were significant for serine, cysteine and  $\alpha$ -aminobutyric acid with  $I_{20 \text{ mM}}$  (in % $I_{\text{Gly}}$ ) of 9.2  $\pm$  0.5 vs 50.9  $\pm$  1.1 for L- and D-serine, 1.8  $\pm$  0.2 vs 69.5  $\pm$  1.6 for L- and D-cysteine and 5.0  $\pm$  0.5 vs 26.5  $\pm$  0.7 for L- and D- $\alpha$ -aminobutyric acid ( $p < 0.01$ ,  $n = 6$ , Table 1).

Furthermore, the apparent affinities of the D-amino acids were generally higher than those of the equivalent L-enantiomers with 4.4-fold in the case of serine (69  $\pm$  5 vs 15.6  $\pm$  1.4 mM for L- and D-serine, respectively) and  $\sim 1.3$ -fold in the case of  $\alpha$ -aminobutyric acid (48  $\pm$  8 vs 36  $\pm$  2 mM for L- and D- $\alpha$ -aminobutyric acid, respectively). Due to the very low currents of L-Cys of less than 2% of the glycine currents (20 mM) (Boll *et al.* 2002), one was not able to

264

M. Boll et al.

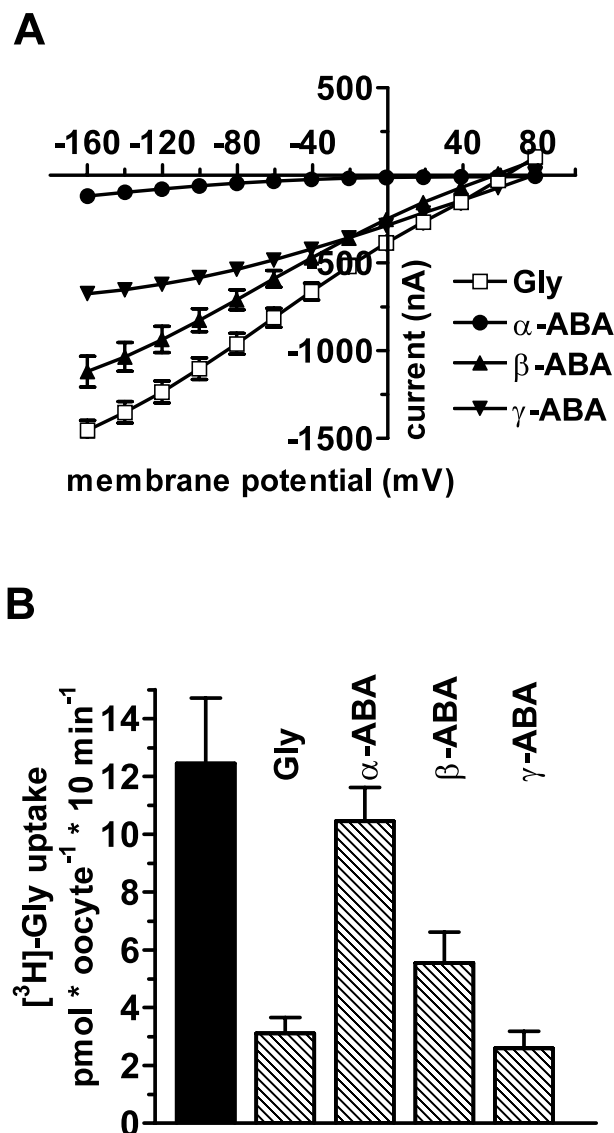


Figure 2. The position of the amino group has a pronounced effect on amino acid transport by PAT1. (a) Current-voltage relationship (I-V curve) of different aminobutyric acids varying in the amino group position in PAT1-expressing oocytes. (b) Inhibition of glycine uptake by aminobutyric acid derivatives in PAT1 expressing oocytes.

determine its apparent affinity, whereas the  $K_m$  value of D-Cys was determined as  $24.0 \pm 0.9$  mM (Table 1). The inhibitory potency of D-amino acids on glycine uptake in PAT1-expressing oocytes showed the same rank order as the affinities determined by electrophysiology (D-Ala > D-Ser > D-Cys > D- $\alpha$ -ABA) (Figure 3(b)). The D-amino acids D-aspartate and D-leucine failed, similar to the L- $\alpha$ -amino acids with a more bulky side chain, to inhibit glycine uptake significantly (Figure 3(b)).

#### Different effects of methyl-substitutions of the carboxyl or amino group on substrate recognition by PAT1

It was also tested whether modifications of the carboxyl or the amino group of amino acids affect PAT1-mediated

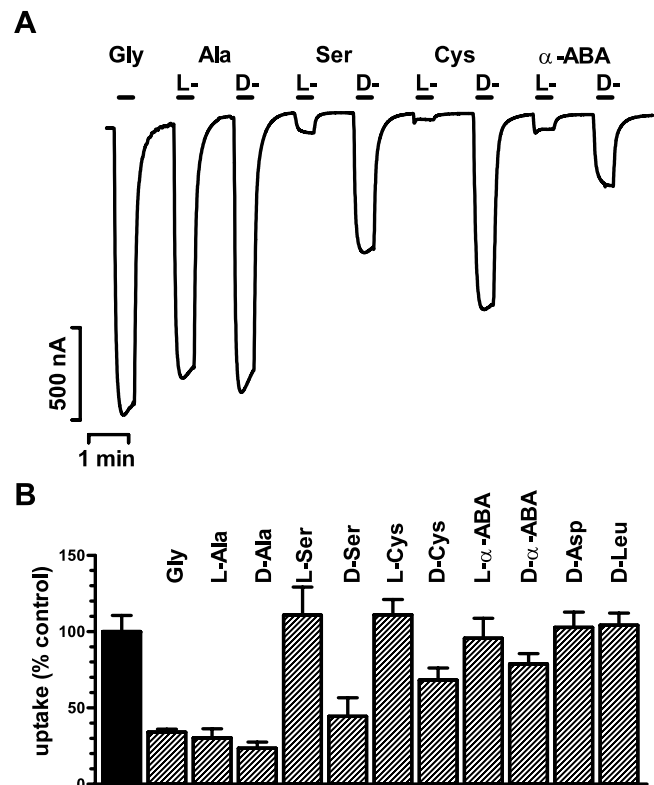


Figure 3. Stereoselectivity of the PAT1 transporter. (a) Representative current trace of PAT1 expressing oocytes showing current responses following the successive addition of the indicated L- and D- $\alpha$ -amino acids at a concentration of 20 mM in  $\text{Na}^+$  free buffer (pH 6.5). In control oocytes, no current change for any test compound has been observed (data not shown). (b) Inhibition of glycine uptake by L- and D- $\alpha$ -amino acids in PAT1 expressing oocytes. The PAT1 mediated glycine uptake (% of control) is shown in the absence (filled bar) or presence (hatched bars) of 10 mM of the indicated amino acids.

substrate transport and affinity. The methyl-substitution of the carboxyl group of glycine and alanine diminished the substrate-evoked currents. Gly-O-methyl and Ala-O-methyl esters evoked only  $13.3 \pm 2.4\%$  and  $21.5 \pm 1.9\%$  of control glycine currents at a concentration of 20 mM (Table 1). In inhibition studies, 20 mM Gly-O-methyl or Ala-O-methyl failed to reduce significantly glycine influx, demonstrating a very low affinity of the O-methylated amino acids (Figure 4).

In contrast to the carboxyl terminus, methyl-substitutions of the amino group of glycine were well tolerated. As shown in Figure 5(a), the N-methylation of glycine has only minor effects on the magnitude of PAT1-mediated currents at  $-60$  mV and in the corresponding I-V relationships with sarcosine induced even slightly higher currents (110%) than glycine, whereas N,N-dimethylglycine and betaine induced 74.8% and 66.8% of glycine currents, respectively. Moreover, all three compounds inhibited glycine influx (Figure 5(b)) and the apparent affinities of sarcosine ( $K_m$   $3.2 \pm 0.3$  mM) N,N-dimethylglycine ( $K_m$   $7.8 \pm 0.6$  mM) and betaine ( $K_m$   $5.4 \pm 0.3$  mM) are very similar to that of glycine ( $K_m$  7.0 mM) under the same experimental conditions (Table 1). Since transport of betaine is of particular interest in view of its function as an osmolyte, it was assessed whether  $\text{H}^+$ /betaine influx via

## Substrate recognition by PAT1

265

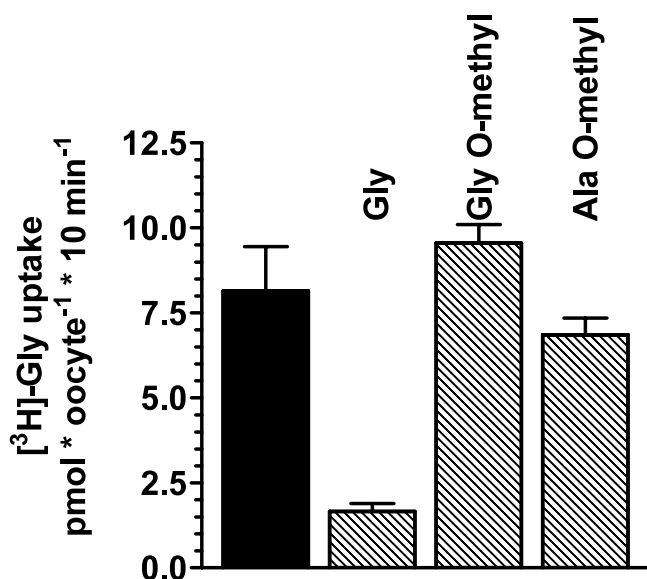


Figure 4. Methylation of the carboxyl group of glycine and L-alanine diminishes the substrate/PAT1 transporter interaction. Inhibition of glycine uptake by O-methylated amino acids in PAT1 expressing oocytes. Glycine uptake is shown in the absence (filled bar) or presence (hatched bars) of 10 mM O-methyl-glycine or O-methyl-alanine (mean  $\pm$  SEM,  $n = 6-8$  oocytes).

PAT1 causes intracellular acidification with membrane potential clamped to  $-60$  mV (Figure 5(c)). Glycine influx evoked a steady state inward current of 1340 nA and, in

parallel, led to a pronounced decline of  $\text{pH}_{\text{in}}$  from 7.4 to pH 6.4 and betaine produced currents of  $\sim 640$  nA and a decline in  $\text{pH}_{\text{in}}$  within 5 min from pH 7.4 to 6.7. Water-injected control oocytes evoked neither current nor pH changes upon addition of the test compounds (data not shown).

*The substrate recognition pattern of the PAT-system in Caco-2 cells is identical with that of the cloned PAT1 transporter*

To test whether the findings obtained with the heterogeneously expressed PAT1-transporter apply also to the endogenously expressed PAT-activity found in mammalian cells, the Caco-2 cell line was used as a model of differentiated intestinal enterocytes. The kinetics of apical uptake of betaine in Caco-2 cells as a function of the betaine concentration in the presence of a pH gradient and  $\text{Na}^+$ -free conditions clearly shows a saturable component (Figure 6(a)). After subtraction of the non-carrier-mediated component, the apparent affinity of the carrier mediated betaine uptake was determined as 6.1 mM. This is in agreement with the  $K_m$  value of betaine in PAT1-expressing oocytes (5.4 mM). Furthermore, the substrate recognition pattern of the PAT-system in Caco-2 cells was essentially identical to that of the heterologously expressed transporter. Both glycine and alanine (each 10 mM) were able to inhibit betaine uptake significantly (reducing uptake to  $32.2 \pm 5.1\%$  and  $29.7 \pm 3.4\%$  of control values, respectively), whereas no significant inhibition was observed when adding  $\alpha$ -aminobutyric acid,

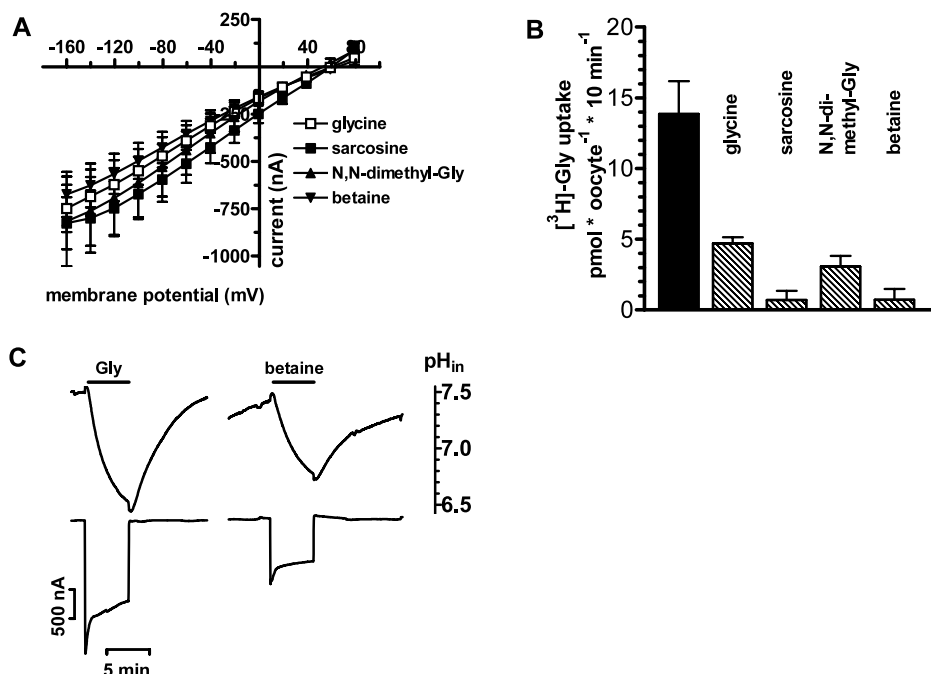


Figure 5. The N-methyl substitution of glycine has only a minor influence on transport and affinity by PAT1. (a) Current-voltage relationships (I-V curve) of different N-methylated glycines (20 mM) in PAT1-expressing oocytes. Data represent the mean  $\pm$  SEM of substrate evoked currents at  $-60$  mV ( $n = 6$ ). (b) Inhibition of glycine uptake by N-methylated glycines in PAT1 expressing oocytes. Data represent the PAT1 mediated glycine uptake in the absence (filled bar) or presence (hatched bars) of 10 mM of the indicated N-methylated glycine. (c) Intra-cellular pH and current recordings following the application of 20 mM glycine or betaine. The upper traces represent the intracellular pH recordings in PAT1 expressing oocytes clamped at  $-60$  mV. The lower traces represent the holding currents. Data are representative of three experiments with PAT1 expressing oocytes.

266

M. Boll et al.

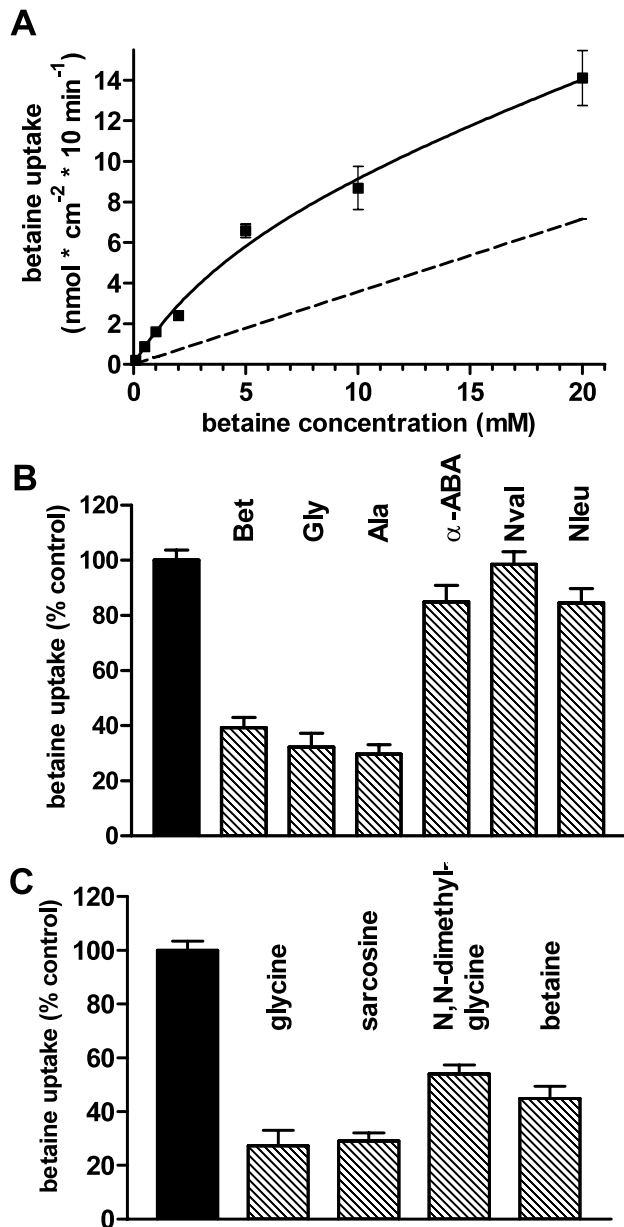


Figure 6. Betaine uptake across the apical membrane of Caco-2 cell monolayers. Betaine ( $0.5 \mu\text{Ci/ml}$ ,  $100 \mu\text{M}$ ) uptake (10 min,  $37^\circ\text{C}$ ) was measured across the apical membrane of Caco-2 cell monolayers. (a) Uptake was measured over a range of betaine concentrations (0–20 mM). The curve represents the best fit using Michaelis-Menten kinetics (one saturable component plus a linear component). For the saturable (hPAT1) component, the  $K_m$  was 6.15 mM and  $V_{\max}$   $8.97 \text{ nmol cm}^{-2} \times 10 \text{ min}^{-1}$  ( $r^2 = 0.99$ ). The linear component was  $0.358 \text{ nmol cm}^{-2} \times 10 \text{ min}^{-1} \text{ mM}^{-1}$  (dashed line). Results are mean  $\pm$  SEM ( $n = 4-6$ ). (b) Betaine uptake in the absence (filled bar) or presence (hatched bars) of a number of amino acids of varying side-chain length (all 10 mM). Results are expressed as % maximum (after subtraction of the non-hPAT1 mediated component) and are mean  $\pm$  SEM ( $n = 9-11$ ). (c) Betaine uptake in the absence (filled bar) or presence (hatched bars) of a number of N-methylated glycines (all 10 mM). Results are expressed as % maximum (after subtraction of the non-hPAT1 mediated component) and are mean  $\pm$  SEM ( $n = 9-11$ ).

norvaline or norleucine to the incubation medium (Figure 6(b)). In addition, all three N-methylated glycines were able to inhibit betaine uptake significantly, as shown by the reduction to  $29.0 \pm 3.1\%$ ,  $54.1 \pm 3.3\%$  and  $44.9 \pm 4.5\%$  of control betaine uptake following addition of 10 mM sarcosine, N,N-dimethylglycine or betaine, respectively (Figure 6(c)).

## Discussion

Proton-dependent amino acid transport systems in epithelial cells participate in the intestinal absorption and renal reabsorption of small neutral amino acids (Rajendran *et al.* 1987, Roigaard-Petersen *et al.* 1987, Jessen *et al.* 1988, 1989, 1991, Thwaites *et al.* 1993a,b, 1994, 1995a,b,c, 2000, Wunz and Wright 1993, Thwaites and Stevens 1999, Boll *et al.* 2002). Based on the phenotypical similarities of the PAT-activity in epithelial cells and that of PAT1 and the presence of PAT1 in the apical membrane, it was proposed that PAT1 is the gene encoding this transport activity. The PAT1-mRNA is expressed in intestinal and renal tissues and apical transport activity (as shown here in Caco-2 cells) resembles in all features PAT1 activity and substrate specificity, as determined in the oocyte test system. PAT1 discriminates its substrates strictly by the size of the side chain and by the charge separation distance within the backbone. Consequently, only glycine and alanine of the proteinogenic aliphatic amino acids are transported, as they fulfil the requirements in side chain size restrictions. However, L-proline has been shown to be transported by PAT1 too (Boll *et al.* 2002), although its side chain is numerically longer than that of L- $\alpha$ -aminobutyric acid that has essentially no affinity. This is most likely due to the ring configuration with its incorporated imino group, making the side chain less bulky than in the aliphatic counterparts. The backbone length restriction allows only  $\beta$ -Ala and GABA to be transported with high affinity by PAT1 which, in the context of PAT1-expression in neurons, addresses its putative role in the clearance of neurotransmitters.

Interestingly, the PAT1 transporter does not show the selectivity for L-amino acids that is observed for almost all other amino acid transporters (Palacin *et al.* 1998). For selected amino acids, e.g. serine and cysteine, the transport currents as well as the apparent affinities are even higher when the substrate is presented as a D-enantiomer. These results are in good agreement with those reported very recently by Chen *et al.* (2003), who determined the  $\text{IC}_{50}$  values of different D-amino acids in human PAT1 transfected HRPE cells. They showed that the D-enantiomers display the same or a higher affinity to PAT1 than the corresponding L-enantiomeric amino acid. The fact that the preferential binding of either L- or D-enantiomers depends upon the amino acid configuration demonstrates that stereoselectivity and physicochemical characteristics are interrelated. The L-configuration of a polar side chain, like in serine and cysteine, may restrict the interaction of the side chain with a proposed hydrophobic binding pocket within the transporter, and this restriction is attenuated in the D-configuration. A second explanation for the better interaction of the D-amino acids with PAT1 might be that the D-configuration, in substrates in

which the side chain is too bulky due to possession of more than one  $\text{CH}_2$ -unit prevents interaction with a size restrictive binding pocket in the PAT1 transporter. The latter explanation is favourable, since the order of the affinities determined for the D-amino acids (D-Ala > D-Ser > D-Cys > D- $\alpha$ -ABA) correlates well with the bulkiness of their side chain. This leads to the assumption that the PAT1 transporter excludes aliphatic amino acids, solely because of their size, accepting amino acids with a more bulky side chain only when present in the D-configuration. Of particular importance appears the efficient transport of D-serine by PAT1. Orally administered D-serine is used in pharmacological doses in the therapy of psychiatric disorders, e.g. in schizophrenia (Wolosker *et al.* 1999, Javitt 2002). PAT1 might play here an important role in the intestinal absorption of orally provided D-serine, due to its localization in the apical membrane of intestinal epithelial cells (Chen *et al.* 2003).

The methylation of both head groups in amino acid substrates differentially alters affinity and transport capability. Modifications of the carboxyl group are critical and markedly reduce affinity. Methylation of the  $\text{COO}^-$  group changes the compound into a predominantly cationic state, whereas the methylation of the amino group does not substantially alter the ionization state (at pH 6.5). It has to be shown whether the impaired interaction of O-methylated amino acids with PAT1 is due to a sterical hindrance of the methyl group and/or due to changes in the ionic state of the amino acid. A pronounced selectivity for the zwitterionic form of substrates has been observed for other transport system, such as the peptide transporter PEPT1 (Doring *et al.* 1998) and the L-type amino acid transporter LAT1 (Uchino *et al.* 2002).

In contrast to the methyl-substitution of the carboxyl group, the attachment of various methyl-groups to the nitrogen of the amino-group is well tolerated allowing efficient transport of compounds such as sarcosine and betaine. The charge of the amino group is not, *per se*, influenced by N-methylation. All three N-methyl-substituted glycines are mainly present in their zwitterionic form at pH 6.5 and the bulkiness of the N-substituents does not impair transport function.

The demonstration of betaine/ $\text{H}^+$ -symport (as shown here) addresses another putative function of the PAT systems, which is osmoregulation. Betaine is a highly effective organic osmolyte in a huge variety of biological systems and in various cell types. Moreover, it is shown here, for the first time, that betaine uptake across the apical membrane of Caco-2 cell monolayers is mediated by the PAT system and is saturable with an apparent affinity of  $\sim 6.5$  mM. Thus, PAT1 may play a role in absorption of dietary betaine in the intestine.

This is the first detailed analysis of the substrate recognition criteria for a carrier of the mammalian AAAP family and may also apply to other members of the different subfamilies. Based on the data, it is proposed that the substrate recognition site of the PAT1-transporter involves at least three domains that participate in substrate binding: one for the binding of the negatively charged carboxyl group (P1), another (P2) for the binding of the positively charged amino group and a third one (P3) that discriminates substrates based on size of the side chain. As given in the model of the binding pockets, together with L-alanine as a model sub-

strate (Figure 7), the intra-molecular distance between pocket P1 and P3 is more restricted than that between pocket P1 and P2. In the L-configuration, a maximum of one  $\text{CH}_2$ -unit is accepted in the amino acid side chain, whereas in the D-configuration an additional hydroxyl- or SH-group is accepted. The P2 binding pocket of the transporter seems to be the most tolerant site, since a three-fold methylation of the amino group is accepted, as in betaine. These results may also be relevant in search of new pharmacologically relevant agonists or antagonists of the inhibitory neurotransmitters glycine or GABA to obtain orally available drugs utilising PAT1 as a delivery system.

## Experimental procedures

### Materials

Female *X. laevis* oocytes were purchased from Nasco (Fort Atkinson, WI). Amino acids and related compounds were obtained from Sigma-Aldrich (Deisenhofen, Germany) or Merck (Darmstadt, Germany) in pa quality. In the case of  $\beta$ -amino butyric acid, only a preparation containing D- and L-enantiomers was available. [ $^3\text{H}$ ]Glycine, specific activity 56.4 Ci/mmol, was purchased from ICN (Irvine, CA, USA); [ $^{14}\text{C}$ ]N,N,N-Trimethylglycine (betaine) (specific activity 55 mCi/mmol) was from American Radiolabelled Chemicals Inc. (St. Louis, MO, USA). Cell culture media, FCS and supplements were from Sigma-Aldrich (Deisenhofen, Germany).

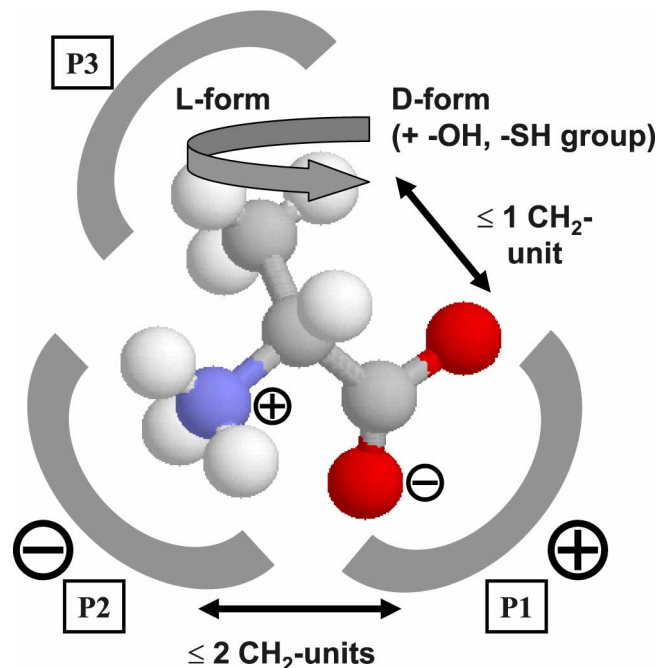


Figure 7. Proposed model for the substrate-binding site of PAT1. The proposed mechanisms of substrate recognition are shown schematically for PAT1 and L-alanine as a model substrate. The binding site of PAT1 is proposed to be composed of three sites: two for the binding of the positively charged amino group (P1) and the negatively charged carboxyl group (P2) (indicated by + and - symbols at the transporter site) and the third for the interaction with the substrate amino acid side chains (P3). The P3 binding site of PAT1 is proposed to accept only moieties with a length of not more than 1  $\text{CH}_2$ -unit of L-enantiomers, whereas in D-enantiomers additional hydroxyl and thiol groups are tolerated.

*Xenopus laevis* oocytes handling and cRNA injection

Oocyte handling and cRNA injection has been described in detail previously (Boll *et al.* 1994). Briefly, oocytes were treated with collagenase A (Roche Diagnostics) for 1.5–2 h at room temperature in Ca<sup>2+</sup>-free ORII solution (82.5 mM NaCl, 2 mM KCl, 1 mM MgCl<sub>2</sub> and 10 mM HEPES, pH 7.5) to remove follicular cells. After sorting, healthy oocytes of stage V and VI were kept at 18°C in modified Barth solution containing 88 mM NaCl, 1 mM KCl, 0.8 mM MgSO<sub>4</sub>, 0.4 mM CaCl<sub>2</sub>, 0.3 mM Ca(NO<sub>3</sub>)<sub>2</sub>, 2.4 mM NaHCO<sub>3</sub> and 10 mM HEPES (pH 7.5). The next day oocytes were injected with 27 nl sterile water (control) or 27 nl murine PAT1 cRNA (10 ng cRNA/oocyte). The oocytes were kept in modified Barth solution at 18°C until further use (3–5 days after injection).

*Amino acid uptake in Xenopus laevis* oocytes

Eight oocytes (water- or PAT1-cRNA-injected) per uptake experiment were pre-incubated at room temperature for 2 min in Na<sup>+</sup>-free standard uptake buffer (100 mM choline chloride, 2 mM KCl, 1 mM MgCl<sub>2</sub>, 1 mM CaCl<sub>2</sub>, 10 mM MES pH 6.5). The buffer was then replaced by the respective uptake buffer supplemented with 100 µM glycine including 5 µCi/ml [<sup>3</sup>H]glycine in the absence (control) or presence of 10 mM competitor. After 10 min of incubation, the oocytes were washed three times with 3 ml of ice cold wash buffer (uptake buffer containing 20 mM glycine) and distributed to individual vials. After oocyte lysis in 10% SDS, radioactivity was counted by liquid scintillation. Uptake values of water-injected control oocytes at each condition were subtracted from those in PAT1-cRNA injected oocytes. Data represent the mean ± SEM of six-to-eight oocytes from a representative uptake experiment out of three experiments with three different batches of oocytes.

*Two-electrode voltage clamp recordings*

Two-electrode voltage clamp experiments were performed as described previously (Boll *et al.* 1996). Briefly, the oocyte was placed in an open chamber and continuously superfused with incubation buffer (100 mM choline chloride, 2 mM KCl, 1 mM MgCl<sub>2</sub>, 1 mM CaCl<sub>2</sub>, 10 mM MES, pH 6.5) in the absence or presence of amino acids. Oocytes were voltage clamped at –60 mV and current-voltage (I-V) relations were measured using short (100 ms) pulses separated by 200 ms pauses in the potential range –160 to +80 mV. I-V measurements were made immediately before and 20–30 s after substrate application when current flow reached steady state. The current evoked by PAT1 at a given membrane potential was calculated as the difference between the currents measured in the presence and the absence of substrate. Kinetic constants were derived from experiments employing five (for substrates with a K<sub>m</sub> < 25 mM) or four (for substrates with a K<sub>m</sub> > 25 mM) different amino acid concentrations in Na<sup>+</sup>-free buffer at pH 6.5 with five-to-seven individual oocytes from at least two different oocyte batches for each substrate. Substrate-evoked currents were transformed according to Eadie-Hofstee and after linear regression the apparent K<sub>m</sub> values were derived.

*Intracellular pH recordings in Xenopus laevis* oocytes

The pH microelectrodes were made from borosilicate capillaries pulled to ~10 µm tip diameter. Electrodes were silanized as described previously (Kottra *et al.* 2002) and the tip was filled with Fluka hydrogen ionophore I cocktail B (Sigma-Aldrich, Deisenhofen, Germany) overnight. Electrodes were backfilled prior to use with a solution containing 40 mM KH<sub>2</sub>PO<sub>4</sub>, 23 mM NaOH, 15 mM NaCl, pH 7.0. The pH electrodes were connected to an FD223 amplifier (WPI, Berlin, Germany). The reference channel of the amplifier was connected to the voltage output signal of the TEC-05 amplifier. The electrodes were calibrated using solutions with different pH and only electrodes with a slope of > 55 and < 60 mV/pH unit and stable calibration were used.

*Cell culture*

Caco-2 cells (passage number 99–100) were cultured as described previously (Thwaites *et al.* 1995a). Cell monolayers were prepared by seeding cells at high density (4.0–5.0 × 10<sup>5</sup> cells cm<sup>-2</sup>) on 12 mM diameter Transwell polycarbonate filters (Costar). Cell monolayers were maintained in culture at 37°C in a humidified atmosphere of 5% CO<sub>2</sub> in air. Experiments were performed 12–14 days after seeding and 18–24 h after feeding.

*Amino acid uptake in Caco-2 cell monolayers*

The cell monolayers were washed in 4 × 500 ml volumes of modified Krebs' solution (pH 7.4) of composition: 137 choline chloride, 5.4 mM KCl, 0.99 mM MgSO<sub>4</sub>, 0.34 mM KH<sub>2</sub>PO<sub>4</sub>, 2.8 mM CaCl<sub>2</sub>, 10 mM Glucose. Solution pH was adjusted at 37°C by addition of either 10 mM MES (pH 6.5) or 10 mM HEPES (pH 7.4) and TRIS base. In all experiments, the apical solution was pH 6.5 and the basolateral solution pH 7.4. [<sup>14</sup>C]Betaine (0.5 µCi ml<sup>-1</sup>, 100 µM) uptake was measured for 10 min (37°C) across the apical membrane of Caco-2 cell monolayers in the presence or absence of unlabelled betaine (0–20 mM), 10 mM unlabelled amino acids or 30 mM β-alanine. Mannitol was added to maintain isoosmolarity between experimental solutions. At the end of the incubation period, the cell monolayers were washed in 3 × 500 ml volumes of ice-cold modified Krebs' (pH 7.4) (to remove any loosely associated radiolabel) and removed from the insert. Data are expressed either as nmol cm<sup>-2</sup> × 10min<sup>-1</sup> or as% control (after subtraction of non-carrier-mediated uptake estimated by uptake in the presence of 30 mM β-alanine). Results are expressed as mean ± SEM (*n*).

**Acknowledgements**

This study was supported by the DFG Grant (BO 1857/1) to MB and by an MRC Career Establishment Grant (G9801704) to DTT. CMHA is supported by a BBSRC Agri-Food Committee Studentship.

**References**

- Boll, M., Foltz, M., Rubio-Aliaga, I., Kottra, G. and Daniel, H., 2002, Functional characterization of two novel mammalian electrogenic proton dependent amino acid cotransporters. *Journal of Biological Chemistry*, **277**, 22966–22973.
- Boll, M., Herget, M., Wagener, M., Weber, W. M., Markovich, D., Biber, J., Clauss, W., Murer, H. and Daniel, H., 1996, Expression cloning and functional characterization of the kidney cortex high-affinity proton-coupled peptide transporter. *Proceedings of the National Academy of Sciences (USA)*, **93**, 284–289.
- Boll, M., Markovich, D., Weber, W. M., Korte, H., Daniel, H. and Murer, H., 1994, Expression cloning of a cDNA from rabbit small intestine related to proton-coupled transport of peptides, beta-lactam antibiotics and ACE-inhibitors. *Pflugers Archives*, **429**, 146–149.
- Chang, H. C. and Bush, D. R., 1997, Topology of NAT2, a prototypical example of a new family of amino acid transporters. *Journal of Biological Chemistry*, **272**, 30552–30557.
- Chaudhry, F. A., Krizaj, D., Larsson, P., Reimer, R. J., Wreden, C., Storm-Mathisen, J., Copenhagen, D., Kavanaugh, M. and Edwards, R. H., 2001, Coupled and uncoupled proton movement by amino acid transport system N. *EMBO Journal*, **20**, 7041–7051.
- Chaudhry, F. A., Reimer, R. J., Krizaj, D., Barber, D., Storm-Mathisen, J., Copenhagen, D. R. and Edwards, R. H., 1999, Molecular analysis of system N suggests novel physiological roles in nitrogen metabolism and synaptic transmission. *Cell*, **99**, 769–780.
- Chaudhry, F. A., Schmitz, D., Reimer, R. J., Larsson, P., Gray, A. T., Nicoll, R., Kavanaugh, M. and Edwards, R. H., 2002, Glutamine uptake by neurons: interaction of protons with system A transporters. *Journal of Neuroscience*, **22**, 62–72.
- Chen, Z., Fei, Y. J., Anderson, C. M. H., Wake, K. A., Miyauchi, S., Huang, W., Thwaites, D. T. and Ganapathy, V., 2003, Structure,

- function and immunolocalization of a proton-coupled amino acid transporter (hPAT1) in the human intestinal cell line Caco-2. *Journal of Physiology*, in press [AQ1], doi 10.1113/jphysiol.2002.026500.
- Doring, F., Will, J., Amasheh, S., Clauss, W., Ahlbrecht, H. and Daniel, H., 1998, Minimal molecular determinants of substrates for recognition by the intestinal peptide transporter. *Journal of Biological Chemistry*, **273**, 23211–23218.
- Hatanaka, T., Huang, W., Ling, R., Prasad, P. D., Sugawara, M., Leibach, F. H. and Ganapathy, V., 2001, Evidence for the transport of neutral as well as cationic amino acids by ATA3, a novel and liver-specific subtype of amino acid transport system A. *Biochimica et Biophysica Acta*, **1510**, 10–17.
- Javitt, D. C., 2002, Glycine modulators in schizophrenia. *Current Opinions in Investigative. Drugs*, **3**, 1067–1072.
- Jessen, H., Jorgensen, K. E., Roigaard-Petersen, H. and Sheikh, M. I., 1989, Demonstration of H<sup>+</sup>- and Na<sup>+</sup>-coupled co-transport of  $\beta$ -alanine by luminal membrane vesicles of rabbit proximal tubule. *Journal of Physiology*, **411**, 517–528.
- Jessen, H., Vorum, H., Jorgensen, K. E. and Sheikh, M. I., 1988, Characteristics of D-alanine transport by luminal membrane vesicles from pars convoluta and pars recta of rabbit proximal tubule. *Biochimica et Biophysica Acta*, **942**, 262–270.
- Jessen, H., Vorum, H., Jorgensen, K. E. and Sheikh, M. I., 1991, Na<sup>+</sup>- and H<sup>+</sup>-gradient-dependent transport of  $\alpha$ -aminoisobutyrate by luminal membrane vesicles from rabbit proximal tubule. *Journal of Physiology*, **436**, 149–167.
- Kotra, G., Stamford, A. and Daniel, H., 2002, PEPT1 as a paradigm for membrane carriers that mediate electrogenic bidirectional transport of anionic, cationic and neutral substrates. *Journal of Biological Chemistry*, **277**, 32683–32691.
- McIntire, S. L., Reimer, R. J., Schuske, K., Edwards, R. H. and Jorgensen, E. M., 1997, Identification and characterization of the vesicular GABA transporter. *Nature*, **389**, 870–876.
- Nakanishi, T., Kekuda, R., Fei, Y. J., Hatanaka, T., Sugawara, M., Martindale, R. G., Leibach, F. H., Prasad, P. D. and Ganapathy, V., 2001, Cloning and functional characterization of a new subtype of the amino acid transport system N. *American Journal of Physiology and Cell Physiology*, **281**, C1757–C1768.
- Palacin, M., Estevez, R., Bertran, J. and Zorzano, A., 1998, Molecular biology of mammalian plasma membrane amino acid transporters. *Physiology Review*, **78**, 969–1054.
- Rajendran, V. M., Barry, J. A., Kleinman, J. G. and Ramaswamy, K., 1987, Proton gradient-dependent transport of glycine in rabbit renal brush-border membrane vesicles. *Journal of Biological Chemistry*, **262**, 14974–14977.
- Reimer, R. J., Chaudhry, F. A., Gray, A. T. and Edwards, R. H., 2000, Amino acid transport system A resembles system N in sequence but differs in mechanism. *Proceedings of the National Academy of Sciences (USA)*, **97**, 7715–7720.
- Roigaard-Petersen, H., Jacobsen, C. and Sheikh, M. I., 1987, H<sup>+</sup>-L-proline cotransport by vesicles from pars convoluta of rabbit proximal tubule. *American Journal of Physiology*, **253**, F15–F20.
- Sagne, C., Agulhon, C., Ravassard, P., Darmon, M., Hamon, M., El Mestikawy, S., Gasnier, B. and Giros, B., 2001, Identification and characterization of a lysosomal transporter for small neutral amino acids. *Proceedings of the National Academy of Sciences (USA)*, **98**, 7206–7211.
- Sagne, C., El Mestikawy, S., Isambert, M. F., Hamon, M., Henry, J. P., Giros, B. and Gasnier, B., 1997, Cloning of a functional vesicular GABA and glycine transporter by screening of genome databases. *FEBS Letters*, **417**, 177–183.
- Sugawara, M., Nakanishi, T., Fei, Y. J., Huang, W., Ganapathy, M. E., Leibach, F. H. and Ganapathy, V., 2000, Cloning of an amino acid transporter with functional characteristics and tissue expression pattern identical to that of system A. *Journal of Biological Chemistry*, **275**, 16473–16477.
- Thwaites, D. T. and Stevens, B. C., 1999, H<sup>+</sup>/zwitterionic amino acid symport at the brush-border membrane of human intestinal epithelial (Caco-2) cells. *Experimental Physiology*, **84**, 275–284.
- Thwaites, D. T., Armstrong, G., Hirst, B. H. and Simmons, N. L., 1995a, D-Cycloserine transport in human intestinal epithelial (Caco-2) cells is mediated by a H<sup>+</sup>-coupled amino acid transporter. *British Journal of Pharmacology*, **115**, 761–766.
- Thwaites, D. T., Basterfield, L., McCleave, P. M. J., Carter, S. M. and Simmons, N. L., 2000, Gamma-aminobutyric acid (GABA) transport across human intestinal epithelial (Caco-2) cell monolayers. *British Journal of Pharmacology*, **129**, 457–464.
- Thwaites, D. T., McEwan, G. T. A. and Simmons, N. L., 1995c, The role of the proton electrochemical gradient in the transepithelial absorption of amino acids by human intestinal Caco-2 cell monolayers. *Journal of Membrane Biology*, **145**, 245–256.
- Thwaites, D. T., McEwan, G. T. A., Brown, C. D. A., Hirst, B. H. and Simmons, N. L., 1993a, Na<sup>+</sup>-independent, H<sup>+</sup>-coupled transepithelial  $\beta$ -alanine absorption by human intestinal Caco-2 cell monolayers. *Journal of Biological Chemistry*, **268**, 18438–18441.
- Thwaites, D. T., McEwan, G. T. A., Brown, C. D. A., Hirst, B. H. and Simmons, N. L., 1994, L-Alanine absorption in human intestinal cells driven by the proton electrochemical gradient. *Journal of Membrane Biology*, **140**, 143–151.
- Thwaites, D. T., McEwan, G. T. A., Cook, M. J., Hirst, B. H. and Simmons, N. L., 1993b, H<sup>+</sup>-coupled (Na<sup>+</sup>-independent) proline transport in human intestinal (Caco-2) epithelial cell monolayers. *FEBS Letters*, **333**, 78–82.
- Thwaites, D. T., McEwan, G. T. A., Hirst, B. H. and Simmons, N. L., 1995b, H<sup>+</sup>-coupled  $\alpha$ -methylaminoisobutyric acid transport in human intestinal Caco-2 cells. *Biochimica et Biophysica Acta*, **1234**, 111–118.
- Uchino, H., Kanai, Y., Kim do, K., Wempe, M. F., Chairoungdua, A., Morimoto, E., Anders, M. W. and Endou, H., 2002, Transport of amino acid-related compounds mediated by L-type amino acid transporter 1 (LAT1): insights into the mechanisms of substrate recognition. *Molecular Pharmacology*, **61**, 729–737.
- Wolosker, H., Sheth, K. N., Takahashi, M., Mothet, J. P., Brady Jr., R. O., Ferris, C. D. and Snyder, S. H., 1999, Purification of serine racemase: biosynthesis of the neuromodulator D-serine. *Proceedings of the National Academy of Sciences (USA)*, **96**, 721–725.
- Wunz, T. M. and Wright, S. H., 1993, Betaine transport in rabbit renal brush-border membrane vesicles. *American Journal of Physiology*, **264**, F948–F955.
- Young, G. B., Jack, D. L., Smith, D. W. and Saier Jr., M. H., 1999, The amino acid/auxin:proton symport permease family. *Biochimica et Biophysica Acta*, **1415**, 306–322.

Received 1 November 2002; and in revised form 13 January 2003.

## APPENDIX 4

published in *Journal of Biological Chemistry*

## The Proton/Amino Acid Cotransporter PAT2 Is Expressed in Neurons with a Different Subcellular Localization than Its Paralog PAT1\*

Received for publication, May 28, 2003, and in revised form, September 24, 2003  
Published, JBC Papers in Press, November 3, 2003, DOI 10.1074/jbc.M305556200

Isabel Rubio-Aliaga<sup>‡§¶</sup>, Michael Boll<sup>‡¶</sup>, Daniela M. Vogt Weisenhorn<sup>||</sup>, Martin Foltz<sup>‡</sup>,  
Gabor Kottra<sup>‡</sup>, and Hannelore Daniel<sup>‡\*\*</sup>

From the <sup>‡</sup>Molecular Nutrition Unit, Technical University of Munich, Hochfeldweg 2, D-85350 Freising-Weihenstephan, Germany and the <sup>||</sup>National Research Center, Institute of Developmental Genetics, Ingostädter Landstrasse 1, D-85764 Neuherberg, Germany

The new member of the mammalian amino acid/auxin permease family, PAT2, has been cloned recently and represents an electrogenic proton/amino acid symporter. PAT2 and its paralog, PAT1/LYAAT-1, are transporters for small amino acids such as glycine, alanine, and proline. Our immunodetection studies revealed that the PAT2 protein is expressed in spinal cord and brain. It is found in neuronal cell bodies in the anterior horn in spinal cord and in brain stem, cerebellum, hippocampus, hypothalamus, rhinencephalon, cerebral cortex, and olfactory bulb in the brain. PAT2 is expressed in neurons positive for the *N*-methyl-D-aspartate subtype glutamate receptor subunit NR1. PAT2 is not found in lysosomes, unlike its paralog PAT1, but is present in the endoplasmic reticulum and recycling endosomes in neurons. PAT2 has a high external proton affinity causing half-maximal transport activation already at a pH of 8.3, suggesting that its activity is most likely not altered by physiological pH changes. Transport of amino acids by PAT2 activity is dependent on membrane potential and can occur bidirectionally; membrane depolarization causes net glycine outward currents. Our data suggest that PAT2 contributes to neuronal transport and sequestration of amino acids such as glycine, alanine, and/or proline, whereby the transport direction is dependent on the sum of the driving forces such as substrate concentration, pH gradient, and membrane potential.

The amino acid/auxin permease (AAP) family is one of the largest families of amino acid transporters identified so far, with members found in virtually all eukaryotic organisms (1–3). Hitherto, three different subfamilies of the AAP transporters have been identified in mammals as represented by the

following: (a) the vesicular GABA transporter (VGAT) (4, 5); (b) the system A/N subfamily (6–10); and (c) the recently described proton/amino acid transporter (PAT) subfamily (11, 12). Although there is no pronounced sequence similarity among the AAP transporters, they all recognize certain amino acids or closely related compounds and are highly sensitive to alterations in intracellular or extracellular proton concentrations.

The first mammalian AAP transporter identified was the vesicular GABA transporter VGAT, also designated the vesicular inhibitory amino acid transporter (VIAAT). VGAT mediates the transport of the two inhibitory neurotransmitters, GABA and glycine, and appears to be expressed solely in the brain. As a neurotransmitter/proton antiporter (4, 5), it plays a crucial role in glycinergic and GABAergic transmission by accumulation of glycine and GABA in secretory vesicles in presynaptic nerve terminals.

The second subfamily comprises three different types of system A transporters (SAT1–3/ATA1–3) and two types of system N transporters (SN1 and SN2) (6–10, 13). Both classes play important roles in the homeostasis of various neutral amino acids in different tissues. Particularly in the brain system, A and N transporters possess a central role in the glutamate-glutamine cycle between astrocytes and neurons involved in recycling glutamate for its role in neurotransmission (14). Both systems are Na<sup>+</sup>-dependent co-transporters but differ with respect to the role of protons in the transport process. System N mediates H<sup>+</sup> efflux during Na<sup>+</sup>-dependent amino acid influx (9), whereas system A members do not translocate protons, although their activity is markedly affected by the extracellular proton concentration (15).

The third mammalian AAP subfamily is represented by the PAT1 to PAT4 proteins that were cloned recently (3, 11, 12). PAT3 and PAT4 are orphan transporters, whereas PAT1 (also designated as LYAAT1) and PAT2 are characterized as electrogenic amino acid/proton co-transporters with a high selectivity for amino acids with apolar and small side chains (3, 16). PAT1 was shown to transport glycine, L-alanine, and L-proline as well as GABA and D-serine (11, 12, 17–19). It is present in almost all tissues analyzed and shows high expression levels in brain, small intestine, kidney, and colon. In brain, PAT1 is mainly found in lysosomes in neurons, where it is involved in proton-driven export of amino acids from lysosomal protein breakdown (11). To some extent, PAT1 is also found in the plasma membrane (19).

Here we report that, like the other mammalian members of the AAP family, PAT2 is well expressed in the central nervous system and is found predominantly in recycling endosomes and in the endoplasmic reticulum in neurons. Furthermore, we

\* This research was supported by Deutsche Forschungsgemeinschaft (FSG) Grant BO 1857/1 (to M. B.). The costs of publication of this article were defrayed in part by the payment of page charges. This article must therefore be hereby marked "advertisement" in accordance with 18 U.S.C. Section 1734 solely to indicate this fact.

§ Present address: Division of Hematology, Children's Hospital, Harvard Medical School, 300 Longwood Ave., Boston, MA 02115.

¶ These authors contributed equally to this work.

\*\* To whom correspondence should be addressed. Tel.: 49-8161-713400; Fax: 49-8161-713999; E-mail: daniel@wzw.tum.de.

<sup>1</sup> The abbreviations used are: AAP, amino acid/auxin permease; PAT, proton/amino acid transporter; LYAAT, lysosomal amino acid transporter; GABA,  $\gamma$ -aminobutyric acid; VGAT, vesicular GABA transporter; RT, reverse transcription; GAPDH, glyceraldehyde-3-phosphate dehydrogenase; TBS, Tris-buffered saline; TEVC, two-electrode voltage clamp; GLYT, glycine transporter; NMDA, *N*-methyl-D-aspartate; NR, NMDA receptor; GAD65/67, glutamate decarboxylase 65/67.

## Proton/Amino Acid Cotransporter PAT2 in Neurons

2755

demonstrate that transport activity of PAT2 is dependent on external pH and membrane potential and that the protein has the ability to transport in the reverse mode.

## EXPERIMENTAL PROCEDURES

**RNA Isolation and RT-PCR**—Total RNA from different mouse brain regions (olfactory bulb, cortex, thalamus, cerebellum, and brain stem) and spinal cord was isolated with RNawiz (Ambion), following the supplier's protocol. 5  $\mu$ g of total RNA were reverse transcribed by using oligo(dT) as primer and the Retroscrip kit (Ambion). 2  $\mu$ l of each RT reaction were subjected to PCR reactions with the following primer pairs: 1) PAT2-F1 (5'-ATG TCT GTG ACC AAG AGT GCC-3') and PAT2-B546 (5'-GCA GCT GAT GGT TGT GCT GTT-3'); and 2) GAPDH-F (5'-GAC CAC AGT CCA TGA CAT CAC T-3') and GAPDH-B (5'-TCC ACC ACC CTG TTG CTG TAG-3'). PCR conditions were 94 °C for 1 min and 30  $\times$  (94 °C for 30 s, 58 °C for 30 s, and 72 °C for 45 s).

**Anti-PAT2 Antibody Production and Western Blot**—A polyclonal antibody raised against the peptide CLDLIKSGNSPAL (amino acid residues 457–469 of the mouse PAT2 protein, GenBank™ accession number AAM80481) with the N-terminal cysteine coupled to keyhole limpet hemocyanin was produced in rabbit (Davids Biotechnologie). The antibody was affinity-purified on the peptide linked to Affi-Gel.

For Western blot analysis, 50  $\mu$ g of crude protein prepared from mouse brain was separated by 10% SDS-PAGE followed by transfer onto a polyvinylidene difluoride membrane by using a semi-dry blotter (Bio-Rad). After blocking, the blot was immunostained with the anti-PAT2 antibody diluted 1:500 or the pre-absorbed antibody with the corresponding antigenic peptide. After washing with TBS, the blots were incubated with a horseradish peroxidase-conjugated anti-rabbit IgG antibody (1:1000; Dianova) and detected by 3-amino-9-ethyl-carbazole staining.

**Heterologous Expression of PAT2 in *Xenopus laevis* Oocytes**—Oocytes were handled as described previously (12), and either 25 nl (25 ng) of the mouse PAT2-cRNA or 25 nl of water (control) were injected into individual cells. Transport studies were performed 3 days after injection, as described previously (12). The two-electrode voltage clamp (TEVC) experiments were performed as reported (20). Briefly, steady state current-voltage (*I-V*) relationships were measured in incubation buffer (100 mM choline chloride or sodium chloride, 2 mM KCl, 1 mM MgCl<sub>2</sub>, 1 mM CaCl<sub>2</sub>, and 10 mM Tris at pH 7.5–9) in the absence or presence of glycine. Oocytes were clamped at –60 mV, and *I-V* relations were measured using short (100 ms) pulses separated by 200-ms pauses in the potential range of –160 to 80 mV. All values are expressed as mean  $\pm$  S.E.

Giant patch clamp experiments were performed as described previously (20) with patch pipettes filled with 10 mM NaCl, 80 mM sodium isethionate, 1 mM MgSO<sub>4</sub>, 1 mM Ca(NO<sub>3</sub>)<sub>2</sub>, and 10 mM HEPES (pH 7.5) and an incubation buffer comprised of 100 mM potassium aspartate, 20 mM KCl, 4 mM MgCl<sub>2</sub>, 2 mM EGTA, and 10 mM HEPES (pH 7.5) containing nothing or 20 mM glycine on the patch cytosolic surface. During perfusion, the membrane potential was clamped to –30 mV, and *I-V* relations in the potential range of –80 to 60 mV were measured in the same way as described for TEVC. For immunolocalization in oocytes, cells injected with the PAT2-cRNA were initially checked for expression of the transporter by measuring positive inward currents induced by 20 mM glycine using the TEVC method. Oocytes were then fixed in 4% paraformaldehyde for 15 min at room temperature and processed for embedment in paraffin wax. Deparaffinized sections (10  $\mu$ m) were used for immunofluorescence analysis.

**Immunodetection Studies**—Immunohistochemistry and immunofluorescence detection of PAT2 were performed on deparaffinized brain or spinal cord sections from adult mouse transcardially perfused for 15 min with 4% paraformaldehyde in buffer 1 (100 mM sucrose, 100 mM NaCl, and 10 mM HEPES, pH 7.4) and washed for 5 min with buffer 1. Tissues were processed for embedding in paraffin wax. Antigen retrieval was carried out by incubating the slices in citrate buffer (pH 6) in a microwave oven. For immunohistochemistry, 5- $\mu$ m sections were blocked for 20 min with 3% goat serum in TBS and incubated overnight with the affinity-purified anti-PAT2 antibody diluted 1:100. On the following day, sections were rinsed with TBS and incubated for 30 min with biotinylated goat anti-rabbit immunoglobulins (1:800; Dako), rinsed with TBS, and incubated for 30 min with peroxidase-conjugated streptavidin (1:300; Dako). After washing with TBS, the sections were stained for 5–10 min with DAB peroxidase substrate (Sigma). Control incubations in parallel sections were carried out by pre-absorption of the primary antibody with the corresponding antigenic peptide. For immunofluorescence analysis, 10- $\mu$ m sections were blocked for 20 min

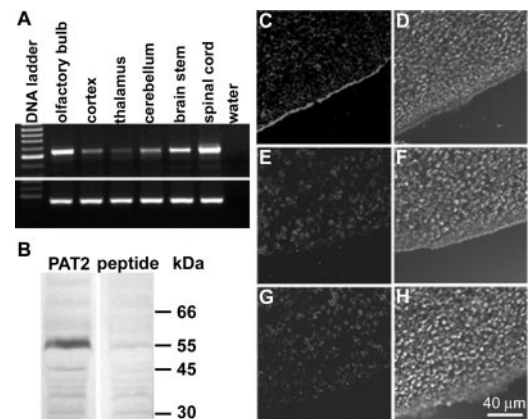


**FIG. 1. Detection of PAT2 mRNA and protein in mouse brain and determination of anti-PAT2 antibody specificity.** A, the RT-PCR analysis was performed with 5  $\mu$ g of total RNA extracted from the different brain regions indicated and water as a negative control. In the PCR reaction, PAT2-cDNA-specific primers were used to detect mRNA (top). The expected size of the product was 546 bp. As a control for RNA integrity, the GAPDH PCR product was amplified (bottom; expected size, 453 bp). B, the Western blot analysis was performed with a crude protein preparation isolated from murine brain and incubated with an anti-PAT2 antibody (left) or the antibody pre-absorbed with the antigenic peptide (right). C–H, for determination of anti-PAT2 antibody specificity, immunofluorescence studies were performed with 10- $\mu$ m slices of *X. laevis* oocytes injected with PAT2-cRNA (C) or *X. laevis* oocytes injected with water (E) and incubated with the anti-PAT2 antibody. An additional control was performed by incubating 10- $\mu$ m slices of *X. laevis* oocytes injected with PAT2-cRNA with the pre-absorbed anti-PAT2 antibody (E). D, F, and H are phase-contrast micrographs of C, E, and G, respectively. Scale bar in H applies to C–H.

with 3% goat serum and incubated overnight with the affinity-purified anti-PAT2 antibody diluted 1:100 or the affinity-purified anti-LYAAT-1 (1:500; kindly provided by B. Giros, INSERM U513, Créteil, France). Colocalization analysis was performed with 10- $\mu$ m sections incubated overnight with the affinity-purified anti-PAT2 antibody diluted 1:100 and mouse anti-BiP/GRP78, mouse anti-GM130, mouse anti-Rab4, mouse anti-EEA1 (all diluted 1:50; BD Transduction Laboratories), goat anti-NR1, goat anti-gephyrin, goat anti-GAD65/67 (all diluted 1:25; Santa Cruz Biotechnology), or goat anti-GLYT2 (1:250; Chemicon). Slices were rinsed with TBS and incubated for 30 min with the following: (a) Cy3-conjugated donkey anti-rabbit IgG (1:800; Dianova) and Alexa Fluor 633 goat anti-mouse IgG (1:1000; Molecular Probes); or (b) Cy5-conjugated donkey anti-rabbit IgG (1:500; Dianova) and Alexa Fluor 488-conjugated donkey anti-goat IgG (1:500; Molecular Probes). Slices were rinsed with TBS and viewed using a confocal laser-scanning microscope (model TCS SP2; Leica Microsystems). Colocalization analysis was performed with a Multicolor software package (Leica Microsystems). All images were generated with Adobe Photoshop 7.0 (Adobe Systems).

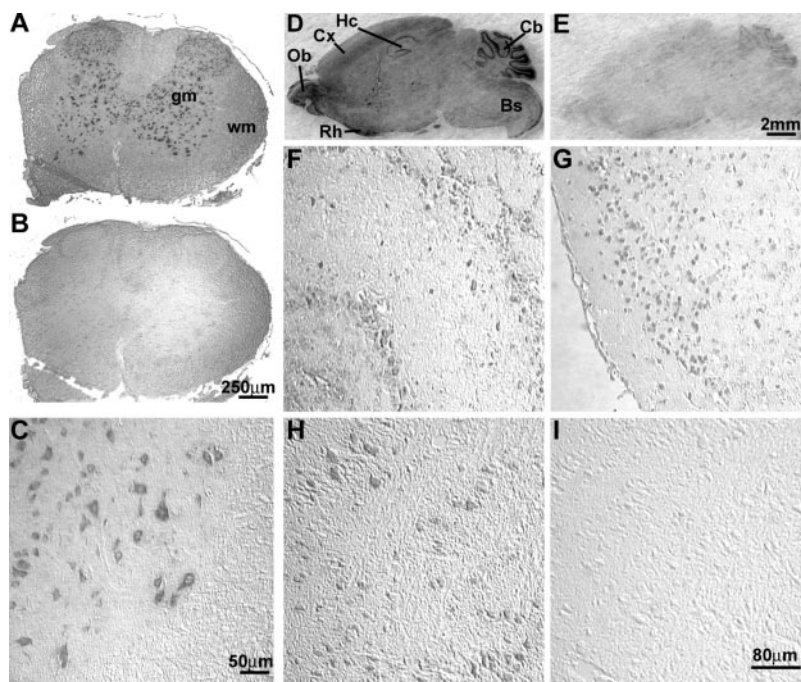
## RESULTS

A BLAST analysis of the murine PAT2 cDNA sequence with the expressed sequence tag (EST) data base revealed the presence of PAT2-EST clones obtained from the nervous system. Because in our previous report we could not detect the PAT2-mRNA in brain by using Northern blot analysis (12), we here applied RT-PCR analysis and show that the PAT2 mRNA was detectable in all nervous system regions analyzed. As shown in Fig. 1A, a 546-bp fragment was amplified from olfactory bulb, cortex, thalamus, cerebellum, brain stem, and spinal cord. The presence of the PAT2 protein in the brain was confirmed by using an anti-PAT2 antibody raised against 13 amino acids of the C-terminal sequence of the PAT2 protein. Western blot analysis using this antibody revealed the PAT2 protein to be present in the brain with an apparent molecular mass of 55 kDa (Fig. 1B). The specificity of the antibody was demonstrated by immunofluorescence studies in *X. laevis* oocytes after expression of PAT2 (Fig. 1, C–H) with water-injected oocytes as a negative control. Only in membranes of oocytes expressing

2756

## Proton/Amino Acid Cotransporter PAT2 in Neurons

**FIG. 2. Immunohistochemistry in cross-sections of the spinal cord (A–C) and parasagittal sections of the mouse brain with an anti-PAT2 antibody (D–I).** Images A–C are in spinal cord. A, image of PAT2 immunoreactivity in spinal cord. *gm*, gray matter; *wm*, white matter. B, incubation with the antibody pre-absorbed with the antigenic peptide in an adjacent section. C, high power magnification of the ventral horn shows the presence of PAT2 in motoneurons and interneurons. Images D–I are in brain. D, image of PAT2 immunoreactivity in the whole brain. *Ob*, olfactory bulb; *Cx*, cerebral cortex; *Hc*, hippocampus; *Cb*, cerebellum; *Bs*, brain stem; *Rh*, rhinencephalon. E, pre-absorption of the anti-PAT2 antibody with the antigenic peptide showed no significant immunoreactivity on an adjacent section. High power magnifications of olfactory bulb (F), cerebral cortex (G), and brain stem (H) are shown. In all regions, pre-absorption of the anti-PAT2 antibody with the antigenic peptide abolished the immunoreactivity on an adjacent section, as shown in panel I for brain stem. Scale bars in B, C, E, and I apply to A and B, C, D–E, and F–I, respectively.



PAT2, a fluorescence signal was detected (Fig. 1C) that was blocked when the anti-PAT2 antibody was pre-absorbed with the antigenic peptide (Fig. 1G).

**Immunolocalization of PAT2 in the Nervous System**—Immunodetection studies revealed that the PAT2 protein is expressed in spinal cord and brain. As shown in Fig. 2A, in spinal cord, PAT2 is highly expressed in the gray matter and is not detectable in the white matter. The signals were abolished in an adjacent section by incubation with the antibody pre-absorbed with the antigenic peptide (Fig. 2B). In the anterior horn, PAT2 is present in motoneurons and interneurons (Fig. 2C) and in interneurons of the posterior horn (data not shown). In brain, PAT2 is found in various regions, with prominent expression in brain stem, cerebellum, hippocampus, hypothalamus, rhinencephalon, cerebral cortex, and olfactory bulb (Fig. 2D). In an adjacent section, signals were abolished by incubation of slices with the antibody pre-absorbed with the antigenic peptide (Fig. 2E). Colocalization studies using the glia marker GFAP (glial fibrillary acidic protein) showed that the PAT2 protein is solely detectable in neurons and not in astrocytes (data not shown). High power magnification demonstrates the expression of PAT2 in neurons of the mitral cell layer and interneurons in the olfactory bulb (Fig. 2F) as well as in neurons of the cerebral cortex (Fig. 2G) and large neurons in brainstem (Fig. 2H).

**Cell-specific Expression of the PAT2 Protein**—PAT2 is expressed in “NMDAergic” neurons in different regions of the central nervous system (Fig. 3A). PAT2 immunoreactivity is found in cells expressing the NMDA receptor subunit NR1, such as motoneurons and interneurons in the spinal cord and brainstem, Purkinje cells in the cerebellar cortex, neurons in the dentate gyrus, the CA1 and CA3 regions of the hippocampus, and neurons in different layers of the cerebral cortex (Fig. 3A). Moreover, a subset of neurons in the molecular layers of the hippocampal formation and the molecular and granular layers of the cerebellum show both NR1 and PAT2 immunoreactivity (Fig. 3, A and B). NR1 and PAT2 showed very similar staining intensities along the neuronal cell bodies; e.g. pyramidal cells of the hippocampal CA3 region stained stronger than the granule cells of the CA1 region. At higher magnification, a

partial subcellular colocalization of both proteins becomes evident (Fig. 3B). This subcellular colocalization is probably due to the expression of both proteins in the endoplasmic reticulum, as shown for PAT2 (see Fig. 4B) and previously for the NR1 subunit (27). No clear correlation of expression pattern was observed between PAT2 and the glycinergic marker protein GLYT2 (glycine transporter 2), the glycine-and-GABAergic marker gephyrin, and the GABAergic marker glutamate decarboxylase GAD65/67 (Fig. 3B). Whereas PAT2 is expressed at higher levels in Purkinje cells of the cerebellum, the glycine and GABAergic markers displayed higher expression levels in the molecular and/or granular layer. Such differential expression patterns in the colocalization of PAT2 with proteins of the glycine and GABAergic systems were also observed in other regions of the brain (data not shown), suggesting that PAT2 plays no role in the inhibitory glycine and GABAergic system. The missing correlation with the GABAergic system is not surprising, because GABA displays only a very low affinity to PAT2 (12).

**Subcellular Localization of PAT2 in Neurons**—We have shown previously that PAT2, unlike its paralog PAT1, is not detected in lysosomes and possesses a different subcellular distribution after expression in HeLa cells (12). As shown in Fig. 4A, in neurons of the brainstem, PAT2 is found mainly in the somata, predominantly in the cytoplasm and probably also partially in the plasma membrane. Its distribution, therefore, differs from the distribution pattern observed for PAT1. Colocalization studies using antibodies against different intracellular marker proteins in cross-sections of spinal cord were carried out for determining the subcellular compartments in which PAT2 is localized. Various regions of the nervous system have been examined, and in all cases the PAT2 protein did not colocalize with the Golgi marker protein GM130 or the early endosome marker protein EAA1 (Fig. 4B). On the other hand, it partly colocalized with the endoplasmic reticulum marker protein BiP/GRP78 and the early and recycling endosome marker protein Rab4. Quantification of PAT2 immunoreactive puncta indicated  $\sim 34 \pm 3\%$  ( $n = 12$ ) and  $\sim 31 \pm 3\%$  ( $n = 15$ ) colocalized with the endoplasmic reticulum marker protein and the recycling endosome marker protein, respectively. There-

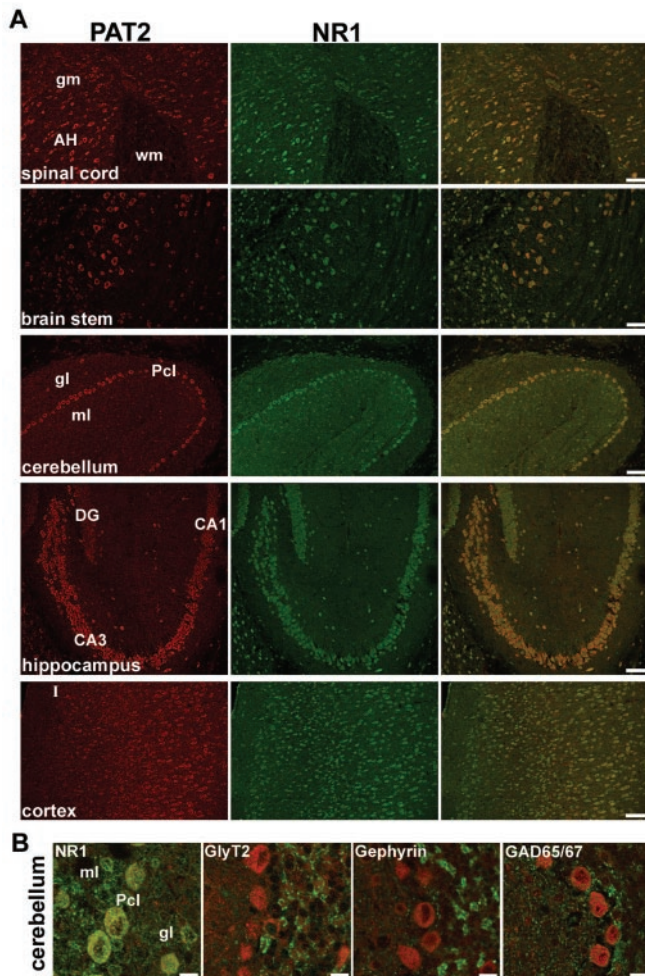


**FIG. 3. Cell-specific expression of PAT2.** *A*, confocal, laser-scanning, double immunofluorescence microscopy in parasagittal sections of different regions of the central nervous system with anti-PAT2 antibody (red) and anti-NR1 (green) antibody. The superimposed images are depicted on the right. *B*, higher resolution of double staining with anti-PAT2 (red) and anti-NR1, anti-GLYT2, anti-Gephyrin, or anti-GAD65/67 (green) antibodies. Colocalization appears in the superimposed images as yellow. *gm*, gray matter; *wm*, white matter; *AH*, anterior horn of spinal cord; *gl*, glomerular layer; *ml*, molecular layer; *Pcl*, Purkinje cell layer of cerebellum; *DG*, dentate gyrus, *CA1*, CA1 region; *CA3*, CA3 region of hippocampus; *I*, neuronal layer I of the cerebral cortex. Scale bars represent 80  $\mu\text{m}$  (*A*) and 10  $\mu\text{m}$  (*B*).

fore, PAT2 is found in endoplasmic reticulum and recycling endosomes, whereas the remaining fraction is localized in other compartments, including the cell membrane.

**Functional Analysis of PAT2**—Whereas in our previous report we demonstrated that PAT1 and PAT2 activities are generally dependent on extracellular pH and membrane potential (12), here we analyzed in more detail the kinetics of glycine transport (Fig. 5). Applying the TEVC technique in oocytes expressing PAT2, the glycine/ $\text{H}^+$  symport at saturating (10 mM) external glycine concentrations induced positive inward currents that increased by decreasing external pH from 9 to 7.5 (Fig. 5A). A further reduction of pH from 7.5 to 5.5 did not further enhance glycine currents (data not shown), and no current responses were observed in the water-injected oocytes. As shown in Fig. 5B, PAT2-mediated inward currents followed Michaelis-Menten kinetics when plotted as a function of apparent external proton concentration. The corresponding Eadie-Hofstee transformation (Fig. 5C) revealed an apparent half-maximal proton activation constant of  $4.7 \pm 0.2$  nM and an  $I_{\text{max}}$  of  $462 \pm 12$  nA. From this data it can be concluded that the

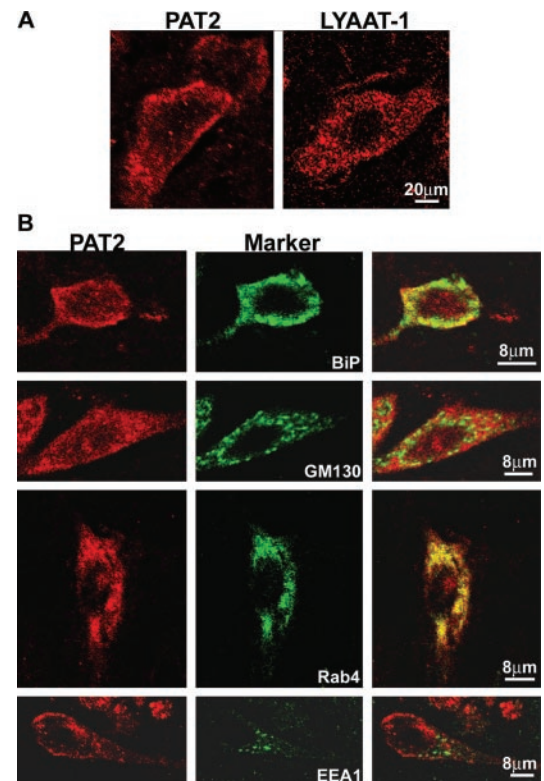


**FIG. 4. Subcellular localization of PAT2 in neurons.** *A*, immunofluorescence analysis with an anti-PAT2 (left) or an anti-LYAAT-1/PAT1 (right) antibody in adjacent brain stem slices. *B*, confocal, laser-scanning, double immunofluorescence microscopy in spinal cord cross-sections with anti-PAT2 antibody and antibodies against subcellular markers. PAT2 immunoreactivity is shown in red, and the marker immunoreactivity in green. The superimposed images are depicted on the right. *BiP*, endoplasmic reticulum marker; *GM130*, cis-Golgi marker; *Rab4*, early/recycling endosome marker; *EEA1*, early endosome marker.

external pH necessary for a half-maximal transport activation at a membrane potential of  $-60$  mV is 8.3, suggesting that, at a physiological pH of 7.3 or in a more acidic environment, PAT2 operates already with a maximal transport rate.

Alterations in membrane potential play an important role in the brain in the regulation of membrane protein functions. Here we demonstrate that PAT2-mediated glycine currents are significantly altered by changes in the membrane potential (Fig. 5D). A hyperpolarization of the membrane increases inward currents, and voltage effects are more pronounced at higher glycine concentrations. Moreover, at low glycine concentrations (0.1 mM) a depolarization of the membrane induces outward currents represented by a reversed transport mode.

**PAT2 Is Capable for Bidirectional Transport of Amino Acids**—To characterize the capability of PAT2 for glycine efflux, we employed the giant patch clamp technique with membrane patches obtained from oocytes expressing PAT2. Positive outward currents were induced by 20 mM glycine (Fig. 6A) and showed pronounced voltage dependence. No comparable currents were obtained in water-injected oocytes (data not shown). The glycine-induced outward currents followed Michaelis-Menten kinetics as a function of substrate concentration (Fig. 6B), and the transformation of substrate-evoked currents according to Eadie-Hofstee revealed an apparent affinity ( $K_m$ ) of glycine outward transport of  $8.5 \pm 0.5$  mM at a membrane potential of  $-30$  mV. Therefore, PAT2 can transport glycine bidirectionally with the direction of transport determined by membrane potential and/or the substrate/proton gradients.

**Sarcosine Inhibition of Glycine Transport**—Sarcosine is a

2758

## Proton/Amino Acid Cotransporter PAT2 in Neurons

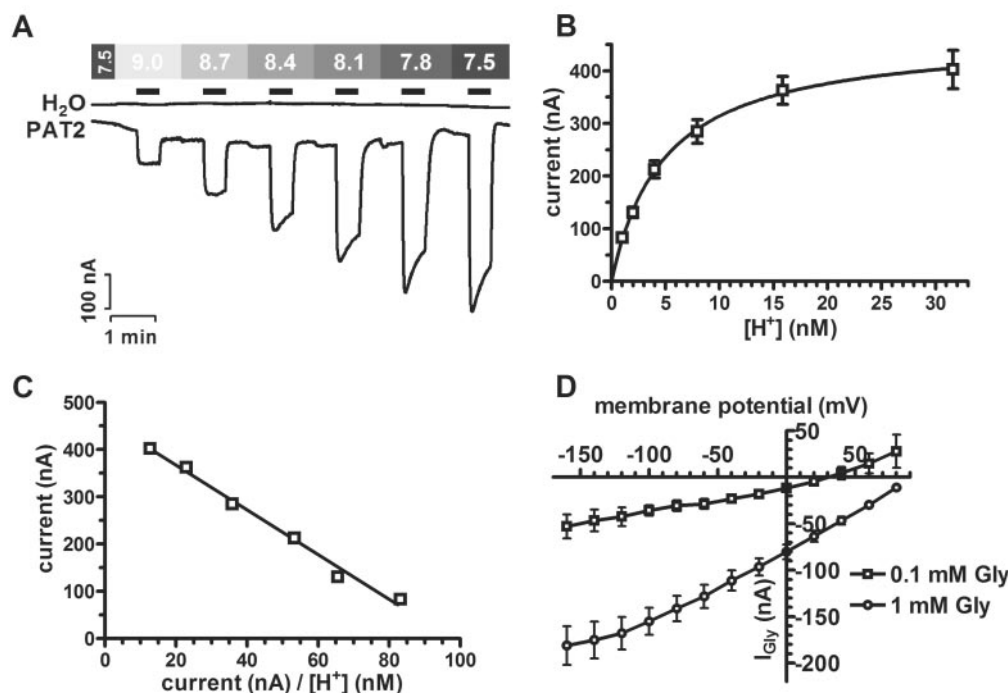


FIG. 5. **pH and membrane potential dependence of PAT2 activity.** *A*, oocytes injected with PAT2-cRNA or water clamped at  $-40$  mV were perfused with incubation buffers adjusted to different pH rankings from 9 to 7.5 in the presence of 10 mM glycine. *B*, saturation kinetics of mediated currents by 10 mM glycine in the function of proton concentration ( $n = 9$  oocytes) and the corresponding Eadie-Hofstee transformation (*C*). *D*,  $I$ - $V$  relationship of glycine-evoked inward currents ( $n = 4$  oocytes) at pH 6.5 and two different glycine concentrations, 0.1 and 1 mM.

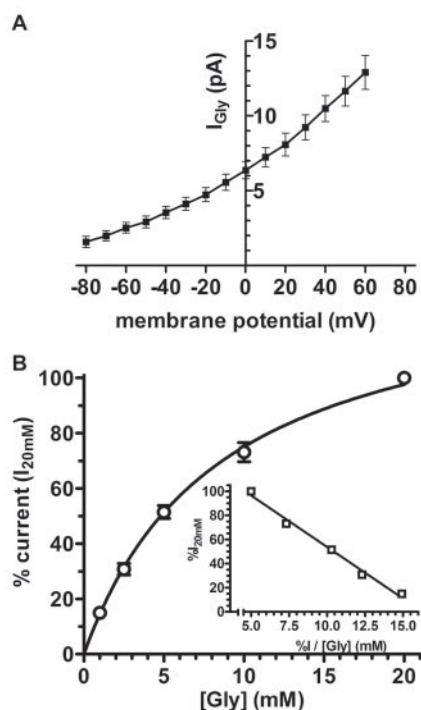


FIG. 6. **Characteristics of the PAT2 outward transport mode using the inside-out giant patch clamp technique.** *A*,  $I$ - $V$  relationship of glycine-evoked outward currents (20 mM) at pH 7.5 ( $n = 4$  oocytes). *B*, saturation kinetics of outward currents as a function of substrate concentrations and the corresponding Eadie-Hofstee transformation (*inset*).

known selective inhibitor of glycine transport in the brain (21, 22) and inhibits glycine influx mediated by the glycine transporter GLYT1 but not by the GLYT2 transporter. Here we

demonstrate that sarcosine is likewise able to inhibit glycine uptake mediated by PAT2. Flux studies performed with radio-labeled glycine in oocytes expressing PAT2 demonstrate that the uptake can be reduced by 10 mM sarcosine to almost the same extent as that obtained by 10 mM glycine as a competitor (Fig. 7A). In water-injected oocytes, no detectable uptake or inhibition was observed. Additionally, by using the TEVC technique we demonstrate that sarcosine induces inward currents that display saturation kinetics as a function of sarcosine concentration. The Eadie-Hofstee transformation of the substrate-evoked currents as a function of sarcosine concentration revealed an apparent  $K_m$  of  $208 \pm 2 \mu\text{M}$  and an  $I_{\text{max}}$  of  $130 \pm 4$  nA (Fig. 7B).

## DISCUSSION

All members of the mammalian subfamilies of the amino acid/auxin permease family are expressed in the nervous system, where they fulfill different physiological roles. Immunolocalization studies indicated the presence of VGAT in glycinergic, GABAergic, and mixed glycine and GABAergic synapses (4, 23). VGAT is responsible for the accumulation of the inhibitory neurotransmitters GABA and glycine in vesicles in presynaptic neurons. In the nervous system, the members of the system N/A subfamily show different cellular and subcellular expression patterns and are central for neurotransmission (14, 24, 25) by their role in the glutamate-glutamine cycle (14). SN1 is mainly responsible for the efflux of glutamine from the astrocytes, and the system A transporters 2 or 1 are responsible for its uptake into the neurons where it is converted to glutamate, allowing the recovery of glutamate to the presynaptic neurons. The proton/amino acid co-transporters PAT1 and PAT2 are present as well in the nervous system. PAT1 has been reported to be present in neurons of the hippocampus, cerebral cortex, cerebellum, and the thalamic and pontine nuclei (11, 19) with a more detailed cellular analysis reported recently (26). We demonstrate here by RT-PCR that the PAT2-mRNA is found in

## Proton/Amino Acid Cotransporter PAT2 in Neurons

2759

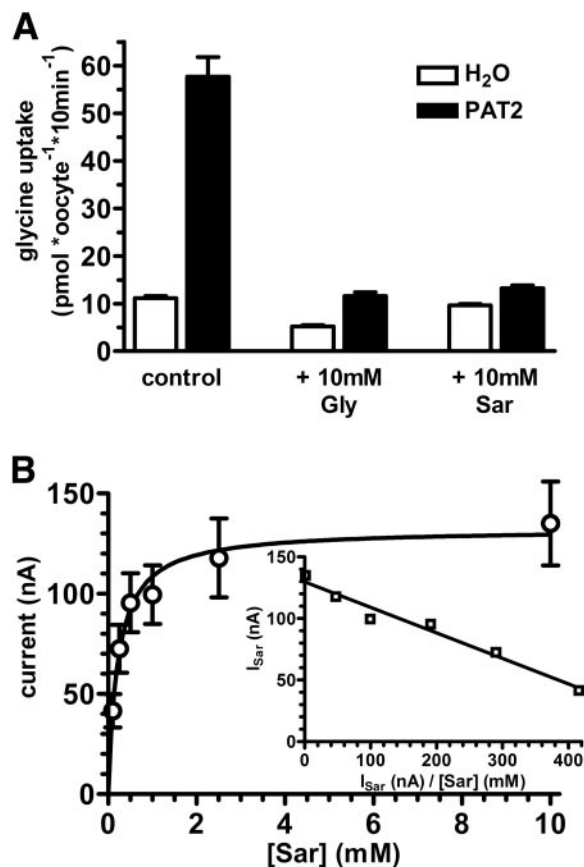


FIG. 7. Sarcosine (Sar) inhibits PAT2-mediated glycine transport. A, water and PAT2-cRNA-injected oocytes ( $n = 8$ ) were incubated with  $100 \mu\text{M}$   $^3\text{H}$ -glycine in the presence or absence of 10 mM sarcosine or 10 mM glycine. B, saturation kinetics of inward currents as a function of sarcosine concentrations at pH 6.5 and held at a membrane potential of  $-60 \text{ mV}$  ( $n = 5$  oocytes), and the corresponding Eadie-Hofstee plot (inset).

all brain regions analyzed. The PAT2 protein was identified with an apparent molecular mass of 55 kDa and localized by immunodetection studies in spinal cord, brain stem, cerebellum, hippocampus, hypothalamus, rhinencephalon, cerebral cortex, and the olfactory bulb. By colocalization with a glial marker protein in various brain regions, PAT2 was exclusively found in neurons similar to its orthologue PAT1.

It has been shown that PAT1 is expressed particularly in regions rich in glutamatergic neurons (11, 19, 26). Here, we show that the cell-specific expression pattern of PAT2 strongly resembles that of the NMDA receptor subunit NR1 (27, 28). The NR1 subunit forms, together with the different NR2 or NR3 subunits, the hetero-oligomeric NMDA subtype of ionotropic glutamate receptors. They serve critical functions in several processes in the central nervous system, including neuronal development, plasticity, and neurodegeneration (29). Receptor activation usually requires the two agonists glutamate and glycine (30). However, recently it has been shown that NMDA receptors comprised of the NR1 and NR3A/B subunits require solely glycine for activation (31). The observed overlapping cell type-specific expression pattern of PAT2 and NR1 suggests, but does not prove, a functional role of PAT2 in the excitatory glycinergic neurotransmission.

Although the transport mode and the general distribution pattern of the two PAT transporters are similar, there are marked differences in their subcellular localization and functional characteristics. PAT1 has broader substrate specificity than PAT2 and can, in addition to small amino acids, also transport GABA and other amino acid derivatives (11, 12, 17).

PAT2, in contrast, is restricted to alanine, glycine, and proline, but has much higher substrate affinities than PAT1 ( $\mu\text{M}$  versus mM). PAT1 and PAT2 also differ in their subcellular localization. PAT1 was shown to be localized in the lysosomes and, to a small extent, in the plasma membrane of neurons (11, 19), and a recent report demonstrated that PAT2 is not present in lysosomes in teased fibers (32). When PAT2 is expressed in HeLa cells, the protein is localized in the plasma membrane and intracellular compartments but not in lysosomes (12). Here we show that, within the cell, PAT2 is present in the endoplasmic reticulum and in recycling endosomes. PAT2, as a high affinity/low capacity system, may therefore play a role in the export of amino acids from the endosomes to the cytoplasm, whereas PAT1, as the low affinity/high capacity system, may serve for lysosomal export of amino acids derived from protein breakdown. Both transporters act as rheogenic  $\text{H}^+$ -coupled symporters and, therefore, changes in the extracellular pH alter their function. PAT1 activity is strongly pH-dependent, and its maximal transport rate is reached at an external pH of 5.5–6. Here we show that PAT2 operates with full activity at physiological pH ( $\leq 7.5$ ), and its activity declines when external pH becomes alkaline. Both transporters therefore show maximal transport rates at pH conditions characteristic for those in recycling endosomes (around pH 6.7) and lysosomes ( $\sim 5.5$ ).

With its presence in recycling endosomes, PAT2 may also, on occasion, reach the plasma membrane where it could serve as an import or export system for glycine or the other amino acids. Previous studies on the kinetics of glycine transport in the rat central nervous system already suggest the existence of a low and a high affinity transport system for glycine with apparent  $K_m$  values of  $\sim 800$  and  $26 \mu\text{M}$ , respectively (33). The two cloned glycine transport systems, GLYT1 and GLYT2, are considered to represent the molecular entities of the high affinity glycine transport pathway (21, 22, 34–36), whereas the low affinity glycine transport system, shown to be sodium independent (37), is not yet known. By its apparent affinity of  $590 \pm 4 \mu\text{M}$  for glycine (12), it may be speculated that PAT2 represents that low affinity glycine transport mechanism. In addition, glycine transport in brain is inhibited by sarcosine. Whereas the GLYT1 transporter displays a  $\text{IC}_{50}$  value of around  $100 \mu\text{M}$  for sarcosine inhibition of glycine influx and sarcosine transport (38), PAT2 likewise transports sarcosine with an apparent substrate of  $208 \mu\text{M}$  and shows glycine transport inhibition in the presence of sarcosine. As demonstrated by heterologous expression in oocytes, PAT2 activity is affected by membrane potential, and hyperpolarization increases glycine-evoked currents. In inhibitory synapses, this could have a physiological role by enhancing glycine transport via PAT2 after membrane hyperpolarization induced by activation of the glycine receptor. We also demonstrate another feature of PAT2, and this is its ability for bidirectional glycine transport. A depolarization of the plasma membrane results in an increased outward current when glycine is provided on the cytosolic side. Although the apparent affinity of glycine for binding to the internal substrate binding domain is lower than that on the outside, a glycine efflux via PAT2 could occur when intracellular glycine concentrations rise. In glutamatergic neurons, the coactivation of the NMDA receptors by glycine induces a depolarization of the neuronal membrane that could initiate a reversed glycine transport by PAT2. This non-vesicular release could then contribute to a sustained glycine signal, as proposed for selected synapses (39). This would be of importance for some glycinergic nerve terminals that failed to show the presence of VGAT. Transmembrane concentration gradients of its substrates and membrane potential finally determine the direction and velocity of amino acid transport mediated by PAT2.

2760

## Proton/Amino Acid Cotransporter PAT2 in Neurons

In conclusion, PAT2 is present in the nervous system where it, together with PAT1, may contribute to the handling of amino acids such as glycine, alanine, and proline in the endosomal/lysosomal system, but possibly also in the plasma membrane. At present, we cannot answer the question of whether PAT2-mediated transport of its specific amino acid substrates is of physiological importance in the mammalian brain, but PAT2 is a candidate protein for a still missing low affinity-type glycine transporter in the central nervous system. Together with GLYT1 and GLYT2, PAT2 could be responsible for the regulation of intracellular and extracellular concentrations of glycine that modulate glycine and glutamatergic neurotransmission.

**Acknowledgment**—We thank B. Giros for providing the anti-LYAAT1 antibody.

## REFERENCES

- Saier, M. H., Jr. (2000) *Microbiology* **146**, 1775–1795
- Young, G. B., Jack, D. L., Smith, D. W., and Saier, M. H., Jr. (1999) *Biochim. Biophys. Acta* **1415**, 306–322
- Boll, M., Foltz, M., Rubio-Aliaga, I., and Daniel, H. (2003) *Genomics* **82**, 47–56
- McIntire, S. H., Reimer, R. J., Schuske, K., Edwards, R. H., and Jorgensen, E. M. (1997) *Nature* **389**, 870–876
- Sagne, C., El Mestikawy, S., Isambert, M. F., Hamon, M., Henry, J. P., Giros, B., and Gasnier, B. (1997) *FEBS Lett.* **417**, 177–183
- Varoqui, H., Zhu, H., Yao, D., Ming, H., and Erickson, J. D. (2000) *J. Biol. Chem.* **275**, 4049–4054
- Sugawara, M., Nakanishi, T., Fei, Y. J., Huang, W., Ganapathy, M. E., Leibach, F. H., and Ganapathy, V. (2000) *J. Biol. Chem.* **275**, 16473–16477
- Sugawara, M., Nakanishi, T., Fei, Y. J., Martindale, R. G., Ganapathy, M. E., Leibach, F. H., and Ganapathy, V. (2000) *Biochim. Biophys. Acta*, **1509**, 7–13
- Chaudhry, F. A., Reimer, R. J., Krizaj, D., Barber, D., Storm-Mathisen, J., Copenhagen, D. R., and Edwards, R. H. (1999) *Cell* **99**, 769–780
- Nakanishi, T., Sugawara, M., Huang, W., Martindale, R. G., Leibach, F. H., Ganapathy, M. E., Prasad, P. D., and Ganapathy, V. (2001) *Biochem. Biophys. Res. Commun.* **281**, 1343–1348
- Sagne, C., Agulhon, C., Ravassard, P., Darmon, M., Hamon, M., El Mestikawy, S., Gasnier, B., and Giros, B. (2001) *Proc. Natl. Acad. Sci. U. S. A.* **98**, 7206–7211
- Boll, M., Foltz, M., Rubio-Aliaga, I., Kottra, G., and Daniel, H. (2002) *J. Biol. Chem.* **277**, 22966–22973
- Nakanishi, T., Kekuda, R., Fei, Y. J., Hatanaka, T., Sugawara, M., Martindale, R. G., Leibach, F. H., Prasad, P. D., and Ganapathy, V. (2001) *Am. J. Physiol.* **281**, C1757–C1768
- Chaudhry, F. A., Reimer, R. J., and Edwards, R. H. (2002) *J. Cell Biol.* **157**, 349–355
- Chaudhry, F. A., Schmitz, D., Reimer, R. J., Larsson, P., Gray, A. T., Nicoll, R., Kavanaugh, M., and Edwards, R. H. (2002) *J. Neurosci.* **22**, 62–72
- Boll, M., Daniel, H., and Gasnier, B. (2004) *Pflügers Arch.* DOI: 10.1007/s00424-003-1073-4
- Boll, M., Foltz, M., Anderson, C. M. H., Oechsler, C., Kottra, G., Thwaites, D. T., and Daniel, H. (2003) *Mol. Membr. Biol.* **20**, 261–269
- Chen, Z., Fei, Y.-J., Anderson, C. M. H., Wake, K. A., Miyauchi, S., Huang, W., Thwaites, D. T., and Ganapathy, V. (2003) *J. Physiol.* **546**, 349–361
- Wreden, C. C., Johnson, J., Tran, C., Seal, R. P., Copenhagen, D. R., Reimer, R. J., and Edwards, R. H. (2003) *J. Neurosci.* **23**, 1265–1275
- Kottra, G., and Daniel, H. (2001) *J. Physiol.* **536**, 495–503
- Smith, K. E., Borden, L. A., Hartig, P. R., Branchek, T., and Weinshank, R. L. (1992) *Neuron* **8**, 927–935
- Liu, Q. R., Lopez-Corcuera, B., Mandiyan, S., Nelson, H., and Nelson, N. (1993) *J. Biol. Chem.* **268**, 22802–22808
- Dumolin, A., Rostaing, P., Bedet, C., Levi, S., Isambert, M. F., Henry, J. P., Triller, A., and Gasnier, B. (1999) *J. Cell Sci.* **112**, 22802–22808
- Reimer, R. J., Chaudhry, F. A., Gray, A. T., and Edwards, R. H. (2000) *Proc. Natl. Acad. Sci. U. S. A.* **97**, 7715–7720
- Armano, S., Coco, S., Bacci, A., Pravettoni, E., Schenk, U., Verderio, C., Varoqui, H., Erickson, J. D., and Matteoli, M. (2002) *J. Biol. Chem.* **277**, 10467–10473
- Agulhon, C., Rostaing, P., Ravassard, P., Sagne, C., Triller, A., and Giros, B. (2003) *J. Comp. Neurol.* **462**, 71–89
- Petralia, R. S., Yokotani, N., and Wenthold, R. J. (1994) *J. Neurosci.* **14**, 667–696
- Moriyoshi, K., Masu, M., Ishii, T., Shigemoto, R., Mizuno, N., and Nakanishi, S. (1991) *Nature* **354**, 31–37
- Cull-Candy, S., Brickley, S., and Farrant, M. (2001) *Curr. Opin. Neurobiol.* **11**, 327–335
- Monyer, H., Sprengel, R., Schoepfer, R., Herb, A., Higuchi, M., Lomeli, H., Burnashev, N., Sakmann, B., and Seeburg, P. H. (1992) *Science* **256**, 1217–1221
- Chatterton, J. E., Awobuluyi, M., Premkumar, L. S., Takahashi, H., Talantova, M., Shin, Y., Cui, J., Tu, S., Sevarino, K. A., Nakanishi, N., Tong, G., Lipton, S. A., and Zhang, D. (2002) *Nature* **415**, 793–798
- Birmingham, J. R., Jr., Shumas, S., Whisenhunt, T., Sirkowski, E. E., O'Connell, S., Scherer, S. S., and Rosenfeld, M. G. (2002) *J. Neurosci.* **22**, 10217–10231
- Logan, W. J., and Snyder, S. H. (1971) *Nature* **234**, 297–299
- Guastella, J., Brecha, N., Weigmann, C., Lester, H. A., and Davison, N. (1992) *Proc. Natl. Acad. Sci. U. S. A.* **89**, 7189–7193
- Liu, Q. R., Nelson, H., Mandiyan, S., Lopez-Corcuera, B., and Nelson, N. (1992) *FEBS Lett.* **305**, 110–114
- Zafra, F., Aragon, C., Olivares, L., Danbolt, N. C., Gimenez, C., and Storm-Mathisen, J. (1995) *J. Neurosci.* **15**, 3952–3969
- Bennett, J. P., Jr., Logan, W. J., and Snyder, S. H. (1972) *Science* **178**, 997–999
- Supplisson, S., and Bergman, C. (1997) *J. Neurosci.* **17**, 4580–4590
- Attwell, D., and Bergman, C. (1993) *Neuron* **11**, 401–407

## **APPENDIX 5**

published in *The FASEB Journal*

*The FASEB Journal* express article 10.1096/fj.03-1387fje. Published online September 2, 2004.

## **A novel bifunctionality: PAT1 and PAT2 mediate electrogenic proton/amino acid and electroneutral proton/fatty acid symport**

Martin Foltz, Michael Boll, Ladislav Raschka, Gabor Kottra, and Hannelore Daniel

Molecular Nutrition Unit, Institute of Nutritional Sciences, Technical University of Munich, D-85350 Freising-Weihenstephan, Germany

Corresponding author: Dr. Hannelore Daniel, Center of Life and Food Sciences, Technical University of Munich, Hochfeldweg 2, D-85350 Freising-Weihenstephan, Germany. E-mail: daniel@wzw.tum.de

### **ABSTRACT**

Recently, the PAT family of proton-dependent amino acid transporters has been identified as a novel class of mammalian amino acid symporters. PAT1 and PAT2 members mediate electrogenic uptake of small, neutral amino acids and derivatives by cotransport of protons. Analysis of the structural requirements for substrate recognition by PAT1 identified that a free amino group in a substrate is not essential for recognition. We therefore hypothesized that PAT1 and its ortholog PAT2 may also be able to recognize and transport the homologous short-chain fatty acids (SCFAs) such as acetate, propionate, and butyrate. We examined in *Xenopus laevis* oocytes whether the SCFAs interact with the transporter by employing flux studies, electrophysiology and intracellular pH recordings. SCFAs did not induce positive inward currents but inhibited glycine-induced transport currents. PAT-mediated uptake of radiolabeled proline was also dose-dependently reduced by SCFA and could be described by first order competition kinetics with apparent  $K_i$ -values for butyrate of  $6.0 \pm 0.7$  and  $7.6 \pm 1.3$  mM for PAT1 and PAT2, respectively. Acetate as well as propionate uptake was significantly enhanced in oocytes expressing PAT1 or PAT2. An electroneutral  $H^+$ /SCFA symport mode was demonstrated by recording intracellular pH changes under voltage clamp conditions with rate constants for the initial intracellular acidification in the presence of SCFAs significantly increased in PAT-expressing oocytes. In conclusion, our data demonstrate that the PAT1 and PAT2 proteins are capable to transport selected SCFAs in an electroneutral and the homologous amino acids in an electrogenic mode and are therefore a paradigm for bifunctional solute carriers.

Key words: *Xenopus laevis* oocytes • SCFA • proton symporter • ph-recording

**A**mino acid transport across the plasma membrane is mediated by multiple transport proteins, which are distinguished primarily by substrate selectivity and ionic dependence (1, 2). Beside numerous ion-independent amino acid transport systems that predominantly operate as obligatory exchangers, rheogenic transporters are mainly sodium-dependent symporters (3). Only very recently proton-driven amino acid transporter proteins have been found in plasma membranes of specialized mammalian cells (4, 5). Although functionally

described in apical plasma membranes of mammalian epithelial cells (6–10) and in the human intestinal cell line Caco-2 (11–14), the molecular structure of the underlying protein entities was not known.

By means of homology based cloning, a family of proton-dependent amino acid transporters, designated as PAT1 and LYAAT (proton/amino acid transporter; lysosomal amino acid transporter), was identified and characterized at the molecular level (15–18). The PAT family comprises four members, PAT1 to PAT4, of which only the first two members, PAT1/LYAAT-1 and PAT2, have been shown experimentally to mediate proton-coupled symport of amino acids with a high selectivity for amino acids with small and apolar side chains (19). PAT1 was shown to transport glycine, L-alanine, and L-proline as well as D-serine and the neurotransmitter  $\gamma$ -aminobutyrate (GABA) (15, 17–20), whereas PAT2 recognizes in addition to small L- $\alpha$ -amino acids also D-proline (15, 16, 21). Both transporters possess a 1:1 flux coupling stoichiometry for proline transport. Substrate affinities range from around 2.8 to 7.5 mM (PAT1) and 0.1 to 0.7 mM (PAT2) for the same substrates (15, 22). The cloning of the human PAT1-cDNA from the Caco-2 cell line and the immunolocalization of the PAT1-protein in the apical membrane of Caco-2 cells proved that PAT1 represents the molecular entity of the described previously PAT system (17). The murine isoform PAT1 is expressed in a variety of tissues and shows highest expression levels in small intestine, kidney and in both proximal and distal colon (15, 17). PAT1 is also strongly expressed in brain and was found there in lysosomes and the plasma membrane of neurons in several regions of the brain (18, 22, 23). The expression pattern of PAT2 differs from that of PAT1. High expression levels are found in lung and heart; weaker signals are detected in kidney, testis, and muscle (15). Immunodetection studies revealed that PAT2 is expressed in spinal cord and brain where it is abundantly found in neuronal cell bodies of *N*-methyl-D-aspartate receptor subunit NR1 positive neurons (21). Subcellular localization studies revealed that the PAT2 protein is targeted to the plasma membrane of *X. laevis* oocytes, and with the use of brain slices, it has been demonstrated that endogenous PAT2 localizes, at least in part, to the plasma membrane of neurons (21).

We have recently analyzed the structural requirements in substrates in terms of variability of the side chain, backbone length and the role of the terminal head groups for interaction with the cloned murine PAT1-protein (20). A remarkable characteristic of PAT1 is the discrimination of substrates by the size of the side chain and by the charge separation distance within the backbone. In L-amino acids, a maximum of one CH<sub>2</sub>-unit in the side chain is accepted. Beside L- $\alpha$ -amino acids, PAT1 also tolerates  $\omega$ -amino acids with a maximal distance of two CH<sub>2</sub>-units between amino and carboxy group, represented by GABA as a high-affinity substrate of PAT1. Methylation of the carboxy group reduces transport capability whereas a methylation of the amino group has only a minor effect on affinity and transport capacity (20). This mainly applies also to PAT2. Therefore, a free amino group in a substrate is not essential for substrate recognition by PAT1 and PAT2. We consequently asked whether PAT1 and/or PAT2 are able to recognize also short-chain fatty acids (SCFAs) such as acetate, propionate, and butyrate as substrates. SCFAs are abundant organic anions and serve as energy substrates and particularly the colonic mucosa utilizes them (24, 25). Moreover, butyrate is an important modulator of gene expression and cell cycle control (26–29). We examined the interaction of SCFAs with the PAT1 and PAT2 proteins using flux studies, electrophysiology, and intracellular pH measurements in *X. laevis* oocytes expressing either PAT1 or PAT2 and demonstrate a novel bifunctional transport mode for these two symporters.

## METHODS

### Materials

Female *X. laevis* frogs were purchased from Nasco (Fort Atkinson, WI). Amino acids and related compounds were obtained from Sigma Chemie (Deisenhofen, Germany) or Merck (Darmstadt, Germany) in p.a. quality. Tritium-labeled compounds ([ $3\text{-}^3\text{H}$ ]glycine, specific activity 56,4 Ci/mmol; L-[ $3,4\text{-}^3\text{H}$ ]proline, 40 Ci/mmol; [ $^3\text{H}$ ]acetate, 150 mCi/mmol; [ $1\text{-}^{14}\text{C}$ ]propionic acid, 60 mCi/mmol) were purchased by ICN (Irvine, CA) or Biotrend (Cologne, Germany). Collagenase A was obtained from Roche Molecular Biochemicals (Mannheim, Germany).

### Amino acid and SCFA uptake experiments

*X. laevis* oocytes handling and cRNA injection have been described previously (15). Oocytes were injected with 10 nl sterile water (control), 10 nl murine PAT1-cRNA (5 ng), 10 nl murine PAT2-cRNA (20 ng), and 10 nl rabbit PEPT1-cRNA (15 ng), respectively. The oocytes were kept in modified Barth solution (88 mM NaCl, 1 mM KCl, 0.8 mM  $\text{MgSO}_4$ , 0.4 mM  $\text{CaCl}_2$ , 0.3 mM  $\text{Ca}(\text{NO}_3)_2$ , 2.4 mM  $\text{NaHCO}_3$ , and 10 mM HEPES, pH 7.5) at 18°C until further use (3-5 days after injection).

Ten oocytes (water- or cRNA-injected) per uptake experiment were preincubated at room temperature for 2 min in standard uptake buffer solution (100 mM sodium chloride, 2 mM KCl, 1 mM  $\text{MgCl}_2$ , 1 mM  $\text{CaCl}_2$ , 10 mM MESpH 5.5). The buffer solution was then replaced by the respective uptake buffer solution supplemented with 100  $\mu\text{M}$  amino acid or SCFA and the corresponding L-[ $^3\text{H}$ ]amino acid or [ $^3\text{H}$ ]acetate or [ $^{14}\text{C}$ ]propionate as a tracer (10  $\mu\text{Ci/ml}$ ). After 5 min (acetate and propionate uptake), or 10 min incubation (amino acid uptake) the oocytes were washed three times with 3 ml of ice cold wash buffer solution (standard uptake buffer solution) and distributed to individual vials. After oocyte lysis in 10% SDS, radioactivity was counted by liquid scintillation. Kinetics of inhibition of amino acid uptake by SCFAs were constructed from experiments employing six different inhibitor concentrations in standard uptake buffer solution at pH 5.5 with 10 oocytes expressing mPAT1 or mPAT2 from at least two different oocyte batches. The osmolarity in all buffer solutions was adjusted by replacement of mannitol. PAT-specific uptake rates were obtained after subtraction of baseline uptake rates in water-injected control oocytes.

### Two electrode voltage clamp experiments

Two-electrode voltage clamp experiments were performed as described previously (30). Oocytes were placed in an open chamber, voltage clamped at -40 mV, and continuously superfused with standard perfusion buffer (100 mM sodium chloride, 2 mM KCl, 1 mM  $\text{MgCl}_2$ , 1 mM  $\text{CaCl}_2$ , 10 mM MES, or HEPES at pH 5.5) in the absence or presence of amino acids. Current traces were recorded during voltage clamping and substrates were perfused at concentrations of 20 mM for 20 s. Kinetics of inhibition of amino acid induced currents by SCFAs were constructed from experiments employing seven different concentrations in sodium-containing buffer solution at pH 5.5 with eight individual oocytes expressing PAT1 from at least two different oocyte batches. The osmolarity in all buffer solutions was adjusted by replacement of mannitol.

## Intracellular pH recordings in *X. laevis* oocytes

Intracellular pH recordings were performed as described previously (20). We only used pH microelectrodes with slopes of 57–59 mV/pH unit and a very rapid response time. Initial acidification rates in response to perfusion with different substrates were determined in the same oocyte. Acidification was always linear in a time range of 10–30 s after substrate application and the slope of the initial acidification was calculated by linear regression of the data obtained in this time range. To exclude variations in acidification rates by different functional expression levels of the PAT1 transporter in different oocytes, a complete set of substrates (acetate, propionate, butyrate and glycine) was always measured in the same oocyte and only those oocytes were chosen that showed similar glycine induced charge movements.

## Calculations and statistics

All data are means  $\pm$  SE of at least two independent experiments with  $n = 8$ –10 oocytes per data point. Significant differences in data were calculated using paired or unpaired two-tailed Student's  $t$  test or ANOVA (using the Bonferroni multiple comparisons post-test). Apparent  $K_i$ -values were determined from  $IC_{50}$  values based on competition curves and by the least-squares method. All calculations were performed using Prism software (GraphPad, San Diego, CA).

## RESULTS

### Interaction of SCFAs with the substrate binding side of the proton/amino acid cotransporters PAT1 and PAT2

Glycine, a prototype substrate of PAT1 evoked high inward currents in PAT1 expressing oocytes, whereas neither the monoamine propylamine nor the monocarboxylate propionate caused any inward currents at concentrations as high as 20 mM and at a pH of 5.5 (Fig. 1A). Similar data were obtained in oocytes expressing PAT2 (not shown). Whereas transport currents of 0.5 mM glycine also remained unaffected by coperfusion with 10 mM propylamine, 10 mM propionate reduced glycine currents to  $35.0 \pm 4.7\%$  of control values (Fig. 1B and C). Similar to propionate, neither acetate nor butyrate alone did induce any measurable currents by PAT1 (Fig. 2A) or PAT2 (Fig. 2B). However, all three SCFAs reduced glycine currents by PAT1 when provided in an 20-fold excess to  $56.5 \pm 8.6\%$  (acetate),  $32.9 \pm 1.6$  (propionate) or  $21.2 \pm 1.9\%$  (butyrate) as shown in Fig. 2C. Fatty acid induced inhibition on glycine currents was also observed in the presence of pentanoate and hexanoate with  $35.5 \pm 2.0\%$  and  $41.3 \pm 5.2\%$  of residual glycine currents, respectively. However, a further increase in the carbon chain length to octanoic acid resulted in a weak inhibition ( $81.2 \pm 6.1\%$ ). When the PAT2 protein was expressed in *X. laevis* oocytes, glycine (1 mM) elicited currents of  $411 \text{ nA} \pm 30 \text{ nA}$  and those were reduced by 20 mM acetate to  $23.1 \pm 1.6\%$  and by propionate to  $26.7 \pm 4.0\%$  of control values, respectively. In contrast to those SCFA, neither lactate nor pyruvate reduced glycine currents; they even increased slightly to  $120.7 \pm 7.5$  and  $114.7 \pm 4.6\%$  of control values (Fig. 2C). This finding strongly suggests that the introduction of a polar residue into the aliphatic chain in SCFA prevents any interaction of the fatty acids with the transporters binding site whereas fatty acids with a carbon chain length up to six carbons are effective competitors.

Since the SCFA by pH-partition and nonionic diffusion of the nonionized species could cause a decline in intracellular pH and in turn by reducing transmembrane  $\Delta\text{pH}$  reduce the driving force for proton-dependent glycine symport, we assessed whether the SCFA also modify transport of the di- and tripeptide transporter PEPT1 protein that is also an electrogenic proton-dependent symporter with similar transport characteristics. As shown in [Fig. 2D](#), PEPT1-mediated dipeptide currents at 1 mM substrate concentration were not affected significantly ( $P>0.05$ ) by the addition of 20 mM propionate with  $87.8 \pm 11.9\%$  ( $n=6$ ) of current remaining when compared with the control.

Inhibition studies with the tracer L- $^3\text{H}$ ]proline confirmed the inhibitory effect of SCFAs on amino acid transport of PAT1 and PAT2. Acetate, propionate, butyrate, pentanoate and hexanoate at concentrations of 20 mM, decreased PAT1 mediated uptake of radiolabeled proline to  $48 \pm 6$ ,  $47 \pm 9$ ,  $33 \pm 7$ ,  $33.1 \pm 5$ , and  $48 \pm 8\%$  of control values, respectively. Octanoate perfusion resulted in a weaker, but still significant ( $P<0.05$ ), decrease in proline uptake to  $69 \pm 8\%$  of that in controls. In contrast, lactate and pyruvate did not influence uptake of L-proline ([Fig. 3A](#)). PAT2-mediated L-proline influx was similarly reduced by acetate, propionate, and butyrate to  $37.8 \pm 2.7$ ,  $40.0 \pm 4.5$ , and  $26.0 \pm 2.5\%$  of control uptake ([Fig. 3B](#)). To demonstrate that the SCFAs inhibit in a concentration dependent manner, we determined the kinetics of L- $^3\text{H}$ ]proline uptake (100  $\mu\text{M}$ ) in the absence and the presence of increasing SCFA concentrations (0-50 mM) at pH 5.5. Inhibition by all three SCFAs followed typical first order competition kinetics. Proline uptake by PAT1 was inhibited by acetate, propionate and butyrate with apparent  $K_i$ -values of  $7.9 \pm 0.5$ ,  $12.0 \pm 1.6$ , and  $5.6 \pm 0.7$  mM, respectively ([Fig. 4A](#)). For PAT2, butyrate exhibited a  $K_i$ -value of  $7.6 \pm 1.3$  mM. Moreover, PAT1-mediated glycine currents also displayed a similar dose-dependent inhibition by propionate ([Fig. 4B](#), inset) under voltage clamp conditions with an apparent  $K_i$ -value of  $9.6 \pm 0.9$  mM ([Fig. 4B](#)). This apparent affinity is similar to that obtained in the tracer flux studies with proline. Taken together, these findings establish that SCFA such as acetate, butyrate, and propionate do specifically and in a concentration dependent manner interact with the substrate binding site of PAT1 and PAT2 without generating any inward currents themselves.

### Transport properties of radiolabeled SCFAs

To investigate whether the PAT-proteins do mediate SCFA transport into oocytes, uptake of 100  $\mu\text{M}$   $^3\text{H}$ ]acetate as well as  $^{14}\text{C}$ ]propionate was determined. Control oocytes possessed a very low intrinsic proline uptake capacity, but acetate and propionate were taken up at pH 5.5 at very high rates. Nevertheless, expression of PAT1 increased acetate and propionate influx to  $131 \pm 7$  ([Fig. 5A](#)) and  $127 \pm 3\%$  ([Fig. 5B](#)) of control, respectively. When the PAT2 protein was expressed in the oocytes acetate uptake was increased 2.3 fold ([Fig. 5A](#)) and propionate uptake 1.5 fold ([Fig. 5B](#)). In presence of 20 mM D-proline, PAT-specific acetate influx was almost completely inhibited to control values of  $148.7 \pm 6.1$  and  $176.1 \pm 12.4$  pmol/oocyte/5 min for PAT1 and PAT2, respectively ([Fig. 5A](#)). For PAT1 this value was not significantly ( $P>0.05$ ) different from that in control oocytes ( $144.8 \pm 5.1$  pmol/oocyte/5 min).

## Analysis of PAT1-mediated SCFA transport by combined voltage clamp and $\text{pH}_{\text{in}}$ measurements

Although PAT1 and PAT2 appear to transport acetate and propionate, TEVC studies show that this process is not electrogenic. The most plausible explanation would be a proton to substrate stoichiometry of 1:1 for the ionized species of the SCFA. To prove this assumption, we measured the corresponding changes in intracellular pH during SCFA transport under voltage clamp conditions. In response to acetate, propionate, and butyrate transport of SCFA by either PAT1 or PAT2 should cause a decline in  $\text{pH}_{\text{in}}$  larger than in water injected control oocytes in which acidification occurs either by nonionic diffusion or via an endogenous transporter. [Figure 6A](#) shows the changes in intracellular pH in comparison to current responses. SCFA did never cause an inward current but reduced significantly  $\text{pH}_{\text{in}}$ , whereas glycine induced a strong inward current in PAT1-expressing oocytes with a concomitant reduction in pH ([Fig. 6A](#)). Perfusion with SCFA caused always a higher intracellular acidification in oocytes expressing PAT1 than in control oocytes. [Figure 6B](#) and [Table 1](#) show the initial acidification rates induced by SCFA or by glycine in oocytes expressing PAT1 in comparison to control oocytes. The slopes of the PAT1-mediated decline in  $\text{pH}_{\text{in}}$  in response to SCFA perfusion were 2.5 times (propionate) and 2.8 times (butyrate) higher than those obtained in control oocytes. As expected, a glycine-induced decrease of intracellular pH was only observed in oocytes expressing PAT1 with an acidification rate of  $-0.013 \pm 0.002 \Delta\text{pH}/\text{sec}$ ; thus, it was very similar to that induced by butyrate. Furthermore, glycine induced charge movements (always measured as a control at the end of each experiment) correlated significantly with the acidification rates as measured for propionate, butyrate and glycine with  $r^2$  values of 0.869, 0.888, and 0.862, respectively. [Figure 6C](#) demonstrates that an increase in PAT1-mediated glycine transport activity resulted always in a concomitant increase in acidification rates for all of the tested SCFAs.

## DISCUSSION

The presence of proton/amino acid cotransport systems in the apical membranes of epithelial cells of rabbit renal tubules (6–10) or confluent monolayers of the epithelial cell line Caco-2 (12–14, 31) was shown functionally. Postcloning analysis of PAT1 suggests that this protein could be the responsible transporter for proton-dependent amino acid uptake in intestinal and renal cells. When expressed in *X. laevis* oocytes, PAT1 but also PAT2 mediate electrogenic proton-amino acid symport (15, 20) for small neutral amino acids. A further analysis of substrate recognition established that a free amino group is not an essential requirement for binding (20) and therefore we analyzed whether the PAT-transporters are able to transport the homologous SCFAs.

By electrophysiological analysis and uptake inhibition experiments with glycine and proline as substrates, we demonstrate that acetate, butyrate, and propionate are competing substrates for uptake by PAT1 and PAT2. Also pentanoate and hexanoate were found to inhibit PAT1 transport, whereas a further increase in chain length, as in octanoic acid reduced inhibition. Whether these medium chain fatty acids do serve as substrates is not known. However, this observation confirms our recent finding that  $\delta$ -amino-pentanoic acid is transported electrogenically via PAT1, whereas a further elongation of the amino acid backbone abolishes the interaction with the PAT1 transporter (20). We assume that the inhibition of PAT1-mediated amino acid transport by medium chain fatty acids results from their unrestricted conformation

that allows them to be accommodated within the substrate binding pocket easily. In contrast, lactate and pyruvate do not interfere with the substrate binding site of the PAT-carriers showing that only unsubstituted monocarboxylic acids are recognized. This is in accordance with the previous observation that amino acids with polar side chains are only recognized by PAT1 (20) with very low affinity. Using radiolabeled acetate and propionate, we show that expression of PAT1 and PAT2 in oocytes increases SCFA uptake and that this influx is inhibited by amino acids. However, electrophysiology failed to demonstrate any associated transport currents when SCFA are provided as substrates. Recordings of intracellular pH changes established that SCFA uptake is associated with proton influx under voltage clamp conditions which strongly suggests that SCFA-influx occurs by proton symport most likely by transport of the SCFA-anion with a proton by a 1:1 flux coupling stoichiometry as shown also for proline (15, 22). Initial rates of intracellular acidification by PAT1 caused by either butyrate or glycine uptake were similar whereas in case of propionate, acidification was twofold higher than with glycine. Similarly, acetate induced also twofold higher acidification rates (data not shown) than glycine. This suggests that the maximal transport rates by which PAT1 mediates propionate and acetate uptake are different from those obtained for glycine. Different maximal transport rates have also been observed for PAT1 with glycine and betaine despite very similar substrate affinities (20). The higher initial acidification rates in case of propionate and acetate are mirrored by higher uptake rates of the corresponding radiolabeled substrates. Whereas proline uptake reached ~5 pmol/oocyte/min, acetate and propionate uptake rates reached around 10 pmol/oocyte/min, within the linear phase.

Acetate, propionate, and butyrate showed concentration dependent inhibition and exhibited apparent  $K_i$ -values (5.6-12.0 mM) for PAT1 in the same range as the apparent  $K_m$  (1-10 mM) values determined for its amino acid substrates (15, 20). In comparison, PAT2 displays affinities in the range of 100-700  $\mu$ M for the amino acid substrates (glycine, alanine, proline) but butyrate displayed an affinity almost 13-fold lower than that of glycine. This is in conformity with the observation that PAT2 is more restrictive with regard to the structural requirements in substrates for high affinity recognition than is PAT1 (15).

Transmembrane transport of SCFAs is assumed to occur by different processes including nonionic diffusion, SCFA/anion-exchange and SCFA/proton symport. Permeation of the nonionized species of a SCFA occurs rapidly by the apolar character followed by fast intracellular dissociation (32, 33). Driving forces for this process are the transmembrane concentration gradient of the SCFA and the transmembrane pH-gradient. Although transmembrane SCFA-movement after pH partition is a general phenomenon, the quantitative importance of this process in comparison to carrier-mediated SCFA-uptake mechanisms is discussed controversial.

In particular in colonic tissues, various studies have assessed the transport mode for SCFA that are produced in huge quantities by bacterial fermentation and it is believed that SCFA transport here occurs via an anion/SCFA exchange mechanism. SCFA uptake into isolated proximal colonic membrane vesicles was increased in the presence of outwardly directed bicarbonate, butyrate, or propionate gradients (34–37) and Ussing chamber experiments also revealed that SCFAs are transported into the tissue via a bicarbonate/SCFA exchange mechanism (38). Besides anion exchange processes, also a proton/SCFA symport mechanism was proposed.

Studies in the intestinal epithelial cell line Caco-2 (39) and in isolated epithelial cells from rabbit proximal colon (40) provided evidence for such a proton/SCFA cotransport system.

Until recently, only two transporter proteins mediating uptake of SCFAs have been characterized at the molecular level, the monocarboxylate cotransporter MCT1 (SLC16A1) (41), and the newly identified sodium-coupled monocarboxylate transporter SMCT (SLC5A8) (42). MCT1 has been demonstrated to catalyze the proton-coupled transport of monocarboxylates such as lactate, pyruvate, acetate, propionate, and butyrate and ketone bodies (41). MCT1 is expressed in almost all tissues, inter alia in cecum, colon, and in kidney cortex (43). Whether MCT1 is localized in the apical or basolateral membrane of epithelial cells is still not clear (44), but it appears mainly to represent the basolateral form of the MCT series. The recently cloned SMCT transporters in contrast mediates  $\text{Na}^+$ -coupled SCFA uptake and is expressed at high levels in colonic tissue. It transports lactate, pyruvate, acetate, butyrate, and propionate by an electrogenic  $\text{Na}^+$ :SCFA cotransport mechanism (42).

With the data described here for PAT-mediated transport of the acetate, propionate, and butyrate, we add two new protein entities to the list of membrane carriers that can transport selected SCFA. The PAT1-mRNA is abundantly expressed with almost the same intensity along the gastrointestinal tract between stomach and descending colon, except in cecum (15, 17). Additionally, the PAT1-protein was recently shown to localize to the apical membrane of cells of the human colon cancer cell line Caco-2 (17). Besides ingestion of SCFA with the diet, acetate, propionate and butyrate are produced by microbial fermentation of nondigestible carbohydrates in colon and are present in the lumen in concentrations of 70-120 mM (45). Whether PAT1 in the intestinal tissues contributes to overall SCFA uptake into the organism is currently not known. SCFAs are metabolized by colonic epithelial cells as a prime energy source but portal blood of different species has concentrations of SCFAs in the range from 0.4 mM and 5.3 mM (45, 46) and SCFAs delivered to circulation serve also as metabolic fuel of the liver and other peripheral tissues (45, 47). PAT1- and also PAT2-mRNA expression is also fairly strong in liver, testis, muscle, brain, and heart (19), but their cellular and/or subcellular localization in these tissues is not known. Therefore, it appears to early to hypothesize that the PAT proteins do play a role in transport of SCFAs or that SCFA modulate PAT-mediated amino acid transport in these tissues and cell types.

In summary, we demonstrate that the mammalian PAT-proteins 1 and 2 are novel bifunctional proton-coupled symporters that operate in an electrogenic mode with amino acid substrates such as glycine, alanine, proline or GABA or in an electroneutral mode when the substrates lack an amino group. The demonstration of PAT-mediated proton/SCFA symport addresses a putative new function of these transporters in mammalian biology.

## ACKNOWLEDGMENTS

This work was supported by Grant BO 1857/1 from the Deutsche Forschungsgemeinschaft (to M. Boll). The costs of publication of this article were defrayed in part by the payment of page charges. The article must therefore be hereby marked "advertisement" in accordance with 18 U.S.C. Section 1734 solely to indicate this fact.

## REFERENCES

1. Palacin, M., Estevez, R., Bertran, J., and Zorzano, A. (1998) Molecular biology of mammalian plasma membrane amino acid transporters. *Physiol. Rev.* **78**, 969–1054
2. Malandro, M. S., and Kilberg, M. S. (1996) Molecular biology of mammalian amino acid transporters. *Annu. Rev. Biochem.* **65**, 305–336
3. Hediger, M. A., Kanai, Y., You, G., and Nussberger, S. (1995) Mammalian ion-coupled solute transporters. *J. Physiol.* **482**, 7S–17S
4. Boll, M., Daniel, H., and Gasnier, B. (2004) The SLC36 family: proton-coupled transporters for the absorption of selected amino acids from extracellular and intracellular proteolysis. *Pflugers Arch.* **447**, 776–779
5. Gasnier, B. (2004) The SLC32 transporter, a key protein for the synaptic release of inhibitory amino acids. *Pflugers Arch.* **447**, 756–759
6. Rajendran, V. M., Barry, J. A., Kleinman, J. G., and Ramaswamy, K. (1987) Proton gradient-dependent transport of glycine in rabbit renal brush-border membrane vesicles. *J. Biol. Chem.* **262**, 14974–14977
7. Jessen, H., Vorum, H., Jorgensen, K. E., and Sheikh, M. I. (1988) Characteristics of D-alanine transport by luminal membrane vesicles from pars convoluta and pars recta of rabbit proximal tubule. *Biochim. Biophys. Acta* **942**, 262–270
8. Jessen, H., Vorum, H., Jorgensen, K. E., and Sheikh, M. I. (1991) Na(+)- and H(+)-gradient-dependent transport of alpha-aminoisobutyrate by luminal membrane vesicles from rabbit proximal tubule. *J. Physiol.* **436**, 149–167
9. Roigaard-Petersen, H., Jacobsen, C., and Iqbal, S. M. (1987) H<sup>+</sup>-L-proline cotransport by vesicles from pars convoluta of rabbit proximal tubule. *Am. J. Physiol.* **253**, 15–20
10. Wunz, T. M., and Wright, S. H. (1993) Betaine transport in rabbit renal brush-border membrane vesicles. *Am. J. Physiol.* **264**, F948–F955
11. Thwaites, D. T., McEwan, G. T., Cook, M. J., Hirst, B. H., and Simmons, N. L. (1993) H<sup>+</sup>-coupled (Na<sup>+</sup>-independent) proline transport in human intestinal (Caco-2) epithelial cell monolayers. *FEBS Lett.* **333**, 78–82
12. Thwaites, D. T., McEwan, G. T., Brown, C. D., Hirst, B. H., and Simmons, N. L. (1994) L-alanine absorption in human intestinal Caco-2 cells driven by the proton electrochemical gradient. *J. Membr. Biol.* **140**, 143–151
13. Thwaites, D. T., McEwan, G. T., and Simmons, N. L. (1995) The role of the proton electrochemical gradient in the transepithelial absorption of amino acids by human intestinal Caco-2 cell monolayers. *J. Membr. Biol.* **145**, 245–256

14. Thwaites, D. T., Armstrong, G., Hirst, B. H., and Simmons, N. L. (1995) D-cycloserine transport in human intestinal epithelial (Caco-2) cells: mediation by a H(+)-coupled amino acid transporter. *Br. J. Pharmacol.* **115**, 761–766
15. Boll, M., Foltz, M., Rubio-Aliaga, I., Kottra, G., and Daniel, H. (2002) Functional characterization of two novel mammalian electrogenic proton-dependent amino acid cotransporters. *J. Biol. Chem.* **277**, 22966–22973
16. Chen, Z., Kennedy, D. J., Wake, K. A., Zhuang, L., Ganapathy, V., and Thwaites, D. T. (2003) Structure, tissue expression pattern, and function of the amino acid transporter rat PAT2. *Biochem. Biophys. Res. Commun.* **304**, 747–754
17. Chen, Z., Fei, Y. J., Anderson, C. M., Wake, K. A., Miyauchi, S., Huang, W., Thwaites, D. T., and Ganapathy, V. (2003) Structure, function and immunolocalization of a proton-coupled amino acid transporter (hPAT1) in the human intestinal cell line Caco-2. *J. Physiol.* **546**, 349–361
18. Sagne, C., Agulhon, C., Ravassard, P., Darmon, M., Hamon, M., El Mestikawy, S., Gasnier, B., and Giros, B. (2001) Identification and characterization of a lysosomal transporter for small neutral amino acids. *Proc. Natl. Acad. Sci. USA* **98**, 7206–7211
19. Boll, M., Foltz, M., Rubio-Aliaga, I., and Daniel, H. (2003) A cluster of proton/amino acid transporter genes in the human and mouse genomes. *Genomics* **82**, 47–56
20. Boll, M., Foltz, M., Anderson, C. M., Oechsler, C., Kottra, G., Thwaites, D. T., and Daniel, H. (2003) Substrate recognition by the mammalian proton-dependent amino acid transporter PAT1. *Mol. Membr. Biol.* **20**, 261–269
21. Rubio-Aliaga, I.; Boll, M.; D.M.; Foltz, M.; Kottra, G.; and Daniel, H. (2004) The proton/amino acid cotransporter PAT2 is expressed in neurons with a different subcellular localization than its paralog PAT1. *J. Biol. Chem.* **279**, 2754–2760
22. Wreden, C. C., Johnson, J., Tran, C., Seal, R. P., Copenhagen, D. R., Reimer, R. J., and Edwards, R. H. (2003) The H<sup>+</sup>-coupled electrogenic lysosomal amino acid transporter LYAAT1 localizes to the axon and plasma membrane of hippocampal neurons. *J. Neurosci.* **23**, 1265–1275
23. Agulhon, C., Rostaing, P., Ravassard, P., Sagne, C., Triller, A., and Giros, B. (2003) Lysosomal amino acid transporter LYAAT-1 in the rat central nervous system: an in situ hybridization and immunohistochemical study. *J. Comp. Neurol.* **462**, 71–89
24. Clausen, M. R., and Mortensen, P. B. (1994) Kinetic studies on the metabolism of short-chain fatty acids and glucose by isolated rat colonocytes. *Gastroenterology* **106**, 423–432
25. Cook, S.I. and Sellin, J.H. (1998) Review article: short chain fatty acids in health and disease. *Aliment. Pharmacol. Ther.* **12**, 499–507

26. Cavaglieri, C. R., Nishiyama, A., Fernandes, L. C., Curi, R., Miles, E. A., and Calder, P. C. (2003) Differential effects of short-chain fatty acids on proliferation and production of pro- and anti-inflammatory cytokines by cultured lymphocytes. *Life Sci.* **73**, 1683–1690
27. Massillon, D., Arinze, I. J., Xu, C., and Bone, F. (2003) Regulation of glucose-6-phosphatase gene expression in cultured hepatocytes and H4IIE cells by short-chain fatty acids: role of hepatic nuclear factor-4alpha. *J. Biol. Chem.* **278**, 40694–40701
28. Mortensen, F. V., Hesso, I., Birke, H., Korsgaard, N., and Nielsen, H. (1991) Microcirculatory and trophic effects of short chain fatty acids in the human rectum after Hartmann's procedure. *Br. J. Surg.* **78**, 1208–1211
29. Ogawa, H., Rafiee, P., Fisher, P. J., Johnson, N. A., Otterson, M. F., and Binion, D. G. (2003) Butyrate modulates gene and protein expression in human intestinal endothelial cells. *Biochem. Biophys. Res. Commun.* **309**, 512–519
30. Kottra, G., Stamford, A., and Daniel, H. (2002) PEPT1 as a paradigm for membrane carriers that mediate electrogenic bidirectional transport of anionic, cationic, and neutral substrates. *J. Biol. Chem.* **277**, 32683–32691
31. Thwaites, D. T., Basterfield, L., McCleave, P. M., Carter, S. M., and Simmons, N. L. (2000) Gamma-aminobutyric acid (GABA) transport across human intestinal epithelial (Caco-2) cell monolayers. *Br. J. Pharmacol.* **129**, 457–464
32. Charney, A. N., Micic, L., and Egnor, R. W. (1998) Nonionic diffusion of short-chain fatty acids across rat colon. *Am. J. Physiol.* **274**, 518–524
33. Ruppin, H., Bar-Meir, S., Soergel, K. H., Wood, C. M., and Schmitt, M. G. J. (1980) Absorption of short-chain fatty acids by the colon. *Gastroenterology* **78**, 1500–1507
34. Mascolo, N., Rajendran, V. M., and Binder, H. J. (1991) Mechanism of short-chain fatty acid uptake by apical membrane vesicles of rat distal colon. *Gastroenterology* **101**, 331–338
35. Reynolds, D. A., Rajendran, V. M., and Binder, H. J. (1993) Bicarbonate-stimulated [<sup>14</sup>C]butyrate uptake in basolateral membrane vesicles of rat distal colon. *Gastroenterology* **105**, 725–732
36. Ritzhaupt, A., Ellis, A., Hosie, K. B., and Shirazi-Beechey, S. P. (1998) The characterization of butyrate transport across pig and human colonic luminal membrane. *J. Physiol.* **507**, 819–830
37. Tyagi, S., Venugopalakrishnan, J., Ramaswamy, K., and Dudeja, P. K. (2002) Mechanism of n-butyrate uptake in the human proximal colonic basolateral membranes. *Am. J. Physiol. Gastrointest. Liver Physiol.* **282**, G676–G682
38. von Engelhardt, W., Gros, G., Burmester, M., Hansen, K., Becker, G., and Rechkemmer, G. (1994) Functional role of bicarbonate in propionate transport across guinea-pig isolated caecum and proximal colon. *J. Physiol.* **477**, 365–371

39. Stein, J., Zores, M., and Schroder, O. (2000) Short-chain fatty acid (SCFA) uptake into Caco-2 cells by a pH-dependent and carrier mediated transport mechanism. *Eur. J. Nutr.* **39**, 121–125
40. DeSoignie, R., and Sellin, J. H. (1994) Propionate-initiated changes in intracellular pH in rabbit colonocytes. *Gastroenterology* **107**, 347–356
41. Halestrap, A. P., and Meredith, D. (2004) The SLC16 gene family—from monocarboxylate transporters (MCTs) to aromatic amino acid transporters and beyond. *Pflugers Arch.* **447**, 619–628
42. Miyauchi, S., Gopal, E., Fei, Y. J., and Ganapathy, V. (2004) Functional Identification of SLC5A8, a Tumor Suppressor Down-regulated in Colon Cancer, as a Na<sup>+</sup>-coupled Transporter for Short-chain Fatty Acids. *J. Biol. Chem.* **279**, 13293–13296
43. Halestrap, A. P., and Price, N. T. (1999) The proton-linked monocarboxylate transporter (MCT) family: structure, function and regulation. *Biochem. J.* **343**, 281–299
44. Garcia, C. K., Brown, M. S., Pathak, R. K., and Goldstein, J. L. (1995) cDNA cloning of MCT2, a second monocarboxylate transporter expressed in different cells than MCT1. *J. Biol. Chem.* **270**, 1843–1849
45. Bergman, E. N. (1990) Energy contributions of volatile fatty acids from the gastrointestinal tract in various species. *Physiol. Rev.* **70**, 567–590
46. Pomare, E. W., Branch, W. J., and Cummings, J. H. (1985) Carbohydrate fermentation in the human colon and its relation to acetate concentrations in venous blood. *J. Clin. Invest.* **75**, 1448–1454
47. Remesy, C., Demigne, C., and Chartier, F. (1980) Origin and utilization of volatile fatty acids in the rat. *Reprod. Nutr. Dev.* **20**, 1339–1349

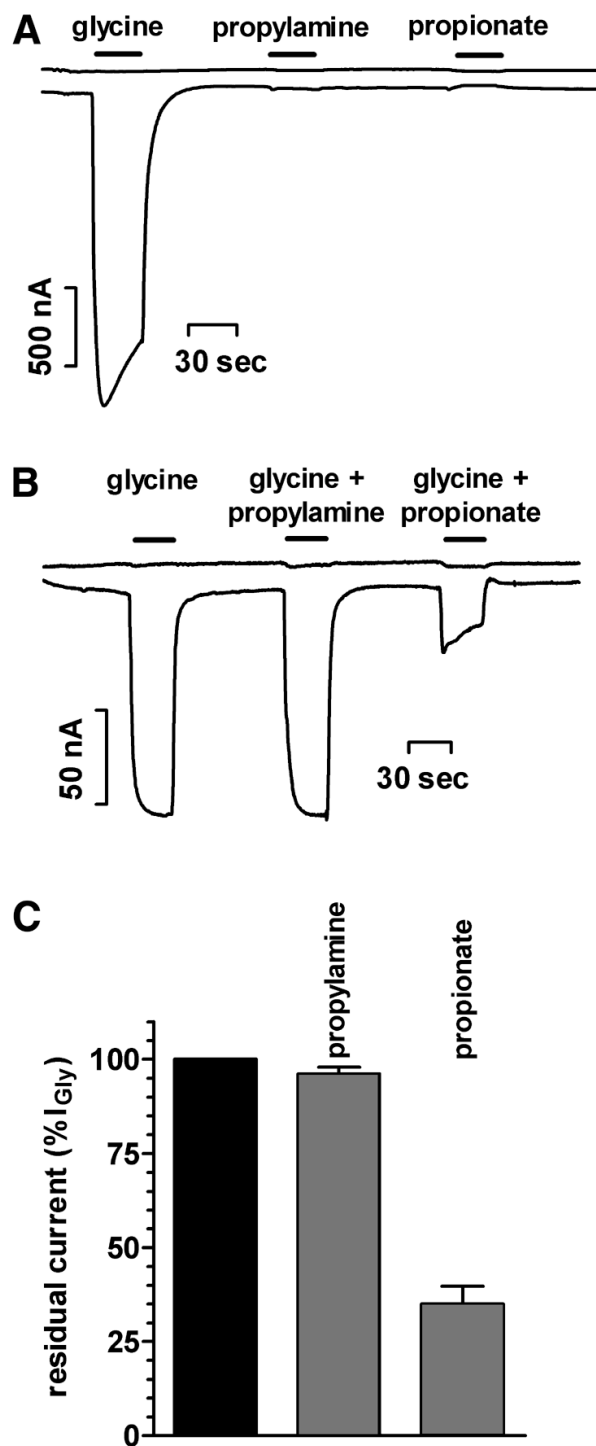
*Received January 12, 2004 ; accepted July 12, 2004.*

**Table 1****Determining intracellular acidification induced by short-chain fatty acids**

<b>Substrate</b>	<b>PAT1-mediated (<math>\Delta\text{pH}/\text{sec}</math>)</b>	<b>Control (<math>\Delta\text{pH}/\text{sec}</math>)</b>	<b>Ratio PAT1/control</b>
Propionate	$-0.026 \pm 0.008$	$-0.011 \pm 0.002$	2.5
Butyrate	$-0.013 \pm 0.002$	$-0.005 \pm 0.001$	2.8
Glycine	$-0.013 \pm 0.003$	-	-

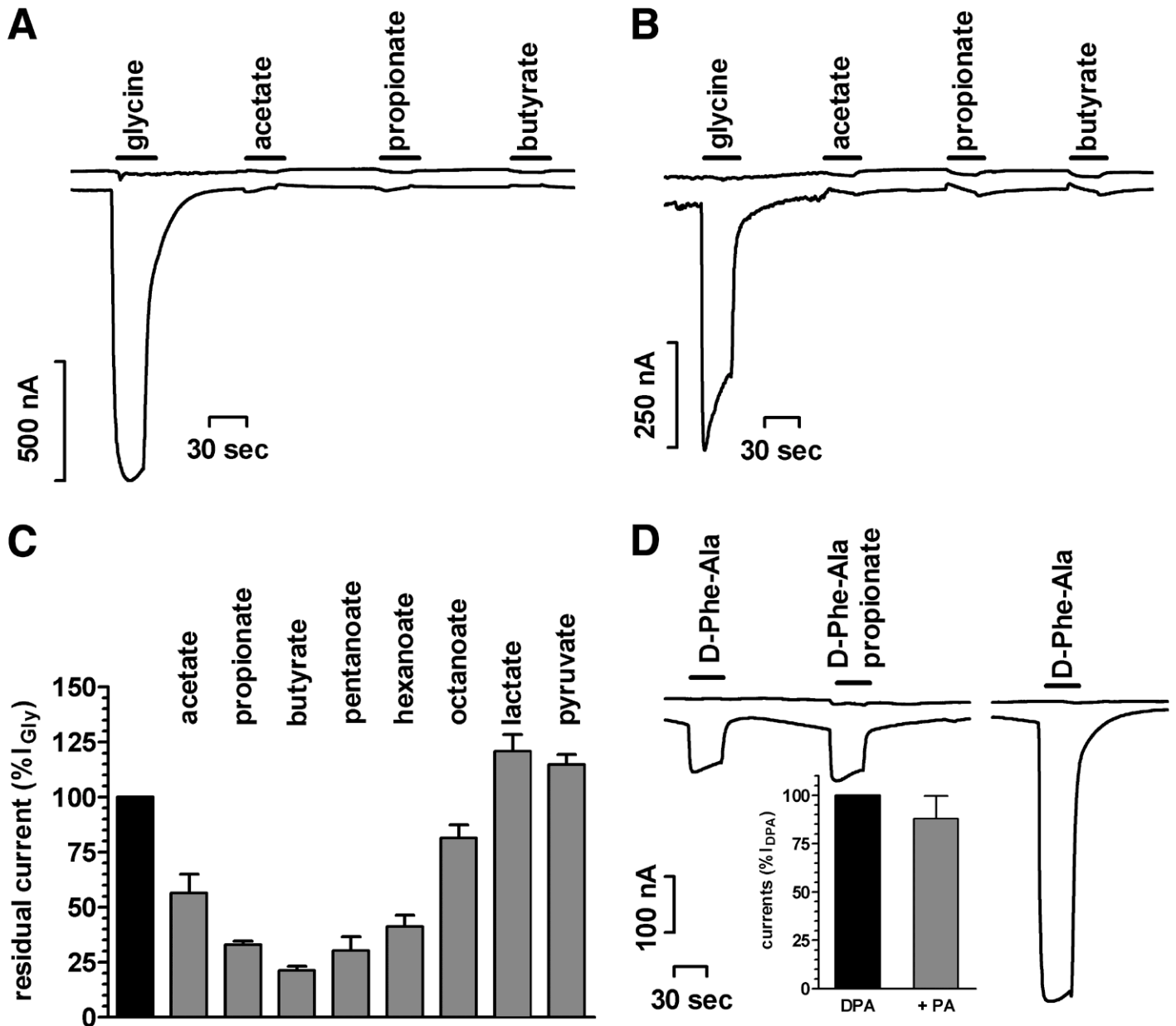
All substrates were applied at a concentration of 20 mM at pH 5.5. Slope of acidification was determined after linear regression of data obtained in the first 20 s of linear acidification after substrate application. PAT1-mediated data are baseline corrected by subtracting pH changes recorded in control oocytes from total pH changes in PAT1-expressing oocytes. Data in last column are relative as a quotient of slope of acidification determined for a substrate in PAT1 expressing oocytes divided by slope values in control oocytes and given as *x*-fold increase regarding to control oocytes.

Fig. 1



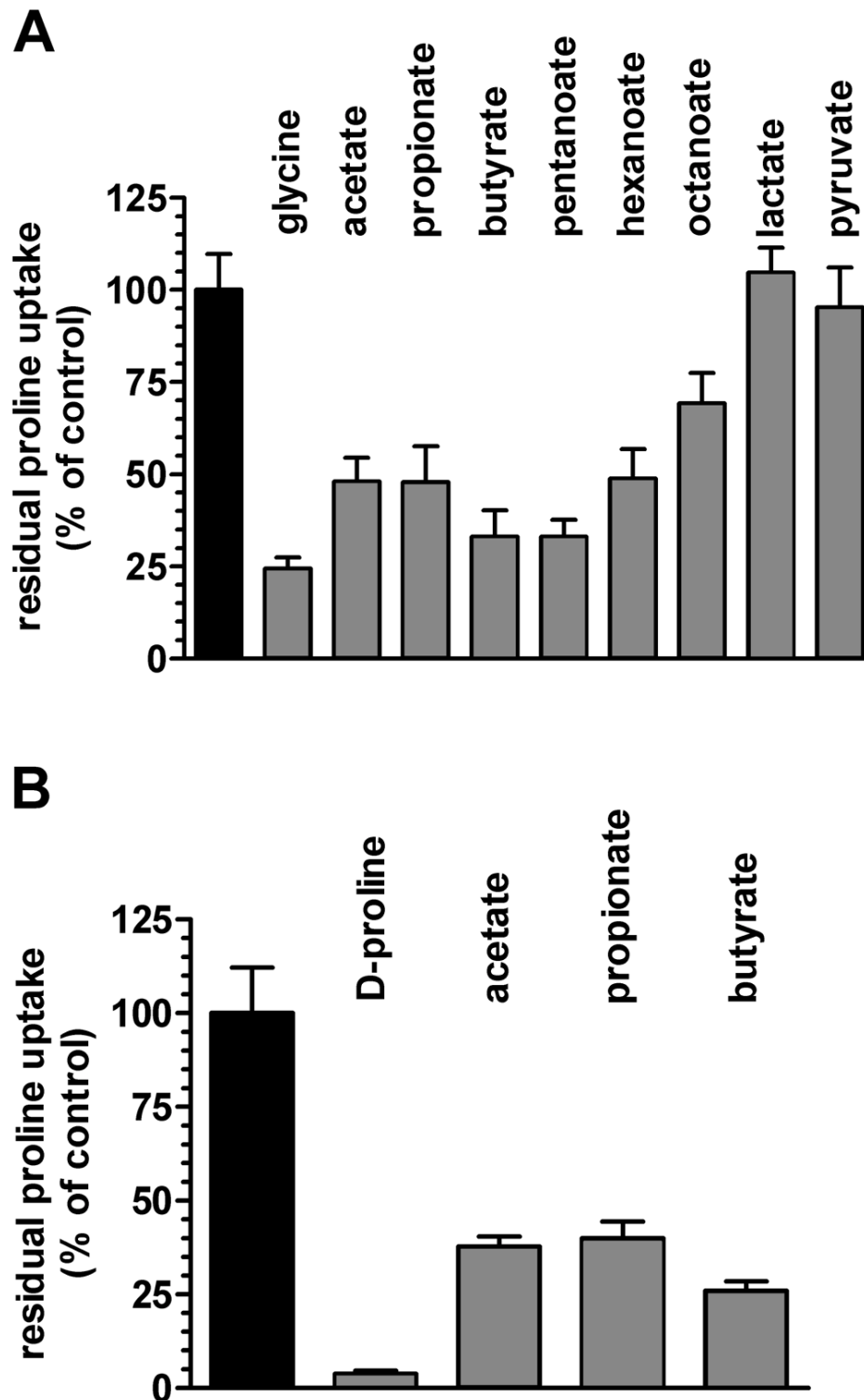
**Figure 1. Current trace and glycine induced current inhibition by monoamines and monocarboxylates in PAT1 expressing *X. laevis* oocytes.** **A**) Representative current trace of a PAT1-expressing oocyte showing current responses after successive addition of glycine, propylamine, and propionate at a concentration of 20 mM in standard perfusion buffer (pH 5.5). In control oocytes, no current change for any test compound has been observed (data not shown). **B**) Current trace of a PAT1 expressing oocyte of a representative inhibition experiment. Currents were induced by 0.5 mM glycine, and inhibitory effect of propylamine and propionate was obtained at concentration of 10 mM. **C**) Inhibition of glycine induced currents by propylamine and propionate in PAT1 expressing oocytes. PAT1-mediated currents, induced by 0.5 mM glycine, are shown in the absence (black bar) or presence (gray bar) of 10 mM of indicated compound. Currents are displayed relative to glycine induced currents ( $I_{Gly}=96 \pm 11$  nA,  $n=6$ ).

Fig. 2



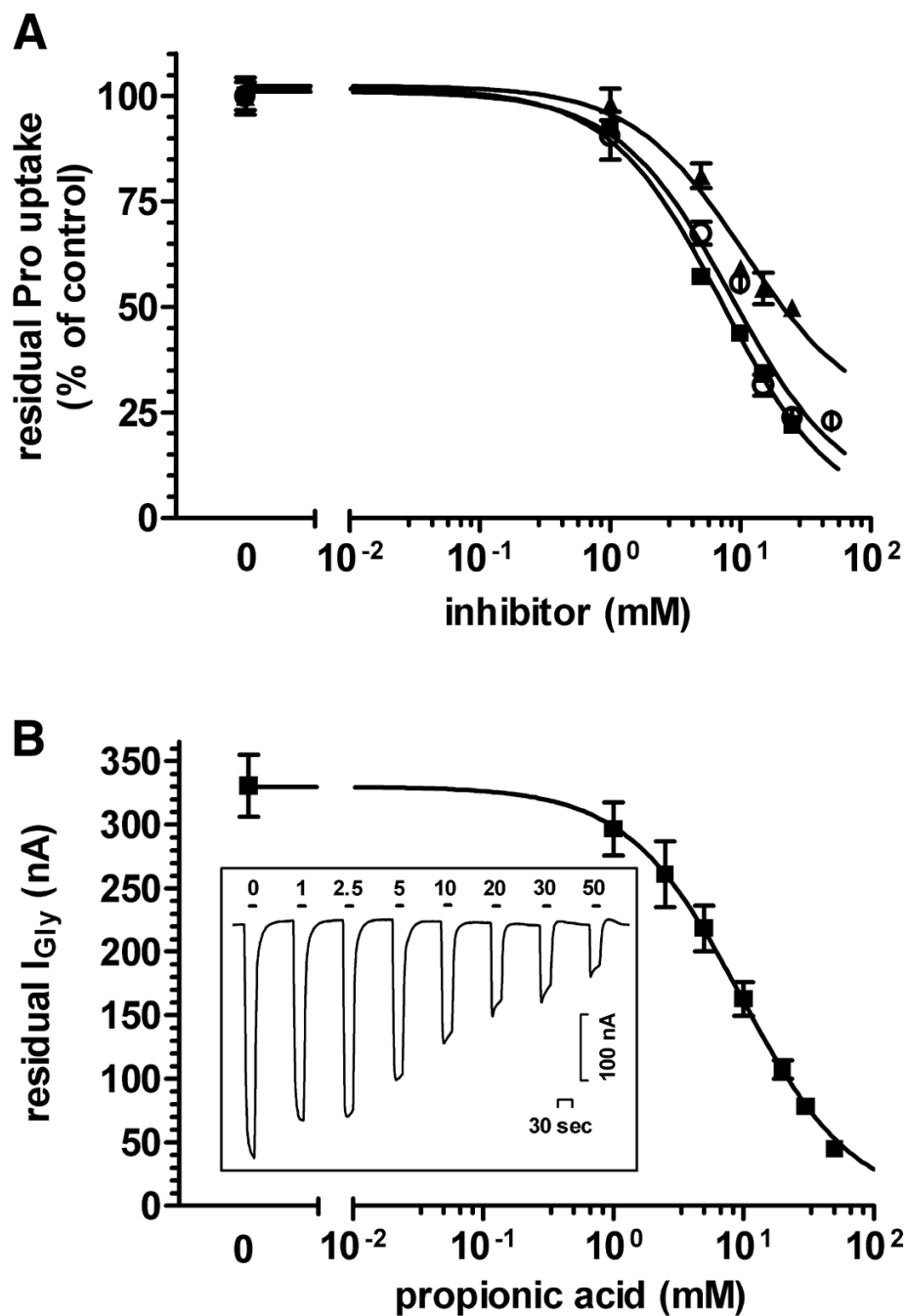
**Figure 2. Short-chain fatty acids are not transported electrogenically via PAT1 and PAT2 but are able to inhibit glycine induced currents of PAT substrates.** Representative current trace of a PAT1 (**A**) and PAT2 (**B**) expressing oocyte showing current responses following the successive addition of the indicated compounds (20 mM, pH 5.5). In control oocytes, no current change for any tested compound has been observed (upper traces). **C**) Inhibition of glycine induced currents by different monocarboxylates in PAT1 expressing oocytes. PAT1-mediated currents, induced by 1 mM glycine, are shown in the absence (black bar) or presence (gray bars) of 20 mM of indicated monocarboxylate. Currents are displayed relative to glycine induced currents ( $I_{Gly}=409\pm 48$  nA,  $n=8$ ). **D**) Representative current trace of a PEPT1 expressing oocyte showing current responses after perfusion of D-Phe-Ala (1 mM) and a combination of D-Phe-Ala (1 mM) and propionate (20 mM) followed by control perfusion with 10 mM D-Phe-Ala. **Inset**) Inhibition of D-Phe-Ala (DPA, 1 mM, black bar) induced currents by coperfusion of 20 mM propionate (+PA; gray bar) in PEPT1 expressing oocytes. Results are expressed as % of PEPT1 mediated 1 mM D-Phe-Ala currents and are means  $\pm$  SE ( $I_{D-Phe-Ala}=121\pm 19$  nA,  $n=4$ ).

Fig. 3



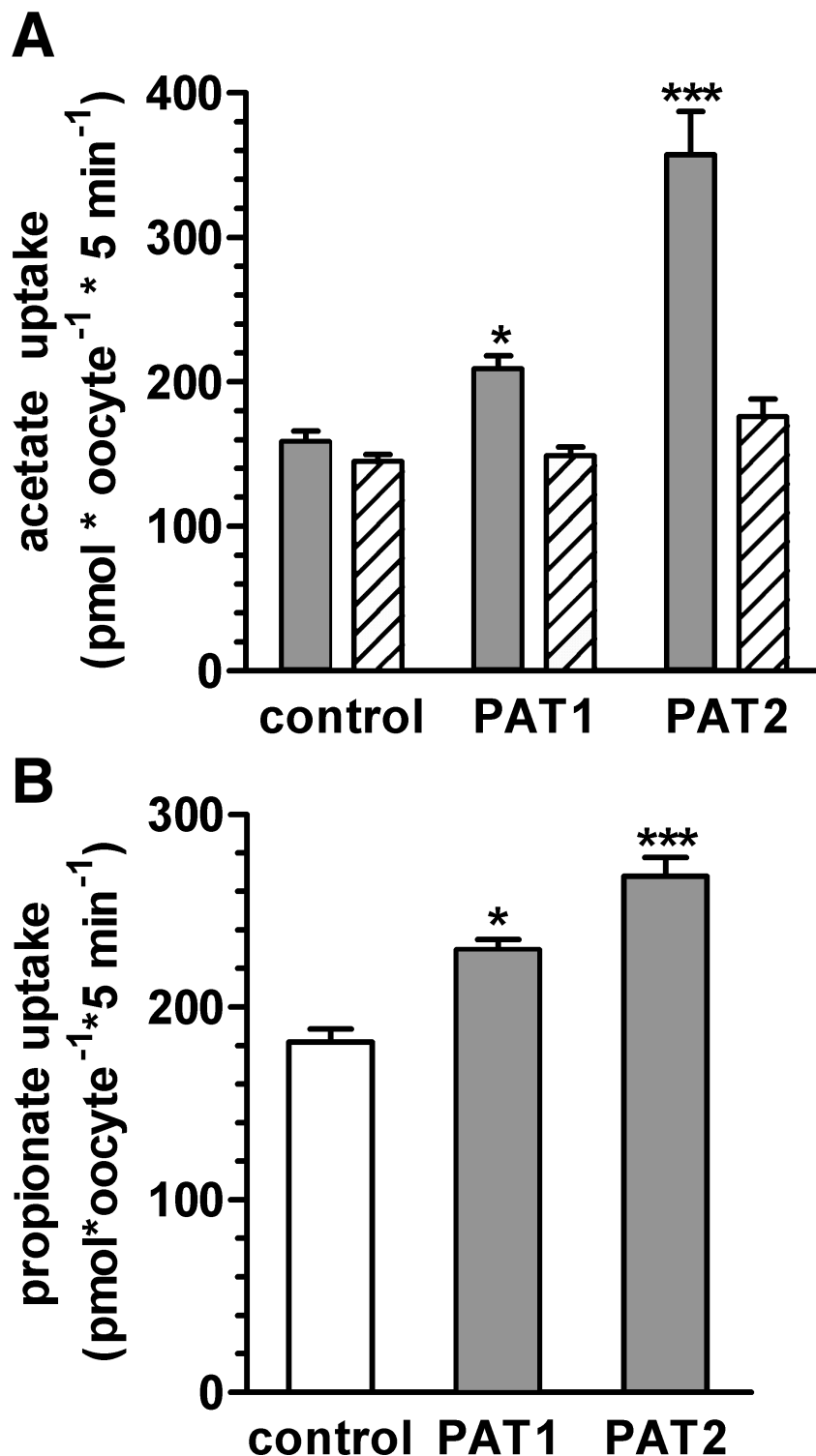
**Figure 3.** Inhibitory effect of short-chain fatty acids on PAT-mediated L-proline uptake. Inhibition of L-proline uptake (100  $\mu$ M) by different short-chain fatty acids into PAT1 (**A**) and PAT2 (**B**) expressing oocytes. Proline uptake is shown in the absence (black bars) or presence (gray bars) of 20 mM unlabeled short-chain fatty acid. Uptake is displayed relative to L-proline uptake (PAT1:  $36.9 \pm 3.9$ ; PAT2:  $55.6 \pm 6.8$  pmol/oocyte/10 min) as means  $\pm$  SE ( $n=8-10$ ).

Fig. 4



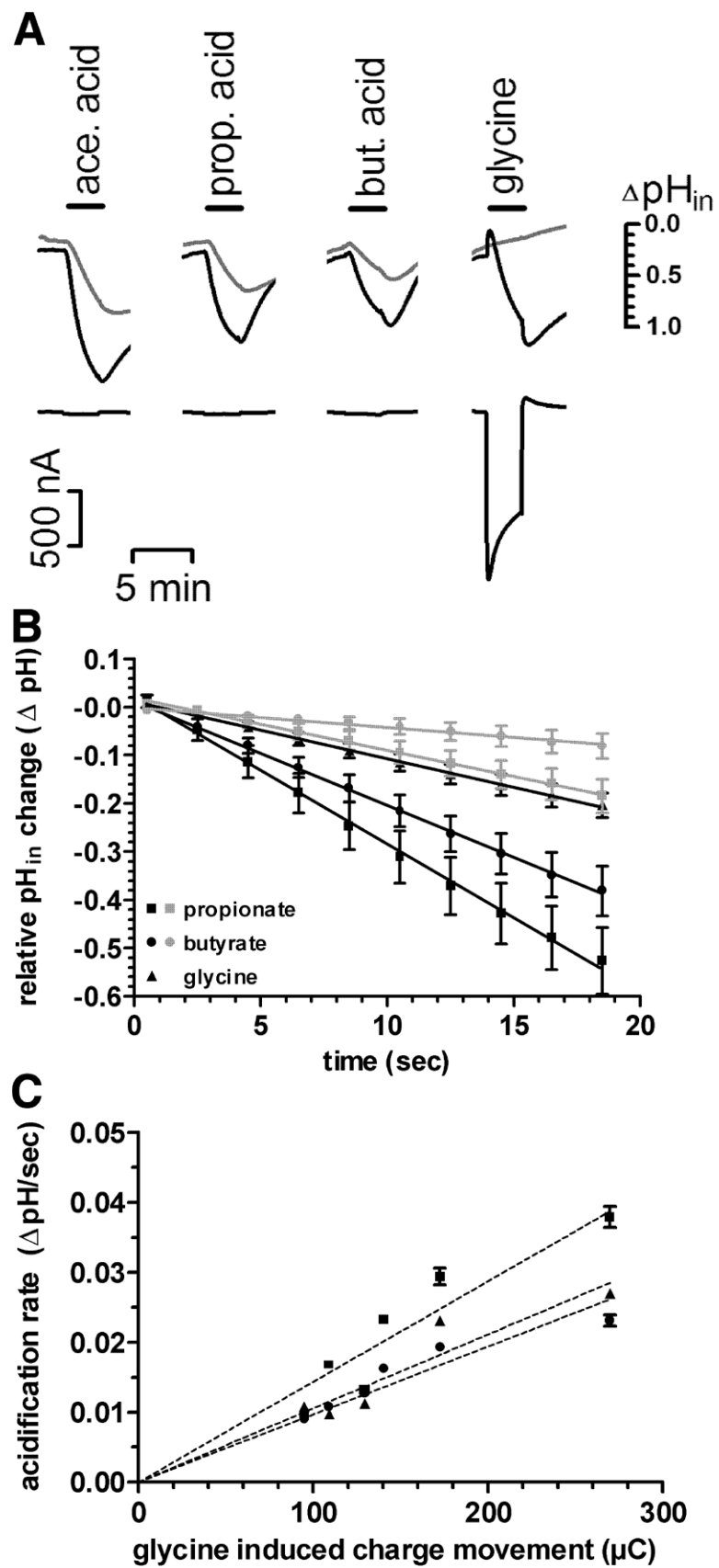
**Figure 4. Concentration dependent inhibition of PAT mediated amino acid transport by different short-chain fatty acids.** **A)** Uptake of L-[<sup>3</sup>H]proline (100  $\mu$ M) into PAT1 expressing oocytes measured as a function of increasing acetate (open circles), propionate (triangles), and butyrate (squares) concentrations (0-50 mM). Curves are best fit using first order competition kinetics. Data are means  $\pm$  SE of  $n = 3$  experiments with  $n = 8-10$  oocytes per condition. **B)** Competition analysis of the inhibitory effect of propionate on Gly currents. Oocytes expressing PAT1 were held at a membrane potential of -40 mV and perfused with standard perfusion buffer at a pH of 5.5 in the absence or presence of 1mM glycine in combination with increasing concentrations of propionate (0-50 mM). Curve represents best fit using first order competition kinetics. Data are shown as means  $\pm$  SE ( $n=8$ ). **Inset)** representative current trace of a PAT1 expressing oocyte, black lines mark time period when substrate was present in perfusate (15 s, respectively), and numbers indicate respective propionate concentration including 1 mM glycine.

Fig. 5



**Figure 5. Uptake of [<sup>3</sup>H]acetate and [<sup>14</sup>C]propionate is significantly enhanced in PAT1 and PAT2 expressing oocytes.** Uptake of [<sup>3</sup>H]acetate and [<sup>14</sup>C]propionate (100 μM) into control oocytes as well as PAT1 and PAT2 expressing *Xenopus* oocytes was measured for 5 min of incubation at pH 5.5 in standard uptake buffer. **A)** Uptake rates of 100 μM acetate in the absence (gray bars) or presence of 20 mM D-proline (dashed bars) are shown. **B)** Uptake of [<sup>14</sup>C]propionate into control oocytes or oocytes expressing PAT1 or PAT2. Transport rates are means ± SE ( $n=8-10$ ) of a representative uptake experiment. \*\*\* $P < 0.001$ , \* $P < 0.05$ , compared with corresponding values in control oocytes.

Fig. 6



**Figure 6. PAT1-mediated intracellular acidification in *X. laevis* oocytes induced by short-chain fatty acids.** **A)** Intracellular pH and current recordings after application of 20 mM of indicated short-chain fatty acid or glycine. Upper traces are intracellular pH recordings as  $\Delta\text{pH}$  in PAT1-expressing (black line) and control oocytes (gray line) clamped at  $-40$  mV. Fast pH changes at the beginning and end of glycine application are virtual and reflect potential differences between the tips of voltage recording and pH microelectrode by changes of the clamp current. Lower traces represent the holding current recorded for a PAT1 expressing oocyte. **B)** Initial acidification rates in PAT1 expressing (black symbols) and control oocytes (gray symbols) during perfusion with either propionate, butyrate, or glycine. Slope of total acidification was determined after linear regression of the first 20 s of linear acidification recorded in PAT1 and control oocytes. Data are means  $\pm$  SE of  $n = 10$  experiments. **C)** Shown are acidification rates of propionate (squares), butyrate (circles), and glycine (triangles) obtained in individual oocytes as function of charge movement induced by glycine in same oocyte as measured at end of each experiment.



## APPENDIX 6

published in the *Biochemical Journal* (accepted manuscript)

**Title: Kinetics of bidirectional H<sup>+</sup> and substrate transport by the proton-dependent amino acid symporter PAT1**

Authors: Martin Foltz, Manuela Mertl, Veronika Dietz, Michael Boll, Gabor Kottra, and Hannelore Daniel

Institution: Molecular Nutrition Unit, Center of Life and Food Sciences, Technical University of Munich, D-85350 Freising-Weihenstephan, Germany

Short title: transport mode of PAT1

Keywords: proton/amino acid transporter, electrophysiology, giant patch clamp, presteady state currents, efflux characteristics, *Xenopus laevis* oocytes

Correspondence: Prof. Dr. Hannelore Daniel, Institute of Nutritional Sciences, Center of Life and Food Sciences, Technical University of Munich, Hochfeldweg 2, D-85350 Freising-Weihenstephan, Germany.

Email: [daniel@wzw.tum.de](mailto:daniel@wzw.tum.de), Phone: +49 8161 71 3400, Fax: +49 8161 71 3999

**SUMMARY**

PAT1 is a recently identified member of the PAT family of proton/amino acid cotransporters with predominant expression in the plasma membrane of enterocytes and in lysosomal membranes of neurons. Previous studies in *Xenopus* oocytes expressing PAT1 established proton-substrate cotransport associated with positive inward currents for a variety of small neutral amino acids. Here we provide a detailed analysis of the transport mode of the murine PAT1 in oocytes using the two electrode voltage clamp technique to measure steady state and presteady state currents. The giant patch clamp technique and efflux studies were employed to characterise the reversed transport mode. Kinetic parameters ( $K_m$  and  $I_{max}$ ) for transport of various substrates revealed a dependence on membrane potential, hyperpolarization increases the substrate affinity and maximal transport velocity. Proton affinity for interaction with PAT1 is in the range of 100 nM, corresponding to a pH of around 7.0 and independent of substrate. Kinetic analysis revealed that binding of proton most likely occurs before substrate binding and that proton and substrate are translocated in a simultaneous step. No evidence for a substrate-uncoupled proton shunt was observed. As shown by efflux studies and current measurements by the giant patch clamp technique, PAT1 allows bidirectional amino acid transport. Surprisingly, PAT1 exhibits no presteady-state currents in the absence of substrate even at low temperatures and therefore PAT1 takes an exceptional position among the ion-coupled cotransporters.

## INTRODUCTION

Proton-coupled amino acid transport across biological membranes is a common phenomenon in prokaryotes and lower eukaryotes (1). However, in mammalian species such proton-coupled amino acid transporting systems are scarce. Based on work in isolated vesicles from brush border membranes of kidney first evidence for the presence of proton-coupled transporters for small polar amino was obtained in the late 1980's and 1990's (2-4). Similarly, in the human intestinal cell line Caco-2 the existence of a proton-coupled system capable of transporting glycine, alanine,  $\beta$ -alanine, prolin and amino acid derivatives such as GABA<sup>1</sup>, and D-cycloserine was demonstrated (5-9) and these systems have been termed PAT for proton-dependent amino acid transporters.

The molecular entities of this transporter family have been identified and in the last years four different transporter cDNAs (PAT1-PAT4) have been cloned (10). All members represent proteins with 483 - 500 amino acid residues with predicted 11 transmembrane domains and a mean similarity of > 65% to each other. Whereas two of the proteins still are orphan transporters, PAT1 and PAT2 proteins have been functionally characterised as proton-coupled symporters. PAT1, cloned so far from rat, mouse and human (10-13) appears to represent the functionally well characterised PAT-system from the apical membranes of the enterocytes and renal proximal tubular epithelial cells. In fact, the human PAT1 cDNA has been cloned from the human intestinal cell line Caco-2 and the PAT1-protein could be localised in the apical membrane of Caco-2 cells (12). The cDNA of PAT1 was initially cloned from rat brain and the protein was found in lysosomal membranes of neuronal cells by immunohistochemistry (13). Here the transporter is proposed to mediate lysosomal export of small amino acids from intralysosomal protein breakdown. In primary neuronal cells prepared from rat hippocampus the transporter localises to specific plasma membrane domains, called the exocyst complex (14). Whether this finding is of significance *in vivo* in the developing or mature brain in the neuronal uptake or release of neurotransmitters such as glycine and GABA - both PAT1 substrates - is so far not known.

The basic functional properties of PAT1 when heterologously expressed have been elucidated in COS-7 and Hela cells and in *Xenopus laevis* oocytes. The substrate specificity is well described and besides small L- $\alpha$ -amino acids (Gly, Ala, Pro) also certain  $\beta$ - and  $\gamma$ -amino acids (e.g.  $\beta$ -alanine, GABA), D-amino acids (e.g. D-Ser, D-Ala), and osmolytes such as sarcosine (N-methyl-glycine) and betaine (N-trimethyl-glycine) were shown to be transported. Critical structural features of substrates that show electrogenic transport by PAT1 are a short size of the amino acid side chain, a free negatively charged (carboxy-) group, and a short spacing between amino and carboxy group whereas a free amino group is not essential for PAT1 interaction (15).

PAT1-mediated transport is highly dependent on the extracellular pH and on membrane potential. The transport of protons and the zwitterionic form of amino acid substrates is electrogenic with a stoichiometry of 1:1, the latter shown for the model substrate L-proline. Substrate-dependent proton translocation by PAT1 has been directly shown by recording intracellular acidification in oocytes expressing PAT1 (11).

Here we present a more detailed analysis of the transport mode of the murine PAT1 protein expressed in *Xenopus laevis* oocytes. By recording steady state currents, the transport characteristics of different substrates have been analysed with respect to substrate and proton binding affinities and their dependence on membrane potential. Moreover, the ability of PAT1 for bidirectional transport and the asymmetry of the binding site in the in- and outward facing direction is demonstrated for the first time and an analysis of presteady state currents is provided. The results help to understand amino acid transport by PAT1 in its different locations such as lysosomal membranes or the brush border of epithelial cells.

## METHODS

### **Materials**

*Xenopus laevis* frogs were purchased from Nasco (Fort Atkinson, WI). All experiments with *X. laevis* were approved by the state ethics committee and followed the German guidelines for care and handling of laboratory animals. Amino acids and related compounds were obtained from Sigma Chemie (Deisenhofen, Germany) or Merck (Darmstadt, Germany) in p. a. quality. Tritium labelled proline (L-[3,4-<sup>3</sup>H]proline, 60 Ci/mmol) was purchased by Amersham Biosciences (Freiburg, Germany). Collagenase A was obtained from Roche Molecular Biochemicals (Mannheim, Germany).

### ***Xenopus laevis* oocytes handling and cRNA injection**

Oocytes were treated with collagenase A (Roche Diagnostics) for 1.5 - 2 h at room temperature in Ca<sup>2+</sup>-free ORII solution (82.5 mM NaCl, 2 mM KCl, 1 mM MgCl<sub>2</sub> and 10 mM HEPES, pH 7.5) to remove follicular cells. After sorting, healthy oocytes of stage V and VI were kept at 18°C in modified Barth solution containing 88 mM NaCl, 1 mM KCl, 0.8 mM MgSO<sub>4</sub>, 0.4 mM CaCl<sub>2</sub>, 0.3 mM Ca(NO<sub>3</sub>)<sub>2</sub>, 2.4 mM NaHCO<sub>3</sub> and 10 mM HEPES (pH 7.5). The next day, oocytes were injected with 27 nl sterile water (control), 27 nl murine PAT1-cRNA or 13 nl rabbit PEPT1-cRNA (10 ng cRNA/oocyte, respectively) and were kept in modified Barth solution at 18°C until further use (3 - 5 days after injection).

### **Two electrode voltage clamp**

Two-electrode voltage clamp experiments were performed as described previously (11). Briefly, the oocyte was placed in an open chamber and continuously superfused with incubation buffer (100 mM choline chloride, 2 mM KCl, 1 mM MgCl<sub>2</sub>, 1 mM CaCl<sub>2</sub>, 10 mM MES or HEPES at pH 5.5-8.5) in the absence or presence of the substances studied. Oocytes were voltage clamped at -60 mV using a TEC-05 amplifier (NPI Electronic, Tamm, Germany), and current-voltage (I-V) relations were measured using short (100 ms) pulses separated by 200 ms pauses in the potential range -160 to +80 mV. I-V measurements were made immediately before and 20-30 s after substrate application when current flow reached steady state. The current evoked by PAT1 at a given membrane potential was calculated as the difference between the currents measured in the presence and the absence of substrate. Positive currents denote positive charges flowing out of the oocyte. (see Figure 6 and 8).

Kinetics of substrate-dependent currents were constructed from experiments employing five different amino acid concentrations in Na<sup>+</sup>-free buffer at pH 6.5 with at least 8 individual oocytes expressing PAT1 from at least two different oocyte batches for each substrate. Substrate-evoked currents were transformed according to Eadie-Hofstee and after linear regression analysis the substrate concentrations that cause half-maximal transport activity were derived. Transport parameters are defined by apparent K<sub>m</sub> (mM) and I<sub>max</sub> (nA).

Kinetics for proton-interaction with PAT1 were obtained under conditions of substrate saturation (50 mM). Such high concentrations were chosen to exclude pH-effects on the titration of the substrate in the pH range used and to allow even at the lowest pH (pH 5.5) substrate saturation for the zwitterionic species. Substrate free buffer has been for comparison osmotically adjusted with 50 mM mannitol. The standard incubation medium was buffered with 10 mM HEPES (> pH 6.0) or MES (pH < 6.0) and adjusted in the presence of substrate to the respective pH values. The apparent  $K_m$  values were derived by linear regression after Eadie-Hofstee transformation of inward currents induced by 6 different apparent proton concentrations. It is noteworthy that the data points could always be fit best to a single kinetics with no indication for unspecific proton binding effects or an allosteric proton binding mechanism.

### ***Giant patch clamp experiments***

GPC experiments were performed as described previously (16). Patch pipettes of 20-30  $\mu\text{m}$  diameter were prepared from thin-walled borosilicate glass capillaries (MTW-150, WPI, Berlin, Germany) and were filled with a solution containing (in mM) NaCl 10, NaISE 80, MgSO<sub>4</sub> 1, Ca(NO<sub>3</sub>)<sub>2</sub> 1, HEPES 10, titrated to pH 7.5, and connected to an EPC-9 amplifier. After removing of the vitelline layer and gigaseal (1-10 gigohms) formation pipettes were moved to a perfusion chamber and continuously superfused with the control bath solution composed of (in mM) potassium aspartate 100, KCl 20, MgCl<sub>2</sub> 4, EGTA 2, HEPES 10 (pH 7.5). During experiments the membrane potential was clamped to 30 mV, and IV relations in the potential range of -80 to +60 mV were measured in the same way as described for TEVC experiments. The data were recorded with the PULSE (HEKA, Lambrecht, Germany) and evaluated with the PATCH (courtesy of Dr. Bernd Letz) program.

The transport parameters  $K_m$  (mM) and  $I_{\text{max}}$  (pA) were obtained from least square fits to the Michaelis-Menten equation. Since  $I_{\text{max}}$  values depend on the expression level of the transporter all parameters (altered substrate concentrations and pH) were always analysed in the same oocyte. This required a reduction of the number of data points for analysis to 5 in these experiments with substrate concentrations of 1, 2.5, 5, 10, and 20 mM for all substrates at pH 7.5.

### ***Presteady state measurements***

Presteady currents were measured with the same equipment and similar to the recordings of the IV-relations. The membrane potential was stepped from the holding potential of -60 mV to -160 to +80 mV in 40 mV steps, however, the pulse length was only 40 ms and the recorded signals were low-pass filtered at 1 kHz. To obtain a good resolution of both, the high-amplitude current peak loading the membrane capacitance and the low amplitude presteady component, the current was recorded first with low amplification (0.2 V/ $\mu\text{A}$ ) and than with high amplification (1 V/ $\mu\text{A}$ ). The time resolution was for both runs 0.16

ms. In the high-amplification mode the peaks of the capacitive currents were cut off by the analog-digital conversion. To reduce measurement noise five runs with each setting were recorded, stored and averaged. The data were evaluated offline by using self-written programs in VBA for Excel and using the Solver routine for least-square fitting. After averaging the data the following function containing two exponential relaxations was fitted to the data points recorded with the low amplification.

$$I_{v,t} = I_{cap,v} * \exp(-t/\tau_{cap,v}) + I_{pre,v} * \exp(-t/\tau_{pre,v}) + I_{s_v}$$

with  $I_{v,t}$  current at the membrane potential „ $V$ “ and at the time „ $t$ “  
 $I_{cap,v}$  peak capacitive current at „ $V$ “  
 $\tau_{cap,v}$  time constant of the capacitive current component at „ $V$ “  
 $I_{pre,v}$  peak presteady current at „ $V$ “  
 $\tau_{pre,v}$  time constant of the presteady current component at „ $V$ “  
 $I_{s_v}$  steady (DC) component of the current at „ $V$ “

Due to the limited speed of the voltage clamp the first 1.12 ms of the current records (i.e. the first 7 data points) were omitted from the fit procedure. When the best fit with the low amplification data was reached, the parameters  $I_{pre,v}$ ,  $\tau_{pre,v}$  and  $I_{s_v}$  were then refitted using the data points recorded with the high amplification, whereas the parameters  $I_{cap,v}$  and  $\tau_{cap,v}$  were fixed at their values obtained in the previous fit. The charge movement due to presteady currents at „ $V$ “ was calculated as the time integral of the relaxation function.

For analysis at low temperatures the measuring chamber was perfused with solutions cooled down from the room temperature (22° C) to about 10° C. This was achieved by filling cooled solutions into thermally isolated reservoirs and by further cooling the perfusate by a Peltier-element in the very neighbourhood of the chamber. In a part of experiments the temperature was measured at the chamber outflow and verified a solution temperature of about 10 °C or lower.

### ***Efflux measurements***

8 oocytes (water- or cRNA-injected) per experiment were injected with 100  $\mu$ M [ $^3$ H]L-proline (2.5 nCi/oocyte) in efflux buffer (100 mM choline chloride, 2 mM KCl, 1 mM MgCl<sub>2</sub>, 1 mM CaCl<sub>2</sub>, 10 mM HEPES, pH 7.5). After 1 min of regeneration at room temperature in efflux buffer, oocytes were briefly washed and immediately transferred to individual wells of a 96-well plate (0.5 ml volume/well). 200  $\mu$ l standard incubation buffer was added with a multi channel pipette. After the indicated time intervals 100  $\mu$ l medium were withdrawn for determination of radioactivity and replaced by new buffer. At the end of the experiment, oocytes were solubilized by adding 100  $\mu$ l 10% (w/v) SDS. Radioactivity of the efflux buffer at the different time points and in the oocyte was counted by liquid scintillation.

**Statistics**

All calculations (linear as well as non-linear regression analyses) were performed using Prism software (GraphPad, San Diego, CA). Transport measurements in *Xenopus* oocytes were performed with at least 8 oocytes from two different oocyte batches. Data are presented as mean  $\pm$  S.E.M. Statistically significant differences were determined using ANOVA analysis followed by Newman-Keuls multiple comparison test.

## RESULTS

### ***H<sup>+</sup>/amino acid steady state kinetics: Proton activation constants***

We first determined the affinity for proton interaction ( $K_m^{H^+}$ ) with PAT1 under saturating substrate concentrations (50 mM) by varying the extracellular pH from pH 7.0 to pH 5.5. As shown in figure 1A, proton-dependent inward currents followed typical Michaelis-Menten kinetics with apparent  $K_m^{H^+}$  values of  $133 \pm 4.3$  nM in case of glycine and  $111 \pm 6.8$  nM in the presence of GABA. The determined  $K_m^{H^+}$  values were independent of the amino acid substrate, as they did not significantly differed from each other ( $p > 0.05$ ) and correspond to a pH value of about pH 6.9 that causes half-maximal stimulation of transport. When currents were recorded at different membrane voltages, the apparent proton affinity with glycine as substrate decreased nearly 9-fold by depolarising the membrane from -140 mV to +20 mV (Fig. 1B). Interestingly, the  $I_{max}^{H^+}$  values for proton-dependent glycine transport at saturating substrate concentrations decreased only 2.4-fold by depolarisation from -140 mV to +20 mV (data not shown).

### ***H<sup>+</sup>/amino acid steady state kinetics: Voltage dependence***

To determine the effect of membrane voltage on the kinetic parameters  $K_m$  and  $I_{max}$  of PAT1 substrates, inward currents were recorded as a function of increasing L-Ala concentrations (0.2 mM - 20 mM). Figure 2A demonstrates that under non-saturating substrate concentrations, inward currents almost linearly depend on membrane potential and only at 20 mM L-Ala currents show a tendency towards saturation at negative membrane potentials. A comparative analysis of membrane voltage effects on the  $K_m$  values for Gly, L-Pro, betaine and taurine is provided in figure 2B. Membrane depolarisation had only a minor effect on affinity of Gly with a decline of  $K_m$  value of about 1.5-fold and similarly, L-Ala, and  $\beta$ -Ala affinities only modestly changed (data not shown). Affinities of L-Pro, betaine, and taurine decreased between 2.1- and 4.1-fold by shifting the membrane potential from -160 mV to 0 mV (Fig. 2B) and similar changes in apparent  $K_m$  were obtained for D-Pro, D-Ala, sarcosine, and GABA (data not shown). All  $I_{max}$  values for the different substrates decreased by 70-80% when membrane voltage was changed from -160 mV to 0 mV (data not shown).

### ***H<sup>+</sup>/amino acid steady state kinetics: Order of binding***

For assessing whether binding of protons and amino acids to PAT1 follows an ordered or random mechanism, we determined apparent  $K_m^{Gly}$  and  $I_{max}^{Gly}$  at two different pH values (pH 6.5 =  $0.316 \mu\text{M} [\text{H}^+]$ , pH 5.0 =  $10 \mu\text{M} [\text{H}^+]$ ). At both pH values substrate-dependent inward currents showed simple Michaelis-Menten kinetics and decreasing external pH from pH 6.5 to pH 5.0 did not change significantly the maximal inward currents but reduced significantly ( $p < 0.001$ ) the  $K_m$  for glycine (Fig. 3A and 3B, Table 1). When currents were

determined at two different glycine concentrations in dependence of the external  $H^+$  concentration (pH 7.0 to 5.5), the apparent  $K_m^{H^+}$  for proton binding increased more than 4.4-fold and the proton-dependent  $I_{max}^{H^+}$  increased 2.3-fold when glycine concentration was increased from 2 mM to 20 mM (Fig. 3C and D; Table 1). These data strongly suggest that there is an ordered binding mechanism with protons binding first followed by substrate.

#### **No substrate uncoupled proton conductance**

We also addressed the question of whether PAT1 exhibits a proton conductance in the absence of amino acid substrates. For this, current-voltage relationships were recorded in oocytes expressing PAT1 and in water-injected controls and oocytes were perfused with buffer solutions of varying  $H^+$  concentrations (pH 7.0 to pH 5.5) in the absence of amino acids. Figure 4A and 4B demonstrate based on I-V relationships and Figure 4C by intracellular pH-recordings that alterations in extracellular pH over a large range does not cause a proton or charge influx different from the changes observed in water-injected control oocytes. We also calculated by linear regression analysis the reversal potential at each pH value tested. Only a slight conversion to less negative potentials, from  $-31 \pm 2.5$  mV (pH 7.5) to  $-27 \pm 1.5$  mV (pH 5.0), was observed in oocytes expressing PAT1 (Fig. 4A). However, this shift was not significantly different ( $p > 0.05$ ) from that obtained in control oocytes ( $-23 \pm 1.6$  mV to  $-20 \pm 1.2$  mV) (Fig. 4B). These observation argue against a capacity of PAT1 to translocate protons in the absence of amino acids.

#### **Presteady state kinetics**

Analysis of presteady state currents of other electrogenic ion-coupled solute transporters has been very helpful to define their transport mode. We have determined for the first time the presteady state currents of PAT1 in direct comparison to PEPT1 as another proton-dependent electrogenic symporter. Figure 5 shows typical current records in response to potential steps for the rabbit PEPT1 and mouse PAT1. In both cases, the upper panels show the currents in the absence and the lower panels in the presence of substrate. It becomes obvious that PEPT1-mediated currents show in addition to the fast capacitive component an additional potential-dependent slow component which disappears in the presence of substrate. No such slow component could be detected in case of PAT1, although the substrate-dependent steady state current was even higher than that of PEPT1 (1206 nA vs 730 nA at  $-60$  mV). These results were consistently found in at least 7 oocytes from two donor animals in the same oocyte batch. The mean transport current in these oocytes was  $600 \pm 83$  nA (at  $-60$  mV). The calculated presteady charge movement was, however, very small ( $0.74 \pm 0.22$  nC,  $n=7$  at  $-160$  mV and pH 7.5), became still lower at pH 6.5 ( $0.55 \pm 0.18$  nC) and was not significantly different from zero at pH 5.5 ( $0.45 \pm 0.21$  nC). For comparison, the presteady-state charge transfer in oocytes expressing PEPT1 with a

mean transport current of  $450 \pm 30$  nA (at  $-60$  mV) amounted to  $16.6 \pm 1.9$  nC, ( $n=16$ ) at  $-160$  mV and pH 7.5.

In addition to the differences in the presteady charge movements, the time constants for the capacitive component were also different between PAT1 and PEPT1. For both transporters they were - as expected - independent of membrane potential, and averaged  $0.393 \pm 0.036$  ms ( $n=7$ ) for PAT1 and  $0.715 \pm 0.059$  ms for PEPT1. This difference suggests differences in the plasma membrane area and is supported also by capacitance measurements which show a considerable increase of the membrane capacitance proportional to the transport current in oocytes expressing PEPT1, but a nearly unchanged membrane area of PAT1-expressing oocytes (unpublished data).

One possible reason for the lack of significant presteady-state currents in PAT1 could be a very short time constant for the reorientation of the unloaded protein in the membrane in response to potential steps that than would be indistinguishable from the time constant of the capacitive currents. To better discriminate these two parameters, we performed the same experiments at low temperature. The results of 7 identical experiments at low temperature revealed a decrease of transport currents from  $594 \pm 145$  nA at room temperature to  $165 \pm 60$  nA in the cooled state, thus reducing the turnover rate of the transporter by  $77 \pm 5$  %. However, we did not observe any significant increase of a current component with slow time constant ( $0.71 \pm 0.34$  nC at room temperature,  $0.31 \pm 0.17$  nC at low temperature) demonstrating the lack of any detectable presteady state currents in PAT1.

#### ***Bidirectional transport: PAT1-mediated amino acid efflux***

For assessing whether PAT1 is able to transport amino acids also in the outward direction, we loaded oocytes expressing PAT1 with glycine and determined outward-directed transport currents. As shown in figure 6, PAT1-expressing oocytes were perfused at  $-40$  mV with 20 mM glycine at pH 5.5 for 5 min while inward directed current was recorded. A fast wash-out of substrate and a shift of external pH to 7.5 led to significant outward currents of up to 520 nA at a  $V_m$  of  $-40$  mV. These outward currents in the wash-out period were dependent on the PAT1-expression level and the length of substrate application period (data not shown). To confirm transport in the outward direction, efflux studies using radiolabelled proline were performed. After injection of oocytes with radiolabelled proline (5 nmol/oocyte), efflux of the tracer from oocytes expressing PAT1 was significantly higher than from control oocytes (Fig. 7A). The presence of the extracellular substrates such as glycine or alanine increased efflux via PAT1 further by 1.9-fold (glycine) and 1.5-fold (alanine) as compared with the efflux in the absence of amino acids (Fig. 7A). Proline efflux from preloaded oocytes followed Michaelis-Menten kinetics when determined as a function of extracellular glycine concentrations with an apparent affinity constant for glycine of  $1.6 \pm 0.2$  mM (Fig. 7B).

To characterise in more detail the reversed transport mode of PAT1, we employed the giant patch clamp technique with membrane patches obtained from oocytes expressing PAT1. With increasing concentrations of D-Ala provided on the internal membrane side, outward directed currents were recorded even at negative membrane potentials of -80 mV (Fig. 8A). Like inward transport, outward transport currents were strongly dependent on membrane potential and increased from  $1.1 \pm 0.8$  pA at -80 mV to  $12.1 \pm 2.8$  pA at +60 mV in the presence of 50 mM D-alanine. No substrate induced currents were observed in membrane patches obtained from control oocytes (data not shown). The amino acid induced outward currents followed typical Michaelis-Menten kinetics as a function of increasing concentrations of D-alanine (Fig. 8B). We next determined apparent  $K_m$  values for different substrates from Michaelis-Menten kinetics of outward transport recorded at a membrane voltage of +60 mV. Affinities ranged from around 10 mM (L-Pro and D-Pro) to 45 mM (L-Ala) and were therefore almost 7-fold lower than the apparent  $K_m$  values for the same substrates as determined for the inward direction under the same conditions and at a membrane voltage of -60 mV (Fig. 8C). As the most interesting observation, a significant linear relationship in affinities for substrate binding to PAT1 in its outward facing or its inward facing direction was observed. Affinities of substrates such as proline or glycine showed a dependence on membrane potential with a decline at more negative voltages (Fig. 8D). Additionally, maximal transport velocity determined for the outward direction exhibited a similar dependency on membrane potential as described for the inward direction. Alteration of membrane potential by 80 mV decreased the  $I_{max}$  values of all substrates tested between 40% and 60%. (data not shown). These results clearly establish that PAT1 is capable to transport its substrates bidirectionally with the direction of transport determined by the electrical and chemical proton gradient as well as the substrate gradient but a defined asymmetry in the conformation of the substrate binding domain.

## DISCUSSION

Proton-dependent amino acid transport systems with a selectivity for small neutral amino acids and their derivatives amino have been demonstrated in intestinal and renal epithelial cells (2-8). It is now accepted that the PAT1 gene encodes the PAT-activity in these epithelia (12) and the heterologously expressed PAT1 displays essentially all expected functional features (15). We here provide an extended analysis of the functional characteristics of the PAT1-protein by electrophysiological and flux studies that do provide new and unexpected findings.

PAT1 exhibits an apparent proton affinity of around 100 nM that corresponds to a pH of 7.0 and which is almost 50-fold lower than proton affinity reported for the ortholog PAT2 (17). Since the pH at the vicinity of the cell membrane is slightly acidic (pH 6.1 - pH 6.8) by a surface microclimate (18), PAT1 operates most likely in intestinal epithelia under proton saturation. Based on the functional coupling of proton recycling via  $\text{Na}^+/\text{H}^+$  exchanger NHE3 from the cytosol to the apical membranes changes in NHE3 activity secondarily can affect PAT transport activity as shown in the Caco2 cell system (19). In lysosomes of neurons were PAT1 is also found, pH values of  $\leq$  pH 5.5 also would provide conditions allowing maximal rates for amino acid export (20). Proton binding affinity is independent of the substrate species but strongly dependent on membrane voltage with highest affinity at hyperpolarised voltages. Apparent affinities of the various amino acid substrates for PAT1 are also dependent on membrane potential with more pronounced effects at subsaturating proton concentrations (pH 6.5), whereas at low pH (pH 5.0) membrane voltage effects are only modest. Also apparent proton affinities under amino acid saturating conditions were strongly dependent on membrane voltage with decreasing affinities by depolarising potentials. The loss of amino acid binding affinity at less negative potentials under subsaturating proton concentrations is therefore mainly a reflection of the loss of the proton binding affinity.

The observation that the proton affinity constants are essentially independent of the substrates nature suggests that PAT1 possesses an ordered binding mechanism, with protons binding first followed by the amino acid. The maximal transport rate for glycine ( $I_{\max}^{\text{Gly}}$ ) also barely responded to a 30-fold increase of  $\text{H}^+$  concentration. Moreover, the reduction in the  $K_m^{\text{Gly}}$  by lowering pH was much less than expected for a cotransporter with a random substrate/cosubstrate binding mechanism (21-24). However, the substrate concentration drastically affected the  $I_{\max}^{\text{H}^+}$  for  $\text{H}^+$ -dependent currents but we also observed that at high glycine concentrations and at more negative membrane potentials the saturating current became independent of the  $\text{H}^+$  concentration. This also supports an ordered binding mechanism with initial  $\text{H}^+$  binding.

Binding of proton and substrate is followed by a translocation step in which most likely  $H^+$  and amino acid are simultaneously transported across the membrane. This is supported by the observation that, at least at potentials more positive than -100 mV, the  $K_m^{Gly}$  increases at diminishing  $H^+$  concentrations (e.g. at -60 mV  $K_m^{Gly}$  increases strongly with increasing external pH, table 2). In addition, the ratio  $I_{max}^{Gly} / K_m^{Gly}$  was strongly dependent on the external  $H^+$  concentration and this can be taken as additional evidence for an ordered binding, simultaneous transport model (21;25).

In the transport model of PAT1 an uncoupled  $H^+$  influx can essentially be excluded based on only minimal shifts in reversal potential in response to pH jumps and the absence of intracellular pH changes in the absence of substrates. The strong potential dependence of apparent proton binding affinity, may be explained by the “ion-well” effect, i.e. that  $H^+$  has to traverse a part of the transmembrane voltage for entering the proton binding site (21). In this respect PAT1 shares general features such as the voltage dependence of affinities, the ordered binding mechanism and the “ion-well” effect with other symporters like the proton-coupled peptide transporter PEPT1, the sodium-coupled hexose transporter SGLT1 or the system A transporter SA2 (26-28), the latter belonging to the same super family as PAT1.

Analysis of presteady state currents of PAT1 performed at room temperature and 10°C yielded unexpected results. In contrast to most other ion-coupled transporters and also in contrast to PEPT1, with significant potential- and pH-dependent presteady-state charge movements, these were virtually absent in PAT1. There are two possible explanations for this lack of presteady charge movements. It could be that a) PAT1 has an almost symmetric charge distribution within the protein that in turn would not produce a potential-dependent reorientation within the membrane or b) that the movement of the empty transporter in response to potential steps is so fast that the presteady-state currents become indistinguishable from the capacitive currents. Our approach to reduce the turnover rate by lowering the temperature only reduced steady state currents, but did not uncover a presteady current component. Another possible reason for the lack of presteady state currents could be that the turnover rate of mPAT1 is much higher than that for example of PEPT1 and therefore a much smaller number of transporters generates the same rate of maximal currents as for example PEPT1. As a consequence of this, the charge movements induced by the reorientation of the transporters in response to potential steps would be too small to be detected - even at low temperature. That PAT1 could indeed have a very high turnover rate is supported by the following observations: a) comparable inward currents after injection of equal amounts of cRNA of PAT1 and PEPT1 into oocytes can be obtained at least one day earlier in case of PAT1 and b) PAT1-expression yields a lower oocyte membrane surface area and smaller capacitive time constants as PEPT1. Taken together, our analysis does in its present state not allow a final conclusion to be drawn about the lack of detectable

presteady state currents in PAT1 but circumstantial evidence argues for an exceptionally high turnover rate.

The capability of PAT1 for bidirectional transport is demonstrated here for the first time. The apparent substrate affinities determined for inward-directed and outward-directed transport under identical conditions reveal an identical substrate binding pattern but affinities for the binding side when facing the cytosol are generally around 7-fold lower. This indicates a consistent conformational difference of the substrate binding pocket in its inward- and outward-facing state that determines for all substrates an almost identical difference in affinity. In terms of the normal transport cycle, the lower affinity inside could promote the release of the substrate into the cytosol. Similar to the inward direction of transport,  $K_m$  and  $I_{max}$  values for outward transport of substrates are dependent on membrane voltage. Whether PAT1-mediated outward transport of amino acid substrates plays a physiological role is currently not known. However, we show that outward transport can occur even at inside negative membrane potentials, which resembles physiological conditions. The observed strong outward currents observed in the TEVC experiments after loading of oocytes with glycine is a consequence of the reversed driving forces, i.e. the pH- and substrate gradients. PAT1-mediated amino acid transport has been shown to cause intracellular acidification of up to 1 pH unit (15) and therefore after a longer substrate perfusion period, pH-gradients could be outwardly directed. When the intracellular glycine concentration in oocytes perfused with glycine was calculated based on charge movement and using the Faraday constant (oocyte volume at 1.1 mm diameter: 697 nl with around 37% aqueous phase) concentrations of 22 mM to 32 mM were determined and it can be anticipated that those are even higher in the vicinity of the membrane. Under these conditions PAT1 is capable to release substrates from the cells. Moreover, PAT1-mediated efflux of labelled L-proline from oocytes can be demonstrated even in the absence of an outwardly directed pH-gradient and L-Pro release was strongly stimulated by the presence of extracellular amino acid substrates with a half maximal transactivation constant of around 1 mM. Extracellular concentrations of glycine, alanine, and proline are in the range of 0.2 mM and 0.4 mM (29) and in the sum are therefore high enough to stimulate PAT1-mediated efflux of amino acids from cells. In addition, intracellular concentrations of PAT1-substrates such as glycine but in particular of taurine or betaine are fairly high, which would allow PAT1-mediated outward transport for example in the absence of a pH gradient or after membrane depolarisation. Uptake and efflux of the osmolyte taurine via PAT1 could thereby contribute to the maintenance of a constant cell volume under hypo- or hyperosmotic conditions. This proposed role of PAT1 may also be of relevance in non-epithelial cells with high intracellular concentrations of taurine and betaine such as muscle, in which the PAT1-mRNA is expressed at considerable levels (10). Whether this is indeed a physiological function of PAT1 needs to be established.

---

In summary, PAT1 is an electrogenic H<sup>+</sup>-coupled amino acid symporter with the capability for bidirectional amino acid transport. Proton and substrate binding affinities are strongly voltage-dependent but the transport occurs most likely in an ordered fashion in which the proton binds before the amino acid is bound followed by simultaneous substrate and proton translocation. Substrate interaction with the protein binding sites in extracellular or intracellular orientation is determined by an asymmetry with a characteristic conformational difference and generally lower affinities in the outward facing state. In contrast to many other cotransporters the PAT1 transporter does not possess detectable presteady state currents either by a symmetric charge distribution within the transporter protein or due to an exceptionally high turnover rate. Although the prime function of PAT1 may be amino acid influx followed by intracellular amino acid accumulation, under certain conditions PAT1 may even serve as an electrogenic proton/amino acid efflux transporter.

**ACKNOWLEDGEMENT**

This work was supported by the Deutsche Forschungsgemeinschaft (BO 1857/1) to MB. For excellent technical assistance with the GPC technique we greatly acknowledge the support by Adelmar Stamford.

## REFERENCES

1. Saier, M.H.J. (2000) *Microbiology*. **146**, 1775-1795
2. Roigaard-Petersen, H., Jacobsen, C., and Iqbal, S.M. (1987) *Am. J. Physiol.* **253**, 15-20
3. Roigaard-Petersen, H., Jacobsen, C., Jessen, H., Mollerup, S., and Sheikh, M.I. (1989) *Biochim. Biophys. Acta* **984**, 231-237
4. Roigaard-Petersen, H., Jessen, H., Mollerup, S., Jorgensen, K.E., Jacobsen, C., and Sheikh, M.I. (1990) *Am. J. Physiol.* **258**, F388-F396
5. Thwaites, D.T., McEwan, G.T., Cook, M.J., Hirst, B.H., and Simmons, N.L. (1993) *FEBS Lett* **333**, 78-82
6. Thwaites, D.T., McEwan, G.T., Brown, C.D., Hirst, B.H., and Simmons, N.L. (1993) *J. Biol. Chem.* **268**, 18438-18441
7. Thwaites, D.T., Armstrong, G., Hirst, B.H., and Simmons, N.L. (1995) *Br. J. Pharmacol.* **115**, 761-766
8. Thwaites, D.T., McEwan, G.T., and Simmons, N.L. (1995) *J. Membr. Biol.* **145**, 245-256
9. Thwaites, D.T., Basterfield, L., McCleave, P.M., Carter, S.M., and Simmons, N.L. (2000) *Br. J. Pharmacol.* **129**, 457-464
10. Boll, M., Foltz, M., Rubio-Aliaga, I., and Daniel, H. (2003) *Genomics* **82**, 47-56
11. Boll, M., Foltz, M., Rubio-Aliaga, I., Kottra, G., and Daniel, H. (2002) *J. Biol. Chem.* **277**, 22966-22973
12. Chen, Z., Fei, Y.J., Anderson, C.M., Wake, K.A., Miyauchi, S., Huang, W., Thwaites, D.T., and Ganapathy, V. (2003) *J. Physiol.* **546**, 349-361
13. Sagne, C., Agulhon, C., Ravassard, P., Darmon, M., Hamon, M., El Mestikawy, S., Gasnier, B., and Giros, B. (2001) *Proc. Natl. Acad. Sci. U S A* **98**, 7206-7211
14. Wreden, C.C., Johnson, J., Tran, C., Seal, R.P., Copenhagen, D.R., Reimer, R.J., and Edwards, R.H. (2003) *J. Neurosci.* **23**, 1265-1275
15. Boll, M., Foltz, M., Anderson, C.M., Oechsler, C., Kottra, G., Thwaites, D.T., and Daniel, H. (2003) *Mol. Membr. Biol.* **20**, 261-269
16. Kottra, G. and Daniel, H. (2001) *J. Physiol.* **536**, 495-503
17. Rubio-Aliaga, I., Boll, M., D.M., Foltz, M., Kottra, G., and Daniel, H. (2004) *J. Biol. Chem.* **279**, 2754-2760
18. Daniel, H., Fett, C., and Kratz, A. (1989) *Am. J. Physiol.* **257**, G489-G495
19. Thwaites, D.T., Ford, D., Glanville, M., and Simmons, N.L. (1999) *J. Clin. Invest.* **104**, 629-635
20. Golabek, A.A., Kida, E., Walus, M., Kaczmarek, W., Michalewski, M., and Wisniewski, K.E. (2000) *Mol. Genet. Metab.* **70**, 203-213
21. Jauch, P. and Lauger, P. (1986) *J. Membr. Biol.* **94**, 117-127
22. Mackenzie, B., Loo, D.D., Panayotova-Heiermann, M., and Wright, E.M. (1996) *J. Biol. Chem.* **271**, 32678-32683
23. Klamo, E.M., Drew, M.E., Landfear, S.M., and Kavanaugh, M.P. (1996) *J. Biol. Chem.* **271**, 14937-14943
24. Stein, W.D. (1989) *Methods. Enzymol.* **171**, 23-62
25. Eskandari, S., Loo, D.D., Dai, G., Levy, O., Wright, E.M., and Carrasco, N. (1997) *J. Biol. Chem.* **272**, 27230-27238
26. Mackenzie, B., Loo, D.D., Fei, Y., Liu, W.J., Ganapathy, V., Leibach, F.H., and Wright, E.M. (1996) *J. Biol. Chem.* **271**, 5430-5437
27. Loo, D.D., Hirayama, B.A., Gallardo, E.M., Lam, J.T., Turk, E., and Wright, E.M. (1998) *Proc. Natl. Acad. Sci. U S A* **95**, 7789-7794
28. Chaudhry, F.A., Schmitz, D., Reimer, R.J., Larsson, P., Gray, A.T., Nicoll, R., Kavanaugh, M., and Edwards, R.H. (2002) *J. Neurosci.* **22**, 62-72
29. Chih-Kuang, C., Shuan-Pei, L., Shyue-Jye, L., and Tuan-Jen, W. (2002) *Clin. Chem. Lab. Med.* **40**, 378-382

**FOOTNOTES**

<sup>1</sup> The abbreviations used are: GABA,  $\gamma$ -aminobutyric acid; PAT, proton/amino acid transporter; PEPT1, peptide transporter 1; MES, 4-Morpholineethanesulfonic acid; HEPES, 4-(2-Hydroxyethyl)-1-piperazineethanesulfonic acid; TRIS, 2-Amino-2-(hydroxymethyl)-1,3-propanediol; TEVC, two electrode voltage clamp, GPC, giant patch clamp,  $V_m$ , membrane potential

**LEGENDS FOR FIGURES****Figure 1 A and B: Kinetics of proton-dependent activation of amino acid induced steady-state currents in *X. laevis* oocytes expressing PAT1.**

**A.** Currents induced by 50 mM glycine (■) and 50 mM GABA (●) were determined as a function of the extracellular H<sup>+</sup>-concentration (H<sup>+</sup>-activity) in the concentration range of 100 nM (pH 7.0) to 3.1 μM (pH 5.5) and apparent K<sub>m</sub> values were calculated from the mean currents. **B.** Apparent K<sub>m</sub><sup>H<sup>+</sup></sup>-value as a function of membrane potential determined in the presence of 50 mM glycine. Data are presented as mean ± SE (n = 11).

**Figure 2 A and B: Apparent substrate affinities of PAT1-mediated transport currents as a function of membrane potential.**

**A.** Representative PAT1-mediated inward currents induced by different L-Ala concentrations (0.2 mM to 20 mM) at pH<sub>out</sub> 6.5 as a function of membrane potential. **B.** Apparent substrate affinity constants of glycine (■); proline (▲); taurine (○); and betaine (●) as a function of membrane potential in oocytes expressing PAT1 determined by two electrode voltage clamp in Na<sup>+</sup>-free perfusion solutions at pH 6.5. Data represent the K<sub>m</sub> values derived from Eadie-Hofstee transformations of inward currents as a function of substrate concentration and are represented as mean ± SE of 8 oocytes. For error bars not visible, standard error of means are smaller than symbols.

**Figure 3 A-D: PAT1-mediated inward currents induced by different substrate concentrations and varying pH<sub>out</sub> as a function of membrane potential**

**Upper panel:** Currents recorded at 6 different concentrations of glycine (1mM to 20mM) at extracellular pH 5.0 (**A**), or pH 6.5 (**B**) as a function of membrane potential. **Lower panel:** Proton-dependent kinetics of glycine-induced currents determined at 6 different pH values ranging from pH 7.0 to pH 5.5 in the presence of either 2mM glycine (**C**) or 20mM glycine (**D**) as a function of membrane potential. Data are the mean ± SE of average currents determined in 6 individual oocytes. The apparent K<sub>m</sub> and I<sub>max</sub> values derived from these experiments are compiled in Table 1.

**Figure 4 A-C: Recordings of I-V relationships and intracellular pH changes in oocytes expressing PAT1 in the absence of amino acid substrates**

**Upper panel:** Inward currents recorded in oocytes expressing PAT1 (**A**) or water (**B**) injected controls were perfused with Na<sup>+</sup>-free buffer solutions of 6 different pH-values (pH 7.0 to 5.5). Oocytes were clamped to -40 mV, and current-voltage (I-V) relationships were recorded in the potential range between +20 mV and -140 mV. At the end of the experiment oocytes

expressing PAT1 were perfused with 20 mM GABA at pH 5.5 and inward currents of  $900 \pm 89$  nA were obtained for demonstrating the functional PAT1-expression level. No significant changes in the reversal potential could be determined between water-injected and PAT-expressing oocytes upon alterations in  $pH_{out}$  and membrane voltage. Data represent the mean  $\pm$  SE of at least 8 oocytes in each experiment.

**Lower panel:** Representative intracellular pH changes ( $\Delta pH$ ) in oocytes injected with water or PAT1 cRNA and perfused with buffer pH 7.5 or pH 5.0 in the absence of substrate. Oocytes were clamped to -40 mV and intracellular pH as well as holding currents were recorded (holding currents not shown). As a control, at the end of the experiment the functional PAT1-expression level was determined by measuring the current and  $\Delta pH$  induced by 20mM glycine at pH 5.0 (current  $1704 \pm 169$  nA;  $\Delta pH$   $0.57 \pm 0.15$ ;  $n = 3$ ).

**Figure 5 A-D: Comparative analysis of presteady-state and steady-state in oocytes expressing either PEPT1 and PAT1**

**Upper panel:** Current recordings in the absence of substrates for PEPT1 (**A**) and PAT1 (**B**) with fast capacitive current components obtained for both transporters but a slow presteady-state current component only present in PEPT1.

**Lower panel:** Current recordings obtained in the presence of either 20mM glycine-glutamine in case of PEPT1 (**C**) or 20mM glycine in case of PAT1 (**D**) with increased steady currents observed for both transporters but the presteady-state component virtually completely suppressed only in case of PEPT1. For further details, see text.

**Figure 6: PAT1-mediated amino acid-induced outward transport currents measured in two electrode voltage clamp experiments.**

A representative current trace as obtained in an oocyte expressing PAT1 and clamped at -40 mV while continuously superfused for 4 min with 20mM glycine at  $pH_{out}$  5.5, followed by a fast wash out with a substrate-free buffer solution of pH 7.5.

**Figure 7 A and B: Demonstration of PAT1-mediated amino acid efflux.**

**A.** Individual oocytes were injected with 5 nmol of L-Pro (including 1pmol of L- $^3H$ Pro as a tracer) and efflux was measured in the absence (○) or the presence of 20 mM glycine (■), and alanine (●) in the incubation medium. Efflux of L- $^3H$ Pro from water-injected control oocytes is also shown (○).

**B.** PAT1-mediated efflux of proline from preloaded oocytes (injection of 5 nmol of L-Pro including 1pmol of L- $^3H$  per oocyte) as a function of increasing concentrations of glycine (1mM to 20 mM) in the incubation buffer. Efflux rates of labelled L-Pro were determined after

10 min of incubation under the various conditions and represent the mean  $\pm$  SE of at least 8 oocytes per variable.

**Figure 8 A-D: PAT1-mediated amino acid-induced outward currents determined in giant patch clamp experiments.**

**A.** Recording of an I-V relationship as difference curves in the presence and the absence of increasing concentrations of D-alanine (0 to 50 mM) at the cytosolic side in response to potential pulses between -80 and +60 mV. The pH of the buffer solutions was 7.5 on both sides of the membrane. **B.** Kinetics of D-alanine-induced outward currents as a function of substrate concentration at pH 7.5 on both sides and holding potentials of +60 mV (■); +30 mV (▲) and 0 mV (▼). Presented is the mean  $\pm$  SE from 6 different oocytes. Note that  $K_m$  values presented in the text and tables are the means of constants as calculated from individual oocytes. **C.** Apparent  $K_m$  values for a variety of substrates as derived from kinetic analysis of transport for the inward and outward directions. Transport currents for the outward direction were determined by the GPC technique in Na<sup>+</sup>-free perfusion solutions containing the different substrates at a  $V_m$  of +60 mV (pH 7.5 at both sides). Transport currents for inward-directed transport were determined under the same experimental conditions in TEVC experiments in Na<sup>+</sup>-free perfusion solutions containing the different substrates at a  $V_m$  of -60 mV (pH<sub>out</sub> 7.5). Based on current-voltage (I-V) relationships  $K_m$  values were determined by fitting the data to the Michaelis-Menten equation. **D.** Apparent  $K_m$  values for PAT1-mediated transport in the outward direction as a function of membrane potential. Data represent the mean  $\pm$  SE of at least 6 oocytes perfusion with either glycine (■); proline (▲); betaine ( ) or alanine (●). If error bars are visible, standard error of means is smaller than symbol.

**Table 1: Kinetic constants for H<sup>+</sup>-dependent and glycine-dependent transport currents as a function of membrane potential**

The apparent  $K_m$  values for glycine were determined in TEVC studies in individual oocytes at two different  $pH_{out}$  (6.5 and 5.0) using 5 different glycine concentrations (1mM to 20mM). Additionally, apparent proton affinity constants ( $K_m^{[H^+]}$ ) were determined in individual oocytes at two different glycine concentrations (2mM and 20mM) and at pH-values varying between 7.0 and 5.0. Substrate induced currents were transformed according to Eadie-Hofstee and  $K_m$  and  $I_{max}$  values were calculated by linear regression analysis. Currents are normalized to the maximum current observed in an individual oocyte at  $pH_{out}$  6.5 ( $I/I_{[H^+] pH6.5}$ ) or at 2 mM glycine ( $I/I_{[Gly] 2mM}$ ).  $K_m$  and  $I_{max}$  values are presented as the mean  $\pm$  SE of at least 6 independent experiments.

Condition	$V_m$ (mV)	$K_m$ Gly (mM)	$I/I_{pH 6.5}$
<b>pH 6.5</b>	-100	9.6 $\pm$ 0.5	1
	-60	13.1 $\pm$ 1.0	1
	-20	13.5 $\pm$ 1.4	1
<b>pH 5.0</b>	-100	5.5 $\pm$ 0.6	1.26 $\pm$ 0.10
	-60	6.0 $\pm$ 0.6	1.40 $\pm$ 0.12
	-20	6.4 $\pm$ 0.5	1.55 $\pm$ 0.09
		$K_m$ H <sup>+</sup> (nM)	$I/I_{[Gly] 2mM}$
<b>2 mM Gly</b>	-100	361 $\pm$ 38	1
	-60	554 $\pm$ 61	1
	-20	861 $\pm$ 80	1
<b>20 mM Gly</b>	-100	77 $\pm$ 15	2.37 $\pm$ 0.28
	-60	130 $\pm$ 18	2.45 $\pm$ 0.29
	-20	194 $\pm$ 27	2.37 $\pm$ 0.25

Figure 1

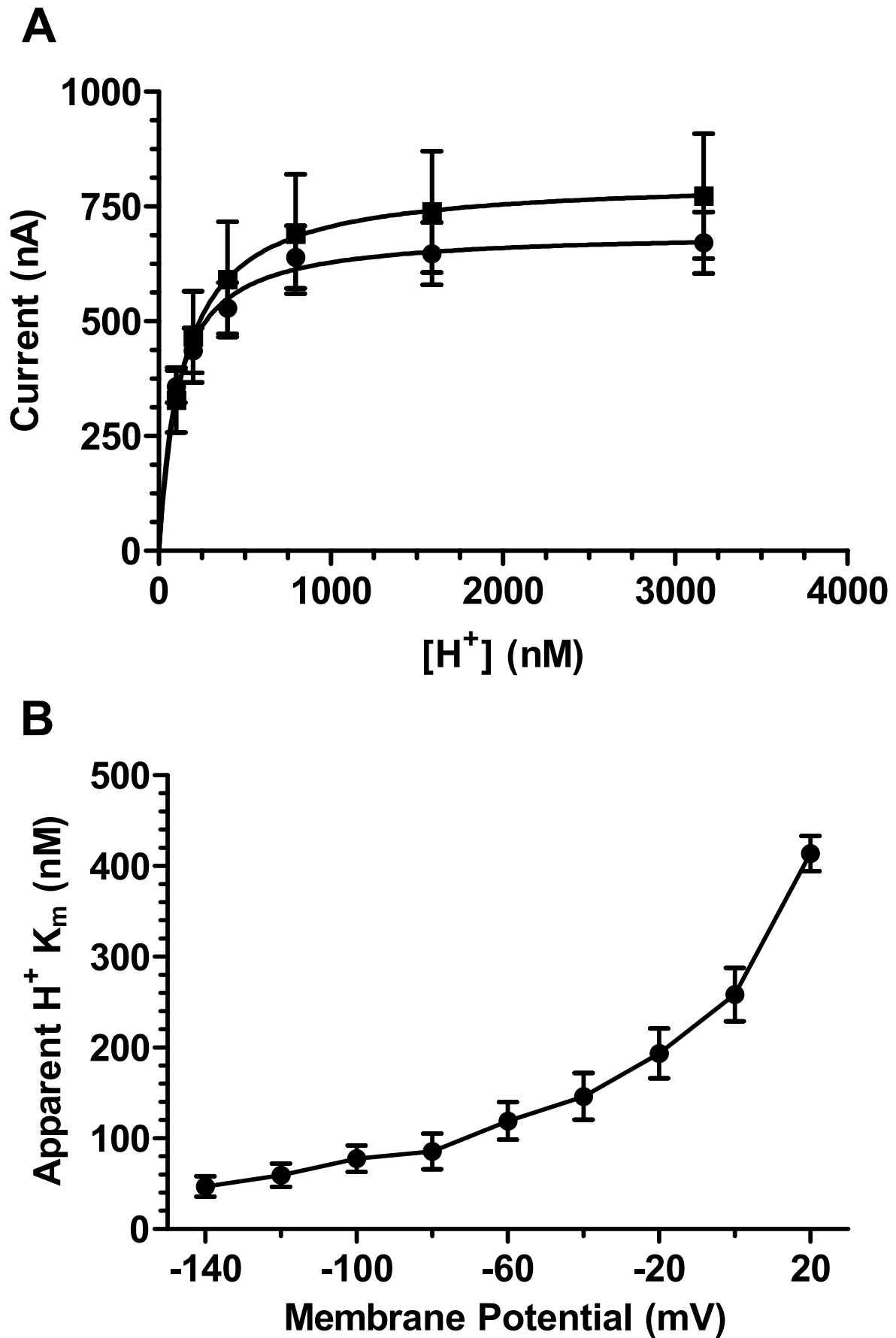


Figure 2

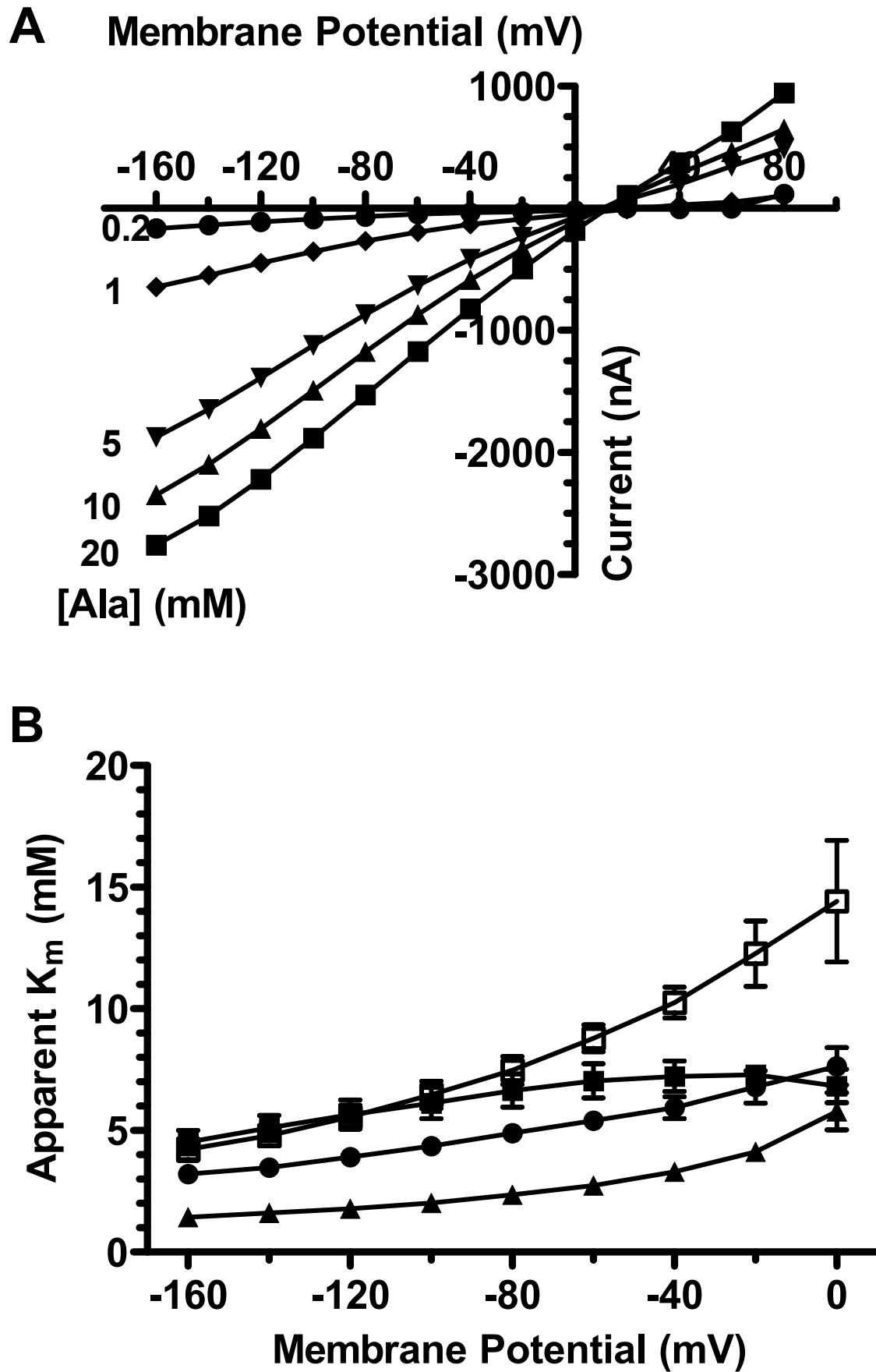


Figure 3

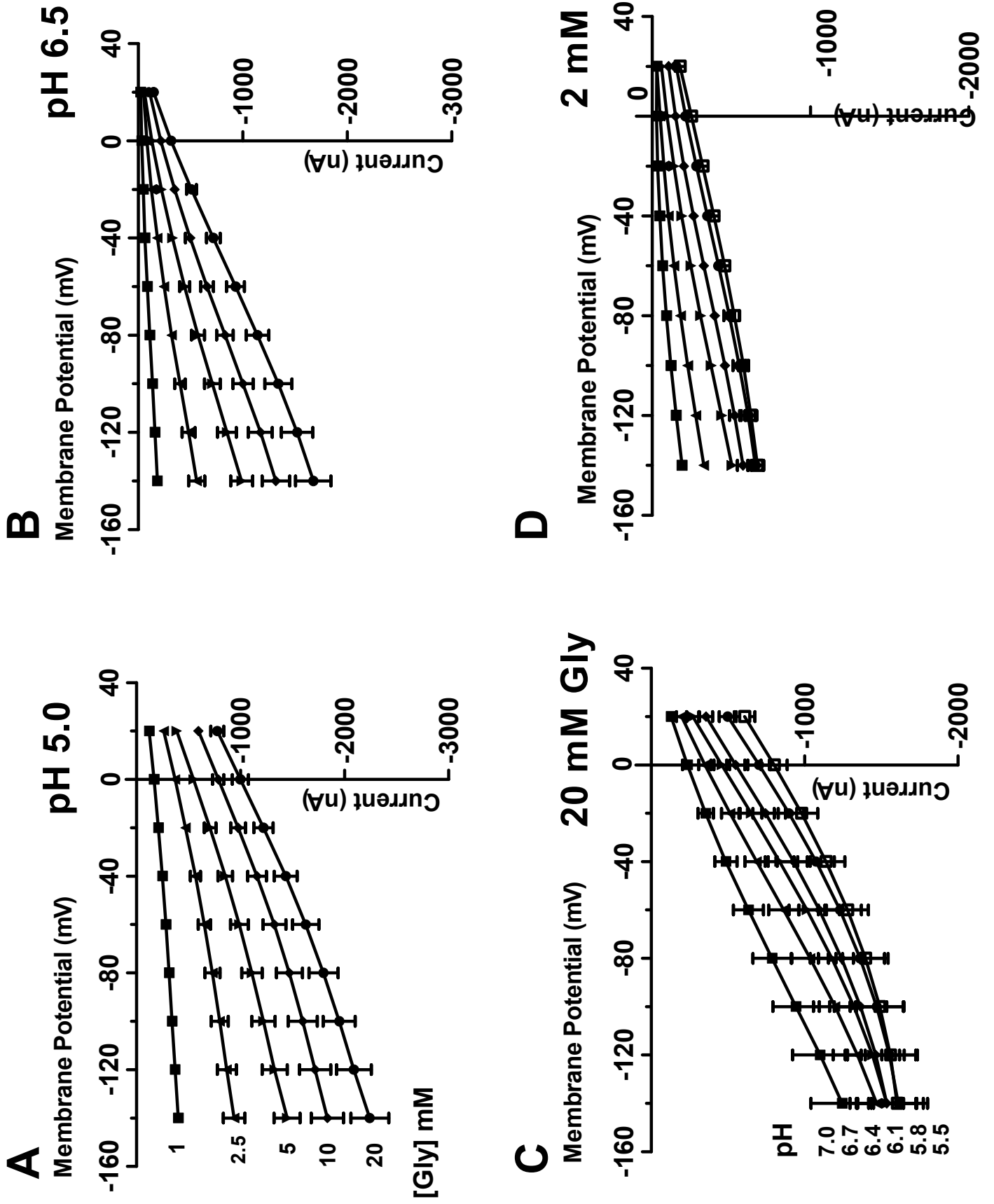


Figure 4

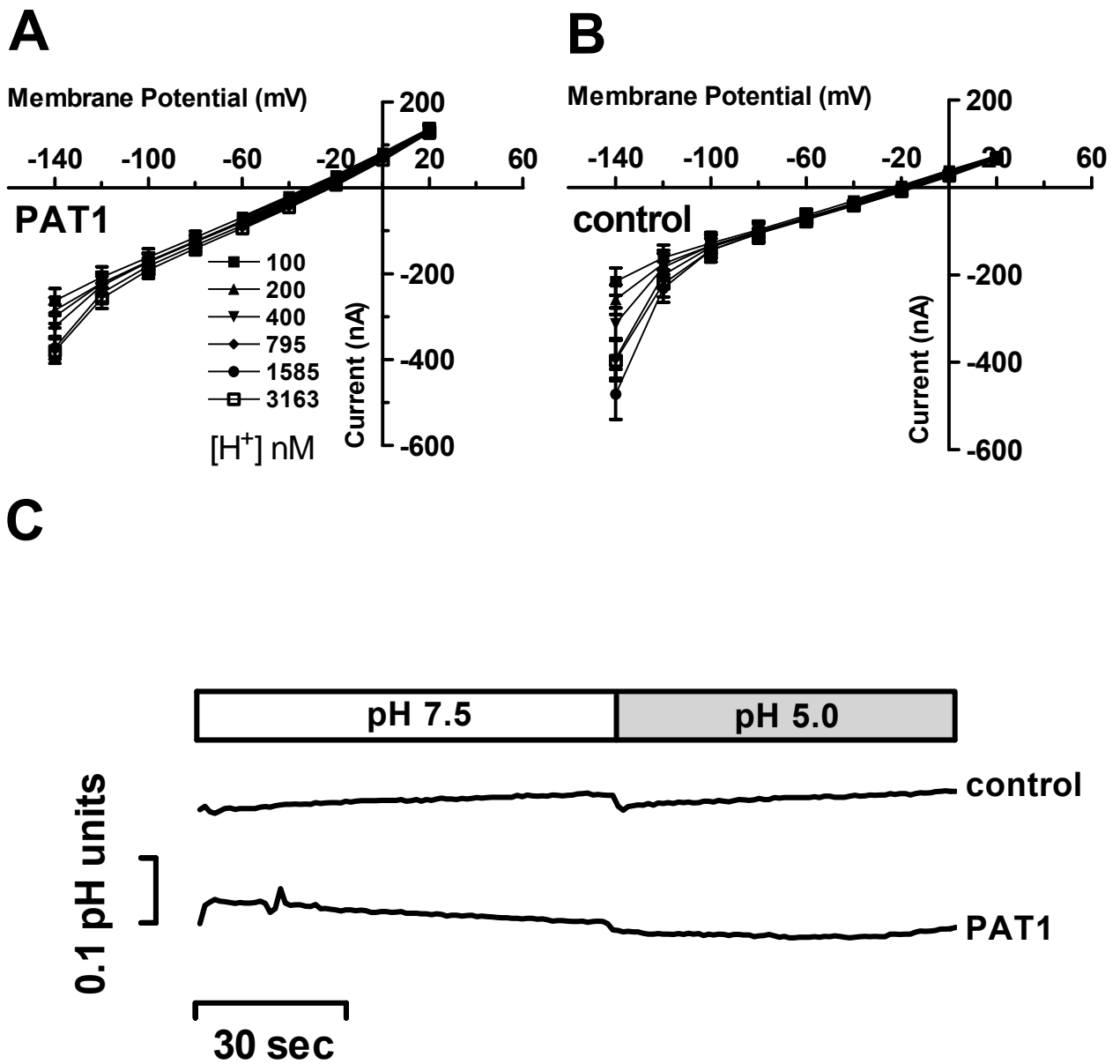


Figure 5

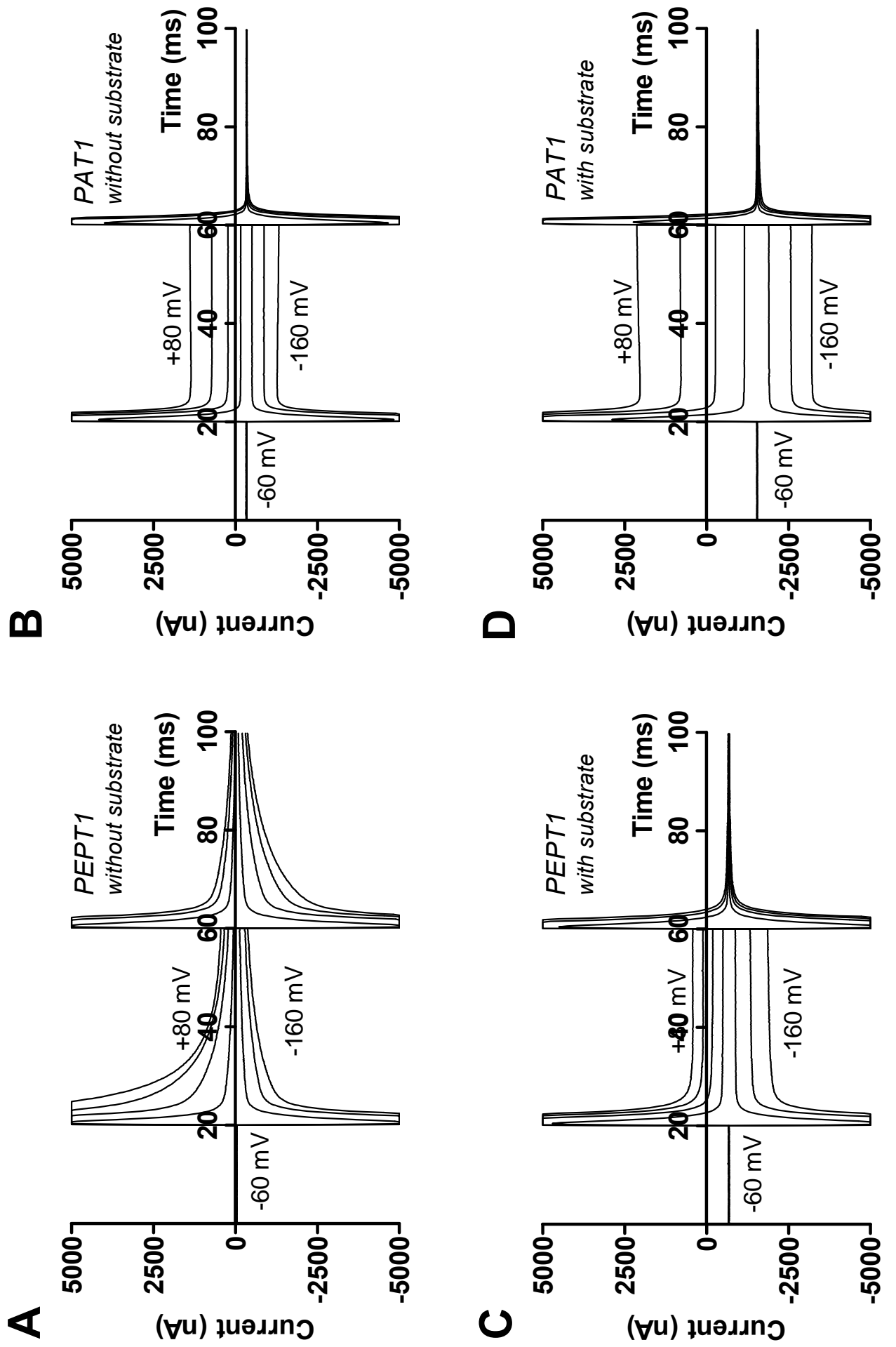


Figure 6

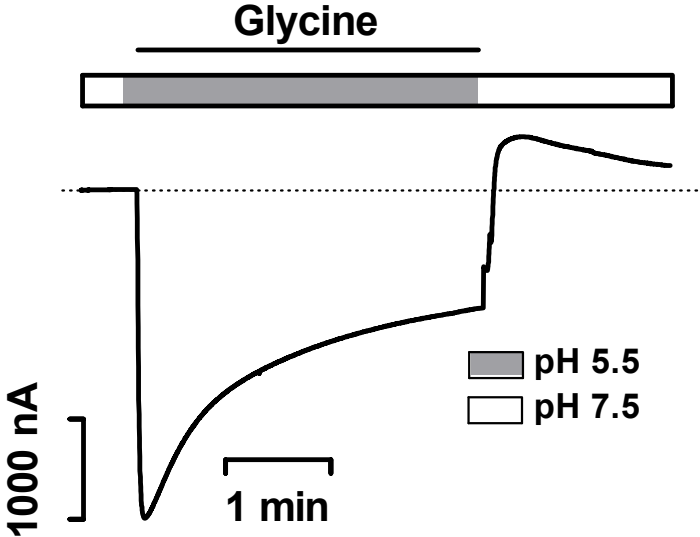


Figure 7

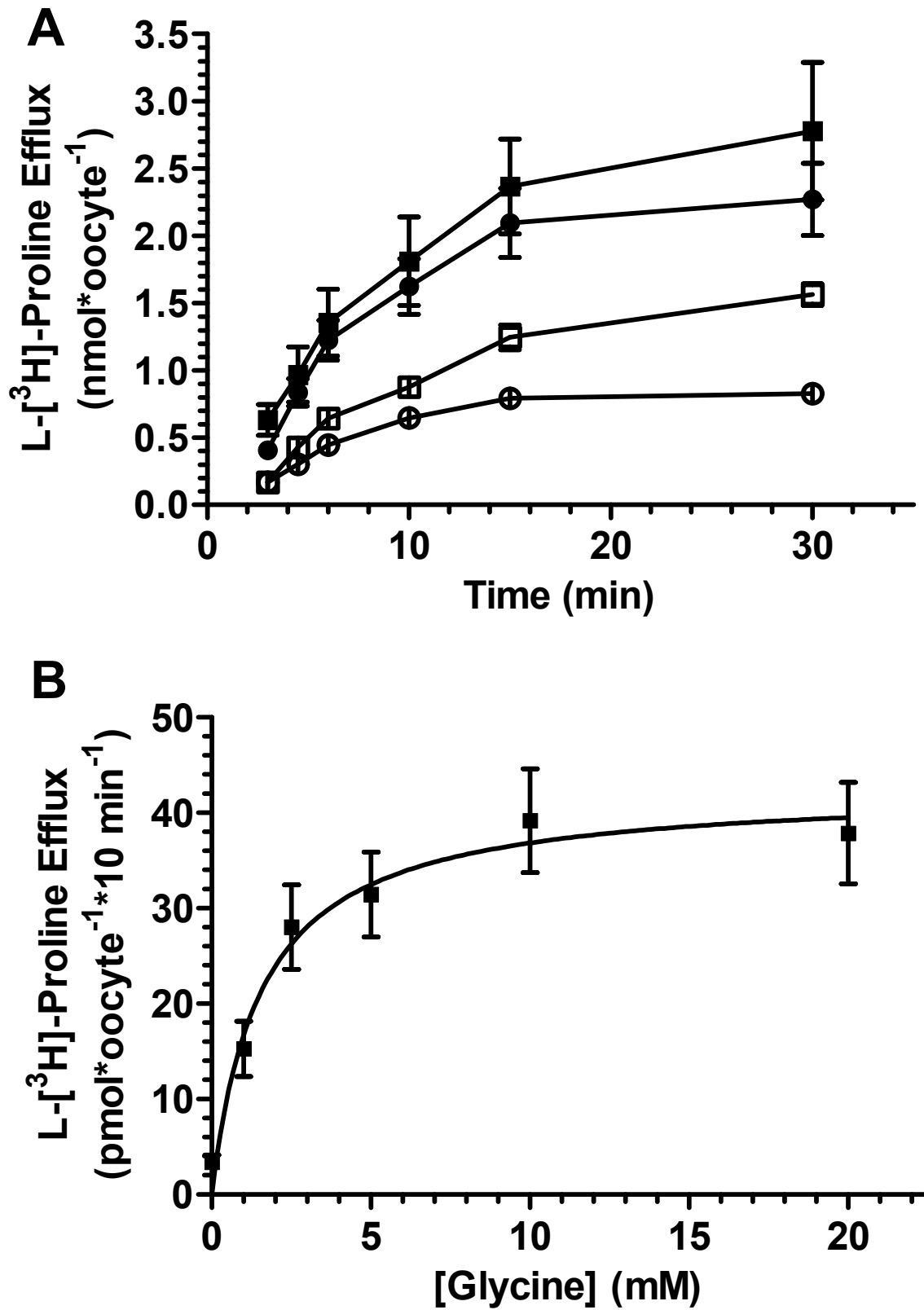
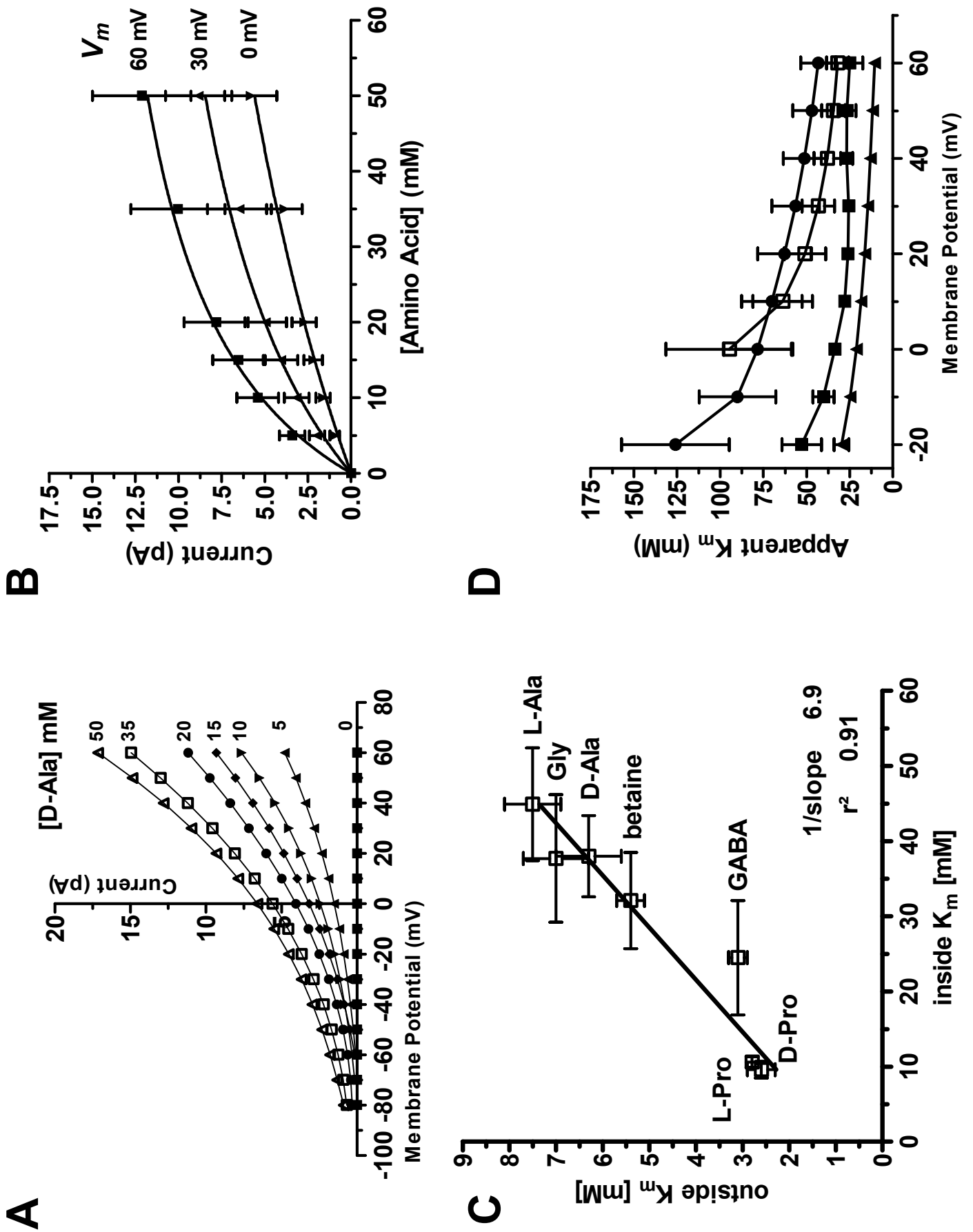


Figure 8



## APPENDIX 7

published in *European Journal of Biochemistry*

## Substrate specificity and transport mode of the proton-dependent amino acid transporter mPAT2

Martin Foltz, Carmen Oechsler, Michael Boll, Gabor Kottra and Hannelore Daniel

Molecular Nutrition Unit, Center of Life and Food Sciences, Technical University of Munich, Germany

The PAT2 transporter has been shown to act as an electrogenic proton/amino acid symporter. The PAT2 cDNA has been cloned from various human, mouse and rat tissues and belongs to a group of four genes (*pat1* to *pat4*) with PAT3 and PAT4 still resembling orphan transporters. The first immunolocalization studies demonstrated that the PAT2 protein is found in the murine central nervous system in neuronal cells with a proposed role in the intra and/or intercellular amino acid transport. Here we provide a detailed analysis of the transport mode and substrate specificity of the murine PAT2 transporter after expression in *Xenopus laevis* oocytes, by electrophysiological techniques and flux studies. The structural requirements to the PAT2 substrates – when considering both low and high affinity type substrates – are similar to those reported for the PAT1 protein with the essential features of a free carboxy group and a small side chain. For high affinity binding, however,

PAT2 requires the amino group to be located in an  $\alpha$ -position, tolerates only one methyl function attached to the amino group and is highly selective for the L-enantiomers. Electrophysiological analysis revealed pronounced effects of membrane potential on proton binding affinity, but substrate affinities and maximal transport currents only modestly respond to changes in membrane voltage. Whereas substrate affinity is dependent on extracellular pH, proton binding affinity to PAT2 is substrate-independent, favouring a sequential binding of proton followed by substrate. Maximal transport currents are substrate-dependent which suggests that the translocation of the loaded carrier to the internal side is the rate-limiting step.

**Keywords:** electrophysiology; functional characterization; proton symporter; substrate recognition; transport mode.

The proton/amino acid transporter family PAT (SLC36) has been identified from human, mouse and rat origin during the last three years [1–7]. The PAT family is comprised of four members (PAT1–PAT4, SLC36A1–4); the PAT proteins consist of around 470–500 amino acids and are thought to represent integral membrane proteins with a > 60% similarity to each other [8]. The orthologous proteins from mouse, rat and human show an identity of more than 90% to each other. The expression pattern of the four different transporter mRNAs is quite different. The PAT1 mRNA shows widespread expression with high levels in brain, intestine and kidney whereas the PAT2 mRNA is highly abundant in lung, kidney and brain. PAT3 mRNA is found solely in testis, whereas PAT4 mRNA shows ubiquitous expression [8].

So far, only PAT1 and PAT2 have been characterized functionally. They have an exceptional position among the mammalian amino acid transporters, as they act as electrogenic amino acid/proton symporters. Transport is depend-

ent on the extracellular pH, but is independent of sodium, chloride, and potassium ions [1,2,4,7]. Moreover, PAT1 and PAT2 mediated amino acid influx leads to a pronounced intracellular acidification [2,9] by cotransport of the zwitterionic amino acid substrates and protons with a stoichiometric coupling of 1 : 1 as shown for the model substrate L-proline [2]. Substrates of both transporters are the small apolar amino acids glycine, L-alanine, and L-proline [1,2,4–8]. Besides these common functional properties, distinct differences became obvious within substrate recognition and electrophysiological characteristics of the two transporters. PAT2 represents the high affinity transporter type with apparent  $K_m$  values for its substrate in the range of 100–700  $\mu\text{M}$ , whereas those of PAT1 are in the range of 1–15 mM [2,7,9,10]. PAT1 recognizes, besides L- $\alpha$  amino acids, a number of additional substrates, e.g.  $\beta$ -alanine,  $\gamma$ -aminobutyrate (GABA), betaine, D-Ser, and D-Ala [1,2,5,6,9], whereas for the PAT2 transporter only sarcosine has been identified as an additional high affinity substrate beside the normal L- $\alpha$  amino acid substrates [2,10].

Recent studies on PAT1 suggest it to play a dual role in mammalian cells [8]. Based on its localization in lysosomal membranes in neurons [1,6] it is considered to act as an export system for amino acids out of lysosomes after their intralysosomal release from proteolytic processes. However, in intestinal epithelial cells PAT1 is responsible for the proton-dependent absorption of small amino acids and derivatives in the small intestine, as shown by its endogenous functional expression in the apical membrane of the human intestinal cell line Caco-2 [4,11]. In contrast, the

Correspondence to H. Daniel, Center of Life and Food Sciences, Technical University of Munich, Hochfeldweg 2, D-85350 Freising-Weißenstephan, Germany. Fax: + 49 8161 71 3999, Tel.: + 49 8161 71 3400, E-mail: daniel@wzw.tum.de

Abbreviations: GABA,  $\gamma$ -aminobutyrate; PAT, proton/amino acid transporter; mPAT2, murine proton/amino acid transporter 2; OH-Pro, L-4-hydroxyproline; I–V, current–voltage.

(Received 7 May 2004, revised 21 June 2004, accepted 24 June 2004)

© FEBS 2004

Functional properties of mPAT2 (*Eur. J. Biochem.* 271) 3341

physiological role of the PAT2 transporter is currently not known. We previously reported the PAT2 protein expression pattern in the mouse brain [10] and demonstrated that it is highly expressed in *N*-methyl-D-aspartate receptor positive neuronal cells throughout the central nervous system. The subcellular localization differs markedly from that of PAT1 in neuronal cells with a lack of detection in lysosomes, but localization in recycling endosomes and endoplasmic reticulum. Whether the endoplasmic reticulum localization is due to a specific role of PAT2 in this compartment or whether it just represents newly synthesized transporters is not clear yet. The localization in recycling endosomes suggests a possible insertion of PAT2 into the neuronal plasma membrane and we proposed PAT2 as a candidate protein for the still missing Na<sup>+</sup>-independent low affinity glycine transport system in the central nervous system [12,13]. PAT2 could be responsible, along with the high affinity glycine transporters GLYT1 and GLYT2, for the regulation of intracellular and extracellular concentrations of glycine that modulate glycinergic and glutamatergic neurotransmission [14,15]. Moreover, Bermingham *et al.* suggested a role for PAT2 in the differentiation of Schwann cells in rat sciatic nerves [3]. In other tissues than the nervous system, cellular and subcellular expression pattern of the PAT2 protein have not been examined so far, although the mRNA is expressed in various organs such as in lung, kidney, and heart [2,5,7].

To get a better understanding of the physiological function of the PAT2 transporter in the various cell types and organelles, we here provide a detailed functional analysis of the murine PAT2 (mPAT2) protein when expressed in *Xenopus laevis* oocytes. We explored the substrate recognition parameters and describe the critical features for high affinity substrate binding. Moreover, we demonstrate that there is no proton-leak pathway and that the kinetic parameters depend on the membrane potential and the proton electrochemical gradient that in turn support the existence of an ordered binding mechanism for protons and substrate.

## Materials and methods

### Materials

All experiments with *Xenopus laevis* followed our institutional guidelines for care and handling of laboratory animals, in full agreement with the German guidelines, and the studies were approved by the state ethics committee. *Xenopus laevis* frogs were purchased from Nasco (Fort Atkinson, WI, USA). Amino acids and related compounds were obtained from Sigma Chemie (Deisenhofen, Germany) or Merck (Darmstadt, Germany) of pro analysi quality. Salts and all other chemicals were obtained from Sigma and Carl Roth AG (Karlsruhe, Germany) of pro analysi quality. L-[3,4-<sup>3</sup>H]proline (specific activity 60 Ci·mmol<sup>-1</sup>) was purchased from ICN (Irvine, CA, USA). Collagenase A was obtained from Roche Molecular Biochemicals (Mannheim, Germany).

### *Xenopus laevis* oocytes handling and cRNA injection

Oocytes were treated with collagenase A (Roche Diagnostics) for 1.5–2 h at room temperature in Ca<sup>2+</sup>-free ORII

solution (82.5 mM NaCl, 2 mM KCl, 1 mM MgCl<sub>2</sub> and 10 mM Hepes, pH 7.5) to remove follicular cells. After sorting, healthy oocytes of stage V and VI were kept at 18 °C in modified Barth solution containing 88 mM NaCl, 1 mM KCl, 0.8 mM MgSO<sub>4</sub>, 0.4 mM CaCl<sub>2</sub>, 0.3 mM Ca(NO<sub>3</sub>)<sub>2</sub>, 2.4 mM NaHCO<sub>3</sub> and 10 mM Hepes (pH 7.5). The next day oocytes were injected with 27 nL sterile water (control) or 27 nL mPAT2-cRNA (27 ng cRNA·oocyte<sup>-1</sup>). The oocytes were kept in modified Barth solution at 18 °C until further use (3–5 days after injection).

### Amino acid uptake

Ten oocytes (water- or cRNA-injected) per uptake experiment were preincubated at room temperature for 2 min in Na<sup>+</sup>-free standard uptake buffer (100 mM choline chloride, 2 mM KCl, 1 mM MgCl<sub>2</sub>, 1 mM CaCl<sub>2</sub>, 10 mM MES pH 6.5). The buffer was then replaced by the respective uptake buffer supplemented with 100 μM L-proline including L-[3,4-<sup>3</sup>H]proline as a tracer (5 μCi·mL<sup>-1</sup>) without (control) or with the addition of 10 mM of the test compounds. After 10 min of incubation, the oocytes were washed three times with 3 mL of ice cold uptake buffer and immediately distributed to individual vials. After oocyte lysis in 10% (w/v) SDS, radioactivity was counted by liquid scintillation.

### Two-electrode voltage clamp

Two-electrode voltage clamp experiments were performed as described previously [2]. Briefly, the oocyte was placed in an open chamber and continuously superfused with incubation buffer (100 mM choline chloride, 2 mM KCl, 1 mM MgCl<sub>2</sub>, 1 mM CaCl<sub>2</sub>, 10 mM MES or HEPES at pH 5.5–8.5) in the absence or presence of amino acids. Oocytes were voltage clamped at –60 mV, and current–voltage (I–V) relations were measured using short (100 ms) pulses separated by 200 ms pauses in the potential range –160 to +80 mV. I–V measurements were made immediately before and 20–30 s after substrate application when current flow reached steady state. The current evoked by PAT2 at a given membrane potential was calculated as the difference between the currents measured in the presence and the absence of substrate. Substrate concentration kinetics were constructed from experiments employing five different amino acid concentrations in Na<sup>+</sup>-free buffer at pH 6.5 with five to seven individual mPAT2 expressing oocytes from at least two different oocyte batches for each substrate. The buffer pH of 6.5 was chosen to measure under full proton saturating conditions and additionally to ensure high enough inward currents even at lower expression level. Substrate-evoked currents were transformed according to Eadie–Hofstee and after linear regression the apparent substrate concentrations that cause half-maximal transport activity (apparent K<sub>m</sub>) were derived. Kinetics of substrate transport as a function of external proton concentration (apparent proton activity) were performed under substrate saturation with either 20 mM alanine or proline. The standard incubation medium was buffered with 10 mM Tris and adjusted to pH values between pH 7.5 and pH 9.0. The apparent K<sub>m</sub> values for proton binding were derived by linear regression after Eadie–Hofstee transformation of

3342 M. Foltz *et al.* (*Eur. J. Biochem.* 271)

© FEBS 2004

inward currents induced by six different external pH values. Data points in all cases could be best-fit by linear regression analysis after transformation according to Eadie–Hofstee to a single kinetic term excluding the possibility that kinetic parameters are substantially affected by unspecific proton binding effects or via an allosteric proton binding site.

### Statistics

All calculations (linear as well as nonlinear regression analyses) were performed using PRISM software (version 4.01, GraphPad, San Diego, CA, USA). Data are presented as mean  $\pm$  SEM. If error bars are not visible within the graphs, they are smaller than the symbols. Statistically significant differences were determined using ANOVA analysis followed by Newman–Keuls multiple comparison test.

### Results

To elucidate the minimal structural requirements which determine the high affinity phenotype of PAT2 a set of amino acids and derivatives divided into different categories with differences in (a) side chain size, (b) backbone length, (c) O- and N-methyl substitutions, (d) stereochemistry and (e) polarity were analysed.

The size of the amino acid side chain was shown to be a critical determinant for substrate interaction with PAT2. Only glycine and alanine were able to induce comparable inward currents in oocytes expressing PAT2 with a high affinity interaction (Fig. 1A and Table 1). The elongation of the side chain by just by one CH<sub>2</sub> unit leading to L- $\alpha$ -amino butyric acid led to a dramatic decrease in substrate

affinity and transport currents (Table 1) and further side chain elongations completely abolished substrate–PAT2 interactions (Table 1). The intramolecular distance between the charged amino- and carboxy-head groups is an even stronger recognition criterion for high affinity. The introduction of one CH<sub>2</sub> unit as in  $\beta$ -alanine substantially reduced PAT2-mediated inward currents paralleled by a pronounced decline in affinity, when compared to glycine or alanine (Table 1). Whereas a further elongation of the backbone as in GABA further decreased inward currents and affinity,  $\delta$ -aminopentanoate or  $\epsilon$ -aminohexanoate failed to induce any transport currents (Table 1). Methyl-substitutions at the amino- or carboxy-group of the  $\alpha$ -amino acids had a differential effect on substrate affinity and transport by PAT2. O-methyl esters of glycine or alanine do not serve as substrates whereas a single N-methylation as in sarcosine is well tolerated as shown by high affinity interaction and high transport currents. However incorporation of a second and third methyl moiety at the amino group as in N,N-dimethylglycine and betaine led to a sequential reduction in PAT2 transport currents as well as markedly lower binding affinity (Fig. 1C and Table 1).

PAT2 does not discriminate completely between D-amino acids as substrates but shows a structure-dependent enantioselectivity. Out of the tested D-amino acids, only D-proline was able to interact in a high affinity mode, D-serine and D-alanine displayed much lower affinities and for D-cysteine no interaction was observed (Table 1). Interestingly, transport currents of the three interacting D-amino acids are not very different to each other despite quite marked differences in affinity, but were substantially lower to those of the reference substrate glycine. This is striking in the case

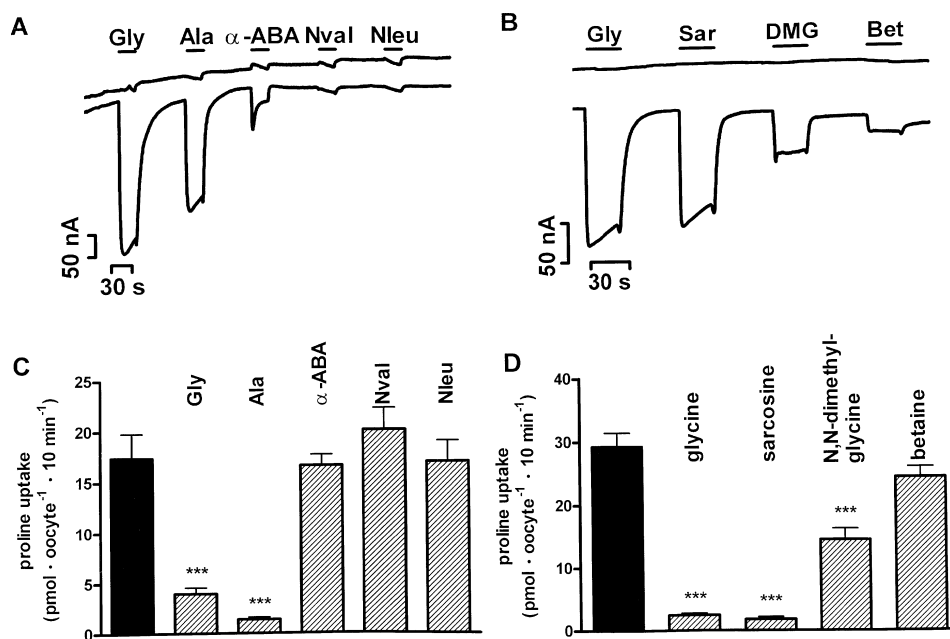


**Fig. 1. Substrate specificity of mPAT2.** (A,B) Representative current traces of oocytes expressing mPAT2 in response to perfusion with 20 mM of the different substrates in Na<sup>+</sup>-free buffer at pH 6.5. (C,D) Inhibition of [<sup>3</sup>H]proline uptake by L- $\alpha$ -amino acids with increasing side chain length (C) or various N-methylated glycines (D). Data represent the specific PAT2-mediated proline uptake in the absence (filled bar) or presence (hatched bars) of 10 mM of competing test compound in Na<sup>+</sup>-free buffer at pH 6.5 (mean  $\pm$  SEM, n = 6–8); \*\*\*, P < 0.001.

© FEBS 2004

Functional properties of mPAT2 (*Eur. J. Biochem.* 271) 3343

**Table 1. Apparent substrate affinities and transport currents of amino acids and derivatives as well as the corresponding inhibitory effect on the uptake of the radiolabelled tracer proline as determined for mPAT2 after expression in *Xenopus* oocytes.** Substrate dependent inward currents as a function of substrate concentration were recorded and transformed according to Eadie–Hofstee to derive the apparent  $K_m$  values by linear regression analysis. Data are presented as the mean  $\pm$  SEM of  $n = 5$ –7 oocytes in each experiment. % $I_{20\text{ mM}}$  ( $I_{\text{Gly}} = 100\%$ ), data are presented as normalized currents (mean  $\pm$  SEM,  $n = 5$ –7) for every test compound at 20 mM relative to the maximal currents of 20 mM glycine at pH 6.5 and at a membrane potential of  $-60$  mV. Compounds with an  $I_{20\text{ mM}}$  not higher than background values as observed in water-injected oocytes ( $P > 0.05$ , Students paired  $t$ -test) are given as  $< 5\%$ . Uptake of L-[ $^3\text{H}$ ]proline (100  $\mu\text{M}$ ) was measured at pH 6.5 for 10 min in the presence of unlabeled amino acids and derivatives at a fixed concentration of 10 mM and are given as percentage inhibition of the control uptake measured in the absence of inhibitor. Data are means  $\pm$  SEM ( $n = 8$ –10). ND, not determined.

Substrate	Apparent $K_m$ value (mM)	% $I_{20\text{ mM}}$ ( $I_{\text{Gly}} = 100\%$ )	% Inhibition of control uptake
Elongation of the side chain			
glycine	0.59 $\pm$ 0.04 <sup>a</sup>	100	90.5 $\pm$ 2.3
L-Alanine	0.25 $\pm$ 0.05 <sup>a</sup>	65.3 $\pm$ 2.6 <sup>a</sup>	95.9 $\pm$ 1.5
L- $\alpha$ -Aminobutyric acid	20.0 $\pm$ 1.5	10.6 $\pm$ 2.0	25.9 $\pm$ 7.3
L-Norvaline	ND	< 5	22.9 $\pm$ 7.6
L-Norleucine	ND	< 5	< 5
Elongation of the backbone			
$\beta$ -Alanine	14.8 $\pm$ 2.5	36.6 $\pm$ 0.7	59.9 $\pm$ 1.3
$\gamma$ -Aminobutyric acid	> 25 <sup>a</sup>	15.3 $\pm$ 0.9	28.5 $\pm$ 5.7
$\delta$ -Aminopentanoic acid	ND	< 5	< 5
$\epsilon$ -Aminohexanoic acid	ND	< 5	10.5 $\pm$ 8.4
O-Methyl substitution			
O-Methyl-glycine	ND	< 5	< 5
O-Methyl-alanine	ND	< 5	6.0 $\pm$ 3.4
N-Methylated glycines			
Sarcosine	0.21 $\pm$ 0.01 <sup>a</sup>	93.8 $\pm$ 3.4	94.3 $\pm$ 1.2
<i>N,N</i> -dimethylglycine	14.7 $\pm$ 2.4	34.2 $\pm$ 2.5	55.3 $\pm$ 5.4
Betaine	> 25	9.4 $\pm$ 1.9	26.9 $\pm$ 7.0
D-Enantiomers			
D-Alanine	6.5 $\pm$ 1.1 <sup>a</sup>	31.2 $\pm$ 1.9	ND
D-Serine	14.7 $\pm$ 0.5	25.4 $\pm$ 2.1	ND
D-Cysteine	ND	< 5	ND
D-Proline	0.25 $\pm$ 0.09	29.9 $\pm$ 0.7	ND
Polar L- $\alpha$ -amino acids			
L-Ser	> 25 <sup>a</sup>	14.5 $\pm$ 0.6 <sup>a</sup>	< 5
L-Cys	ND	< 5	< 5
L-4-Hydroxy-proline	0.72 $\pm$ 0.10	37.2 $\pm$ 1.3	ND

<sup>a</sup>  $K_m$  and % $I_{20\text{ mM}}$  values taken from our previous studies [2,10].

of praline, with 30% of maximal glycine currents at 20 mM concentration and a fairly high affinity of 0.25  $\pm$  0.09 mM. This may be interpreted as the first evidence for a restricted velocity in the translocation step of the loaded transporter by the steric conformation of the substrate.

The introduction of polar side groups in the aliphatic  $\alpha$ -amino acids led to dramatic decreases in transport currents and affinity, as shown for L-cysteine and L-serine (Table 1). However, the polar residue in L-4-hydroxy-proline (OH-Pro) was able to interact in a high affinity mode, although transport currents were substantially smaller when compared to those of glycine. We also studied the potency of various compounds for inhibition of PAT2-mediated proline uptake in *Xenopus laevis* oocytes. The inhibition rates were in close relationship to the apparent affinities as determined by electrophysiology, as shown for  $\alpha$ -amino acids with increasing side chain length as well as for the N-methylated glycines (Fig. 1C,D). This correlation was also observed with all other tested amino acids (Table 1).

Concentration dependent substrate induced transport currents always followed single component saturation

kinetics, as shown for D-proline and  $\beta$ -alanine (Fig. 2). Substrate affinities were, for most compounds, only modestly dependent or independent on changes in membrane potential (Fig. 3A). The apparent  $K_m$  values of D-Pro, D-Ala and OH-Pro increased only 1.5- and 2.1-fold by depolarizing the membrane from  $-120$  to  $-20$  mV. On the other hand, the affinity of  $\beta$ -Ala did not change significantly within this potential range. Maximal transport currents for the various substrates are essentially independent of the membrane potential (Fig. 3B) with changes of less than 30% by alterations of membrane voltage from  $-120$  to  $-20$  mV for all tested substrates.

Next, we addressed the question of whether the substrate affinity depends on extracellular pH, by determining the apparent  $K_m$  values of glycine and alanine at pH values of pH 5.5–8.5 (Fig. 4) and a broad range of membrane potentials. At hyperpolarized membrane potentials  $K_m$  values of glycine and alanine were relatively insensitive towards voltage (Fig. 4A,B). When increasing the pH in the extracellular medium, voltage dependence of the  $K_m$  values became pronounced with a severe reduction in affinity at

3344 M. Foltz *et al.* (*Eur. J. Biochem.* 271)

© FEBS 2004

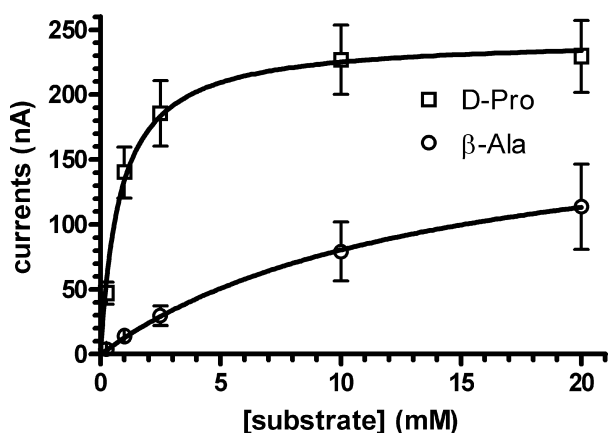


Fig. 2. PAT2-mediated inward currents as a function of substrate concentration. PAT2 expressing oocytes clamped at  $-60$  mV were perfused with increasing concentrations (0.25–20 mM) of D-proline ( $\square$ ) or  $\beta$ -alanine ( $\circ$ ) at an extracellular pH of 6.5. The curves were fitted to a Michaelis–Menten kinetic by nonlinear regression analysis ( $R^2 = 0.78$  and 0.81, respectively). Data represent the mean  $\pm$  SEM ( $n = 5$ ).

neutral and more alkaline pH values for both amino acids at a membrane potential of  $-60$  mV (Fig. 4C). This strongly suggested that the apparent proton concentration (activity) at the outside substrate binding domain affects substrate affinity in a voltage-dependent manner. We therefore varied the extracellular pH from pH 9.0–7.5 at saturating substrate concentration (20 mM alanine or proline) in small pH-steps and recorded currents in the membrane potential range from  $-140$  to  $+20$  mV. As shown in Fig. 5A inward currents increased by lowering extracellular pH, and followed Michaelis–Menten kinetics as a function of external proton concentration, as shown for various voltage steps in Fig. 5B. After Eadie–Hofstee transformation, for each recorded membrane potential the apparent proton binding affinity constant (apparent  $K_m$  value) was determined. The data in all cases could be fitted best to a single kinetics, almost excluding a significant contribution of nonspecific pH-effects and excluding a co-operative (e.g. allosteric) proton binding mechanism. Apparent proton affinities in the presence of alanine and proline at  $-60$  mV were as high as  $0.83 \pm 0.21$  nM and  $0.49 \pm 0.10$  nM, respectively. These values correspond to a pH of 9.1 and pH 9.3 and suggest that PAT2 under physiological conditions at extracellular pH values of 6.8–7.4 operates essentially independent of pH. The apparent proton binding affinities at a given membrane potential were independent of the substrate used but highly dependent on the membrane potential (Fig. 5C). A depolarization of the oocyte membrane from  $-120$  mV to  $-20$  mV led to a 10- to 15-fold decrease in apparent proton affinity in the presence of substrate which suggests that membrane voltage changes are the most critical parameters in PAT2-mediated transport *in vivo*.

To assess whether PAT2 possesses a proton shunt pathway in the absence of substrate by a channel/pore like activity in an uncoupled mode, pH jump studies were performed. Accordingly, membrane potential-dependent currents in PAT2-expressing oocytes were recorded at pH 9.0 and pH 7.5 in the absence of any substrate (Fig. 5D). The I–V relationship did not significantly change

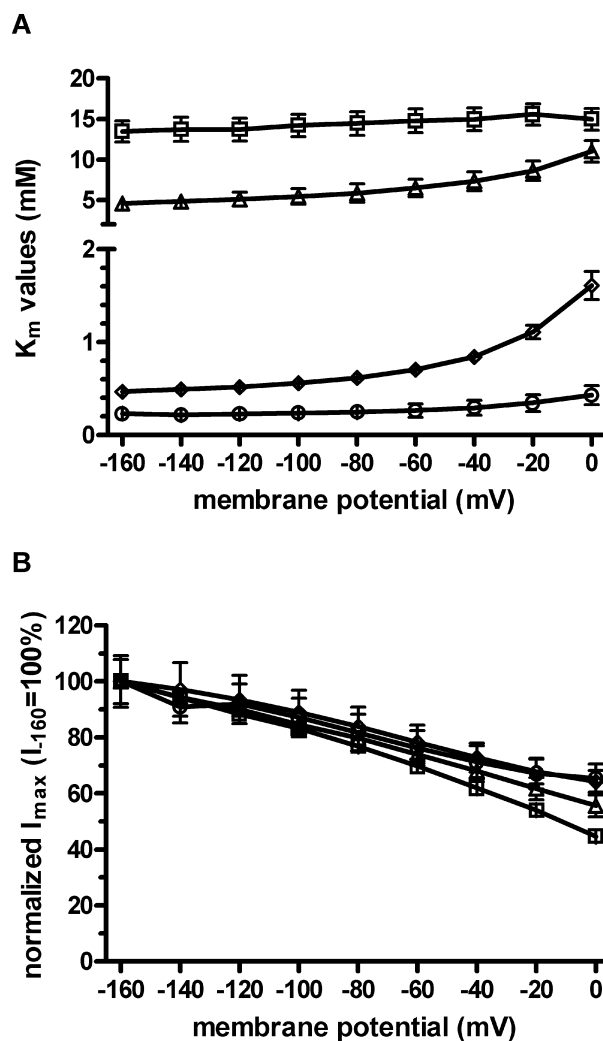


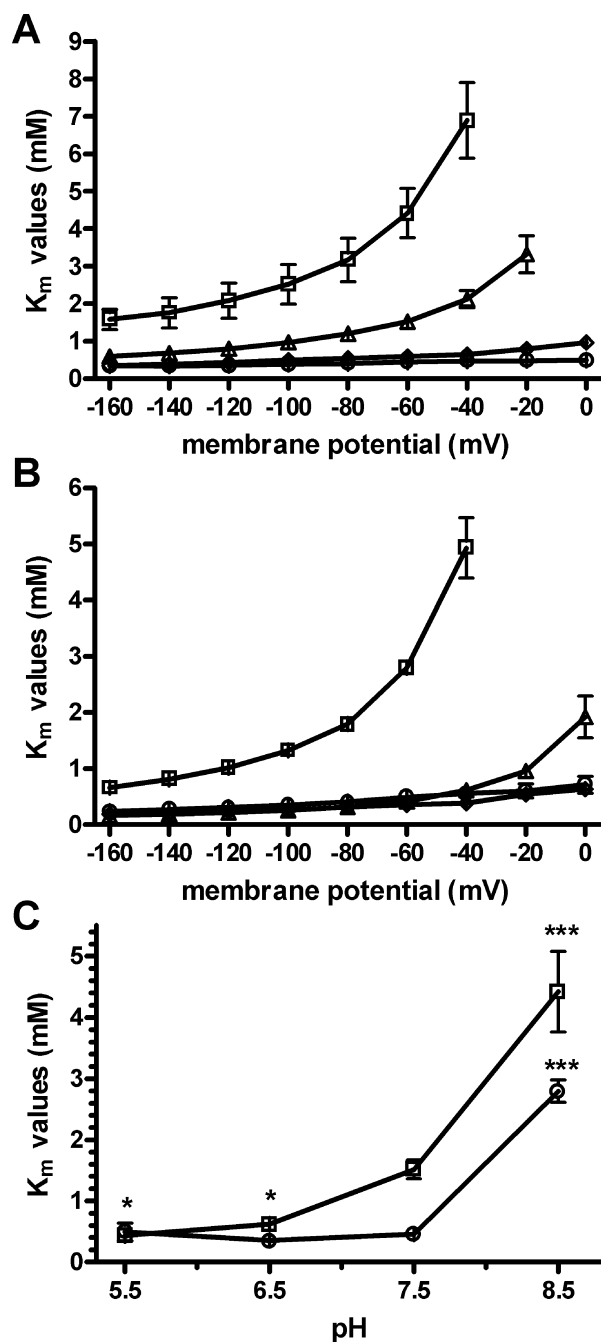
Fig. 3. Apparent  $K_m$  and  $V_{max}$  of various amino acids as a function of the membrane potential in PAT2 expressing oocytes. Membrane potential dependency of the apparent  $K_m$  (A) and  $V_{max}$  (B) values of  $\beta$ -alanine ( $\square$ ), D-alanine ( $\triangle$ ), OH-proline ( $\diamond$ ), and D-proline ( $\circ$ ) at pH 6.5. Data represent the mean  $\pm$  SEM ( $n = 5$ –7).

in response to the pH jump. Moreover, the reversal potential only shifted slightly from  $-24$  mV to  $-19$  mV. This suggests that PAT2 does not have any detectable proton leakage. In the presence of substrate however, the reversal potential shifted markedly to more positive potentials, e.g. from  $-2$  mV to  $+20$  mV by lowering extracellular pH from pH 9.0 to pH 8.7 as a measure of substrate-coupled proton cotransport (Fig. 5A).

## Discussion

In previous studies on the substrate recognition pattern of PAT1 [9] we were able to demonstrate that this transporter has a broader substrate spectrum that includes not only the amino acids glycine, alanine, serine and proline but also osmolytes such as sarcosine and betaine, and the D-enantiomers of serine and alanine. The apparent affinities of PAT1 substrates are mainly in the range of 2–15 mM [1,2,4,6,9]. As shown here, PAT2 is a

© FEBS 2004

Functional properties of mPAT2 (*Eur. J. Biochem.* 271) 3345

**Fig. 4.** Substrate apparent  $K_m$  values as a function of the extracellular pH. (A,B) Membrane potential dependency of the apparent  $K_m$  values of glycine (A) and L-alanine (B) at the extracellular pH 8.5 (□), pH 7.5 (△), pH 6.5 (◇), and pH 5.5 (○) in PAT2 expressing oocytes. (C) Apparent  $K_m$  values of glycine (□) and L-alanine (○) – depicted from (A) and (B) – as a function of the extracellular pH at  $-60$  mV. Data represent the mean  $\pm$  SEM ( $n = 4-7$ ); \*\*\*,  $P < 0.001$ ; \*\*,  $P < 0.01$  when compared with the corresponding values at pH 7.5.

high affinity type amino acid proton symporter that has a more restrictive specificity. In contrast to PAT1, PAT2 preferentially recognizes  $\alpha$ -amino acids, whereas  $\beta$ -alanine and GABA are low affinity substrates and betaine seems not to be recognized by PAT2.

When considering both the high ( $K_m = 0.1-1$  mM) and low affinity ( $K_m = 5-15$  mM) type substrates of PAT2 identified, (a) an unsubstituted negatively charged (carboxy-) group, (b) the small size of the side chain (maximally two  $\text{CH}_2$  units), and (c) a distance not exceeding three  $\text{CH}_2$  units between the charged amino- and carboxy-head groups, are the common and essential substrate features. But PAT2 in contrast to PAT1 tolerates only one (methyl-) substitution at the amino group as in sarcosine. Interestingly, all tested prolines (L-Pro, D-Pro and L-OH-Pro) are recognized as high affinity substrates by PAT2 with D-Pro as the only D-amino acid, and L-OH-Pro as the only polar amino acid accepted with high affinity. Although only speculative, the rigid ring structure of proline may cause a different orientation of the substrate within the substrate binding site of PAT2, and this may simultaneously avoid the interference of the polar side chain with corresponding amino acid residues in the binding pocket. Whether other proline derivatives also serve as substrates of PAT2, as recently shown for its paralog PAT1 [11], is presently not known.

Membrane potential and extracellular pH have quite diverse effects on the kinetics of transport by PAT2. Maximal transport velocity was only moderately affected by both membrane potential and extracellular pH within the physiological ranges. This appears to be a unique feature of PAT2. Similar electrogenic proton-dependent symporters such as PAT1 (M. Foltz, unpublished observation) or the peptide transporters PEPT1 do show a much more pronounced voltage-dependence of maximal transport currents [16].

In contrast to  $V_{\max}$ , apparent substrate affinity strongly decreased more than 7.5-fold when extracellular pH was increased from pH 6.5 to pH 8.5. The effect of membrane potential on substrate affinity is also highly dependent on extracellular pH. Under proton saturation conditions ( $\text{pH} < 7.5$ ), apparent  $K_m$  values were only modestly (around 2-fold) affected by a voltage change from  $-120$  mV to  $-20$  mV whereas at pH 8.5 the voltage effects became apparent with a severe reduction in affinity at low membrane potential. Apparent proton affinity also decreased substantially by depolarization suggesting that the lower substrate affinities under nonsaturating external proton concentrations is mainly a consequence of the decreased proton activity. The extraordinary high affinity of protons for binding to PAT2 with less than 1 nM at physiological membrane voltages suggests that pH changes in the physiological range do not affect transport activity at all. Moreover, affinity of proton binding is not dependent on substrate, whereas the affinity of the substrate is significantly dependent on the actual extracellular proton concentration. This argues for an ordered binding mechanism where the proton binds before the substrate enters the binding domain. Proton transfer to the internal membrane side however, requires the substrate as no intrinsic proton leak or uncoupled proton/charge movement could be observed. A pronounced pH-dependent shift in reversal potential was observed in the presence of substrate and we have previously shown that PAT2 couples proton movement to substrate movement with a 1 : 1 flux coupling stoichiometry. The shift in reversal potential however, was smaller than theoretically predicted for cotransport of a

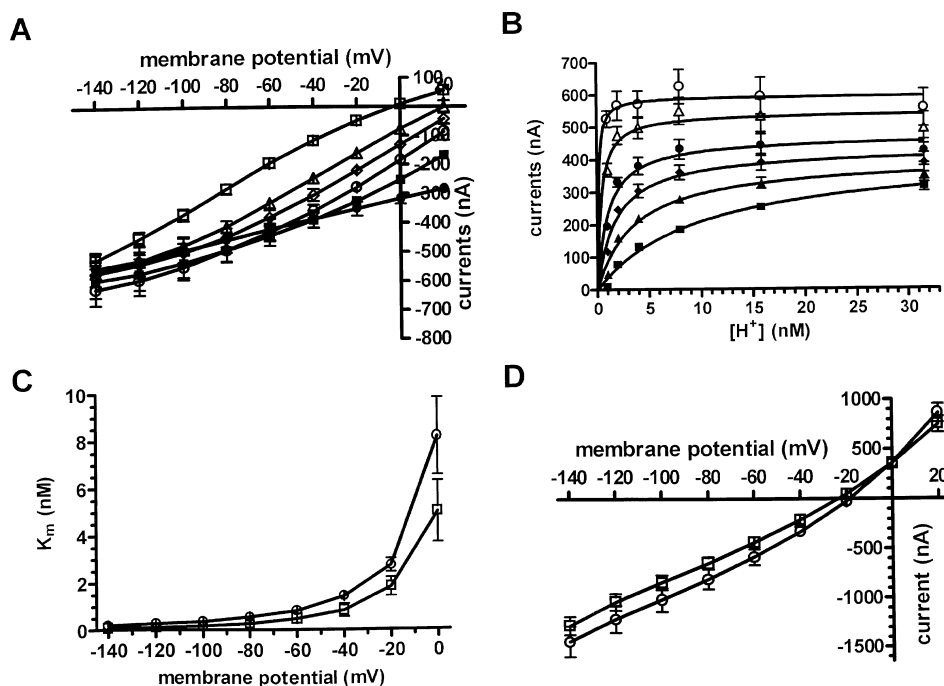


**Fig. 5. Proton kinetics in PAT2 expressing oocytes.** (A) I–V relationship of PAT2 mediated currents induced by 20 mM alanine at extracellular pH 9.0 (□), pH 8.7 (△), pH 8.4 (◇), pH 8.1 (○), pH 7.8 (■), and pH 7.5 (●). (B) PAT2 mediated currents as a function of the extracellular proton concentration at various membrane potentials: 0 mV (■), –20 mV (▲), –40 mV (◆), –60 mV (●), –100 mV (△), and –140 mV (○). Data from (A) were transformed for Michaelis–Menten presentation, pH values are expressed as the corresponding proton concentrations. (C) Apparent  $K_m$  values of protons in the presence of proline (□) and L-alanine (○) as a function of the membrane potential. (D) I–V relationship of non substrate currents in PAT2 expressing oocytes at different extracellular pH values. Oocytes were perfused with standard  $Na^+$ -free buffer at pH 9.0 (□) and pH 7.5 (○). Twenty seconds after pH changes the I–V relationship was recorded in the absence of substrate. Data represent the mean  $\pm$  SEM ( $n = 6$ ).

single positive charge ( $61 \text{ mV} \cdot \text{pH}^{-1}$ ) at an assumed intracellular pH of about 7.5. This deviation most likely results from rapid changes in intracellular pH during the first 20 s of substrate perfusion before the I–V curves were recorded, and such a significant decline in intracellular pH was shown previously by intracellular pH recordings [2,9]. Although the data provide evidence for an ordered process in proton and substrate binding, what appears to be a novel feature of PAT2 are the quite impressive differences in maximal transport activity (at least maximal transport currents) elicited by the different substrates. Most strikingly, substrates with essentially the same affinity such as L-alanine (0.25 mM), sarcosine (0.21 mM), D-proline (0.25 mM) or L-4-OH-Proline (0.72 mM) display  $I_{\max}$  values of  $65 \pm 3$ ,  $94 \pm 3$ ,  $30 \pm 1$  and  $37.2 \pm 1\%$  of the  $I_{\max}$  currents induced by glycine in the same oocytes (Table 1). This can only be taken as an indicator that the translocation of the loaded transporter to the internal membrane side is the rate-limiting step and not – as proposed for most of the other electrogenic symporters – the return of the unloaded transporter to the outside of the membrane [17].

In summary, we show that the mPAT2 protein when expressed heterologously in *Xenopus oocytes* has more restricted substrate specificity and a distinctly different dependence on membrane potential and pH than its paralog PAT1. PAT2 in its physiological setting is predicted to operate independent of pH by its extremely high external proton binding affinity, and substrate

affinity is also only affected via the pH dependence at depolarized potentials. Maximal transport activity is also only modestly dependent on membrane voltage and pH but strongly dependent on the substrate. An ordered proton and substrate binding process is followed by translocation of the loaded carrier – as the rate-limiting step – with delivery of substrate and cotransported ion to the internal side. The lack of transport of the two neuroactive compounds D-Ser and GABA appears particularly interesting with respect to PAT2 expression in the mammalian central nervous system [10].

## Acknowledgements

This work was supported by the DFG Grant (BO 1857/1) to M. B.

## References

- Sagné, C., Aguilhon, C., Ravassard, P., Darmon, M., Hamon, M., El Mestikawy, S., Gasnier, B. & Giros, B. (2001) Identification and characterization of a lysosomal transporter for small neutral amino acids. *Proc. Natl Acad. Sci. USA* **98**, 7206–7211.
- Boll, M., Foltz, M., Rubio-Aliaga, I., Kottra, G. & Daniel, H. (2002) Functional characterization of two novel mammalian electrogenic proton dependent amino acid cotransporters. *J. Biol. Chem.* **277**, 22966–22973.
- Bermingham, J.R. Jr, Shumas, S., Whisenhunt, T., Sirkowski, E.E., O'Connell, S., Scherer, S.S. & Rosenfeld, M.G. (2002)

© FEBS 2004

Functional properties of mPAT2 (*Eur. J. Biochem.* 271) 3347

- Identification of genes that are downregulated in the absence of the POU domain transcription factor pou3f1 (Oct-6, Tst-1, SCIP) in sciatic nerve. *J. Neurosci.* **22**, 10217–10231.
- Chen, Z., Fei, Y.J., Anderson, C.M.H., Wake, K.A., Miyachi, S., Huang, W., Thwaites, D.T. & Ganapathy, V. (2003) Structure, function and immunolocalization of a proton-coupled amino acid transporter (hPAT1) in the human intestinal cell line Caco-2. *J. Physiol.* **546**, 349–361.
  - Boll, M., Foltz, M., Rubio-Aliaga, I. & Daniel, H. (2003) A cluster of proton/amino acid transporter genes in the human and mouse genomes. *Genomics* **82**, 47–56.
  - Wreden, C.C., Johnson, J., Tran, C., Seal, R.P., Copenhagen, D.R., Reimer, R.J. & Edwards, R.H. (2003) The H<sup>+</sup>-coupled electrogenic lysosomal amino acid transporter LYAAT1 localizes to the axon and plasma membrane of hippocampal neurons. *J. Neurosci.* **23**, 1265–1275.
  - Chen, Z., Kennedy, D.J., Wake, K.A., Zhuang, L., Ganapathy, V. & Thwaites, D.T. (2003) Structure, tissue expression pattern, and function of the amino acid transporter rat PAT2. *Biochem. Biophys. Res. Comm.* **304**, 747–754.
  - Boll, M., Daniel, H. & Gasnier, B. (2004) The SLC36 family: proton-coupled transporters for the absorption of selected amino acids from extracellular and intracellular proteolysis. *Pflügers Arch.* **447**, 776–779.
  - Boll, M., Foltz, M., Anderson, C.M., Oechsler, C., Kottra, G., Thwaites, D.T. & Daniel, H. (2003) Substrate recognition by the mammalian proton-dependent amino acid transporter PAT1. *Mol. Membr. Biol.* **20**, 261–269.
  - Rubio-Aliaga, I., Boll, M., Vogt Weisenhorn, D.M., Foltz, M., Kottra, G. & Daniel, H. (2004) The proton/amino acid cotransporter PAT2 is expressed in neurons with a different subcellular localization than its paralog PAT1. *J. Biol. Chem.* **279**, 2754–2760.
  - Metzner, L., Kalbitz, J. & Brandsch, M. (2004) Transport of Pharmacologically Active Proline Derivatives by the Human Proton-Coupled Amino Acid Transporter hPAT1. *J. Pharmacol. Exp. Ther.* **309**, 28–35.
  - Logan, W.J. & Snyder, S.H. (1971) Unique high affinity uptake systems for glycine, glutamic and aspartic acids in central nervous tissue of the rat. *Nature* **234**, 297–299.
  - Bennett, J.P. Jr, Logan, W.J. & Snyder, S.H. (1972) Amino acid neurotransmitter candidates: sodium-dependent high-affinity uptake by unique synaptosomal fractions. *Science* **178**, 997–999.
  - Guastella, J., Brecha, N., Weigmann, C., Lester, H.A. & Davison, N. (1992) Cloning, expression, and localization of a rat brain high-affinity glycine transporter. *Proc. Natl Acad. Sci. USA* **89**, 7189–7193.
  - Liu, Q.R., Nelson, H., Mandiyan, S., Lopez-Corcuera, B. & Nelson, N. (1992) Cloning and expression of a glycine transporter from mouse brain. *FEBS Lett.* **305**, 110–114.
  - Mackenzie, B., Loo, D.D., Fei, Y., Liu, W.J., Ganapathy, V., Leibach, F.H. & Wright, E.M. (1996) Mechanisms of the human intestinal H<sup>+</sup>-coupled oligopeptide transporter hPEPT1. *J. Biol. Chem.* **271**, 5430–5437.
  - Jauch, P. & Lauger, P. (1986) Electrogenic properties of the sodium-alanine cotransporter in pancreatic acinar cells. II. Comparison with transport models. *J. Membr. Biol.* **94**, 117–127.



## APPENDIX 8

published in *Gastroenterology*

## H<sup>+</sup>/Amino Acid Transporter 1 (PAT1) Is the Imino Acid Carrier: An Intestinal Nutrient/Drug Transporter in Human and Rat

CATRIONA M. H. ANDERSON,\* DANIELLE S. GRENADE,\* MICHAEL BOLL,† MARTIN FOLTZ,† KATHERINE A. WAKE,\* DAVID J. KENNEDY,\* LARS K. MUNCK,§ SEIJI MIYAUCHI,|| PETER M. TAYLOR,¶ FREDERICK CHARLES CAMPBELL,# BJARNE G. MUNCK,\*\* HANNELORE DANIEL,† VADIVEL GANAPATHY,|| and DAVID T. THWAITES\*

\*Institute for Cell & Molecular Biosciences, Faculty of Medical Sciences, University of Newcastle Upon Tyne, Newcastle Upon Tyne, United Kingdom; †Molecular Nutrition Unit, Technical University of Munich, Freising-Weihenstephan, Germany; §Department of Medicine, Roskilde County Hospital, Køge, Denmark; ||Biochemistry and Molecular Biology, Medical College of Georgia, Augusta, Georgia; ¶Molecular Physiology, School of Life Sciences, University of Dundee, Dundee, United Kingdom; #Department of Surgery, Queen's University of Belfast, Belfast, United Kingdom; and \*\*Department of Medical Physiology, The PANUM Institute, University of Copenhagen, Copenhagen, Denmark

**Background & Aims:** Amino acid (and related drug) absorption across the human small intestinal wall is an essential intestinal function. Despite the revelation of a number of mammalian genomes, the molecular identity of the classic Na<sup>+</sup>-dependent imino acid transporter (identified functionally in the 1960s) remains elusive. The aims of this study were to determine whether the recently isolated complementary DNA hPAT1 (human proton-coupled amino acid transporter 1), or solute carrier SLC36A1, represents the imino acid carrier; the Na<sup>+</sup>-dependent imino acid transport function measured at the brush-border membrane of intact intestinal epithelia results from a close functional relationship between human proton-coupled amino acid transporter-1 and Na<sup>+</sup>/H<sup>+</sup> exchanger 3 (NHE3). **Methods:** PAT1 function was measured in isolation (*Xenopus laevis* oocytes) and in intact epithelia (Caco-2 cell monolayers and rat small intestine) by measurement of amino acid and/or H<sup>+</sup> influx. Tissue and membrane expression of PAT1 were determined by reverse-transcription polymerase chain reaction and immunohistochemistry. **Results:** PAT1-specific immunofluorescence was localized exclusively to the luminal membrane of Caco-2 cells and human and rat small intestine. The substrate specificity of hPAT1 is identical to that of the imino acid carrier. In intact epithelia, PAT1-mediated amino acid influx is reduced under conditions in which NHE3 is inactive. **Conclusions:** The identification in intact epithelia of a cooperative functional relationship between PAT1 (H<sup>+</sup>/amino acid symport) and NHE3 (Na<sup>+</sup>/H<sup>+</sup> exchange) explains the apparent Na<sup>+</sup> dependence of the imino acid carrier in studies with mammalian intestine. hPAT1 is the high-capacity imino acid carrier localized at the small intestinal luminal membrane that transports nutrients (imino/amino acids) and orally active neuromodulatory agents (used to treat affective disorders).

The intestinal absorption of many nutrients and drug molecules is mediated by ion-driven transport mechanisms in the intestinal enterocyte luminal membrane. Clearly, the establishment and maintenance of the driving forces (transmembrane and transepithelial ion gradients) are vital for maximum absorption to proceed.<sup>1</sup> Intestinal absorptive capacity is thus dependent on the cooperative activity of discrete transport processes involved directly in absorption and on those that mediate cellular (ion) homeostasis. Dietary protein is absorbed across the luminal membrane of the human small intestine in the form of small peptides (di/tripeptides) and amino acids.<sup>2</sup> All di/tripeptide absorption can be accounted for by the function of a single transporter, the H<sup>+</sup>-coupled di/tripeptide transporter hPepT1.<sup>3</sup> In contrast, amino acid transport across the intestinal brush-border membrane is mediated via a number of distinct transport systems that vary in substrate selectivity and ion coupling.<sup>2</sup> Recent genomic revelations have allowed most mammalian amino acid transport functions to be attributed to specific gene products: at least 52 amino acid transporter-related gene products are grouped

**Abbreviations used in this paper:** ABA, aminobutyric acid; BCECF, 2',7'-bis(2-carboxyethyl)-5(6)-carboxyfluorescein; BBMV, brush-border membrane vesicles; bp, base pair; cAMP, 3',5'-cyclic monophosphate; EIPA, N-(ethyl-N-isopropyl)-amiloride; GABA,  $\gamma$ -aminobutyric acid; hPAT1, human proton-coupled amino acid transporter 1; hPepT1, human intestinal di/tripeptide transporter; HRPE, human retinal pigment epithelial; Ki, inhibition constant; K<sub>m</sub>, Michaelis constant; LYAAT1, lysosomal amino acid transporter-1; MeLeu, methylaminoisobutyric acid; MeLeu, methyl-leucine; mPAT1, mouse proton-coupled amino acid transporter 1; NHE, Na<sup>+</sup>/H<sup>+</sup> exchanger; PAT, proton-coupled amino acid transporter; PCR, polymerase chain reaction; PepT1, di/tripeptide transporter; pH<sub>i</sub>, intracellular pH; rBAT, related to b<sup>0,+</sup> amino acid transporter; VIP, vasoactive intestinal polypeptide.

© 2004 by the American Gastroenterological Association  
0016-5085/04/\$30.00

doi:10.1053/j.gastro.2004.08.017

November 2004

INTESTINAL H<sup>+</sup>-COUPLED AMINO ACID ABSORPTION 1411

within 12 solute carrier families.<sup>4</sup> Despite this wealth of information, some intestinal brush-border membrane amino acid transport systems (as characterized by functional studies) have yet to be identified at the molecular level.<sup>5,6</sup> In addition, it is not known how some amino acids (including orally delivered therapeutic agents such as D-cycloserine, D-serine, and betaine)<sup>7-9</sup> are absorbed across the human small intestine. Only with knowledge of the substrate selectivity (and, therefore, the structural limitations of the active centre),<sup>10</sup> ion dependency, tissue distribution, and membrane localization of transporters involved in both nutrient and drug absorption can rational approaches to drug design and treatment of absorptive disorders be implemented.

The degree of understanding of the mechanisms involved in nutrient and drug transport across the human small intestine is limited by the lack of availability of viable human tissues and the interspecies variability observed in studies with animal small intestine.<sup>5,6,11-15</sup> Our own studies using confluent monolayers of the human intestinal epithelial cell line Caco-2 describe a low-affinity, high-capacity, proton-coupled amino acid transporter (PAT) at the brush-border membrane.<sup>16-20</sup> PAT transports the small zwitterionic amino acids glycine, proline, and alanine<sup>17,19</sup> and a number of orally administered compounds, including D-serine (used in the treatment of schizophrenia),<sup>8,18,19</sup> betaine (used in the treatment of homocystinuria),<sup>9,19,21</sup> and D-cycloserine (used as an orally delivered antibiotic and in the treatment of schizophrenia).<sup>7,18,20</sup> In addition, PAT transports the neurotransmitter  $\gamma$ -aminobutyric acid (GABA),<sup>20</sup> several GABA analogues (e.g., nipecotic acid, isonipecotic acid, and 3-amino-1-propanesulfonic acid)<sup>20</sup> that function as GABA receptor agonists or reuptake inhibitors,<sup>22</sup> and the conditionally essential amino acid taurine (which in humans is derived partly from dietary sources, with a particular requirement for absorption in the neonate).<sup>23</sup> Because of the clear potential of this high-capacity transport system to play essential roles in both nutrient and drug absorption, it is perhaps surprising that there are apparently no reports of an H<sup>+</sup>-coupled, PAT-like amino acid transporter in studies with "real" mammalian small intestine.

From the 1960s onward, several groups described a transport system in rat small intestine, named variously the *sarcosine carrier*,<sup>10,24,25</sup> *imino acid carrier*,<sup>11,12</sup> and *methionine-insensitive sarcosine-glycine-proline system*.<sup>26</sup> It is clear from examination of the literature that this rat intestinal transporter (from now on called the *imino acid carrier*) has a similar substrate specificity to PAT characterized in human (Caco-2) enterocytes.<sup>16-20</sup> Nevertheless, reference to the imino acid carrier in recent litera-

ture is limited, because most reviews describe a transporter called the IMINO carrier,<sup>27-29</sup> characterized in studies with rabbit jejunal brush-border membrane vesicles (BBMV).<sup>6</sup> An assumption has perhaps been made that the rat imino acid transporter and the rabbit IMINO carrier represent species-specific variants of a single transport system (the corresponding mechanism in human intestine is unclear because system PAT has generally been ignored). However, the substrate specificity and ion dependency of the imino acid and IMINO carriers are very different.<sup>5,6,13,15</sup> The IMINO carrier has a strong preference for imino acids<sup>6</sup> and excludes many substrates of the imino acid carrier, including  $\alpha$ -aminoisobutyric acid, glycine,  $\beta$ -alanine, and GABA<sup>5,6</sup> (all good substrates for PAT).<sup>16,19,20</sup> In addition, the IMINO carrier has a strong preference for L-proline over D-proline, whereas the imino acid carrier and PAT do not discriminate between these L- and D-enantiomers.<sup>5,6,19</sup> It is interesting to note that of all the classic amino acid transport systems described functionally, the molecular identity of any imino acid/IMINO carrier(s) has yet to be revealed.

The human proton-coupled amino acid transporter 1 (hPAT1), or solute carrier SLC36A1, is a complementary DNA (cDNA) isolated recently from a Caco-2 cDNA library that mediates PAT-like function when expressed in heterologous cell types.<sup>30</sup> The substrate specificity of hPAT1 is identical to that of the endogenous PAT system in Caco-2 cells.<sup>19,30</sup> The similarity in substrate specificity among hPAT1, endogenous PAT, and the rat imino acid carrier suggests that hPAT1 may represent the molecular identity of the human form of the rat imino acid carrier. However, initial comparisons suggest that there are apparently incontrovertible differences in ion dependency. hPAT1, when expressed in isolation (in human retinal pigment epithelial (HRPE) cells or *Xenopus laevis* oocytes), functions in an H<sup>+</sup>-coupled, pH-dependent, Na<sup>+</sup>-independent manner.<sup>30,31</sup> In contrast, the imino acid and IMINO carriers are described as being Na<sup>+</sup> dependent.<sup>5,6</sup> There is, however, an additional difference between rabbit and rat: transport in intact intestinal tissues is Na<sup>+</sup> and Cl<sup>-</sup> dependent in the rabbit (and guinea pig) but is only partially Na<sup>+</sup> dependent (60%) and is Cl<sup>-</sup> independent in the rat.<sup>5,14,15</sup> The Na<sup>+</sup> dependence of the rabbit IMINO carrier is unequivocal: this has been shown with jejunal BBMV.<sup>6</sup> In contrast, there are no reports of the Na<sup>+</sup> dependence of the imino acid carrier with rat intestinal BBMV, and although a slight Na<sup>+</sup> dependence in L-proline uptake was observed in human intestinal BBMV from both adult<sup>32</sup> and fetal<sup>33</sup> tissues, no overshoot was reported.

The partial  $\text{Na}^+$  dependency of imino acid transport in studies with intact tissue preparations is reminiscent of that observed with the di/tripeptide transporter (PepT1).<sup>34–37</sup> The PepT1 clone is an  $\text{H}^+$ -coupled transporter that functions independently of extracellular  $\text{Na}^+$  after heterologous expression.<sup>2,36</sup> The driving force (the  $\text{H}^+$  electrochemical gradient) for  $\text{H}^+$ -coupled nutrient transport in the small intestine is present at the luminal surface as an area of low pH (pH 6.1–6.8) called the *acid microclimate*.<sup>38,39</sup> In intact tissue preparations, dipeptide transport shows partial  $\text{Na}^+$  dependence, whereas no  $\text{Na}^+$  dependence is observed in studies that use intestinal BBMV.<sup>34</sup> These apparently anomalous observations can be explained; in intact intestinal epithelia, there is a close functional coupling between PepT1 and the apically localized  $\text{Na}^+/\text{H}^+$  exchanger 3 (NHE3) such that only with the cooperative activity of these 2 transporters can optimal absorption occur.<sup>34–37</sup> A consequence of  $\text{H}^+$ -coupled dipeptide absorption will be a reduction in the driving force, because  $\text{H}^+$  movement across the luminal membrane will lead to intracellular acidification. Studies with Caco-2 cell monolayers show that PepT1-mediated  $\text{H}^+$  influx leads to selective activation of the apical NHE3 without any activation of basolateral  $\text{Na}^+/\text{H}^+$  exchanger 1 (NHE1).<sup>1</sup> Thus, in intact epithelia, PepT1 and NHE3 function in tandem to mediate dipeptide and  $\text{Na}^+$  absorption, and the driving force for dipeptide transport is maintained (during absorption) by NHE3-mediated  $\text{H}^+$  efflux.<sup>1,34–37</sup> It is interesting to note that in studies with Caco-2 cells, a similar selective activation of NHE3 is observed after PAT-mediated  $\text{H}^+/\beta$ -alanine symport.<sup>1</sup>

We had 3 primary objectives: to determine whether PAT-mediated transport in an intact epithelium (Caco-2 cell monolayer) shows partial  $\text{Na}^+$  dependence (as observed with the rat imino acid transporter) and whether this  $\text{Na}^+$  dependence is due to NHE3 activity; to identify whether PAT1 protein is present at the brush-border membrane of Caco-2 cells and human and rat small intestine; and to determine the identity of the human “imino” carrier by investigation of the substrate selectivity of hPAT1/PAT with a series of substrates chosen to discriminate between transport via an imino acid (rat) or IMINO (rabbit) type of carrier.

## Materials and Methods

### Materials

[<sup>3</sup>H] $\beta$ -Alanine (specific activity, 50 Ci/mmol) and [<sup>3</sup>H]methylaminoisobutyric acid (MeAIB; 60–85 Ci/mmol) were from American Radiolabeled Chemicals (St. Louis, MO). [<sup>3</sup>H]L-Aspartate (17 Ci/mmol) was from ICN Pharmaceuticals (Basingstoke, UK). [<sup>3</sup>H]Proline (43 Ci/mmol) was from Amersham Biosciences (Little Chalfont, UK). The acetoxymethyl ester of 2',7'-Bis(2-carboxyethyl)-5(6)-carboxyfluores-

cein (BCECF) was from Molecular Probes (Leiden, The Netherlands). S1611 and cariporide (HOE642) were from H. J. Lang (Aventis Pharma Deutschland GmbH, Frankfurt/Main, Germany). All other chemicals were from Sigma or VWR (Poole, UK) and were of the highest quality available.

### Amino Acid Uptake Across the Apical Membrane of Caco-2 Cell Monolayers

Caco-2 cells (passage 101–120) were cultured as confluent monolayers on permeable polycarbonate filters (Corning-Costar, High Wycombe, UK), as described previously.<sup>16,35</sup> [<sup>3</sup>H] $\beta$ -Alanine, [<sup>3</sup>H]MeAIB, and [<sup>3</sup>H]L-aspartate (0.5–1  $\mu\text{Ci}/\text{mL}$ ; 20–100  $\mu\text{mol}/\text{L}$ ) uptake across the apical membrane of Caco-2 cell monolayers was measured (over 0.5–90 minutes), as described previously.<sup>16,20,35</sup> Uptake was measured routinely over 15 minutes in the presence or absence of external  $\text{Na}^+$ ; at apical pH 5.5 or 6.5 (basolateral pH 7.4); and in the presence or absence of various compounds (see figure legends for details). Cell monolayer-associated radioactivity was determined by scintillation counting.

### Intracellular pH Measurements

Intracellular pH ( $\text{pH}_i$ ) of Caco-2 cell monolayers loaded with the pH-sensitive dye BCECF was measured by microspectrofluorimetry, as described previously.<sup>16,20,35,37</sup> Cell monolayers were superfused with various amino acids (10 mmol/L; 200 seconds) in the apical superfusate ( $\text{Na}^+$  free; pH 5.5), and the initial rate of acidification induced by each was converted to  $\Delta\text{pH}_i$  per minute and expressed as percentage GABA response.<sup>20</sup> In separate experiments,  $\text{pH}_i$  recovery from  $\beta$ -alanine (20 mmol/L,  $\text{Na}^+$  free, apical pH 5.5, 300 seconds)–induced acidification was investigated: in the presence or absence of apical  $\text{Na}^+$ , at an apical pH of 5.5–7.4, and after 15 minutes of incubation with S1611. Initial  $\text{H}^+$  efflux rates were calculated as described previously.<sup>35,37</sup>

### Functional Expression in *Xenopus laevis* Oocytes

hPAT1 and mouse proton-coupled amino acid transporter-1 (mPAT1) were expressed in *X. laevis* oocytes, as described previously.<sup>21,36,40</sup> [<sup>3</sup>H] $\beta$ -Alanine or [<sup>3</sup>H]proline (5  $\mu\text{Ci}/\text{mL}$ ; 100  $\mu\text{mol}/\text{L}$ ) uptake into  $\text{H}_2\text{O}$  or hPAT1-injected oocytes was measured (40 minutes,  $\text{Na}^+$  free, pH 5.5) in the presence and absence of various compounds or amino acids (as described previously).<sup>36</sup> Two-electrode voltage-clamp experiments were performed on mPAT1- or hPAT1-expressing oocytes (clamped at  $-40$  mV), as described previously.<sup>21,31,40</sup>

### Amino Acid Uptake Into Mammalian Small Intestine

Female rabbits (2500 g), female guinea pigs (400 g) and male Wistar rats (200 g) were maintained with free access to food and water. Animals were killed by intravenous (rabbits) or intraperitoneal (rats and guinea pigs) phenobarbital sodium.

November 2004

INTESTINAL H<sup>+</sup>-COUPLED AMINO ACID ABSORPTION 1413

Excised mid jejunum (rats and guinea pigs) or 30 cm of distal ileum (rabbits) was mounted between Lucite plates so that the mucosa (area, 0.62 cm<sup>2</sup>) was exposed in the bottom of wells in which the solution was stirred and oxygenated by high rates of 100% oxygen flow at 37°C. After 20 minutes of preincubation at the appropriate pH, [<sup>14</sup>C]MeAIB (100 μmol/L) uptake was measured for 30 seconds in the absence of Na<sup>+</sup> and at pH 7.2 or 5.65 by using [<sup>3</sup>H]polyethylene glycol-4000 to correct for extracellular adhesion of MeAIB, essentially as described previously.<sup>5,41</sup>

### Polymerase Chain Reaction

Human multiple tissue and digestive system cDNA panels (BD Biosciences, Cowley, UK) and Caco-2 cDNA (total RNA was isolated from Caco-2 cells by using a midi kit [Qiagen, Crawley, UK] and was reverse-transcribed by using Omniscript [Qiagen]) were screened by using primers specific for hPAT1 (forward, <sub>19</sub>CGGAACGAAGACTACCACGACTAC<sub>42</sub>; reverse, <sub>742</sub>GGCTGGGGTCTGGGATTC<sub>725</sub>; expected product size, 724 base pairs [bp]) and glyceraldehyde phosphate dehydrogenase (forward, <sub>12</sub>TGAAGGTCGGAGTCAACGGATTTGGT<sub>38</sub>; reverse, <sub>994</sub>CATGTGGGCCATGAGGTCCACCAC<sub>970</sub>; expected product size, 983 bp). Polymerase chain reactions (PCRs) were performed in the manufacturers' buffers in 2.5 mmol/L MgCl<sub>2</sub> by using HotStarTaq DNA Polymerase (Qiagen). Thermal cycling parameters were 95°C for 15 minutes as an initial activation step, then 3-step cycling (94°C for 30 seconds, 65°C for 30 seconds, and 72°C for 1 minute) for 35 cycles, and finally 72°C for 10 minutes. PCR products and a 100-bp ladder (New England Biolabs, Hitchin, UK) were separated on a 1% agarose gel.

### Immunolocalization

PAT1 was localized in Caco-2 cell monolayers<sup>30</sup> and in sections of frozen rat ileum and human jejunum by using a specific antibody.<sup>30</sup> Normal human jejunum samples were obtained from 6 cadaver organ donors after relatives' consent and local ethical committee approval were obtained for tissue retrieval for research purposes. After retrieval, jejunal specimens were immediately wrapped in tinfoil, labeled, snap-frozen in liquid nitrogen, and stored until use. Subjects' age and sex were recorded, but details of donor identity were omitted. Tissues were gently thawed before analysis. Tissues and monolayers were fixed (with paraformaldehyde), permeabilized (with Triton X-100), and incubated with an affinity-purified chicken anti-hPAT1-specific antibody (before or after preadsorption with the antigenic peptide). To show monolayer orientation, Caco-2 cells were incubated with antibodies specific to either the basolateral CD98 (BD Biosciences) or apical rBAT (related to b<sup>0,+</sup> amino acid transporter) by using an affinity-purified rabbit polyclonal antibody to a rat rBAT peptide (PRSFKSDK-DGNGD) orthologous to residues 128–141 of human rBAT.<sup>42</sup> The tissues and monolayers were incubated with a fluorescein isothiocyanate-conjugated goat anti-chicken secondary antibody (Sigma) plus either a tetramethylrho-

damine isothiocyanate-conjugated goat anti-mouse (Sigma) or goat anti-rabbit (Zymed, San Francisco, CA) secondary antibody as appropriate.<sup>30,42</sup> Tissue sections or monolayers were mounted in Vectorshield (Vector Laboratories, Peterborough, UK), and fluorescence was observed by using confocal laser scanning microscopy.

### Statistics

Data are mean ± SEM. Statistical comparisons of mean values were made by using paired or unpaired 2-tailed Student *t* tests or analysis of variance (with the Tukey–Kramer or Bonferroni multiple comparisons posttest) as appropriate. Curve fitting was performed by using either GraphPad Prism version 3.00 (GraphPad, San Diego, CA) or FigP software (Biosoft, Cambridge, UK).

## Results

### Partial Na<sup>+</sup> Dependence of PAT-Mediated Amino Acid Uptake in Caco-2 Cell Monolayers

Uptake of the PAT (and imino acid, but not IMINO)<sup>5,6,16,19,20</sup> substrate [<sup>3</sup>H]β-alanine was measured (at 100 μmol/L) across the apical membrane of Caco-2 cell monolayers at an apical pH (pH 6.5) typical of that measured at the luminal surface of mammalian jejunum both in vivo and in vitro.<sup>38,39</sup> Uptake was routinely measured over 15 minutes, where Na<sup>+</sup> removal significantly (*P* < .001) reduced (but did not abolish) β-alanine uptake from 493.0 ± 16.7 pmol/cm<sup>2</sup> (n = 159) to 182.0 ± 6.5 pmol/cm<sup>2</sup> (n = 151; a 63% reduction). This partial Na<sup>+</sup> dependence was also noted for MeAIB (an hPAT1, imino acid, and IMINO substrate)<sup>5,6,19,30</sup> uptake, which was reduced on Na<sup>+</sup> removal by 54.6% ± 2.6% (n = 18; *P* < .001 vs. control [presence of extracellular Na<sup>+</sup>]). In contrast, when the maneuver was performed with L-aspartate (a substrate restricted to the Na<sup>+</sup>-coupled system X<sub>AG</sub><sup>-</sup>),<sup>43</sup> uptake was much more sensitive to Na<sup>+</sup> removal; it was reduced to 11.8% ± 0.9% (n = 18) of control (*P* < .001).

A feature of the partial Na<sup>+</sup> dependence of β-alanine uptake is that the Na<sup>+</sup>-dependent component is variable and depends on the length of time over which uptake is measured. Over 30 seconds, although there was a 17% reduction, no significant difference was noted in the presence (40.6 ± 2.3 pmol/cm<sup>2</sup>; n = 24) or absence (33.6 ± 1.9 pmol/cm<sup>2</sup>; n = 24; *P* > .05) of Na<sup>+</sup> (Figure 1). In contrast, the Na<sup>+</sup>-dependent component represented 59% of total uptake at 15 minutes and 75% over 90 minutes (Figure 1). This phenomenon was also observed with the H<sup>+</sup>-coupled peptide transporter hPepT1, for which dipeptide uptake into Caco-2 cells at pH 6.5 was Na<sup>+</sup>

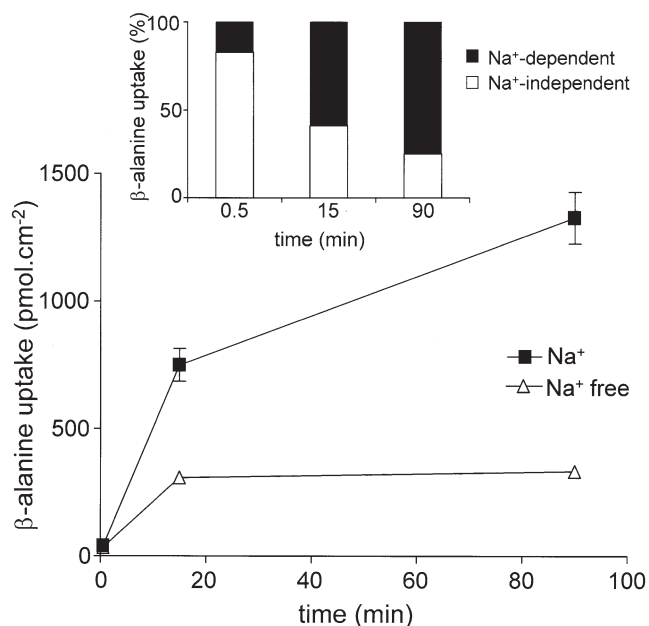


**Figure 1.** Time and  $\text{Na}^+$  dependence of  $\beta$ -alanine uptake across the apical membrane of Caco-2 cell monolayers.  $\beta$ -Alanine (100  $\mu\text{mol/L}$ ) uptake was measured over 0.5–90 minutes at apical pH 6.5 (basolateral pH 7.4) in the presence (filled squares) and absence (open triangles) of  $\text{Na}^+$ . (Insert) Data from the main panel expressed as the percentage of total uptake in the presence of  $\text{Na}^+$ .  $\text{Na}^+$ -dependent uptake (filled bars) was calculated as the difference between uptake in the presence and absence of  $\text{Na}^+$  (open bars). Results are mean  $\pm$  SEM ( $n = 12$ –18).

independent over 30 seconds but became  $\text{Na}^+$  dependent as the time over which measurements were made was lengthened.<sup>35,36</sup> In contrast to the observations in intact epithelia, amino acid uptake into hPAT1-expressing oocytes (as observed with dipeptide uptake into hPepT1-expressing oocytes)<sup>36</sup> was  $\text{Na}^+$  independent even over 40 minutes (data not shown). In the case of dipeptide transport via PepT1, the time-dependent increase in  $\text{Na}^+$  dependency is explained by activation of NHE3, which is required to maintain the  $\text{H}^+$  electrochemical gradient so that dipeptide uptake can continue over the longer time periods required for absorption of a meal.<sup>34,35</sup> To determine whether the effect of  $\text{Na}^+$  removal on  $\beta$ -alanine uptake is through a dependence on functional NHE3-mediated  $\text{Na}^+/\text{H}^+$ , the effects of a number of selective pharmacological  $\text{Na}^+/\text{H}^+$  inhibitors were assessed.

### Pharmacological Inhibition of NHE3 Reduces PAT-Mediated Amino Acid Uptake

The selective NHE3 inhibitor S1611 (3  $\mu\text{mol/L}$ )<sup>44</sup> and the nonselective  $\text{Na}^+/\text{H}^+$  exchange inhibitor *N*-(ethyl-*N*-isopropyl)-amiloride (EIPA; 100  $\mu\text{mol/L}$ ; concentrations that inhibit NHE3) both significantly ( $P <$

.05) reduced  $\beta$ -alanine uptake across the apical membrane of Caco-2 cells in the presence of  $\text{Na}^+$  (Figure 2). In contrast, neither compound had any effect ( $P > .05$  vs. the  $\text{Na}^+$ -free control) in  $\text{Na}^+$ -free conditions (Figure 2).  $\text{Na}^+$ -coupled L-aspartate uptake (over 15 minutes) was unaffected by S1611: it was  $265.9 \pm 18.3$   $\text{pmol/cm}^2$  and  $273.5 \pm 20.6$   $\text{pmol/cm}^2$  ( $n = 12$ ;  $P > .05$ ) in the absence and presence of S1611, respectively. Apical cariporide (HOE642), at a concentration that would inhibit NHE1 and NHE2, but not NHE3,<sup>45</sup> had no effect on  $\beta$ -alanine uptake in Caco-2 cells. The  $\text{Na}^+$ -dependent effect of S1611 was through a reduction in capacity (Figure 2, insert), where maximum velocity decreased from  $43.9 \pm 18.0$  to  $15.4 \pm 5.7$   $\text{nmol} \cdot \text{cm}^{-2} \cdot (15 \text{ min})^{-1}$  in the absence or presence of S1611, respectively (no significant change in the Michaelis constant ( $K_m$ ) was observed). The nonsaturable component was unaffected by S1611 ( $1.0 \pm 0.7$  vs.  $1.0 \pm 0.3$   $\text{nmol} \cdot \text{cm}^{-2} \cdot (15 \text{ min})^{-1}$  in the absence and presence of S1611, respectively). In contrast to PAT-mediated amino acid uptake in Caco-2 cells,  $\beta$ -alanine uptake in hPAT1-expressing oocytes was unaffected by S1611, EIPA, or cariporide ( $P > .05$ ; data not shown). Thus, in the presence of  $\text{Na}^+$ , PAT function in Caco-2 cells can be modulated by compounds known to inhibit NHE3. The lack of effect

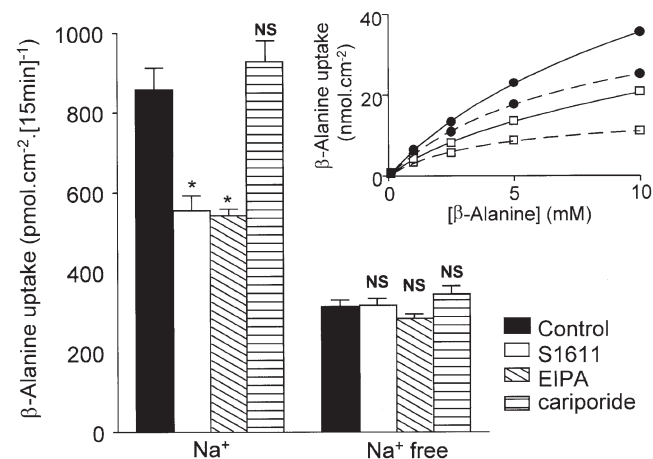


**Figure 2.** Pharmacological modulation of PAT-mediated amino acid uptake. Apical  $\beta$ -alanine (100  $\mu\text{mol/L}$ ) uptake in Caco-2 cells (15 minutes; apical pH 6.5) in the presence and absence of  $\text{Na}^+$  and the NHE3 selective inhibitor S1611 (3  $\mu\text{mol/L}$ ; open bars), the NHE inhibitor EIPA (100  $\mu\text{mol/L}$ ; hatched bars), or the NHE1/NHE2 inhibitor cariporide (10  $\mu\text{mol/L}$ ; horizontal striped bars). Data are mean  $\pm$  SEM ( $n = 12$ ). \* $P < .05$  vs. control in the presence of  $\text{Na}^+$ . NS,  $P > .05$  vs. control. (Insert) Concentration-dependent  $\beta$ -alanine uptake ( $\text{Na}^+$  solutions, 15 minutes, apical pH 6.5) in the presence (open squares) or absence (filled circles) of apical S1611 (3  $\mu\text{mol/L}$ ). Results are mean  $\pm$  SEM ( $n = 11$ –12). Solid lines are the best-fit curves for the hyperbolic Michaelis–Menten kinetics of the data (saturable plus nonsaturable components;  $r^2 = 0.999$  for both curves). The dotted lines represent the carrier-mediated (saturable) uptake (after subtraction of the nonsaturable component).

November 2004

INTESTINAL H<sup>+</sup>-COUPLED AMINO ACID ABSORPTION 1415

of any compound in Na<sup>+</sup>-free conditions or on uptake into hPAT1-expressing oocytes, suggests that the inhibition is not via a direct effect on PAT1 but is rather through inhibition of NHE3. To test this conclusion, NHE3 activity was measured by fluorescent microscopy with BCECF-loaded Caco-2 cell monolayers (Figure 3). We have previously shown (by using <sup>22</sup>Na<sup>+</sup> influx and pH<sub>i</sub> measurements) that H<sup>+</sup>/β-alanine symport in Caco-2 cells leads to selective activation of apical Na<sup>+</sup>/H<sup>+</sup> exchange,<sup>1,18–20</sup> which can be inhibited by 100 μmol/L EIPA (a concentration that would inhibit NHE1, NHE2, and NHE3).<sup>1</sup> pH<sub>i</sub> recovery from β-alanine-induced acidification was dependent on apical pH (Figure 3A) and Na<sup>+</sup> (Figure 3B) in a manner indicative of Na<sup>+</sup>/H<sup>+</sup> exchange.<sup>46</sup> The role of NHE3 was confirmed by the inhibition of Na<sup>+</sup>-dependent recovery by S1611 (Figure 3B). Figure 3C shows that the pH<sub>i</sub> recovery (calculated as the H<sup>+</sup>-efflux rate) after β-alanine-induced acidification was significantly inhibited by decreasing apical pH, Na<sup>+</sup> removal, or incubation with S1611. Under experimental conditions in which the Na<sup>+</sup>-dependent component of β-alanine uptake is inhibited, NHE3 activity is also reduced.

#### PAT1 Messenger RNA (mRNA) and Protein Expression in Human and Rat Tissues

The results presented previously confirm that an H<sup>+</sup>-coupled amino acid transporter (PAT) functions at the apical membrane of Caco-2 cells and that transport (in intact epithelia but not after expression in oocytes) shows partial Na<sup>+</sup> dependence, which is reduced after NHE3 inhibition. To date, there is apparently little functional evidence for the existence of PAT in “real” mammalian tissues. PCR analysis of human cDNA from multiple tissues by using hPAT1-specific primers produced a single band of the predicted size (724 bp) in all tissues, including small intestine (Figure 4A and B). By using a PAT1-specific antibody raised in chicken,<sup>30</sup> PAT1 protein was localized exclusively to the brush-border membrane of Caco-2 cells, as visualized with a fluorescein isothiocyanate-conjugated (*green*) anti-chicken secondary antibody (Figure 4C–K). Apical localization was confirmed by colocalization (*yellow*) with the apical amino acid transport protein rBAT<sup>29</sup> (*red*, Figure 4D–E), but not with the basolateral amino acid transport protein CD98 (*red*, Figure 4G–K).<sup>29,30</sup> To determine whether PAT1 protein is expressed in “real” intestinal tissues, sections of rat ileum were incubated with the PAT1 antibody, which shows clear brush-border membrane staining in the epithelial layer (Figure 4M). The brush-border membrane staining was eliminated by preadsorption with the antigenic peptide (Figure 4N),

thus confirming observations in Caco-2 cells.<sup>30</sup> Immunofluorescence was also detected in the underlying lamina propria, but this was observed with the secondary antibody alone (Figure 4L), so this lamina propria staining does not seem to be specific for PAT1. PAT1 protein was detected at the luminal membrane of the human jejunal epithelium (Figure 4P), and no brush-border staining was detected with the secondary antibody alone (Figure 4O). This provides the first demonstration of PAT1 immunolocalization in “real” intestinal tissues from both human and rat small intestine.

#### PAT/hPAT1 Show the Same Substrate Selectivity as the Rat Imino Acid Transporter

To identify whether hPAT1 is the human homologue of the rat imino acid transporter, the substrate selectivity of the hPAT1 clone (expressed in *X laevis* oocytes or HRPE cells) and the endogenous PAT transporter (in Caco-2 cells) was determined by using a series of compounds chosen to distinguish between transport via an imino acid (rat) or IMINO (rabbit) type of transporter.<sup>5,6,12,13</sup> Experimental conditions (extracellular pH 5.5, Na<sup>+</sup> free) were chosen to allow optimal measurement of transport via hPAT1 (by using a combination of radiolabel uptake/competition experiments and substrate-induced current measurements). To allow direct comparison with the endogenous transporter, transport was measured in Caco-2 cell monolayers under identical experimental conditions (Figure 5). The imino acid carrier has a clear preference for GABA and β-aminobutyric acid (ABA) over α-ABA,<sup>5,12,47</sup> whereas the IMINO transporter prefers α-ABA over β-ABA and has little or no recognition for GABA.<sup>6,13</sup> The IMINO carrier<sup>6,13</sup> has a strong preference for pipecolic (inhibition constant [K<sub>i</sub>] = 0.2 mmol/L) over nipecotic (K<sub>i</sub> = 40 mmol/L) and isonipecotic (K<sub>i</sub> = 153 mmol/L) acid. The imino acid carrier is less selective (a 2-fold difference in affinity) but has a slight preference for isonipecotic over nipecotic over pipecolic acid.<sup>12</sup> Methyl-leucine (MeLeu) is a good substrate for the IMINO carrier<sup>13</sup> but does not interact with the imino acid carrier even at 40 mmol/L.<sup>5</sup> A key feature of the IMINO carrier is the preference for L- over D-amino acids (L-pipecolate is the best substrate for the transporter and has a 39-fold greater affinity than the D-form).<sup>6</sup> In contrast, the imino acid carrier shows weak or reversed stereoselectivity.<sup>5,24,25</sup> A similar weak or reversed stereoselectivity for alanine, serine, proline, and cysteine has been shown previously for PAT/PAT1,<sup>19,30,40</sup> and D-cycloserine is a substrate in Caco-2 cells.<sup>18</sup> The competition experiments shown here in Caco-2 cells (and hPAT1-expressing oocytes [Figure 5C] or HRPE cells [data not shown]) show that PAT/hPAT1

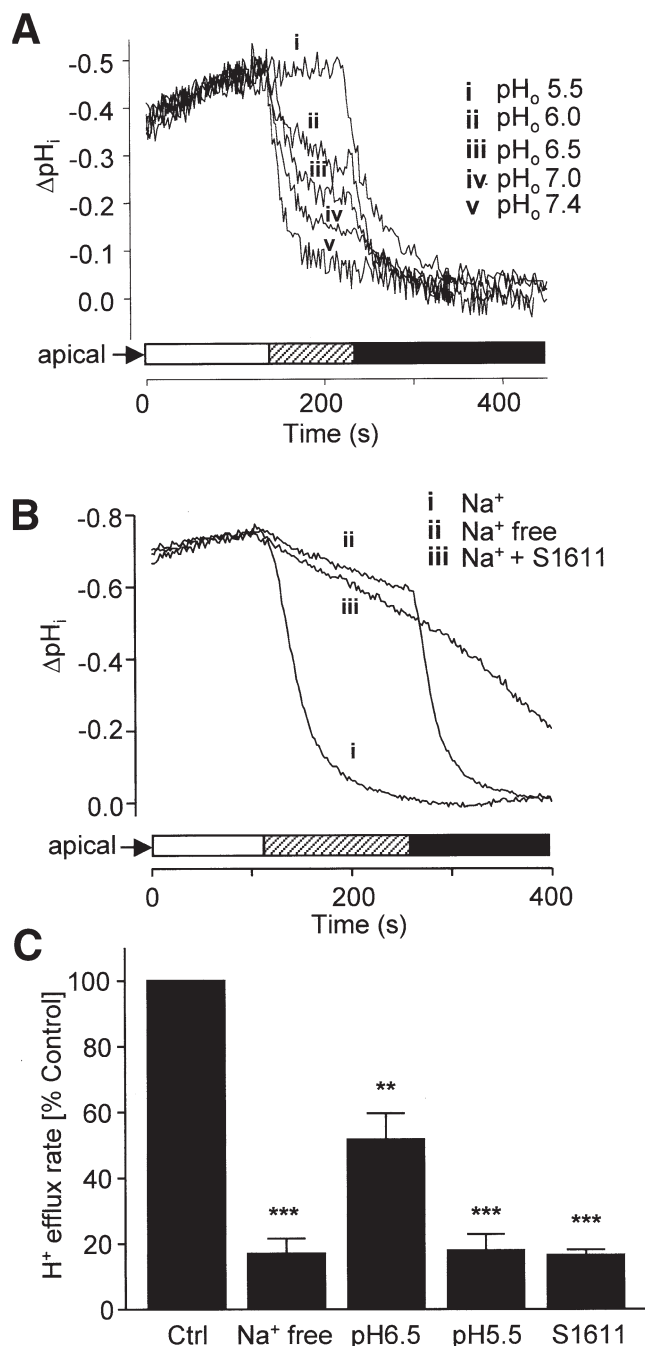


**Figure 3.** NHE3-dependent recovery of  $\text{pH}_i$  after amino acid-induced acidification. BCECF-loaded Caco-2 cell monolayers were exposed to  $\beta$ -alanine (20 mmol/L; 300 seconds; *open bars*) in the apical superfusate ( $\text{Na}^+$  free, pH 5.5; basolateral  $\text{Na}^+$  free, pH 7.4 throughout).  $\text{pH}_i$  recovery was then measured under various conditions (*hatched bars*) before the addition of an  $\text{Na}^+$ -containing, pH 7.4 apical solution (*filled bars*). S1611 was added before (for 10 minutes) and then during exposure to  $\beta$ -alanine (giving a total incubation of 15 minutes before  $\text{pH}_i$  recovery was measured). Composite responses are shown of single monolayers to (A) successive recoveries at apical pH 5.5–7.4 in the presence of  $\text{Na}^+$  and (B) successive recoveries (at apical pH 7.4) in  $\text{Na}^+$ -containing (i) and  $\text{Na}^+$ -free (ii) solution and in  $\text{Na}^+$  after exposure to apical S1611 (3  $\mu\text{mol/L}$ ) (iii). (C) Mean data for (A) and (B).  $\text{H}^+$  efflux was calculated from  $\Delta\text{pH}_i$  over the initial 30 seconds of  $\text{pH}_i$  recovery.<sup>35,37</sup> Data (mean  $\pm$  SEM;  $n = 4$ –7) are expressed as the percentage of  $\text{H}^+$  efflux in control conditions ( $\text{Na}^+$  containing; pH 7.4) and were analyzed by the Student  $t$  test (paired data):  $**P < .01$ ;  $***P < .001$ ; both vs. control.

has the same general characteristics as those determined in rat intestine: there is a slight preference for GABA over  $\beta$ -ABA, and  $\alpha$ -ABA is the weakest inhibitor (Figure 5A); it is inhibited by L-pipecolic (notably not the substrate with highest affinity overall), nipecotic, and isonipecotic acid, but with no difference in affinity (not shown;  $P > .05$ ); it is unaffected by MeLeu (Figure 5B); and it is unable to discriminate significantly between enantiomers of cycloserine (Figure 5B) or pipecolic acid (although a preference for each D-form was observed; data not shown).

The ability of PAT1 to selectively transport the amino acids used in Figure 5A–C was confirmed by measurements of substrate-coupled  $\text{H}^+$  flow (measured as inward current or  $\Delta\text{pH}_i$ ) into PAT1-expressing oocytes and Caco-2 cells. Representative current traces in hPAT1-expressing oocytes after exposure to different amino acids (Figure 5D) show that hPAT1 has a clear preference for GABA and  $\beta$ -ABA over  $\alpha$ -ABA or MeLeu. Experiments with mPAT1-expressing oocytes produced similar responses with  $K_m$  values of  $3.1 \pm 0.2$  mmol/L for GABA,  $4.1 \pm 0.6$  mmol/L for  $\beta$ -ABA, and  $48.0 \pm 8.0$  mmol/L for  $\alpha$ -ABA ( $n = 4$ –7). Similar observations were made when substrate-coupled  $\text{H}^+$  flow was measured via the endogenous Caco-2 transporter, for which  $\Delta\text{pH}_i$  on apical superfusion of  $\alpha$ -ABA or MeLeu was not different ( $P > .05$  vs. control) from control (pH 5.5 solution alone; Figure 5E), whereas GABA and  $\beta$ -ABA caused a significant  $\Delta\text{pH}_i$  ( $P < .001$  vs. control; Figure 5E). The data are summarized in Figure 5F. Substrate inhibition of transport via PAT/PAT1 (Figure 5A–C) is closely related to stimulation of  $\text{H}^+$  flow (Figure 5D–F). The substrate selectivity is consistent with hPAT1 being the human orthologue of the rat imino acid transporter,<sup>5</sup> whereas the rabbit IMINO carrier is distinct.<sup>6</sup>

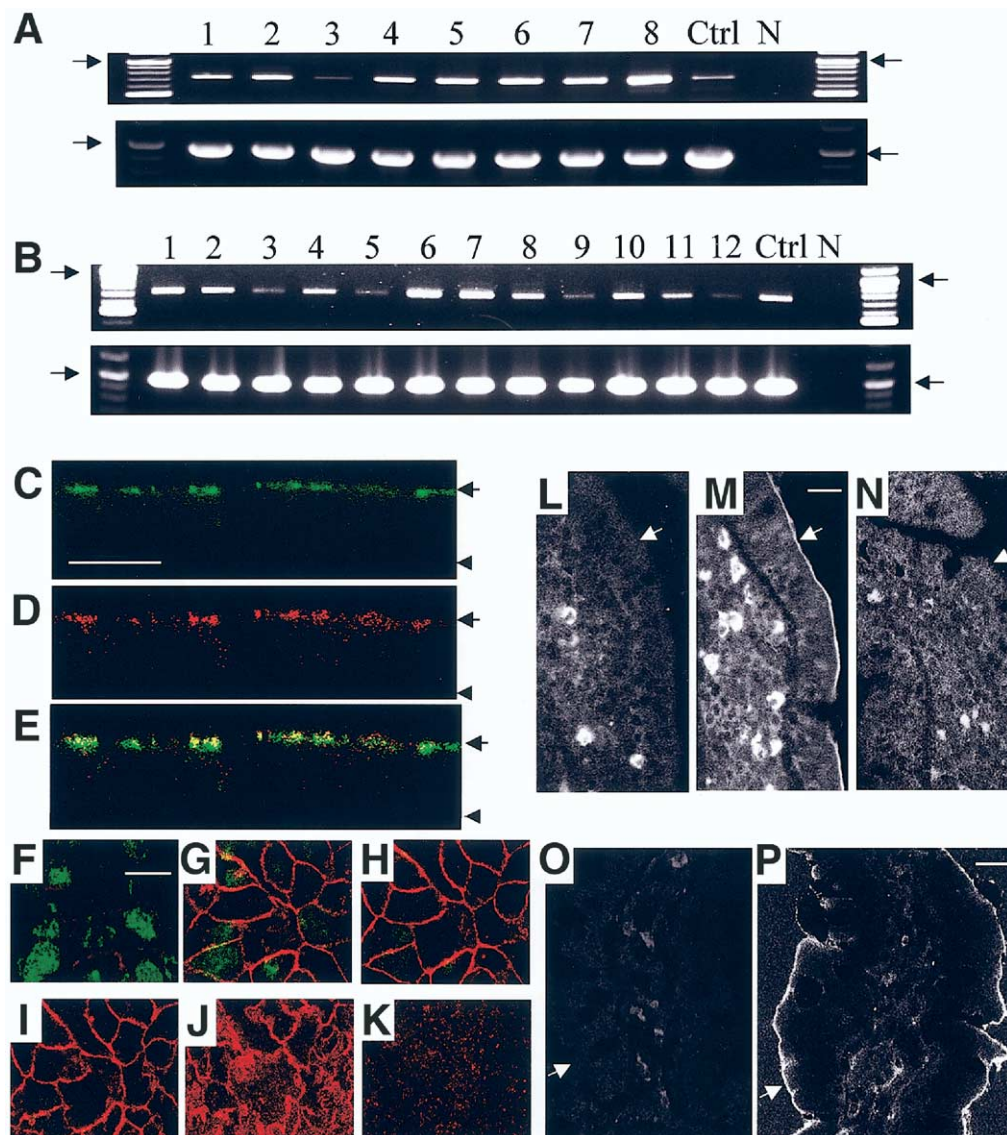
### pH-Dependent, $\text{Na}^+$ -Independent, PAT-Type Transport in Rat Small Intestine

The final confirmation of the existence of functional PAT-like transport in rat intestine requires the demonstration of pH-dependent,  $\text{Na}^+$ -independent amino acid uptake. In the absence of extracellular  $\text{Na}^+$ , MeAIB uptake into rat small intestine was significantly increased ( $P < .001$ ) when the pH of the luminal bathing solution was reduced from 7.2 to 5.65 (Figure 6). In contrast, only a very small ( $P > .05$ ) increase was observed in both guinea pig and rabbit small intestine. In rat small intestine,  $\text{Na}^+$ -independent MeAIB uptake at pH 5.65 was reduced by 68% in the presence of excess  $\beta$ -alanine (1000-fold excess).

### Discussion

The first piece of molecular information on any PAT-related transporter was provided with the isolation

November 2004

INTESTINAL H<sup>+</sup>-COUPLED AMINO ACID ABSORPTION 1417

**Figure 4.** PAT1 messenger RNA and protein expression in human and rat tissues. Products of PCR with human multiple tissue (A) and digestive tract tissue cDNA panels (B) by using primers specific for hPAT1 (upper panels) and glyceraldehyde phosphate dehydrogenase (lower panels). (A) Lanes are as follows: 1, heart; 2, brain; 3, placenta; 4, liver; 5, lung; 6, skeletal muscle; 7, pancreas; 8, kidney. (B) Lanes are as follows: 1, ascending colon; 2, descending colon; 3, transverse colon; 4, duodenum; 5, ileocecum; 6, ileum; 7, jejunum; 8, rectum; 9, cecum; 10, stomach; 11, liver; 12, esophagus. Ctrl lane shows the positive control reaction with Caco-2 cDNA. Lane N shows the negative control reaction (no cDNA). DNA size markers (with the 1000-bp band identified) are shown. (C–E) Cross-sectional (xz) sections through a Caco-2 cell monolayer (arrows indicate apical membrane, and arrowheads indicate basal membrane) showing immunofluorescent detection of (C) PAT1 (green), (D) rBAT (red), and (E) apical colocalization (yellow). (F–K) A stack of xy sections [at 1.8- $\mu$ m intervals moving down from the apical (F) to basal (K) surface] through a Caco-2 cell monolayer showing PAT1 localization to the apical membrane (green), whereas CD98 is solely basolateral (red). PAT1 immunofluorescence in rat ileum (L–N) and human jejunum (O–P) is localized to the brush-border membrane (M and P) (arrows). The PAT1 fluorescence is blocked by preadsorption with the antigenic peptide (N). Some lamina propria (but no brush-border) staining is observed with the secondary antibody alone (L and O). All scale bars are 20  $\mu$ m.

of a rat cDNA named lysosomal amino acid transporter 1 (LYAAT1)<sup>48</sup> because of its predominant lysosomal localization in the neuronal tissue investigated. Recently rat LYAAT1 has been localized to the neuronal cell surface.<sup>49</sup> The mouse<sup>40</sup> and human<sup>30</sup> forms of this transporter were isolated from small intestine and human Caco-2 cells and named PAT1 because of their similarity

in function to PAT.<sup>16–20</sup> There are 4 members (PAT1–4) of this solute carrier family (SLC36A1–4).<sup>4,31,50</sup>

At the mRNA level, PAT1 is ubiquitously expressed in all rat, mouse, and human tissues investigated (Figure 4).<sup>30,31,40,48,49</sup> It is surprising, therefore, that there have been relatively few reports of a functional PAT-type transporter in mammalian tissues. Immunolocalization

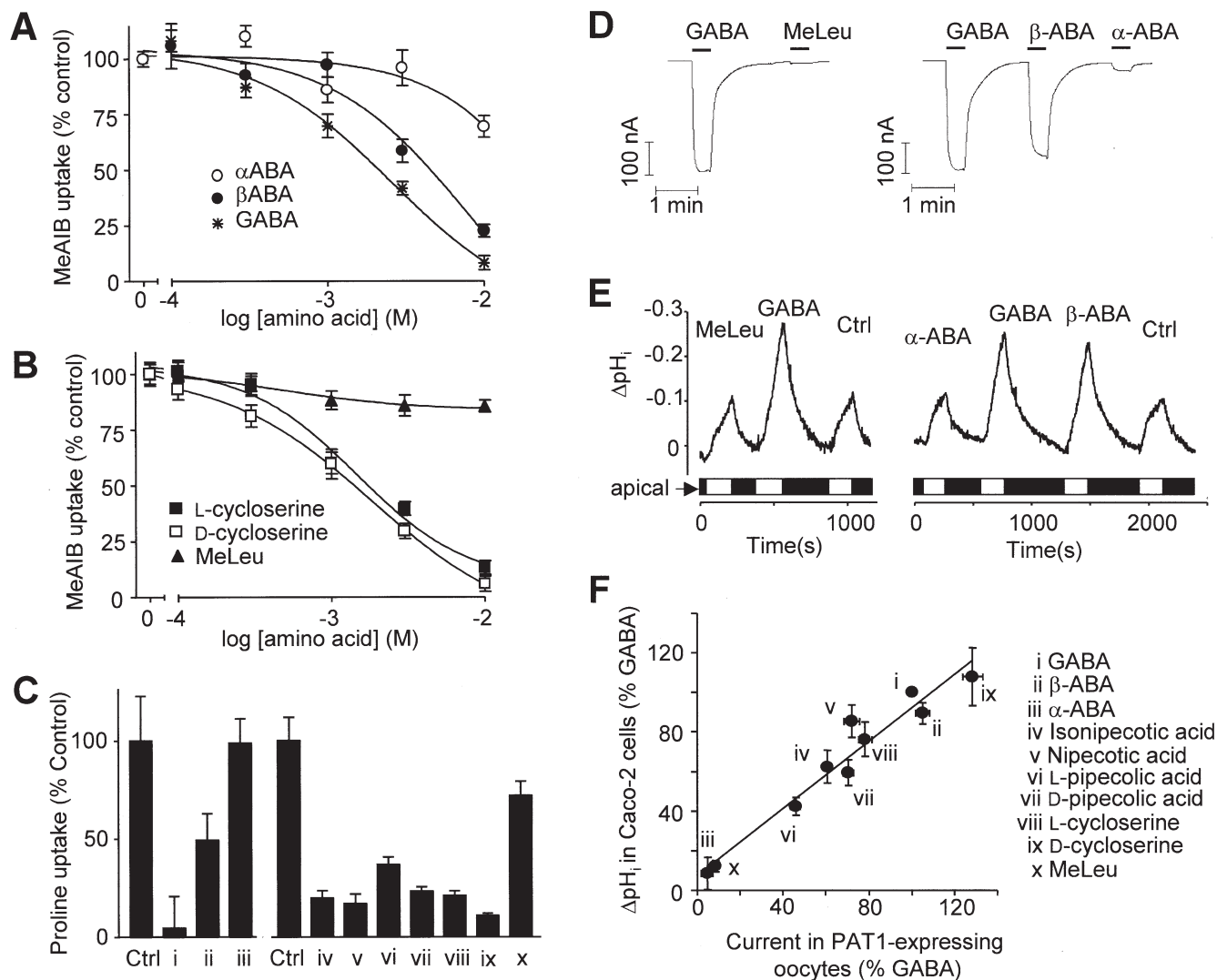


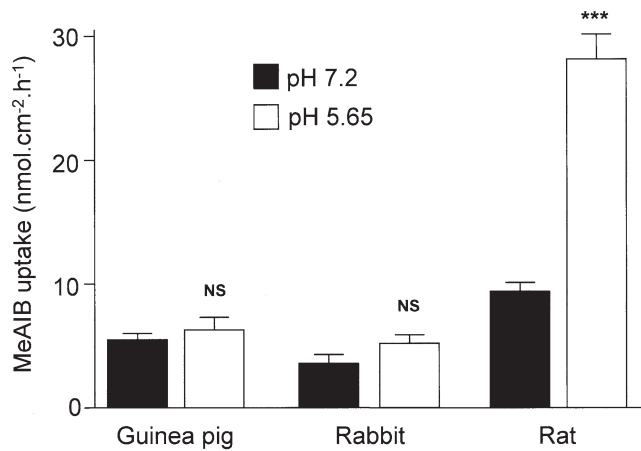
**Figure 5.** PAT/hPAT1 show the same substrate selectivity as the rat imino acid transporter. Apical MeAIB (20  $\mu$ mol/L) uptake in Caco-2 cells in the presence (0.1–10 mmol/L) of (A)  $\alpha$ -ABA,  $\beta$ -ABA, and GABA and (B) L-cycloserine, D-cycloserine, and MeLeu. Data are mean  $\pm$  SEM ( $n = 12$ –20) and are expressed as percentage of control (the absence of competing amino acids). (C) Competition experiments showing the inhibition of proline (100  $\mu$ mol/L) uptake into hPAT1-expressing oocytes by various amino acids (all 10 mmol/L). Substrates are as in (F) below: i, GABA; ii,  $\beta$ -ABA; iii,  $\alpha$ -ABA; iv, isonipecotic acid; v, nipecotic acid; vi, L-pipecolic acid; vii, D-pipecolic acid; viii, L-cycloserine; ix, D-cycloserine; x, MeLeu. Data are mean  $\pm$  SEM ( $n = 9$ –20) and are expressed as percentage of control (Ctrl, the absence of competing amino acids) after subtraction of uptake into water-injected oocytes. (D) Current induced by various amino acids (all 10 mmol/L; pH 5.5;  $Na^+$  free) in 2-electrode voltage-clamped hPAT1-expressing oocytes. (E)  $\Delta pH_i$  in Caco-2 cell monolayers after apical superfusion with various amino acids (10 mmol/L; pH 5.5;  $Na^+$  free; open bars). Closed bars represent pH 7.4  $Na^+$ -containing apical superfusate. Control (Ctrl) indicates the  $\Delta pH_i$  after exposure to the pH 5.5,  $Na^+$ -free superfusate alone. (F) Correlation between amino acid-induced current in mPAT1-expressing oocytes and  $\Delta pH_i$  in Caco-2 cells. Data are mean  $\pm$  SEM and are expressed as percentage of GABA response. The linear relationship ( $r^2 = 0.946$ ) between current and  $\Delta pH_i$  suggests that PAT1 (in oocytes) and PAT (in Caco-2 cells) discriminate between potential substrates in a similar manner.

studies (Figure 4) with a PAT1-specific antibody<sup>30</sup> show exclusive PAT1 protein localization in the brush-border membrane in Caco-2 cells and in human and rat small intestine. Beyond our own studies with Caco-2 cells,<sup>16–20</sup> reports on PAT-like  $H^+$ -coupled amino acid transport are limited to eel and lizard small intestine,<sup>51,52</sup> rabbit renal BBMVs,<sup>53,54</sup> and rat hippocampal neurons.<sup>49</sup> The lack of additional functional evidence may be due to a predominant lysosomal localization in many tissues.<sup>48</sup>

However, the results in Figure 4 show that exclusive lysosomal localization does not account for the lack of functional evidence in “real” mammalian intestine.

For many years we have highlighted the similarity in substrate specificity of the rat imino acid carrier and PAT in Caco-2 cells.<sup>5,16–20,30</sup> Although PAT1 functions in a  $Na^+$ -independent manner when expressed exogenously in isolation, the optimal function of the endogenous PAT transporter is  $Na^+$  dependent and depends on the coexpression

November 2004

INTESTINAL H<sup>+</sup>-COUPLED AMINO ACID ABSORPTION 1419

**Figure 6.** pH-dependent, Na<sup>+</sup>-independent, PAT-type transport in rat small intestine. MeAIB (100 μmol/L) uptake into rat, rabbit, or guinea pig small intestine is shown. Uptake was measured over 30 seconds in the absence of Na<sup>+</sup> at a luminal pH of 7.2 or 5.65. Data are mean ± SEM (n = 8–12). \*\*\**P* < .001; NS, *P* > .05; both vs. pH 7.2.

and functional activity of NHE3. Thus, PAT function in Caco-2 cells shows partial Na<sup>+</sup> dependence, as previously observed for the imino acid carrier.<sup>15</sup> Such functional cooperativity has been described previously for NHE3 and another H<sup>+</sup>-coupled transporter, hPepT1.<sup>34–37</sup> Thus, during H<sup>+</sup>-coupled solute absorption, the driving force (the H<sup>+</sup> electrochemical gradient) is maintained by the activity of NHE3, so the overall effect is a net transport of solute and Na<sup>+</sup> with H<sup>+</sup> recycling.

The identity of PAT/hPAT1 as the human homologue of the rat imino acid carrier and the lack of similarity of either system to the IMINO carrier are confirmed by the results in Figure 5. In this study we carefully selected a series of compounds to discriminate between the imino acid carrier and the IMINO transporter. PAT and hPAT1 (or mPAT1) have similar substrate selectivity to the imino acid carrier, whereas the specificity of the IMINO transporter is very different.<sup>6,13</sup> Na<sup>+</sup>-independent, pH-dependent imino acid transport in “real” mammalian (rat) small intestine is shown for the first time in Figure 6. The differences observed between species both here and in previous studies<sup>5,6,10–15</sup> suggest that there are species differences in the complement of amino acid transporters at the brush-border membrane of the small intestine. The detection of PAT1 immunofluorescence at the brush-border of rat ileum, combined with the large stimulation of MeAIB uptake observed after a decrease in luminal pH (in Na<sup>+</sup>-free conditions), is consistent with expression of a PAT-like transporter. The rat imino acid carrier should be renamed rPAT1 to help reduce further confusion with the IMINO carrier,<sup>6</sup> which is clearly a different entity. The small effect of pH observed in both rabbit and guinea pig small intestine (Figure 6) suggests

either that PAT1 is absent or that the expression levels are relatively low.

Since the revelation of the rPAT1 (LYAAT1)<sup>48</sup> sequence, a number of key observations have been made regarding PAT1 and the potential role it plays in nutrient and drug absorption in the human small intestine. The rat sequence allowed the isolation of hPAT1,<sup>30</sup> which in turn allowed the development of specific tools to identify tissue distribution (mRNA) and membrane (protein) localization, not only in the model system (Caco-2), but also in human and rat small intestine. The availability of hPAT1 allowed identification of the transport characteristics and substrate selectivity in isolation (after expression in heterologous systems)<sup>21,30</sup> and in comparison with transport in the human intestinal epithelium.<sup>21,30</sup> The key observation of brush-border membrane localization led to a re-evaluation of the literature and the hypothesis that hPAT1 was the human imino acid carrier. The identical nature of the substrate specificity of hPAT1 and the imino carrier and the discovery that the apparent Na<sup>+</sup> dependence of PAT1/imino acid transport was due to a functional relationship with NHE3 force a reinterpretation of the published data, in which Na<sup>+</sup> dependency has been incorrectly assigned, thereby revealing a large body of evidence to support the role of PAT1 in the absorption of both nutrients and drug molecules.

Because hPAT1 functions as a low-affinity, high-capacity transporter, it is likely to play an important role in both nutrient and drug absorption. It is interesting to note that to date, PAT-like transport has been identified at the intestinal brush border of carnivorous/omnivorous (rat, human, eel, and lizard), but not herbivorous (guinea pig and rabbit), species. Perhaps brush-border PAT1 expression is an intestinal adaptation to allow the former group to use the abundance of taurine found in meat, fish, and insects (only trace levels are found in most plants),<sup>23</sup> because some meat-eating mammals (e.g., humans) are unable to synthesize adequate amounts of taurine. Alternatively, it may allow meat-eating mammals to decrease taurine synthesis and concentrate valuable energy resources elsewhere. Taurine is an excellent substrate for hPAT1,<sup>19</sup> and high-capacity transport of taurine has been measured in intact epithelia.<sup>5,15</sup> Although this is not its primary function, hPAT1 is almost certainly the transporter involved in taurine absorption from “high-energy” drinks.<sup>55</sup>

Perhaps the greatest potential of this transporter is as a route for oral absorption of therapeutic compounds. hPAT1 is the only small-intestinal transporter capable of transporting a number of orally administered compounds, e.g., D-cycloserine, D-serine, and betaine.<sup>7–9</sup> Al-

though not used orally, L-cycloserine is a hPAT1 substrate and inhibits tumor growth *in vitro*.<sup>56</sup> hPAT1 transports a number of GABA receptor agonists/antagonists and reuptake inhibitors. In addition, hPAT1 transports a number of nitrogen-containing heterocyclic compounds, including pipercolic acid and azetidine-2-carboxylic acid (not shown), that are found in higher plants. Although this was not tested in this study, a single report suggests that acamprosate (used orally to prevent relapse in sober alcoholics) shares a rat intestinal transporter with GABA and taurine.<sup>57</sup>

hPAT1 function may be affected in certain disease states. The unique ability of hPAT1 to transport glycine, proline, and hydroxyproline (combined with the demonstration of pH-dependent glycine and proline transport in renal BBMVs)<sup>53,54</sup> makes this transporter a candidate for the system disrupted in iminoglycinuria,<sup>29</sup> in which defects are observed in renal (and intestinal) capacity to reabsorb certain amino acids. The defective carrier in iminoglycinuria cannot be the IMINO transporter, because glycine is excluded from the latter.<sup>6</sup> More common absorptive problems are likely to result from the dependence of hPAT1 on functional NHE3. NHE3 is down-regulated by protein kinase A after an increase in adenosine 3',5'-cyclic monophosphate (cAMP).<sup>58</sup> A number of pathophysiological conditions (e.g., enterotoxin-induced diarrheal states or those associated with vasoactive intestinal polypeptide (VIP)-producing tumors) are associated with enteric release of VIP or increased plasma VIP levels. In addition, cholera enterotoxin can increase the intracellular cAMP concentration in intestinal epithelial cells directly.<sup>59</sup> Thus, many pathophysiological conditions will have antiabsorptive effects and inhibit solute absorption indirectly after inhibition of NHE3. These antiabsorptive effects have been observed in Caco-2 cells with both hPepT1<sup>35,37</sup> and hPAT1 (Anderson and Thwaites, unpublished data, 2004). In addition, drug-drug interactions may be evident, because compounds such as the orally administered amiloride (an Na<sup>+</sup>/H<sup>+</sup> exchange inhibitor, commonly prescribed as a K<sup>+</sup>-sparing diuretic) may inhibit NHE3 function and indirectly reduce the bioavailability of hPAT1-transported drugs.

To allow the future development of rational approaches to the design of orally delivered drugs, functional foods, and effective treatments for absorptive disorders, the temptation to focus on biology simply at the molecular level must be avoided. Rather, the genomic information revealed over recent years must be translated into functional (physiological) information to aid investigation of biological problems at all levels from the individual molecule up to the entire animal. This study

shows that the optimal absorptive performance of the small intestine depends on the coexpression (in specialized membranes within the enterocyte) and functional cooperation of discrete ion gradient-driven transporters involved in both absorption (hPAT1) and cellular homeostasis (NHE3). This investigation resolves a mystery (the lack of evidence for PAT1 or imino acid transport function in many species) and provides a greater understanding of how these diverse transporters function cooperatively at the luminal membrane of the intact intestinal epithelium to optimize absorption. The breadth of the role played by PAT1 in both nutrient and drug absorption awaits further study.

## References

1. Thwaites DT, Ford D, Glanville M, Simmons NL. H<sup>+</sup>/solute-induced intracellular acidification leads to selective activation of apical Na<sup>+</sup>/H<sup>+</sup> exchange in human intestinal epithelial cells. *J Clin Invest* 1999;104:629–635.
2. Ganapathy V, Brandsch M, Leibach FH. Intestinal transport of amino acids and peptides. In: Johnson LR, ed. *Physiology of the gastrointestinal tract*. New York: Raven, 1994:1773–1794.
3. Liang R, Fei YJ, Prasad PD, Ramamoorthy S, Han H, Yang-Feng TL, Hediger MA, Ganapathy V, Leibach FH. Human intestinal H<sup>+</sup>/peptide cotransporter: cloning, functional expression, and chromosomal localization. *J Biol Chem* 1995;270:6456–6463.
4. Hediger MA, Romero MF, Peng JB, Rolfs A, Takana H, Bruford EA. The ABCs of solute carriers: physiological, pathological and therapeutic implications of human membrane transport proteins—introduction. *Pflugers Arch* 2004;447:1–942.
5. Munck BG, Munck LK, Rasmussen SN, Polache A. Specificity of the imino acid carrier in rat small intestine. *Am J Physiol* 1994; 266:R1154–R1161.
6. Stevens BR, Wright EM. Substrate specificity of the intestinal brush-border proline/sodium (IMINO) transporter. *J Membr Biol* 1985;87:27–34.
7. Ewins AE, Amico E, Posever TA, Toker R, Goff DC. D-Cycloserine added to risperidone in patients with primary negative symptoms of schizophrenia. *Schizophr Res* 2002;56:19–23.
8. Tsai G, Yang P, Chung L-C, Lange N, Coyle JT. D-Serine added to antipsychotics for the treatment of schizophrenia. *Biol Psychiatry* 1998;44:1081–1089.
9. Smolin LA, Benevenga NJ, Berlow S. The use of betaine for the treatment of homocystinuria. *J Pediatr* 1981;99:467–472.
10. Newey H, Smyth DH. The transfer system for neutral amino acids in the rat small intestine. *J Physiol* 1964;170:328–343.
11. Munck BG. Amino acid transport by the small intestine of the rat. *Biochim Biophys Acta* 1966;120:97–103.
12. Munck BG. Intestinal absorption of amino acids. In: Johnson LR, ed. *Physiology of the gastrointestinal tract*. New York: Raven Press, 1981:1097–1122.
13. Munck BG. Transport of imino acids and non- $\alpha$ -amino acid across the brush-border membrane of the rabbit ileum. *J Membr Biol* 1985;83:15–24.
14. Munck LK, Munck BG. Distinction between chloride-dependent transport systems for taurine and  $\beta$ -alanine in rabbit ileum. *Am J Physiol* 1992;262:G609–G615.
15. Munck LK, Munck BG. Chloride-dependent intestinal transport of imino and  $\beta$ -amino acids in the guinea pig and rat. *Am J Physiol* 1994;266:R997–R1007.
16. Thwaites DT, McEwan GTA, Brown CDA, Hirst BH, Simmons NL. Na<sup>+</sup>-independent, H<sup>+</sup>-coupled transepithelial  $\beta$ -alanine absorp-

November 2004

INTESTINAL H<sup>+</sup>-COUPLED AMINO ACID ABSORPTION 1421

- tion by human intestinal Caco-2 cell monolayers. *J Biol Chem* 1993;268:18438–18441.
17. Thwaites DT, McEwan GTA, Cook MJ, Hirst BH, Simmons NL. H<sup>+</sup>-coupled (Na<sup>+</sup>-independent) proline transport in human intestinal (Caco-2) epithelial cell monolayers. *FEBS Lett* 1993;333:78–82.
  18. Thwaites DT, Armstrong G, Hirst BH, Simmons NL. D-Cycloserine transport in human intestinal epithelial (Caco-2) cells: mediation by a H<sup>+</sup>-coupled amino acid transporter. *Br J Pharmacol* 1995;115:761–766.
  19. Thwaites DT, McEwan GTA, Simmons NL. The role of the proton electrochemical gradient in the transepithelial absorption of amino acids by human intestinal Caco-2 cell monolayers. *J Membr Biol* 1995;145:245–256.
  20. Thwaites DT, Basterfield L, McCleave PMJ, Carter SM, Simmons NL. Gamma-aminobutyric acid (GABA) transport across human intestinal epithelial (Caco-2) cell monolayers. *Br J Pharmacol* 2000;129:457–464.
  21. Boll M, Foltz M, Anderson CMH, Oechsler C, Kottra G, Thwaites DT, Daniel H. Substrate recognition by the mammalian proton-dependent amino acid transporter PAT1. *Mol Membr Biol* 2003;20:261–269.
  22. Krogsgaard-Larsen P, Falch E, Larsson OM, Schousboe A. GABA uptake inhibitors: relevance to antiepileptic drug research. *Epilepsy Res* 1987;1:77–93.
  23. Huxtable RJ. Physiological actions of taurine. *Physiol Rev* 1992;72:101–163.
  24. Daniels VG, Newey H, Smyth DH. Stereochemical specificity of neutral amino acid transfer systems in rat small intestine. *Biochim Biophys Acta* 1969;183:637–639.
  25. De la Noue J, Newey H, Smyth DH. Transfer of alanine isomers by rat small intestine. *J Physiol* 1971;214:105–114.
  26. Thompson E, Levin RJ, Jackson MJ. The stimulating effect of low pH on the amino acid transferring systems of the small intestine. *Biochim Biophys Acta* 1970;196:120–122.
  27. Stevens BR, Kaunitz JD, Wright EM. Intestinal transport of amino acids and sugars: advances using membrane vesicles. *Annu Rev Physiol* 1984;46:417–433.
  28. Mailliar ME, Stevens BR, Mann GE. Amino acid transport by small intestinal, hepatic, and pancreatic epithelia. *Gastroenterology* 1995;108:888–910.
  29. Palacin M, Estevez R, Bertran J, Zorzano A. Molecular biology of mammalian plasma membrane amino acid transporters. *Physiol Rev* 1998;78:969–1054.
  30. Chen Z, Fei YJ, Anderson CMH, Wake KA, Miyauchi S, Huang W, Thwaites DT, Ganapathy V. Structure, function and immunolocalization of a proton-coupled amino acid transporter (hPAT1) in the human intestinal cell line Caco-2. *J Physiol* 2003;546:349–361.
  31. Boll M, Foltz M, Rubio-Aliaga I, Daniel H. A cluster of proton/amino acid transporter genes in the human and mouse genomes. *Genomics* 2003;82:47–56.
  32. Rajendran VM, Ansari SA, Harig JM, Adams MB, Khan AH, Ramaswamy K. Transport of glycyl-L-proline by human intestinal brush border membrane vesicles. *Gastroenterology* 1985;89:1298–1304.
  33. Malo C. Multiple pathways for amino acid transport in brush border membrane vesicles isolated from the human fetal small intestine. *Gastroenterology* 1991;100:1644–1652.
  34. Ganapathy V, Leibach FH. Is intestinal peptide transport energized by a proton gradient? *Am J Physiol* 1985;249:G289–G294.
  35. Thwaites DT, Kennedy DJ, Raldua D, Anderson CMH, Mendoza ME, Bladen CL, Simmons NL. H<sup>+</sup>/dipeptide absorption across the human intestinal epithelium is controlled indirectly via a functional Na<sup>+</sup>/H<sup>+</sup> exchanger. *Gastroenterology* 2002;122:1322–1333.
  36. Kennedy DJ, Ganapathy V, Leibach F, Thwaites DT. Optimal absorptive transport of the dipeptide glycylsarcosine is dependent on functional Na<sup>+</sup>/H<sup>+</sup> exchange activity. *Pflugers Arch* 2002;445:139–146.
  37. Anderson CMH, Mendoza ME, Kennedy DJ, Raldua D, Thwaites DT. Inhibition of intestinal dipeptide transport by the neuropeptide VIP is an anti-absorptive effect via the VPAC<sub>1</sub> receptor in a human enterocyte-like cell line (Caco-2). *Br J Pharmacol* 2003;138:564–573.
  38. McEwan GTA, Daniel H, Fett C, Burgess MN, Lucas ML. The effect of *Escherichia coli* STa enterotoxin and other secretagogues on mucosal surface pH of rat small intestine in vivo. *Proc R Soc Lond B* 1988;234:219–237.
  39. Daniel H, Fett C, Kratz A. Demonstration and modification of intervillous pH profiles in rat small intestine in vitro. *Am J Physiol* 1989;257:G489–G495.
  40. Boll M, Foltz M, Rubio-Aliaga I, Kottra G, Daniel H. Functional characterization of two novel mammalian electrogenic proton-dependent amino acid cotransporters. *J Biol Chem* 2002;277:22966–22973.
  41. Munck BG, Munck LK. Effects of pH changes on systems ASC and B in rabbit ileum. *Am J Physiol* 1999;276:G173–G184.
  42. McCloy LRR, Taylor PM, Thwaites DT. Neutral amino acid transport via system L at the basolateral membrane of human intestinal Caco-2 cell monolayers. *J Physiol* 2001;535P:48P–49P.
  43. Kanai Y, Stelzner M, Nussberger S, Khawaja S, Hebert SC, Smith GP, Hediger MA. The neuronal and epithelial human high affinity glutamate transporter. Insights into structure and mechanism of transport. *J Biol Chem* 1994;269:20599–20606.
  44. Wiemann M, Schwark JR, Bonnet U, Jansen HW, Grinstein S, Baker RE, Lang HJ, Wirth K, Bingmann D. Selective inhibition of the Na<sup>+</sup>/H<sup>+</sup> exchanger type 3 activates CO<sub>2</sub>/H<sup>+</sup>-sensitive medullary neurones. *Pflugers Arch* 1999;438:255–262.
  45. Scholtz W, Albus U, Counillon L, Gogelein H, Lang HJ, Linz W, Weichert A, Scholkens BA. Protective effects of HOE642, a selective sodium-hydrogen exchange subtype 1 inhibitor, on cardiac ischaemia and reperfusion. *Cardiovasc Res* 1995;29:260–268.
  46. Orłowski J. Heterologous expression and functional properties of amiloride high affinity (NHE-1) and low affinity (NHE-3) isoforms of the rat Na/H exchanger. *J Biol Chem* 1993;268:16369–16377.
  47. Daniels VG, Dawson AG, Newey H, Smyth DH. Effect of carbon chain length and amino group position on neutral amino acid transport systems in rat small intestine. *Biochim Biophys Acta* 1969;173:575–577.
  48. Sagné C, Agulhon C, Ravassard P, Darmon M, Hamon M, El Mestikawy S, Gasnier B, Giros B. Identification and characterization of a lysosomal transporter for small neutral amino acids. *Proc Natl Acad Sci U S A* 2001;98:7206–7211.
  49. Wreden CC, Johnson J, Tran C, Seal RP, Copenhagen DR, Reimer RJ, Edwards RH. The H<sup>+</sup>-coupled electrogenic lysosomal amino acid transporter LYAAT1 localizes to the axon and plasma membrane of hippocampal neurons. *J Neurosci* 2003;23:1265–1275.
  50. Chen Z, Kennedy DJ, Wake KA, Zhuang L, Ganapathy V, Thwaites DT. Structure, tissue expression pattern, and function of the amino acid transporter rat PAT2. *Biochem Biophys Res Commun* 2003;304:747–754.
  51. Ingrosso L, Marsigliante S, Zonno V, Storelli C, Vilella S. An L-proline-dependent proton flux is located at the apical membrane level of the eel enterocytes. *Am J Physiol* 2000;279:R1619–R1624.
  52. Diaz M, Medina V, Gomez T, Lorenzo A. Membrane mechanisms for electrogenic Na<sup>+</sup>-independent L-alanine transport in the lizard duodenal mucosa. *Am J Physiol* 2000;279:R925–R935.
  53. Rajendran VM, Barry JA, Kleinman JG, Ramaswamy K. Proton gradient dependent transport of glycine in rabbit renal brush border membrane vesicles. *J Biol Chem* 1987;262:14974–14977.

54. Roigaard-Petersen H, Jacobsen C, Sheikh MI. H<sup>+</sup>-L-proline co-transport by vesicles from pars convoluta of rabbit proximal tubule. *Am J Physiol* 1987;253:F15-F20.
55. Alford C, Cox H, Wescott R. The effects of red bull energy drink on human performance and mood. *Amino Acids* 2001;21:139-150.
56. Cinatl J, Cinatl J, Kotchetkov R, Pouckova P, Vogel JU, Rabineau H, Michaelis M, Kornhuber B. Cytotoxicity of L-cycloserine against human neuroblastoma and medulloblastoma cells is associated with the suppression of ganglioside expression. *Anticancer Res* 1999;19:5349-5354.
57. Mas-Serrano P, Granero L, Martin-Algarra RV, Guerri C, Polache A. Kinetic study of acamprosate absorption in rat small intestine. *Alcohol Alcohol* 2000;35:324-330.
58. Yun CHC, Oh S, Zizak M, Steplock D, Tsao S, Tse CM, Weinman EJ, Donowitz M. cAMP-mediated inhibition of the epithelial brush border Na<sup>+</sup>/H<sup>+</sup> exchanger, NHE3, requires an associated regulatory protein. *Proc Natl Acad Sci U S A* 1997;94:3010-3015.
59. Field M. Intestinal ion transport and the pathophysiology of diarrhea. *J Clin Invest* 2003;111:931-943.

---

Received May 6, 2004. Accepted July 29, 2004.

Address requests for reprints to: David T. Thwaites, PhD, Institute for Cell & Molecular Biosciences, Faculty of Medical Sciences, University of Newcastle Upon Tyne, Newcastle Upon Tyne, NE2 4HH, United Kingdom. e-mail: d.t.thwaites@ncl.ac.uk.

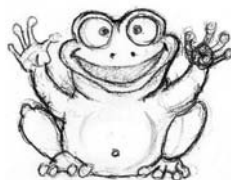
Supported by the Medical Research Council (G9801704) and Biotechnology and Biological Sciences Research Council (13/D17277). S1611 and cariporide were from H. J. Lang (Aventis Pharma Deutschland GmbH, Frankfurt/Main, Germany).

## **DANKSAGUNG**



## DANKSAGUNG

Michael, dir gilt an erster Stelle mein herzlichster Dank! Ohne deine außerordentliche Unterstützung und Hilfe wäre meine Doktorarbeit in dieser Form nicht möglich gewesen. Du warst immer ansprechbar und bereit, dich mit auftauchenden Problemen auseinander zu setzen, mir Anregungen und Hilfestellung zu geben und mich in meiner Arbeit tatkräftig zu unterstützen. Deine Diskussionsbereitschaft bzw. die ständige Aufforderung zur Diskussion hat zu neuen Versuchsansätzen angeregt und die Arbeiten entscheidend vorangetrieben. Dir ist es gelungen, deine Begeisterung für wissenschaftliches Arbeiten und dein kritisches Verständnis bei der Betrachtung von Ergebnissen auf mich zu übertragen. Ohne dich wäre es mir nicht möglich gewesen, im Rahmen meiner Doktorarbeit ein so großes Methodenspektrum zu erlernen. Nach 3 Jahren gemeinsamen Arbeitens kann ich von ganzem Herzen sagen, dass ich es als großes Glück empfunden habe, dich als „meinen“ Betreuer bezeichnen zu dürfen. Natürlich wäre dies alles aber niemals ohne die Unterstützung von Frau Daniel möglich gewesen, die mir die Möglichkeit gegeben hat, meine Doktorarbeit in ihrer Arbeitsgruppe anzufertigen. Ihre konstruktive Kritik hat zum Gelingen dieser Arbeit entscheidend beigetragen. Dass Grundlagenforschung keine karge Kost sein muss, hat Sie mir mit ihrem Enthusiasmus gezeigt und auch meine Horizonte jenseits der Wissenschaft erweitert. Vielen Dank auch an Gabor, der mir die Elektrophysiologie nahe gebracht und bei Problemen mich mit tatkräftiger Hilfe unterstützt hat. Isabel gilt mein Dank für die Einführung in die Immunhistochemie. Laddi, Danke für die Hilfe bei meinen (erfolglosen) Ussing-Kammer-Versuchen, das Lesen der Arbeit und vielmehr noch für die Zeit außerhalb des Instituts in den Bergen. Helene, vielen Dank für die umfangreiche Hilfe bei den Arbeiten rund um die Frösche, dies war mir eine sehr große Erleichterung. Danke Daniela, für den reibungslosen Laborablauf und deine tatkräftigen Unterstützungen bei meinen ersten molekularbiologischen „Gehversuchen“. Didi, Manu und Alex, danke für die witzigen Momente in unserer Schreibstube. Kai, die Männerabende werden unvergessen bleiben. Danke auch an alle weiteren Mitglieder der Arbeitsgruppe, alle namentlich zu nennen ist bei einer DIN A4 Seite leider nicht möglich, die Erinnerungen werden aber bleiben. Ein großer Dank gilt meine Eltern, für Ihre Hilfe, nicht den Blick auf das Wesentliche während der manchmal wirren Promotionszeit zu verlieren. Liebe Dagmar, danke dass Du die Zeit mit „dem Wahnsinnigen“ so tapfer durchgestanden hast und mich trotz Deiner vielen Arbeit so unterstützt hast.





## CURRICULUM VITAE

### Personal

Name: Martin Foltz  
Address: Vöttinger Strasse 46  
85354 Freising, Germany  
Date of birth: February 19<sup>th</sup> 1973  
Place of birth: Ludwigshafen am Rhein / Germany  
Phone: +49 8161 713553  
Email: foltz@wzw.tum.de  
Civil status: Single  
Nationality: German  
Language: English (fluent), German (mother tongue)

### Education

1979 - 1983 Primary school Dudenhofen  
1983 - 1992 Hans Purrmann Gymnasium Speyer  
June 1992 Abitur (general qualification for university entrance)

### University Education

4/1993 - 04/1999 Study of Nutrition and Household Sciences, Main Focus on Human Nutrition, at the Justus-Liebig-University of Giessen, Germany.  
Diploma Thesis: Influence of selenate and  $\alpha$ -tocopherol on selenium metabolism in primary cultures of rabbit hepatocytes

05/1999 - 02/2000 Postgraduate Study of Human Biology and Theoretical Medicine at the Philipps University of Marburg

03/2000 - 10/2004 Completion of PhD work in the group of Prof. Dr. Daniel, Molecular Nutrition Unit, Technical University of Munich, Germany.  
Title: Molecular and functional characterisation of a new mammalian family of proton dependent amino acid transporters

### Additional Qualifications

10/1995 - 05/1999 Collegiate assistant in the group of Prof. Dr. J. Pallauf, Institute of Animal Nutrition and Nutrition Physiology at the Justus Liebig University of Giessen, Germany

2002 Member of the Organization Committee of the International Transporter Meeting 2002, Seon, Deutschland

03/2000 - to date Supervision of students and trainees in biochemical and physiological practical trainings and seminars. Supervision of students preparing their diploma thesis at the Molecular Nutrition Unit

---

**Scientific Awards**

- 01/2000 Award of the H. Wilhelm Schaumann Stiftung (Hamburg) for extraordinary achievement in the field of animal nutrition with the diploma thesis "Influence of selenate and  $\alpha$ -tocopherol on selenium metabolism in primary cultures of rabbit hepatocyte"
- 07/2003 First prize of the poster award at the "FASEB Summer Research Conference", Tucson, USA for the poster entitled "The bifunctionality of mPAT1: electrogenic proton-coupled amino acid and electroneutral proton-coupled short-chain fatty acid cotransport mediated by the same protein"

**Membership**

- since 2002 Member of the Gesellschaft für Biochemie und Molekularbiologie, Study Group Biomembranes
- since 2003 Member of the European Nutrigenomics Organisation

**Activities**

- 1992 - 2000 Literature, cycling, outdoor activities  
Race cyclist of the highest German amateur cycling category

## LIST OF SCIENTIFIC PUBLICATIONS

### Peer reviewed original papers and submitted manuscripts

- 2002 Boll M, **Foltz M**, Rubio-Aliaga I, Kottra G, and Daniel H. Functional characterization of two novel mammalian electrogenic proton dependent amino acid cotransporters. *J. Biol. Chem.*, 277, 22966-22973  
[concept by MB, experimental work by MF, MB, and IRA, technical advice by IRA and GK, writing by MB and MF with editorial help of the co-authors]
- 2003 Boll M, **Foltz M**, Rubio-Aliaga I, Daniel H. A cluster of proton/amino acid transporter genes in the human and mouse genomes. *Genomics*, 82, 47-56  
[concept by MB, genome mapping by MB, alignments and dendograms by MB and MF, oocyte experimental work by MF, writing by MB with editorial help of the co-authors]
- Boll M<sup>#</sup>, **Foltz M**<sup>#</sup>, Anderson CM, Oechsler C, Kottra G, Thwaites DT, Daniel H. Substrate recognition by the mammalian proton-dependent amino acid transporter PAT1. <sup>#</sup>authors contributed equally  
*Mol. Membr. Biol.*, 20, 261-269 (2003)  
[concept by MB and MF, oocyte experimental work by MF and CO, Caco-2 experiments by CMA, writing by MB and MF with editorial help of the co-authors]
- 2004 Knütter I, Hartrodt B, Theis S, **Foltz M**, Rastetter M, Daniel H, Neubert K, Brandsch M. Analysis of the transport properties of side chain modified dipeptides at the mammalian peptide transporter PEPT1. *Eur. J. Pharm.Sci.*, 21, 61-67 (2004)  
[contribution of MF to this paper: *P. pastoris* as well as oocytes experiments and editorial help]
- Rubio-Aliaga I, Boll M, Vogt-Weisenhorn DM, **Foltz M**, Kottra G, Daniel H. The proton/amino acid cotransporter PAT2 is expressed in neurons with a different subcellular localization than its paralog PAT1. *J. Biol. Chem.* 279, 2754-2760  
[contribution of MF to this paper: oocyte experimental work, expression of PAT2-EGFP fusion protein in GT1-1 cells, imaging, and editorial help]
- Foltz M**, Meyer A, Theis S, Demuth HU, Daniel H. Rapid and convenient screening of in vitro transport of DP IV-inhibitors as antidiabetic drug candidates with different peptide transporter expressing systems. *J Pharmacol Exp Ther.* 310, 695-702  
[concept by MF, experimental work by MF and ST, synthesis of test compounds by AM, writing by MF with editorial help of the co-authors]
- Foltz M**, Boll M, Raschka L, Kottra G, Daniel H. A novel bifunctionality: PAT1 and PAT2 mediate electrogenic proton/amino acid and electroneutral proton/short-chain fatty transport. *FASEB J* (accepted and in press)  
[concept by MF, experimental work by MF, technical advice by GK and LR, writing by MF with editorial help of the co-authors]

**Foltz M**, Oechsler C, Boll M, Kottra G, Daniel H. (2004) Substrate specificity and transport properties of the murine proton dependent amino acid transporter PAT2  
*Eur. J. Biochem.* 271, 3340-3347

*[concept by MF, experimental work by MF and CO, writing by MB with editorial help of the co-authors]*

Anderson CMH, Grenade DS, Boll M, **Foltz M**, Wake KA, Kennedy DJ, Munck LK, Miyauchi S, Taylor PM, Campbell FC, Munck BG, Daniel H, Ganapathy V, Thwaites DT (2004) PAT1 (SLC36A1) is a nutrient and drug transporter in human and rat small intestine.

*Gastroenterology* (accepted and in press)

*[concept by DTT, contribution from MF to this work: oocyte experimental work as well as editorial help]*

**Foltz M**, Dietz V, Merti M, Boll M, Kottra G, Daniel H. Kinetics of bidirectional H<sup>+</sup> and substrate transport by the proton-dependent amino acid symporter PAT1.

*Biochem J* (submitted)

*[concept by MF, experimental work by MF, VD, MM, writing by MF with editorial help of the co-authors]*

## Oral Presentations

2001 **Foltz M**, Theis S, Knütter I, Hartrodt B, Brandsch M, Neubert K, Daniel H. Synthesis and characterization of high-affinity inhibitors of the H<sup>+</sup>/peptide transporter PEPT2.  
7<sup>th</sup> International Congress on Amino Acids and Proteins, Wien 2001

2003 **Foltz M**, Boll M, Rubio-Aliaga I, Kottra G, Daniel H. Funktion und Bedeutung des intestinalen und renalen epithelialen Protonen-abhängigen Aminosäure-Transport-systems PAT1  
40<sup>th</sup> Scientific Congress of the German Nutrition Society, Potsdam 2003

**Foltz M**, Boll M, Daniel H. The biofunctional transport proteins PAT1 and PAT2  
Göttinger Transporttage, Göttingen 2003

2004 **Foltz M**, Boll M, Rubio-Aliaga I, Kottra G, Daniel H. Recovering the past - proton dependent amino acid transporters in mammals.  
Institutskolloquium, Freising 2004

**Selected Abstracts of Congressional Contributions**

- 2001 **Foltz M**, Meissner B, Boll M, Daniel H. Die Inaktivierung des *pep-2* Gens führt zu starker Malnutrition in *Caenorhabditis elegans*.  
38<sup>th</sup> Scientific Congress of the German Nutrition Society, Gießen 2001
- 2002 **Foltz M**, Boll M, Daniel H. Identifizierung und funktionelle Charakterisierung eines murinen, elektrogenen H<sup>+</sup>/Aminosäuren-Transporters.  
39<sup>th</sup> Scientific Congress of the German Nutrition Society, Jena 2002
- Foltz M**, Boll M, Rubio-Aliaga I, Kottra G, Daniel H. Cloning and functional characterization of a proton/amino acid transporter from murine small intestine.  
81<sup>st</sup> Congress of the German Physiological Society (DPG) and Federation of European Physiological Societies (FEPS), Tübingen 2002
- Foltz M**, Boll M, Oechsler C, Kottra G, Daniel H, Substrate recognition by the proton amino acid cotransporter PAT1: structure-transport relationship of modified pat1 substrates.  
Congress on Transport of Amino Acids, Amines, Peptides, Nucleosides and Drugs, Kloster Seeon 2002
- 2003 **Foltz M**, Boll M, Oechsler C, Kottra G, Daniel H. Transport of amino acids and derivatives mediated by the Proton amino acid cotransporter PAT1: insights into the mechanism of substrate recognition.  
4<sup>th</sup> Transport Colloquium of the German Society of Biochemistry and Molecular Biology, Study Group Biomembranes, Rauschholzhausen 2003
- Foltz M**, Boll M, Kottra G, Daniel H. The bifunctionality of mPAT1: electrogenic proton-coupled amino acid and electroneutral proton-coupled short-chain fatty acid cotransport mediated by the same protein.  
FASEB Summer Research Conference, Perspectives in Transport Biology, Tucson 2003
- Foltz M**, Boll M, Kottra G, Daniel H. A novel bifunctionality: electrogenic proton-coupled amino acid and electroneutral proton-coupled short-chain fatty acid cotransport mediated by the same protein.  
83<sup>st</sup> Congress of the German Physiological Society (DPG), Leipzig 2004

